Final Technical Report

Grand Valley State University
Lake Michigan Offshore Wind Feasibility Assessment

Award Number DE-EE0000294
September 2009 – March 2014

Principle Investigator – T. Arnold Boezaart
Author – James Edmonson
200 Viridian Drive
Muskegon, Michigan 49440
616.331.6901

GRAND VALLEY STATE UNIVERSITY
MICHIGAN ALTERNATIVE AND RENEWABLE ENERGY CENTER

200 Viridian Drive, Muskegon, Michigan 49441
616.331.6901

Team Members

GVSU School of Engineering
GVSU School of Computing
Michigan Public Service Commission
Michigan State University,
Michigan Natural Features Inventory
Michigan Technological University
Sierra Club of the Great Lakes
University of Michigan
AXYS Technologies
Andrie Specialized

June 30, 2014

Acknowledgement and Disclaimer

Acknowledgements: "This material is based upon work supported by the Department of Energy; Grand Valley State University; Michigan Public Service Commission; We Energies; Sierra Club of the Great Lakes; Grand Valley State University; Michigan State University, Michigan Natural Features Inventory; and the University of Michigan, under Award Number DE-EE0000294. Special acknowledgement and thanks also to the following organizations for technical support: National Oceanic and Atmospheric Administration/Great Lakes Environmental Research Laboratory; National Data Buoy Center; Pacific Northwest National Laboratory; United States Coast Guard; United States Army Corp of Engineers; Michigan Department of Natural Resources; and West Michigan Energy Partners."

Table of Contents

List of Acronyms

AEP	American Electric Power
ANN	Artificial Neutral Networking
AUV	Autonomous Underwater Vehicle
AWEA	American Wind Energy Association
CDMA	Code Division Multiple Access
DB	Decibels
EPA	Environmental Protection Agency
FAA	Federal Aviation Administration
FERC	Federal Energy Regulation Commission
GLERL	Great Lakes Environmental Research Laboratory
DOE	U.S. Department of Energy
GLOW	Great Lakes Wind Council
GVSU	Grand Valley State University
INL	Integral Nonlinearity
LIDAR	Light Detection and Ranging
LWS	Laser Wind Sensor
MAREC	Michigan Alternative and Renewable Energy Center
MATLAB	A language of technical computing
MET	Meteorological
MDEQ	Michigan Department of Environmental Quality
MDNR	Michigan Department of Natural Resources
MDOT	Michigan Department of Transportation
MNFI	Michigan Natural Features Inventory
MPSC	Michigan Public Service Commission
MSU	Michigan State University
MTU	Michigan Technological University
MZEA	Michigan Zoning Enabling Act
NDBC	National Data Buoy Center
NOAA	National Oceanographic and Atmospheric Administration
NREL	National Renewable Energy Laboratory
OADS	Optical Air Data Systems
RFP	Request for Proposals
RLT	Project Research Leadership Team
ROV	Remotely Operated Underwater Vehicle
SM2	Song Monitor
TKE	Turbulent Kinetic Energy
UM	University of Michigan
USACE	United States Army Corp of Engineers
USCG	United States Coast Guard
WS	AXYS Technologies WindSentinel
WQM	Water Quality Monitor

List of Figures

List of Tables

List of Appendices

A. **A Case Study of Laser Wind Sensor Performance Validation by Comparison to an Existing Gage**
Charles Standridge (standric@gvsu.edu) Padnos College of Engineering and Computing, Grand Valley State University, 301 West Fulton, Grand Rapids, Michigan 49504 – Corresponding Author

B. **Lake Michigan Offshore Wind Assessment, 2012 Season Summary Report**
Charles Standridge (standric@gvsu.edu) Padnos College of Engineering and Computing, Grand Valley State University, 301 West Fulton, Grand Rapids, Michigan 49504

C. **Data Summary and Analysis Comparing the 2013 Season and the 2012 Season**
Charles Standridge (standric@gvsu.edu) Padnos College of Engineering and Computing, Grand Valley State University, 301 West Fulton, Grand Rapids, Michigan 49504

D. **Wind Energy Assessment using a Wind Turbine with Dynamic Yaw Control**
Md Nahid Pervez. Padnos College of Engineering and Computing, Grand Valley State University, 301 West Fulton, Grand Rapids, Michigan 49504. April 2013. – A Thesis Submitted to the Graduate Faculty in Partial Fulfillment of the Requirements For the Degree of Master of Science in Engineering School of Engineering.

E. **Great Lakes Wind Energy Analysis of Turbulence and Temporal Averaging Time Constants**
Neel Desai. University of Michigan, Ann Arbor

F. **Wind Gust Analysis**
Bruce M. Williams. University of Delaware. May 2013

G. **Visualizing Lake Michigan Wind with SAS® Software**
Aaron C Clark and David Zeitler, Grand Valley State University. SAS Global Forum, March 22-26 in Washington D.C.

H. **AWRI Summary Report of Water Quality Data from Wetlab's WQM Sensor on board GVSU's Windsentinel Buoy during 2012 and 2013.**
Scott Kendall, Bopi Biddanda, Alan Steinman. Annis Water Resources Institute, Grand Valley State University, Muskegon, MI 49441. April, 2014.

I. **Offshore Bat and Bird Activity at the Lake Michigan Mid-lake Plateau, Considerations for Wind Energy Development**
Klatt, B. J., T. A. Boezzart, J. L. Gehring, K. Walter, and J. Edmonson. 2014. Offshore Bat and Bird Activity at the Lake Michigan Mid-lake Plateau – Considerations for Wind Energy Development.

Michigan Natural Features Inventory, Michigan State University, Report Number 2014-XX, Lansing, MI. Copyright 2014 Michigan State University Board of Trustees.

J. Estimating sound levels from a hypothetical offshore wind farm in Lake Michigan
Erik E. Nordman, Ph.D. Grand Valley State University, Allendale, MI. 2014.

K. Behavioral approaches to environmental policy analysis: a case study of offshore wind energy in the North American Great Lakes
Erik Nordman. Natural Resources Management Program, Biology Department, Grand Valley State University, Allendale, Michigan 49401, 2014.

L. Executive Summary

The purpose of this project was to conduct the first comprehensive offshore wind assessment over Lake Michigan and to advance the body of knowledge needed to support future commercial wind energy development on the Great Lakes. The project involved evaluation and selection of emerging wind measurement technology and the permitting, installation and operation of the first mid-lake wind assessment meteorological (MET) facilities in Michigan's Great Lakes. In addition, the project provided the first opportunity to deploy and field test floating LIDAR and Laser Wind Sensor (LWS) technology, and important research related equipment key to the sitting and permitting of future offshore wind energy development in accordance with public participation guidelines established by the Michigan Great Lakes Wind Council (GLOW). The project created opportunities for public dialogue and community education about offshore wind resource management and continued the dialogue to foster Great Lake wind resource utilization consistent with the focus of the GLOW Council.

Figure 1 – WindSentinel Floating MET Facility

The technology proved to be effective, affordable, mobile, and the methods of data measurement accurate. The public benefited from a substantial increase in knowledge of the wind resources over Lake Michigan and gained insights about the potential environmental impacts of offshore wind turbine placements in the future. The unique first ever hub height wind resource assessment using LWS technology over water and development of related research data along with the permitting, sitting, and deployment of the WindSentinel MET buoy has captured public attention and has helped to increase awareness of the potential of future offshore wind energy development on the Great Lakes.

Specifically, this project supported the acquisition and operation of a WindSentinel (WS) MET wind assessment buoy, and associated research for 549 days over multiple years at three locations on Lake Michigan, *Table 1*. Four research objectives were defined for the project including to: 1) test and validate floating LIDAR technology; 2) collect and access offshore wind data; 3) detect and measure bird and bat activity over Lake Michigan; 4) conduct an over water sound propagation study; 5) prepare and offer a college course on offshore energy, and; 6) collect other environmental, bathometric, and atmospheric data.

GVSU-MAREC WindSentinel Record of Service				
Year	Date Deployed	Date Retrieved	Days in Service	Location
2011	Oct. 7th	Dec. 30th	85	MKG Lake & 6 miles WNW of Muskegon Channel
2012	May 7th	Dec. 18th	225	Mid-lake Plateau
2013	Apr. 27th	Dec. 21st	239	10 miles SW of Muskegon Channel

Table 1 – WindSentinel Deployment Dates and Location

Desk-top research was performed to select anchorage sites and to secure permits to deploy the buoy.

The project also collected and analyzed data essential to wind industry investment decision-making including: deploying highly mobile floating equipment to gather offshore wind data; correlating offshore wind data with conventional on-shore MET tower data; and performing studies that can contribute to the advancement and deployment of offshore wind technologies. Related activities included:

- Siting, permitting, and deploying an offshore floating MET facility;
- Validating the accuracy of floating LWS using near shoreline cup anemometer MET instruments;
- Assessment of laser pulse technology (LIDAR) capability to establish hub height measurement of wind conditions at multiple locations on Lake Michigan;
- Utilizing an extended-season (9-10 month) strategy to collect hub height wind data and weather conditions on Lake Michigan;
- Investigation of technology best suited for wireless data transmission from distant offshore structures;
- Conducting field-validated sound propagation study for a hypothetical offshore wind farm from shoreline locations;
- Identifying the presence or absence of bird and bat species near wind assessment facilities;
- Identifying the presence or absence of benthic and pelagic species near wind assessment facilities;

All proposed project activities were completed with the following major findings:

- Floating Laser Wind Sensors are capable of high quality measurement and recordings of wind resources. The WindSentinel presented no significant operational or statistical limitations in recording wind data technology at a at a high confidence level as compared to traditional anemometer cup technology.

- During storms, mean Turbulent Kinetic Energy (TKE) increases with height above water;

- Sufficient wind resources exist over Lake Michigan to generate 7,684 kWh of power using a 850 kW rated turbine at elevations between 90 - 125 meters, a height lower than originally anticipated for optimum power generation;

- Based on initial assessments, wind characteristics are not significantly different at distant (thirty-two mile) offshore locations as compared to near-shore (six mile) locations;

- Significant cost savings can be achieved in generation wind energy at lower turbine heights and locating closer to shore.
- Siting must be sufficiently distant from shore to minimize visual impact and to address public sentiment about offshore wind development;
- Project results show that birds and bats do frequent the middle of Lake Michigan, bats more so than birds;
- Based on the wind resource assessment and depths of Lake Michigan encountered during the project, future turbine placement will most likely need to incorporate floating or anchored technology;
- The most appropriate siting of offshore wind energy locations will enable direct routing of transmission cables to existing generating and transmission facilities located along the Michigan shoreline;
- Wind turbine noise propagation from a wind energy generating facility at a five mile offshore location will not be audible at the shoreline over normal background sound levels.

Introduction

The nation's reliance on foreign oil and other non-renewable energy sources compromises our physical and economic security as well as our environment. In addition, Michigan, which is one of the nation's leading manufacturing states, continues to experience high unemployment and the loss of manufacturing jobs. The introduction of renewable energy technology including considerable growth in onshore and the potential for offshore wind energy generation, provides an opportunity to strengthen the state's economy and provide new employment opportunities for its citizens. Early stage measurement and validation of offshore wind resources leading to future development and servicing of offshore wind generating facilities on the Great Lakes has the potential to add an important component to Michigan's energy generation portfolio. Michigan is well positioned to secure a portion of the expanding renewable energy and offshore wind industry.

Discussions with investors, developers, manufacturers, utilities and scientists suggests that the Great Lakes look very promising for wind energy production. The type of wind and related research data that will be needed to attract financing and large scale investment in offshore wind energy is inadequate at this time. It is noteworthy that no affordable technology suitable to conduct deep-water wind assessment had been available until this project field tested and validated the WindSentinel platform. The success of this project has made collecting hub-height wind data from multiple near shore and more distant offshore locations both possible and cost-effective.

The establishment of an offshore buoy based MET facility provided opportunities for high quality multi-disciplinary research, including the evaluation of LIDAR and LWS technology in a challenging Great Lakes environment. With a robust buoy research platform designed for an open ocean environment it is now possible to collect wind data using the most advanced technology in deep water locations. Data from this project provides some of the first ever insights on Great Lakes wind resources, the offshore environment and wind development sitting possibilities. Successful field testing and validation of new wind assessment technology and related research equipment in a challenging Great Lakes offshore environment has opened the possibility of future offshore wind energy development. The project outcomes also provide the basis for more effective public policy development and new opportunities for public outreach and engagement.

The project has contributed to advancing the public's greater understanding of offshore wind as a viable and renewable source of energy. and has addressed public concerns about the environmental impact of offshore wind. The project was beneficial to the people of Michigan and the surrounding Great Lakes region. The offshore wind data collected will contribute to a greater understanding of the potential of generating utility scale "green" energy in an untapped environment that has huge energy potential. Advancing a greater understanding of offshore wind and related research and technology also helped to provide the basis for projecting future job creation by other organizations. Development of a commercial wind industry on Lake Michigan will prove beneficial to stimulating private investment and business development opportunities, and will result in new jobs in a wide range of related manufacturing sectors. The project also positioned West Michigan, and the Muskegon Lakeshore, as a promising hub for offshore wind technology, manufacturing, logistical staging and deployment in the Great Lakes region.

The research effort was organized in five core areas, as shown in *Table 2*, and complimented by a sixth outreach and education component.

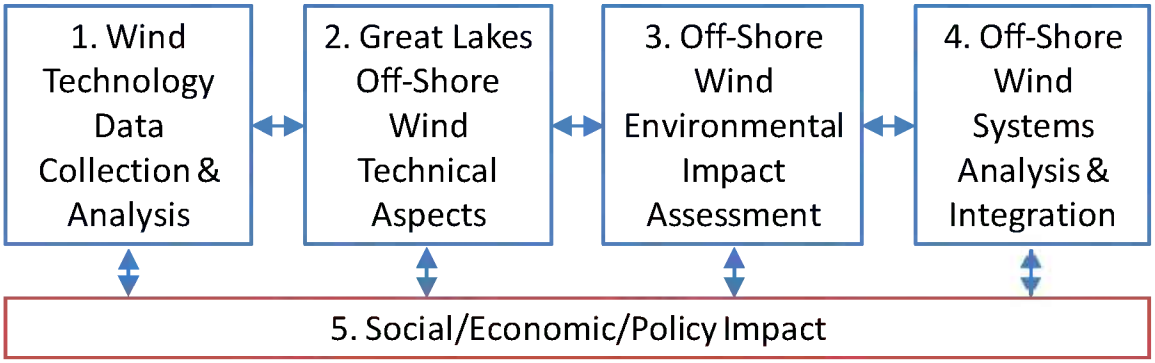

Table 2: 5 Core Areas of Study

Planning for the project began in January 2011 in conjunction with the academic schedule at partnering universities. Equipment deployment and full-scale offshore field studies, equipment validation, and data collection began in October 2011. During the three-year project period, researchers collected previously never available wind data from the WindSentinel buoy, from an on-shore fixed MET

tower on Muskegon Lake for LWS validation study purposes, and from additional NOAA operated offshore and shore based sources for data comparison purposes.

The project advanced the deployment of offshore the commercial wind energy development on the Great Lakes by collecting and analyzing data essential to the wind industry investment decision-making.

Background

The project described herein resulted from a Congressional Earmark secured by then Congressman Pete Hoekstra (Holland, MI) for Grand Valley State University. The Earmark was administered by the U.S. Department of Energy's Golden Colorado Office as Award DE-EE0000294. Matching support was provided by the Michigan Public Service Commission; WE Energies, the Sierra Club of the Great Lakes; the University of Michigan; Michigan State University, Michigan Natural Features Inventory Program; and Michigan Technological University. The Principle Investigator was T. Arnold Boezaart, Director, GVSU-Michigan Alternative and Renewable Energy Center, Muskegon, Michigan.

Project Scope

While valuable lessons can be learned from ocean based offshore wind turbine installations, the Great Lakes region poses particular challenges to the development and deployment of offshore wind powered electric generating resources, particularly with respect to the climatology of the region and the depth of water. Therefore a first step towards fully understanding the potential of offshore wind energy generation in the Great Lakes region required a more detailed analysis of the wind resources available, including their variability in time and space, and the impact on power generation. To this end, the following phases were undertaken:

Phase One: A call for proposals (RFP) was issued by GVSU during the second half of 2010 to seek co-funding for the project, including proposals to design, engineer, procure, construct and deploy a new offshore MET facility, fixed or floating.

Phase Two: The chosen WS met facility was secured and deployed at three Lake Michigan locations.

Phase Three: Using the offshore WS / MET facility and on-board LWS technology, the use of LWS on buoy mounted platform was validated, reliable wind data was gathered and data was analyzed.

Technology and Vendor Selection

GVSU, in collaboration with its project partners, issued a request for proposals for the design, engineering, construction, maintenance, and collection of data needed for the project within project timelines and budgetary constraints on two separate occasions. After receipt of the first bid for a fixed platform MET tower, it was determined the cost ranging from $9-12 million was outside the budgetary constraints of the project.

A second RFP was issued for floating MET tower facilities. This solicitation resulted in equipment costs of $1.5 - $5 million from 3 bidders. The successful bidder was AXYS Technologies offering their WindSentinel floating LWS/LIDAR facility. The WindSentinel was selected based on three factors: affordable cost, the highly mobile nature of the MET platform and instrumentation package, and the ability to measure wind characteristics using cutting edge technology at heights up to 175 meters.

Deployment and Data Collection Plan

Following selection of the equipment vendor, a six month plan was established to support construction and delivery, commissioning of the buoy, and selection of anchorage sites.
The WindSentinel deployment plan was based on accomplishing four Milestones.

Milestone One

Conduct desk-top studies to describe and rank two or more potential sites in Lake Michigan for placing the WS buoy considering costs, partner interests, in proximity to potential offshore wind energy development sites, and in consideration of the GLOW Council's recommended sites for most favorable wind. Four sites were selected. One site was in Muskegon Lake next to a fixed, onshore MET tower for technology and data collection validation purposes, *Figure 2*. The other three sites were located in Lake Michigan for offshore data collection, *Figure 3*.

Figure 2 – Location of WindSentinel and MET tower on Muskegon Lake

Milestone Two

Permit and deploy the WindSentinel at the validation site and the Lake Michigan sites. Initiate meteorological, engineering and habitat data collection. Conduct research and field data collection including floating LWS/LIDAR validation. The WindSentinel was deployed to two sites in late 2011. The first site was on Muskegon Lake within 100 meters of a GVSU MET Tower for validation studies. Table 3 shows the specific location of the WindSentinel LIDAR, elevation above sea level, and test height used for validation purposes. The second site was in Lake Michigan for 30-day field trial data collection and wireless communication testing.

Data Source	Location	Latitude/Longitude	Above Sea Level	Test Heights
Laser sensor	Muskegon Lake	43° 14' 55" N; 86° 14' 55" W	176 m	57.85 m
Met mast	Open field	43° 14' 46" N; 86° 14' 41" W	178 m	50.5 m

Table 3 – Validation site characteristics

Milestone Three

Relocate the WindSentinel to a third site at the Mid-Lake Plateau just east of the Lake Michigan boundary line between Michigan and Wisconsin (approximately thirty-five miles from either shore). Conduct a full season of data collection to support offshore wind assessment and related research.

Milestone Four

Relocate the WindSentinel to a fourth near-shore site located on Lake Michigan. Conduct research and field data collection.

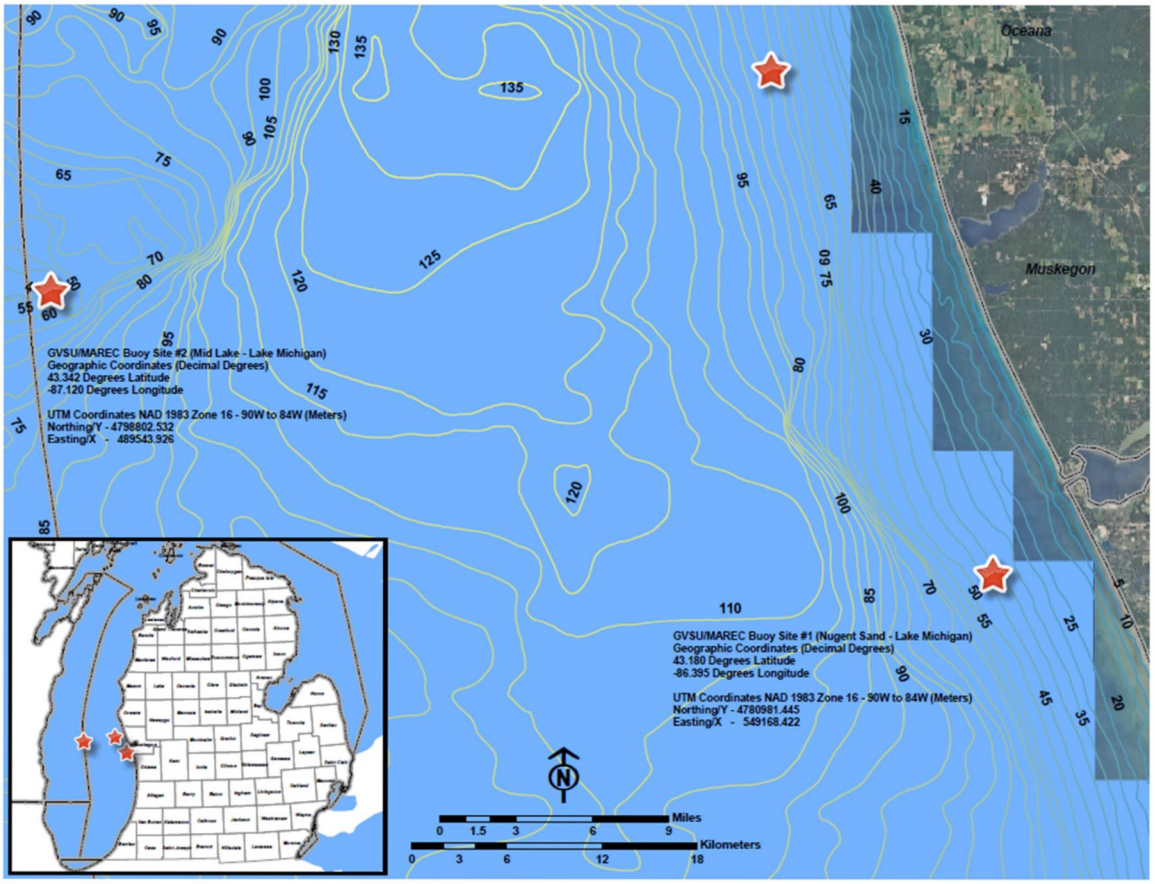

Figure 3 – Lake Michigan anchorage sites for the WindSentinel

To select specific anchorage sites, the project RLT conducted studies to determine desirable wind assessment locations; and established the details of a research program detailing how goals could be fully met without a fixed platform research station. The RLT also conducted pre-deployment lake bottom studies, engaged engineering resources and prepared project details for buoy deployment including location characterizations, mooring design, and employment of an AIS system and wireless data transmission system for each site.

The RLT developed a detailed list of siting options, identified related regulatory issues, established timeline for acquisition of federal/state permits for assessment facilities and obtained necessary permits to support the project. The Team convened meetings and consulted with regulatory agencies to review project requirements, consulted with federal agencies, and began the process of securing permits.

The Michigan Department of Natural Resources and the U.S. Army Corp of Engineers determined that a joint, nationwide, permit application would be suitable. A 3 year Nationwide Permit No. 5 was issued. Also required was an annual Aids to Navigation Permit from the U. S. Coast Guard.

Buoy Anchorage Site Analysis and Assessments

The application included information on historic subsurface features and grab samples of fish and aquatic organisms. A bottom survey was also conducted at the proximity of the two near shore locations and at the mid-lake plateau, *Figures 4, 5 and 6.*

Figure 4 – UM's Iver 2 AUV and Outland 1000 ROV

Figure 5- ROV video images showing patchy Quagga mussel beds.

Figure 6 - Ichthyoplankton net showing flow meter inside the net deployed at the buoy site in 46 m of water.

Following investigations for the near shore locations, the bottom survey indicated a flat level bottom consisting of very fine sands, which are approximately 80 – 90 % covered by quagga mussels. Light penetration from the surface and bottom visibility was exceptional at a depth of 35 meters. Coincident with the ROV observations, a Ponar dredge was lowered from the survey vessel and acquired three repetitive bottom grab samples of the surficial sediments.

The gill net collected five lake trout and fourteen alewives. The lake trout were all clipped (stocked fish) and were determined to be consuming alewives and round gobies. The alewives in turn were found to be consuming zooplankton of various species in sometimes large amounts. The trawl survey collected 4,480 cubic inches of quagga mussels and no fish.

Conclusions at the near shore locations revealed there were no endangered species collected or observed and this area has no rocky reefs or other sedimentary characteristics which would be directly linked to fish spawning. Researchers had expected to see more round gobies and some other fish species in the net hauls.

At the Mid-Lake Plateau, the Ichthyoplankton sampling caught one deepwater sculpin (*Myoxocephalus thompsoni*) larva at the site farthest from the buoy site; the density was 5/1,000 m3. The larva was about 10 mm long. No other larval fish were collected at the other two sites. For the Gill net sampling, the gill nets did not capture any fish during the time it was set on the buoy site. Researchers only observed one small rock and some quagga mussels caught in the net. Preliminary assessment of the buoy site on the mid lake reef showed very little noteworthy results. Researchers caught no fish in the gill nets, saw none during the ROV deployment, and only caught one deepwater sculpin in the larval fish tows; none were caught at the buoy deployment site. Adult burbot were discovered and collected on the reefs and there is significant evidence of higher densities of burbot larvae on the reef as compared with densities off the reef to suggest that spawning is also occurring for this species at the plateau.

The Project Team

GVSU/MAREC senior staff administered the project including oversight of the buoy operation and maintenance, data collection and management, coordination of research efforts among four participating universities, financial management and linkage with federal project officials.

GVSU assembled several teams including a *Grant Administration Team* that oversaw funds, procurement, preparation and approval of 7 budget modifications and submission of quarterly reports. A *Research Leadership Team* (RLT) consisting of representatives from the project partners that designed the final research program, set research objectives and served as liaison with members of the broader research community as well as public and private sector interests to assure maximum public awareness of the project and utilization of the research results. A *WS buoy Logistics Team* that handled the deployment and retrieval of the WS and day-to-day operations during the in-the-water research season. Finally, a *Data Management Team* that managed the download, indexing and archiving of the data. A total of 65 individuals where involved in the project including:

U.S. Department of Energy

- Jose Zayas - DOE HQ Program Manager
- Pamela Brodie - DOE Field Contract Officer
- David Welsh - DOE Field Grants Management Specialist
- Michael Hahn - DOE Field Project Officer
- Gretchen Andrus - DOE/CNJV Project Monitor
- Gary Nowakowski – DOE Senior Project Manager
- Will Shaw – DOE Technical Advisor
- Chris Hart – DOE Technical Advisor

Other Federal and State Agencies

- Marie Colton - Former Director, NOAA/ GLERL
- Steve Ruberg - Manager, Observation Systems & Advanced Technology, NOAA/GLERL
- Gary Fahnenstiel - Ecosystem Dynamics, NOAA/GLERL
- Dennis Donahue - Marine Superintendent, NOAA/GLERL
- D. J. Henman - Program Analyst, NOAA/GLERL
- Jon Grob – U. S. Coast Guard, Lake Michigan Sector
- Tom Graff – Michigan Department of Environmental Quality

Grand Valley State University – Michigan Alternative and Renewable Energy Center

- T. Arnold Boezaart – Director,
- Jim Edmonson – Project Manager, GVSU Contractor
- Silvia Dietrich – Administrative Assistant, MAREC

Grand Valley State University – Office of Sponsored Programs

- Christine Chamberlain – Director

Grand Valley State University – Office of Business and Finance

- Brian Copeland – Associate Vice President
- Pamela Brenzing - Controller
- Brenda Lindberg – Associate Controller
- Kim Patrick – Director of Procurement Services
- Michelle McCloud, Grants, Sr. Accountant
- Matti Sullivan, Grants, Sr. Accountant

Grand Valley State University - Seymour and Esther Padnos College of Engineering and Computing

- Paul Plotkowski – Dean
- Charlie Standridge – Professor and Assistant Dean
- Carl Strebel – Network Systems Supervisor
- Ira Woodring – Laboratory Systems Administrator
- Dave Zeitler – Professor, Statistics Department
- Mehmet Sozen – Professor
- M.M. Azizur Rahman – Professor
- Ron Grew – Lab Supervisor
- Bhakthavathsala Penumalli – Graduate Student
- Md Nahid Pervez – Graduate Student
- Divya Vermula – Graduate Student
- Tyson Spoema – Graduate Student
- Steve Taylor – Graduate Student
- Aaron Clark – Undergraduate Student

Grand Valley State University – Department of Biology

- Erik Nordman – Associate Professor

Grand Valley State University – Robert B. Annis Water Resources Institute

- Alan Steinman – Director and Professor

Dave Kendall – Research Assistant
Kurt Thompson, Research Associate
John Koches, Associate Research Scientist
Bopi Biddanda, Associate Professor

Grand Valley State University – University Libraries
Sarah Beaubien, Head of Collections and Scholarly Communications
Debbie Morrow, Liaison Librarian in Liberal Arts Programs
Max Eckard, Metadata & Digital Curation Librarian

AXYS Technologies and Optical Air Data Systems (OADS)
Fred Belen, OADS
Reo Phillips, AXYS
Graham Howe
Dan Shumuk
George Puritch
Yanis Gryshan

Other Universities
Brian Klatt - Director, Michigan Natural Feature Inventory, Michigan State University
Guy Meadows – Director, Great Lakes Research Center and Adjunct Professor, Michigan Tech University
Dave Jude – Research Scientist Emeritus, Natural Resources and Environment, University of Michigan
Russ Miller – Mechanical Technician, Cooperative Institute of Limnology and Ecosystems, University of Michigan
Frank Marsik – Associate Research Scientist, Atmospheric, Ocean and Space Sciences, University of Michigan
Aline Cotel – Associate Professor, Civil and Environmental Engineering, University of Michigan
Neel Uday Desai – Graduate Student, University of Michigan
Bruce Williams – Graduate Student, University of Delaware

Andrie Specialized
Phil Andrie
Seth Andrie
Leonard Zaug

Results and Discussion

Phases 1 and 2 were successfully accomplished with the selection of the WindSentinel floating MET buoy and deployment to multiple locations. Results show that floating LWS is a valid wind assessment technology and that floating MET facilities are the most economical and least invasive to the environment as compared to placement of fixed MET towers. Phase 3 was divided into four Milestones. Milestone One was achieved by conducting site research and desk-top studies to pick four anchorage sites. The results of Milestones Three and Four are described in brief here and in more detail in the attached papers. The results are divided into seven topic areas: Technology Validation; Wind Data Analysis; Data Management; Offshore Environmental Assessment; Social, Economic, and Policy Impacts Analysis; Outreach and Education, and; New Advancements in Technology.

Technology Validation

The accuracy of the wind data gathered by the WindSentinel equipment was validated and presented in the following report to be submitted to the International Journal of Energy and Environmental Engineering. The entire document can be found in Appendix A.

A Case Study of Laser Wind Sensor Performance Validation by Comparison to an Existing Gage

Charles Standridge (standric@gvsu.edu) Padnos College of Engineering and Computing, Grand Valley State University, 301 West Fulton, Grand Rapids, Michigan 49504 – Corresponding Author

Abstract

A case study concerning validation of wind speed measurements made by a laser wind sensor mounted on a floating platform in Muskegon Lake through comparison with measurements made by pre-existing cup anemometers mounted on a met tower on the shore line is presented. The comparison strategy is to examine the difference in measurements over time using the paired-t statistical method to identify intervals when the measurements were equivalent and to provide explanatory information for the intervals when the measurements were not equivalent.

The data was partitioned into three sets: not windy (average wind speed measured by the cup anemometers ≤ 6.7m/s) windy but no enhanced turbulence (average wind speed measured by the cup anemometers > 6.7m/s), and windy with enhanced turbulence. For the not windy data set, the difference in the average wind speeds was equal in absolute value to the precision of the gages. Similar results were obtained for the windy with no enhanced turbulence data set and the average difference was not statistically significant (□=0.01). The windy with enhanced turbulence data set showed significant differences between the buoy mounted laser wind sensor and the on-shore mast mounted cup anemometers. The sign of the average difference depended on the direction of the winds. Overall, validation evidence is obtained in the absence of enhanced turbulence. In addition, differences in wind speed during enhanced turbulence were isolated in time, studied and explained.

Conclusions

The coefficient of determination R2 has been commonly used in validation studies as the primary metric of equivalency between two gauges. However, this metric cannot identify periods of time when differences in the speed of winds measured by two gages occur. An approach for examining the time series of differences in wind speeds based on the paired-t statistical method has been shown to be effective in identifying and explaining time periods when significant differences in wind speeds were measured even when the overall R2 is greater than 99% and the comparison is constructed with ideal conditions.

This result provides the foundation for validating a LWS unit on a floating platform in Muskegon Lake by comparison to existing cup anemometers installed on a met tower on the shoreline which served as a calibrated and trusted gage. The data was partitioned into three sets: not windy (average wind speed measured by the cup anemometers ≤ 6.7m/s), windy but no enhanced turbulence (average wind speed measured by the cup anemometers > 6.7m/s), and windy with enhanced turbulence (again, average wind speed measured by the cup anemometers > 6.7m/s).

Validation evidence for the wind speed measures made by the LWS unit by comparison to the cup anemometer wind speed measurements were obtained as follows. The paired-t analysis for the not windy data set showed a difference in the average wind speeds of -0.10m/s, equal in absolute value than the 0.1m/s, the smallest value either gage will measure. The negative sign indicates slower wind speed over land as well as at a lower height, which is expected. Furthermore, the magnitude of the coefficient of variation is much greater than (1) indicating that differences in the observations made by the two data sets can be viewed as random variation. Similar results were obtained for the windy with no enhanced turbulence data set. In addition, the average difference was not statistically significant (□=0.01). Thus, credible evidence that the LWS unit could be trusted to provide reliable wind speed measurements was obtained.

The windy with enhanced turbulence data set showed significant differences between the two gauges. The sign of the average difference depends on the direction of the winds. Mean TKE was measured to be greater when flow was predominantly from over land versus when flow was predominantly from Lake Michigan into Muskegon Lake. The higher mean TKE for flow originating over land would likely be due to greater surface roughness experienced by the overland flow. Thus, there is a plausible foundation for the observed difference in average wind speed during enhanced turbulence.

Overall, validation evidence is obtained in the absence of enhanced turbulence. In addition, differences in wind speed during enhanced turbulence were isolated in time, studied and explained.

Wind Data Analysis

Characteristics of the Wind Profile

Data was analyzed on a monthly and yearly basis, including analysis of the difference between years. These individual reports can be found at the project report site http://scholarworks.gvsu.edu/marec/. A representation of a typical report is presented below. Complete reports are provided in the Appendices.

Lake Michigan Offshore Wind Assessment, 2012 Season Summary Report
Charles Standridge (standric@gvsu.edu) Padnos College of Engineering and Computing, Grand Valley State University, 301 West Fulton, Grand Rapids, Michigan 49504

This report summarizes the data collected by the Laser Wind Sensor (LWS) OADS Vindicator #8, mounted on an AXYS NOMAD WindSentinel with collection information as follows:

Location:	Lake Michigan – Mid-lake Plateau (4320.5100N 8707.2057W)
Date:	May 8 through December 17, 2012 (UTC)
Range Gates 1-6:	75, 90, 105, 125, 150, 175 meters
Cup Anemometer:	3 meters mounted on the buoy
Observations:	10-minute averages of wind speed and wind direction stored onboard the buoy

Quantities of Primary Interest: Average wind speed, variation in wind speed, and distribution of wind direction

Independent Variables: Range gate height, month, and location (versus 2011)

Number of Observations: 224 days at 6 observations per hour = 32256 observations

Missing Observations: 35 – (7/9 at 12:30-13:50; 7/24 at 11:10; 8/28 at 14:00 – 15:40; 10/23 at 18:40-18:50; 10/30 at 16:40; 11/8 at 13:10-13:20 and 14:00-15:20)

Good Observations:

32221 (99.9%)

Notes: All high resolution one second data for all wind speeds is stored onboard the buoy and can be used for further detailed post processing as required. Missing observations are those not reported by LWS #8.

Statistic	N001S007 P006 Cup Anemometer	N001S009 P083 75m	N001S009 P084 90m	N001S009 P085 105m	N001S009 P086 125m	N001S009 P087 150m	N001S009 P088 175m
Good Obs.	32216	30076	30951	30882	29265	21101	12226
% of Total (32256)	99.9	93.2	96.0	95.7	90.7	65.4	37.9
Average	6.2	8.7	8.9	9.0	8.9	9.2	9.5
Std. Dev.	3.1	4.7	4.8	4.8	4.9	5.2	5.0
Coeff. of Variation	0.50	0.54	0.54	0.53	0.55	0.57	0.53
Minimum	0.0	0.2	0.2	0.2	0.2	0.2	0.3
Quartile 1	4.0	5.1	5.3	5.4	5.1	5.2	5.7
Median	5.9	8.0	8.3	8.4	8.2	8.4	8.8
Quartile 3	8.2	11.6	11.9	12.0	11.9	12.4	12.5
Maximum	19.3	28.3	28.7	29.2	29.8	30.2	31.5
99% CI– Lower Bound	6.2	8.6	8.8	8.9	8.8	9.1	9.4
99% CI Upper Bound	6.2	8.8	9.0	9.1	9.0	9.3	9.6

Table 4: Horizontal Wind Speed (meters per second)

The report's findings are summarized below for wind speed and LWS performance.

Wind speed:

1. The variation in wind speed is approximately the same for each range gate height as shown by the coefficient of variation values in Tables 4 and 5.
2. The average wind speed is approximately 50% higher at the range gate heights than on the buoy deck as shown in Table 4.
3. The average wind speed in Table 4 generally increases with height. However, the number of observations tends to decrease with height.
4. Given #3, a better comparison of average wind speed is given for those 10 minute intervals where all averages

Statistic	N001S009 P083 75m	N001S009 P084 90m	N001S009 P085 105m	N001S009 P086 125m	N001S009 P087 150m	N001S009 P088 175m
Average	10.3	10.4	10.5	10.5	10.4	9.5
Std. Dev.	4.9	5.0	5.0	5.1	5.2	5.0
Coeff. of Variation	0.48	0.48	0.48	0.49	0.50	0.53
Minimum	0.2	0.2	0.2	0.2	0.2	0.3
Quartile 1	6.7	6.8	6.8	6.8	6.5	5.7
Median	9.7	9.9	9.9	10.0	9.7	8.8
Quartile 3	13.6	13.8	13.9	14.0	13.9	12.5
Maximum	27.3	28.4	29.2	29.8	30.2	31.5
99% CI– Lower Bound	10.2	10.3	10.4	10.4	10.3	9.4
99% CI Upper Bound	10.4	10.5	10.6	10.6	10.5	9.6

Table 5: Horizontal Wind Speed (meters per second) Statistics by Range Gate – All Range Gates with Good Observations (12154/32256= 37.7%)

contain 300 or more 1-second observations. These results are shown in table 5. A comparison of average wind speed between adjacent range gate heights where each average in the pair contains 300 or more 1-second observations is shown in table 5. These results indicate that average wind speed increases between 75m and 105m; levels off and perhaps begins to decrease between 105m and 125m; and continues to decrease up 175m. All differences are statistically significant ($\alpha = 0.01$).

LWS Performance

1. Overall, the LWS made observations for 99.9% of all 10 minute intervals.
2. The number of good observations decreases with height above 90m. Since the LWS relies on detecting particle movement in the airflow, this may be due to a lack of such particles at the mid-lake plateau as height increases that is cleaner air. In addition, there is less mixing of the air layers in the mid-lake versus near shore resulting in less movement of particulate matter.
3. The average wind speed for each range gate shown in table 3 is higher than the corresponding average in Table 4, except for 175m where the two averages are the same. This indicates that observations at 175m are only made at higher wind speeds, which is consistent with reaching the outer observation limits of the LWS.

Table 6 shows the energy generated for each range gate. The amount of energy generated depends on the turbine employed, in this case the Gamesa Elioca G58 850kW. The energy estimate was computed assuming that the turbine will always face the wind.

	All data		Every Range Gate with Good Obs.	
Range Gate	Average Power (MW)	Average Daily Energy (MWh)	Average Power (MW)	Average Daily Energy (MWh)
1	0.414	9.95	0.522	12.54
2	0.429	10.30	0.525	12.60
3	0.431	10.35	0.525	12.59
4	0.418	10.04	0.520	12.48
5	0.426	10.23	0.505	12.11
6	0.425	10.20	0.455	10.93
Buoy Cup	0.248	5.96	0.248	5.96

Table 6: Energy (kWh/time unit) by Range Gate

Discussion points:

1. For each of the heights, the largest average wind speed is in October due to the residual effects of a hurricane Sandy in the Atlantic Ocean.
2. The general pattern in average wind speed is a decline from May through August and increase from September through December, disregarding the October value as discussed in point one. This pattern is also seen in the median values.
3. The difference in average wind speeds for May and June is not statistically significant ($\alpha = 0.01$) for heights: 75m, 90m, 105m, and 125m but is statistically significant for heights 150m and 175m.

4. The difference in average wind speeds for June and July is statistically significant (= 0.01) for all heights.
5. The difference in average wind speeds for July and August is not statistically significant (= 0.01) for height 175m but is statistically significant for heights 75m, 90m, 105m, 125m and 150m.
6. The difference in average wind speeds for August and September is not statistically significant (= 0.01) for height 175m but is statistically significant for heights 75m, 90m, 105m, 125m and 150m.
7. The difference in average wind speeds for November and December is statistically significant (= 0.01) for all heights.
8. The average wind speed pattern based on points 3 through 7 is level average wind speed in May and June, a large drop in average wind speed in July from June, level average wind speed in July and August, and increasing average wind speed starting in September with the average returning to May levels by December.

Wind Direction by Height

The wind rose graphs show the wind speed by direction as well as the percent of time the wind was blowing in each direction. The percent of time the wind was coming from a particular direction is shown by the inner and outer circles. For range gate one, the inner circle represents the wind coming from a particular direction 4% of the time and the outer circle 9% of the time.
Note that for each height, the dominate wind direction is SSW, Figure 7.

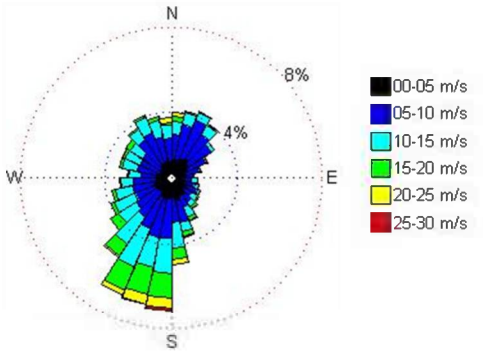

Figure 7 –Average wind speed and direction, mid-lake plateau.

Discussion Points:

1. The predominant wind direction from May through December is SSE-SSW, except for September when the predominant wind direction is NNW-NNE. This is true for heights 75m through 125m and the buoy deck. For these heights, the percent of good observations exceeded 90%.
2. For the heights where the percent of good observations was less than 90%, 150m and 175m, the predominant wind direction is SSE-SSW in September as well. As was discussed in the section on average wind speed by height, this may have to do with the performance of the LWS.
   Discussion points:
3. The difference in average wind speed at range gate heights 75m, 90m, 105m, and 125m is not statistically significant (= 0.01).
4. The average difference at heights 150m and 175m is statistically significant (= 0.01).

5. The average wind speed at 150m and 175m is decreasing with height in 2012 and increasing in 2011.

Overall, the difference in mean wind speed between mid-lake and near shore locations is no more than 10%. Thus, if mean wind speed differences are further verified, the additional cost of a mid-lake installation would need to be balanced against the apparent 10% or less energy output differential . The best height for wind at both locations is 105 meters. Overall, the LWS made observations for 99.5% of all 10 minute intervals. For heights 125m, 150m, and 175m, the percent of good ten minute averages is greater at the near Muskegon location than at the mid-lake location. Since the LWS relies on detecting particle movement in the airflow, this may be due to a lack of such particles at the mid-lake plateau versus near shore as height increases. In addition, there is less mixing of the air layers in the mid-lake versus near shore resulting in less movement of particulate matter.

Conclusions

The differences in the mean are comprised of two components -- difference due to year and difference due to location. The differences are all less than 1m/s and most are less than 0.5m/s.

The difference due to year is estimated by the difference in wind speed on the surface measured by NOAA buoys. Both for the mid-lake and near Muskegon, this difference is 0.3 m/s slower in 2013.

This implies that the difference due to location is actually less than the difference in the average 2012 to 2013 wind speeds.

The data are consistent with the following statement:

Locating a wind turbine farm in the Lake and near Muskegon will result in an approximate 5% energy loss versus locating the same wind turbine farm mid-lake.

This in addition to the data indicating that there is minimal energy loss from using lower in height wind turbines (105m - 125m at the center).

Wind Energy Assessment using a Wind Turbine with Dynamic Yaw Control

Md Nahid Pervez. Padnos College of Engineering and Computing, Grand Valley State University, 301 West Fulton, Grand Rapids, Michigan 49504. April 2013. – A Thesis Submitted to the Graduate Faculty in Partial Fulfillment of the Requirements For the Degree of Master of Science in Engineering, School of Engineering.

Conclusions

This project was conducted to assess the wind potential over Lake Michigan. Wind data was collected at 1 Hz frequency at six different altitudes within the range of 55m-175m at different locations over the entire project period. The data as collected by state-of-art LIDAR sensor mounted on an GVSU's WindSentinel .

A thorough literature review was performed to develop an accurate methodology to analyze the collected wind data and assess the wind potential over Lake Michigan. From the literature review it was determined that the publicly available estimation techniques overestimate the energy output because of not considering the effect of yaw error and dynamic yaw motion in the estimation process. Therefore, a dynamic mathematical model was developed capable of considering the yaw error and dynamic yaw motion in the estimation technique.

This model required a quality controlled continuous stream of daily data set. However, the collected data were at 1 Hz frequency and had some issues such as missing data and time stamps, unnecessary columns, and unrecognized characters in the data set. A refining module for this unrefined data set was developed to address these issues. An averaging module was also developed to average the data set over 30 sec, 1 min, 2 min, 5 min, and 10 min to observe the effect of data set frequency on the energy output. To represent the dominant wind direction and time duration of wind blowing in different wind directions, a wind rose generating model was developed. A wind frequency generating module was also developed.

The dynamic model was developed in such a way that the effect of yaw control can be included or disregarded in the calculation. If the yaw error is disregarded then the results should be same as the INL wind energy model. The dynamic model was validated by comparing a test data set results with the INL wind energy model. For validation process the effect of yaw error was not considered and the dynamic model generated same results as the INL wind energy model with the same data set which confirms the validity of the MATLAB code developed.

The effect of the two important parameters of the dynamic model, yaw rate and delay time, on the energy output was analyzed. The results suggested that the turbine generated more energy if the yaw rate of the turbine increased. Up to 0.05 deg/sec yaw rate the energy increased sharply. Later the increase was not that significant. The effect of delay time was quite unpredictable. The only conclusion that can be drawn is that the turbine generated highest energy at the minimum delay time which is equal to the time step of the data set.

The findings of the dynamic model were then compared with the INL wind energy model. The INL wind energy model overestimated the output energy. The amount of overestimate depends on the time frame of data as the energy is dependent on the time frame of the data set. For the mid-lake deployment the INL energy model overestimated the output energy by 7% at 75 m altitude. The reason for this was that the INL energy did not consider the yaw misalignment in the energy estimation. The dynamic model results were also compared with the other estimation techniques. The results showed that the turbine used for calculation (Gamesa Eolica G52-850 kW) could harness about 24% of the

available wind energy during the mid-lake deployment at 75 m of hub height. The other locations and hub height results were also very close to this.

The dynamic model was a turbine specific estimation technique like INL wind energy model, polynomial model, and one two three equation model. To observe the effect of turbine model on the estimated output energy another turbine, Lagerwey LW72-2000 kW, was used. The energy output was doubled by using this turbine because the turbine was larger in size and had higher rated power output. However, the turbine harnessed about 26% of the available wind energy. The effect of the time step of the data set was also analyzed by using different time averaged data set. The results showed that longer time averaged data sets overestimated energy by small amounts.

The capacity factors of the turbine used in dynamic model (Gamesa Eolica G58-850 kW) were also calculated. The capacity factor varied from 35%~40% for different altitudes and different deployment locations. Note that, the capacity factor calculated was for only a single turbine. A wind farm consists of a large of number of wind turbines. Some of those wind turbines may have a lower capacity factor than the other turbines in that wind farm due to maintenance and unavailability of wind resource. While calculating the capacity factor of the entire wind farm the capacity factors of individual turbines are averaged. Therefore, for an entire wind farm the capacity factor is generally lower than the capacity factor of an individual turbine. The wind roses provided a good representation of the prevailing wind direction and wind speed. The frequency distributions for different deployments and different altitudes were also generated.

The dynamic yaw control model predicted that the potential energy output from the Gamesa Eolica G58-850 kW would be about 7% lower than the prediction of the INL wind energy model for the mid-lake deployment of the Wind Sentinel. Of course it does not take into account the power that goes into the dynamic control of the turbine.

Boundary Layer Analysis

Great Lakes Wind Energy Analysis of Turbulence and Temporal Averaging Time Constants
Neel Desai. University of Michigan, Ann Arbor

- Investigated the possible causes of the observed periods of high Turbulence Kinetic Energy (TKE).
- Observed that the TKE values seem to co-relate better with wind speeds rather than wave heights.
  - Stability
  - Time required for wave development at a given wind speed and fetch
- TKE values determined using Wind Sentinel Observations.

- TKE contours were compared with wind speed data obtained from GLERL buoy (MKGM4), as well as from the cup anemometers on the WindSentinel Buoy.
- Enhanced TKE periods correspond to elevated surface winds from buoys.

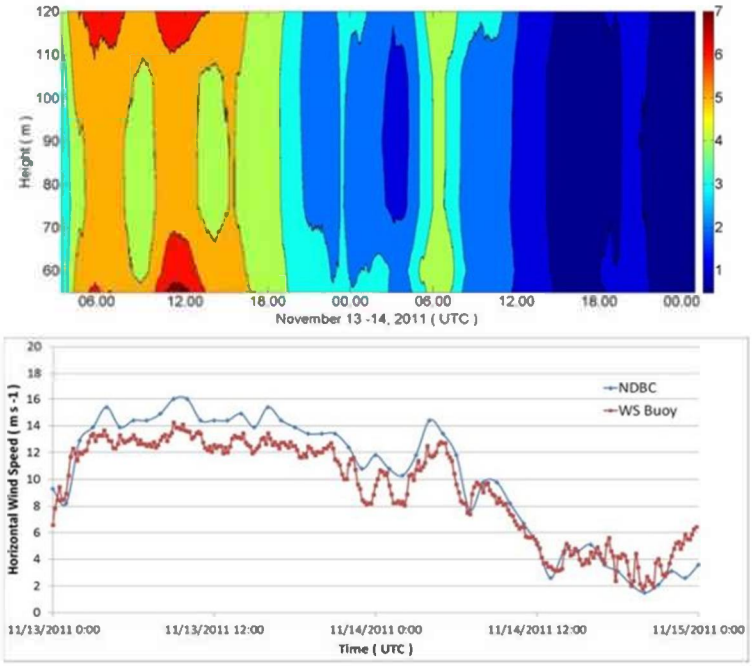

Figure 8 – Turbulence Intensity, 30-second averaging.

Vertical profiles of mean turbulence intensity and kinetic energy were calculated as follows. The instantaneous velocity in three directions (u, v, w, respectively) can be decomposed into average (U, V, W) and fluctuating components (u', v', w'). The average velocity information will be used to determine the vertical profile while the fluctuating component will help determine the effect of turbulence on the overall dynamics, including additional energy generation and gust response. The average velocity and the fluctuating velocity components are often combined in a simple non-dimensional derived turbulence parameter, Turbulence Intensity (TI), where TI in the x direction can be defined as:

$$TI_x = \frac{u'}{\sqrt{U^2 + V^2 + W^2}}$$

Similarly, the Turbulence Intensity can be defined for the other two directions. TI characterizes the amount of turbulent fluctuations with respect to the average resultant velocity. However, if the average velocity is low, TI can appear to be artificially large. In some situations, it is an appropriate measure of turbulence while in others, focusing only on the fluctuations is more relevant.

Understanding that the velocity fluctuations are important in order to accurately monitor and predict wind turbine responses to wind gusts, another parameter commonly used to quantify turbulent flows is the Turbulence Kinetic Energy (TKE), which measures the increase in kinetic energy due to turbulent fluctuations in the flow and is defined as:

$$TKE = \frac{1}{2}\left(u'^2 + v'^2 + w'^2\right)$$

The energy associated with any velocity occurring at a given length scale is proportional to the square of the magnitude of the velocity. Since TKE quantifies the additional energy in the flow due to its turbulent nature, it could help identify areas of increased wind energy potential, as long as time scales associated with the increased TKE are appropriate.

Wind Gust Analysis / Gust Frequency Analysis

Bruce M. Williams, University of Delaware - May 2013

The first analysis was conducted to determine if, and how often. The wind speed ramp rate exceeded the ability of the pitch rate to keep up and maintain optimal pitch. An algorithm was written and run in "C" programming language which estimates the frequency of ramp events by durations and accelerations using a moving time window. As an example, results for a 4 second window are shown in *Figure 9*. The horizontal axis represents the acceleration of the wind, from -1.5 m/s per second to +1.5 m/s per second (pos. and neg. around zero at center), and the vertical axis is the number of occurrences. The highest frequency belongs to the lowest acceleration rates, and the tails belong to the largest acceleration rates.

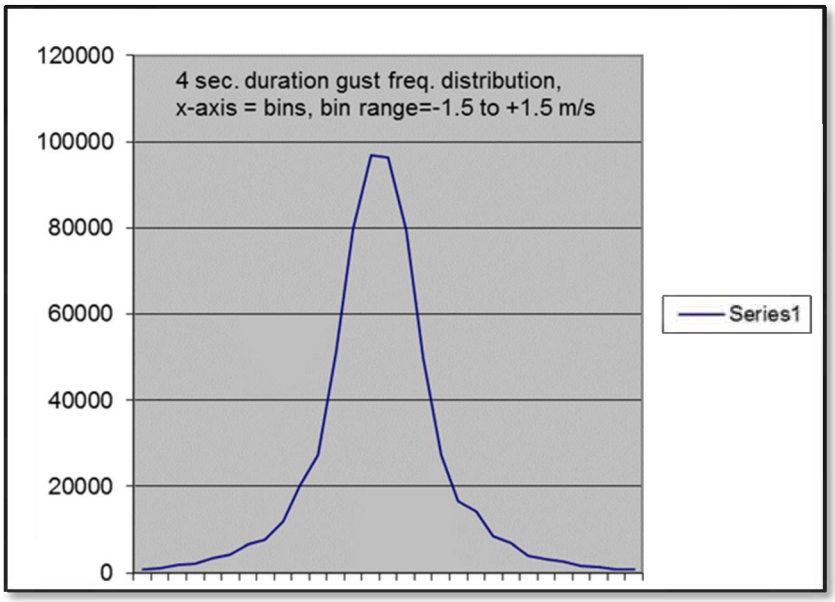

Figure 9 - Wind Acceleration Frequency Distribution for a 4 Second Averaging Time. Acceleration range is from -1.5 m/s/s to +1.5 m/s/s. .

Although this analysis has high levels of uncertainty, and is based on data from Lake Michigan, not the study area, it does not show any evidence of significant gains in AEP from this methodology of pitch control. This agrees with other simulation studies reviewed, which found no direct, significant increase in power production through LIDAR assisted pitch control. Further research is warranted to confirm or revise this observation. However, the reduction in fatigue loading is confirmed by several studies, and can be monetized, as discussed in the following sections.

Data Management

The WindSentinel system collects, maintains, and can communicate over 300 fields of data covering the physical environment above and below the water service as well as bird and bat activity.

These data are reported in 21 messages in either 1 hour, 10 minute, or 1 second intervals. The management of such information falls within range of what is called "big data". This data can be sent wirelessly by cell phone or satellite services. Cost for transmission of data by satellite is prohibited; therefore 10 minute average data was transmitted by cell phone CMDA card. Other data was stored on an on-board flash card and physically retrieved every 4-6 weeks. When the WindSentinel is out of cell phone range, all data was physically retrieved at the same intervals of time.

Table 7 – Data Management Structure

Once retrieved, whether by wireless transmission or physically, the data is entered into two systems. The data is organized as shown in Table 7 and stored on the GVSU server for future use.

Data is also placed in the buoy manufacturer's proprietary software interface, Smartweb, Figure 10. This allows real time access of the 10 minute average data within about 15 minutes of the last reading. Historical data can also be retrieved.

Requests for data from third parties outside GVSU RLT will be able to access and retrieved data through a time sensitive data retrieval web portal.

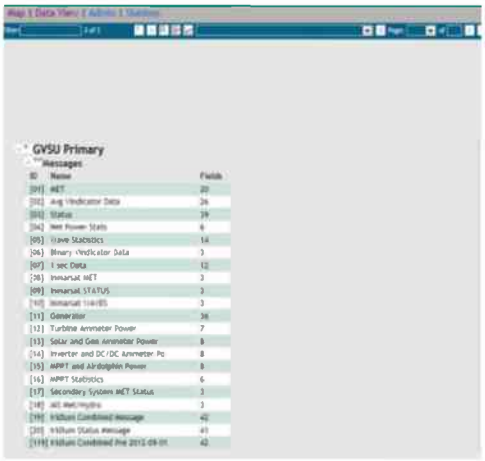

Figure 10 - Screen shot of the Smartweb data portal interface.

With large amounts of data to analyze, it was important for the RLT to identify and test the use of powerful data software. The following abstract describes the use of SAS as presented at the Global Forum, Washington, D.C. March, 2014:

Visualizing Lake Michigan Wind with SAS® Software
Aaron C Clark and David Zeitler, Grand Valley State University. SAS Global Forum, March 22-26 in Washington D.C.

ABSTRACT

A wind resource assessment buoy, residing in Lake Michigan, uses a pulsing laser wind sensor to measure wind speed and direction offshore up to a wind turbine hub-height of 175m and across the blade span every second. Understanding wind behavior would be tedious and fatiguing with such large data sets. However, SAS/GRAPH® 9.4 helps the user grasp wind characteristics over time and at different

altitudes by exploring the data visually. This paper covers graphical approaches to evaluate wind speed validity, seasonal wind speed variation, and storm systems to inform engineers about the energy potential of Lake Michigan offshore wind farms.

In some experimental high altitude cases, the LWS struggles to collect consistent and validated wind speed records due to lack of reflective particulates and movement of existing particles in the atmosphere over the open water. Data quality indicators provided by the LWS vendor have proven to flag relatively good data as bad. Therefore, before exploration of seasonal and storm activity on the lake for a turbine-friendly assessment, we need to ensure we are examining all valid data values. Visualizing the state of these data using SAS® 9.4 will prove useful to identify "bad data" and inform an algorithm to sort it from the "good data." For example, at times, reported wind speeds are too constant or too extreme to be real.

Our solution utilizes a 5-second moving window standard deviation (5-sec stddev). This statistic satisfies our need for a quantitative measure of variability because the window is short enough to measure delicate spikes in wind and long enough to be conservative about how long wind can remain constant.

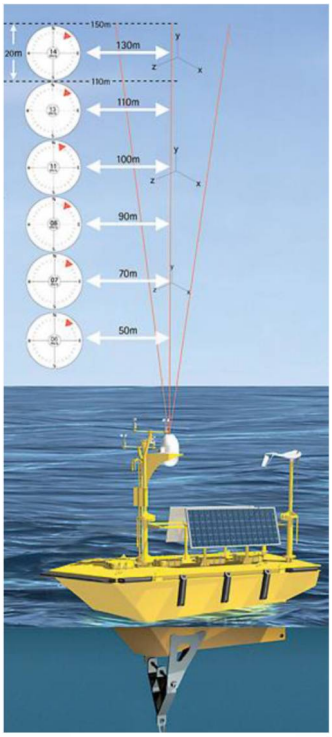

Figure 11 - WindSentinel wind data range gates

Offshore Wind Environmental Assessment

To determine suitable site locations for ultimate construction of offshore wind energy sites that are the least detrimental to aquatic organisms and birds and bats, it is necessary to evaluate potential effects based on distribution of habitat, current communities in the area, and passage of transient populations.

Aquatic Environment Data Collection and Results

The original intent before the loss of State of Michigan research funding was to compile data on aquatic habitat including substrate and bathymetry and to produce related maps. Compile and evaluate available data on benthic macro-invertebrates, zooplankton, larval, juvenile, adult fish; bats and birds. And, to collect invertebrate, zooplankton, and fish data at the buoy sites to complement ongoing or past studies and to characterize conditions at the site. Due to the loss of research funding during the project, data and sample gathering was limited to: 1) anchorage site sampling; 2) water quality data; 3) bird and bat data collection, and; 4) a sound propagation study. A summary of the results are below.

AWRI Summary Report of Water Quality Data from Wetlab's WQM Sensor on board GVSU's Windsentinel Buoy during 2012 and 2013.

Scott Kendall, Bopi Biddanda, Alan Steinman. Annis Water Resources Institute, Grand Valley State University, Muskegon, MI 49441. April, 2014.

During the 2012 and 2013 deployments of the Windsentinel buoy, an onboard Wetlab's Water Quality Monitor (WQM) collected data on several core parameters important for monitoring water quality in Lake Michigan surface waters. Data were collected from May-December in 2012 and April-December in 2013 at 10 minute intervals for conductivity, temperature, sensor depth, dissolved oxygen (2012 only), chlorophyll fluorescence and turbidity. Seasonal patterns of these parameters in Lake Michigan were observed at the Mid-Lake Plateau location in the central basin of southern Lake Michigan during 2012 and the near shore location near Whitehall, Michigan during 2013.

In summary, these data show seasonal trends during the April-December months at the 2012 mid-lake plateau and 2013 coastal locations. The data also allow for a general comparison between the sites, albeit in different years. More effort is needed to determine if the mounting location of the WQM in the WS moon pool is impacting data quality through such artifacts as bio-fouling of the buoy hull.

Avian Environment Data Collection and Results

Offshore Bat and Bird Activity at the Lake Michigan Mid-lake Plateau, Considerations for Wind Energy Development

Klatt, B. J., T. A. Boezaart, J. L. Gehring, K. Walter, and J. Edmonson. 2014. Offshore Bat and Bird Activity at the Lake Michigan Mid-lake Plateau – Considerations for Wind Energy Development. Michigan Natural Features Inventory, Michigan State University, Report Number 2014-XX, Lansing, MI.

Many offshore areas of the Great Lakes are believed to possess wind resources adequate for the efficient generation wind energy. However, this supposition is based on modeling of onshore winds projected out into the lakes. To better assess the actual wind resources available, the Michigan Alternative and Renewable Energy Center (MAREC) of Grand Valley State University assembled a team of researchers to study the issue of offshore wind energy development. The team oversaw the design and construction of a research buoy that included instrumentation to assess a variety of offshore conditions, including actual wind speeds at various assumed wind turbine hub heights. As a member of the MAREC team, the Michigan Natural Features

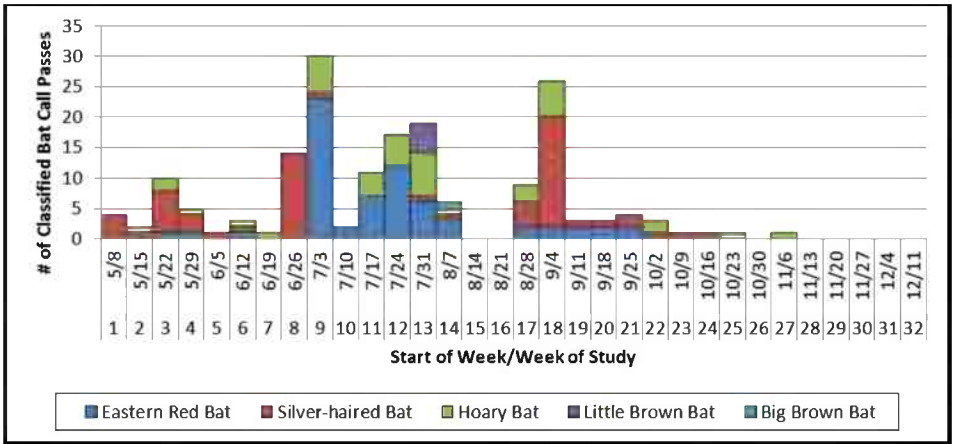

Figure 12 - Number of Classified Bat Calls by Study Week, 2012

Inventory (MNFI) of Michigan State University installed acoustical monitoring instrumentation on the buoy to monitor bird and bat activity over the lake. The buoy was deployed at the Mid-lake Plateau of Lake Michigan during the period of April to December 2012.

During the deployment, bat activity was assessed by monitoring for bat echolocation calls from one half hour before sunset until one half hour after sunrise, using a SM2Bat+ monitor, recording in full spectrum. Recorded calls were analyzed using Sonobat software, which attempts to classify bat calls as to species based on over 60 call characteristics. 177 calls were classified to species, with 3 species accounting for the majority of the calls; the eastern red bat, silver-haired bat, and hoary bat; each accounted for approximately 40-60 calls, Figure 12. Calls from the little brown bat and the big brown bat were also represented in the recordings. The distribution of calls throughout the deployment indicate that there is a fairly steady level of bat activity over the lake throughout the spring, summer, and fall months, with the last bat call recorded at the end of October. This is the first known systematic documentation of bat activity in far offshore (over the horizon) areas of the Great Lakes.

Bird activity was monitored during daylight hours, also using the SM2Bat+ monitor. The bird call recordings were analyzed using Raven software. A total of 2773 bird calls were classified with the majority (2697) being identified as gulls, Figure 13. Also represented were Forster's Tern, Red-winged Blackbird, and American Goldfinch; 36 calls could not be identified beyond general groups (e.g. passerine). All non-gull calls were recorded by early June, after which bird activity remained constant but low.

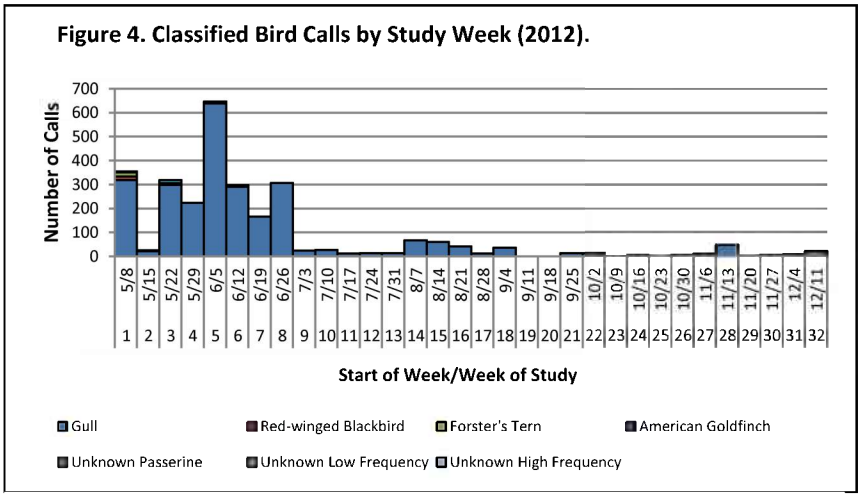

Figure 13 – Classified Bird Calls

Sound Propagation Analysis

Estimating sound levels from a hypothetical offshore wind farm in Lake Michigan

Erik E. Nordman, Ph.D. Grand Valley State University, Allendale, MI. 2014.

Operating wind turbines generate sounds from the rotating blades and electrical components. The sound from operating land-based turbines, and its potential impacts, has been thoroughly studied but the sound from offshore wind turbines has received less attention. This paper seeks to review the

existing literature on sound propagation from offshore wind farms and estimate the potential sound impact on coastal residents and beachgoers from a hypothetical offshore wind farm in Lake Michigan, USA. The paper focuses on the airborne sound propagation from operating turbines. Sounds from the construction and decommissioning phases, as well as underwater sounds, are beyond the scope of this project, but are important considerations for wind farm developers.

The hypothetical wind farm was composed of Vestas V90 3 megawatt (MW) turbines. This turbine model is in use at several European offshore wind farms. Two project configurations were considered: a single row of five turbines and two rows (offset) of five turbines each. In both scenarios, the turbines were spaced 800 meters apart within and between rows. Vestas 90 turbines have a broadband sound power level at the source of 109.3 dB(A).

Sound propagation from offshore wind turbines was estimated using sound models in the WindFarm software package. WindFarm includes two industry-standard sound propagation models: one from the Danish Ministry of the Environment, National Agency for Environmental Protection (henceforth referred to as the Danish model); and the International Organization for Standardization (ISO 9613 Parts I and II, henceforth referred to as the ISO model).

Both the Danish model and the ISO 9613 model were used to estimate sound propagation from the hypothetical offshore wind farm in Lake Michigan. Researchers have noted that the ISO 9613 model is more accurate for calculating air absorption of sound. Utility association guidelines for assessing sound impacts also recommend using the ISO model.

Baseline sound data were recorded using an industry-grade sound level meter. The microphone was mounted on a 2 meter stand outside of Great Lakes Environmental Research Laboratory near the beach. Sound levels were measured from 14 November 2014 to 25 November 2014. On 17 November, however, the study site experienced an intense thunderstorm with a tornado watch. The sound monitoring equipment was dismantled on 17 November and restarted on 19 November. This analysis is based on the post-storm data set. L_{AS90} is the A-weighted sound level that is exceeded 90% of the time is an appropriate estimate for background noise at the receiving site. The background noise at the receiver site (outside GLERL) during the study period was L_{AS90}=49.5 dB(A). Short-term sound measurements (~1 minute each) were taken right at the beach on a calm day. The lowest L_{AS90} reported during these short measurements was 47.4 dB(A) during which the 10 minute average wind speed was 3.9 m/s. The location of the short term measurements was about 10 meters closer to the water than the long-term measurements at the GLERL site.

The sound level under average wind conditions for November 2013 (11.6 m/s at 125 m) from the ten turbine configuration, ISO octave model, was 23.4 dB(A).

The background sound level (L_{AS90}) during the study period was 49.5 dB(A). The ten turbine configuration, under the most extreme wind conditions measured during the study period, produced a

sound level at the receiver of 39.0 (ISO model). Under these conditions, the sound produced by the turbines would not be audible above the background noise (L_{AS90}) at the GLERL site. Only 0.89% of the sound observations during the study period fell below 39.0 dB(A). It is possible, but unlikely; that such conditions would occur it is extremely windy at the turbine site and very calm at the receiving site at the beach. The scenario presented here is a worst-case scenario and under these conditions the turbine sounds are masked by the background noise.

Winds are generally calmer in the summer months when people spend more time at the beach. The GLERL daily average data indicate that summer (Memorial Day to Labor Day) wind speeds average 4.4 m/s. The wind measurements on the calm November day averaged 3.9 m/s which is similar to a calm summer day. The background sound level (LAS90) right at the beach was 47.7 dB(A). This suggests that even under calm summer-like conditions, wind turbines sounds will not be audible above the background noise. Additional data are needed to understand the background noise levels at coastal locations during the summer months.

Social, Economic, and Policy Impacts Analysis

Behavioral approaches to environmental policy analysis: a case study of offshore wind energy in the North American Great Lakes

Erik Nordman, Natural Resources Management Program, Biology Department, Grand Valley State University, Allendale, Michigan 49401, 2014.

Abstract

Behavioral economics, including prospect theory, offers new approaches to environmental policy analysis. The utility of behavioral approaches to environmental policy analysis is illustrated using a case study of offshore wind energy policy in Michigan, USA. Michigan has attempted to clarify the permitting process for offshore wind energy but those efforts have failed. Prospect theory suggests that Michigan legislators are, for the most part, risk averse to policy reforms as the state emerges from its "one-state recession" and into a gains domain. Legislators from some coastal districts perceive offshore wind development as a threat to coastal quality of life, are risk-seeking for policy reforms, and have introduced bills banning offshore wind energy. Framing the discussion from a loss perspective (losing out to competing states) may be an effective strategy for passing offshore wind policy reforms. Results suggest behavioral approaches have utility for other environmental policy challenges, such as climate change.

Conclusions

Behavioral approaches to environmental policy analysis are gaining traction. Though the standard rational choice model of policy actors, including consumers, works well in most cases, environmental economists and policy analysts have catalogued "behavioral failures" in which actors do

not make optimizing choices. While the research focus so far has been on consumers of environmental goods and services, behavioral approaches, including prospect theory, can apply to the actions of policy-makers as well. We have illustrated the utility of the behavioral approach to environmental policy analysis using a case study of offshore wind energy in Michigan's Great Lakes. Our results also suggest that behavioral approaches may be useful for analyzing other environmental policy challenges, including climate change and fracking.

Michigan has outstanding offshore wind energy resources but lacks a clear policy framework through which the private sector can access the state-owned lake bottomlands. While offshore wind energy is not prohibited, the regulatory uncertainty provides a strong disincentive toward such infrastructure investments. Attempts to clear the regulatory hurdles have failed to pass through the state legislature and there seems to be little enthusiasm to sponsor a bill that would facilitate offshore wind energy development in Michigan. On the other hand, several bills have been introduced that would ban offshore wind energy development from Michigan's Great Lakes. Prospect theory can explain some aspects of this policy paralysis. The benefits of offshore wind energy – particularly in reducing air pollution from other generating sources – accrue to a broad range of residents inside and outside Michigan, while the potential, but uncertain and relatively smaller, property value and aesthetic impacts accrue to a particular constituency. There is little incentive for a legislator to advocate for offshore wind energy policy and strong incentives for particular legislators to advocate a ban. Prospect theory's emphasis on risk aversion, status quo bias, and framing add to the explanation and offer ways forward.

We offer several approaches for moving the policy discussion forward. Framing the issue from a loss domain – such as losing out to neighboring states on an emerging industry – could encourage voters and legislators to be more open to the regulatory reform needed to facilitate offshore wind energy development in Michigan's Great Lakes. Framing the policy reform from a gains domain requires the potential for a large, rather than incremental, benefit. The reform would need to go beyond simply permitting to perhaps an industrial policy aimed at making Michigan the Great Lakes hub for offshore wind energy. Regional collaborative approaches, from a federally coordinated MOU to a multi-state compact, could encourage Michigan to adopt a coherent, basin-wide offshore wind permitting system. A ban on offshore wind energy (and associated research) has been proposed but does not, at the moment, have much support. However the uncertainty surrounding Michigan's offshore wind energy permitting system discourages investment and the status quo may be as good as a ban.

The behavioral turn in environmental policy analysis is just beginning. Additional empirical evidence is needed from natural and laboratory experiments to advance the field. Our research, as well as that of others, suggest that prospect theory holds promise for understanding how individuals, whether consumers, citizens, or policy-makers, make decisions under conditions of uncertainty. The 20th century generation of energy infrastructure was built largely without much public input. The 21st century transition to low-carbon, distributed energy systems is happening with a large degree of public input, making the need for a behavioral approach to policy analysis that much greater.

Table 8: Key permitting actions, actors, and statutes regulating offshore wind energy development in Michigan's Great Lakes.

Action	Major Actor	Statute	Coordinating actors
Review and issue Joint Permit	MDEQ	NREPA Part 325	MDNR
	USACE	R&HA, CWA, NHPA	
Issue bottomland lease	MDEQ	NREPA Part 325	MDNR
Conduct EA/EIS	USACE	NEPA	EPA
Issue Notice of Proposed Construction	FAA and MDOT	MI Tall Structures Act, FAA 14 CFR 77	
Issue Permit for Private Aids to Navigation	USCG	33 CFR 64, 66. 67	USACE
Issue Certificate of Public Conveyance and Necessity	MPSC	PA 30 of 1995	FERC
Issue zoning permit for onshore transmission	Local planning and zoning boards	MZEA	

Outreach and Education Programs

The RLT developed an outreach and education strategy with suitable materials to explain the project and educate the public about offshore wind technology development. Publications describe use of the research facilities, instrumentation, and use of new data to advance offshore wind technology on the Great Lakes. Information is broadly shared at wind industry and wind sector collaborative gatherings and with the general public through web site postings. The RLT also assisted in identifying other potential users of the research facilities including state and federal agencies.

A project video, PowerPoint, and handout presentation on the WindSentinel/Vindicator buoy was prepared for distribution on web sites, Facebook, twitter, and others. And, a project poster and handouts prepared for schools and civic clubs.

Prepare class materials on wind assessment techniques, thermo-flow dynamics; and engineering impacts of wind and Great Lakes climate on turbine design, energy output, placement, and fatigue for PCEC and CLAS instructional material development.

Course Title: EGR 406 -- Renewable Energy Systems: Structure, Policy and Analysis

The new general education program requires each student to take two courses in global issues at the junior / senior level. See http://www.gvsu.edu/genedresources/faq-s-34.htm for some more information. EGR 406 will be one such course, offered for the first time in winter 2014.

Course Objectives

Upon successful completion of this course students will be able to:

1) Explain current renewable energy systems.
2) Apply basic knowledge of the technological and public policy issues in renewable energy.
3) Analyze current as well as future renewable energy approaches and strategies.

Course Topics

1) Overview of energy systems including definition of renewable energy and comparison with conventional energy; Introduction to working in teams -- 1 week
2) Energy and society: legal issues, public policy issues, economic issues, and social issues—1 week
3) Renewable solar energy systems – 1 week
4) Renewable wind energy systems: land based and water based – 2 weeks
5) Renewable hydroelectric and other water-based energy systems –2 weeks
6) Energy systems research and analysis: planning and procedures -- 1 week
7) Renewable biomass energy systems – 1 week
8) Geothermal, hydrogen and other renewable energy systems -- 1 week
9) Energy storage and distribution systems including advanced battery technology, distributed energy production, and net zero draw from the electric grid -- 3 weeks
10) Student Presentations – 1 week

Methods of Evaluation

1) In-class assessments (weekly quizzes) 10-20%
2) Reflective journals with weekly entries 10-20%
3) Homework including calculations 10-20%
4) Research Paper & Presentation (1) 10-20%
5) Analysis Project (1) 10-20%
6) Response to peer research and analysis presentations (1 or 2) 10-20%
7) Comprehensive final examination 20-30%

Accomplishments, Conclusions, and Recommendations

New Advancements in Technology

The most notable technology advancements for this project include: demonstrated use of floating LWS LIDAR with motion compensation; the use of recording equipment to inventory birds and

bats far offshore, and; management techniques for "big data". The GVSU WindSentinel was the first such device deployed in U.S. waters. A large element of the project was to assess the capabilities and vulnerabilities of the technology and all on board systems and to validate the accuracy of the captured wind data. The project was also the first attempt to detect the presence of bird and bat activity in offshore locations without the aid of aircraft. Project implementation also coincided with the emergence of "big data" management issues of government, universities as well as business andindustry. Collection and management of WindSentinel data contributed significantly not only to GVSU's capacity to manage big data growth, but also in support of specific industries. These accomplishments are discussed in further detail below.

Despite the $1,000,000 loss of research dollars from the MPSC, the project achieved a great deal thanks to the generous pro-bono support of individual researchers and their institutions. The project successfully demonstrated and validated the use of floating, motion compensated LWS, LIDAR for collection of wind data in remote offshore locations. The project also produced the first ever hub height site specific offshore wind data assessments for the Great Lakes over the course of two research seasons. The success of the GVSU Lake Michigan Offshore Wind Assessment project has led to the use of the WindSentinel system in a number of locations around the world. The collection of offshore wind data using floating platform technology and incorporating laser pulse technology was the first for Lake Michigan and the Great Lakes. The data increased the depth of knowledge about the wind characteristics of Lake Michigan and the logistical aspects of conducting offshore wind assessments on the Great Lakes. It was determined that sufficient wind does exist over the Great Lakes to generate substantial energy resources; wind turbines only need to be 100 meters off the water surface for optimal wind energy generation; and wind turbines will most likely be deployed on floating platform structures.

Other major findings include the results of a sound propagation study which determined that normal background noise levels at the shoreline edge would exceed the noise emanating from a commercial scale wind farm 5 miles offshore. Key environmental data was gathered that adds to the scientific body of knowledge and will be of considerable interest to future wind developers when in-depth site development studies commence and leasing and permitting processes are initiated. An update on policy impacts of offshore wind development on the Great Lakes was also prepared as part of the project documentation.

The project was represented at the AWEA's 2012 Offshore WindPower Conference Poster Session and Exhibition, Chicago, Illinois. The project was also presented at the American Wind Energy Association meeting in Atlanta; the International Association of Great Lakes Research in Cornwall, Ontario; and the Great Lakes Wind Collaborative Annual Meeting in Erie, PA; all in 2012. The final results of the project will be presented at a poster session at the AWEA Offshore WindPower Conference in Atlantic City, New Jersey on October 7, 2014.

The project was also represented for specific topical discussion at various other conferences, as evidenced by the published or presented paper listed in the Appendix. In addition, science students

from the Muskegon County Intermediate School District (K-12) were transported offshore on Muskegon Lake to tour the WindSentinel when it was first deployed in order to learn more about offshore wind power. Numerous undergraduate and graduate students at GVSU had an opportunity to visit the buoy in Lake Michigan during the two full season deployments. The project was also presented a numerous local schools, chamber, and rotary meetings throughout West Michigan. Written documents, reports, the AWEA poster, and other information can be found at: http://scholarworks.gvsu.edu/marec/. Access to the data portal can be obtained by contacting GVSU-MAREC. The project web site is located at: http://gvsu.edu/marec/lake-michigan-offshore-wind-assessment-project-62.htm.

Prior to the launch of the WindSentinel, the process to locate and inventory birds and bats offshore has been to make visual contact by aircraft or other aerial surveillance equipment. The WindSentinel on board recording equipment was the first attempt to simplify and reduce the cost of offshore bird and bat surveillance. The WindSentinel was equipped with a recording system typically used on land and was successfully used to record both birds and bats presence over a 9 month period, 35 miles offshore. In 2012, the equipment successfully detected thousands of calls from both birds and bats. The results of the project were presented as a Great Lakes Commission webinar in May of 2013 and at the American Society of Mammologists in June, 2013. The projects bird and bat work also won NatureServe's Scientific and Technological Achievement Award, April, 2014.

The WindSentinel has the capacity to collects large amount of data. The manipulation and management of such data falls within the emerging science of "big data". The project data management process and specific protocols developed for the project proved to be an unexpected project bonus, and was presented at the SAS Global Forum in Washington, D.C in March, 2014. Two graduate assistants that worked on the project were immediately hired following graduation, one by the Ford Motor Company and the other by Meijer, Inc. of West Michigan to work on "big data" programs within those corporations.

Also to be noted is when preparing power generation calculations (pages 23-25) it was determined that it is not possible to fully align and maintain a turbine with the prevailing wind over time. This results in reduced energy output. A possible solution for this can be the prediction of the wind direction by utilizing the previous wind direction patterns. A time series can be formed to estimate the wind direction for the coming few seconds. Several mathematical estimation techniques can be used such as artificial neural networking (ANN), machine learning approach. .

Figure 14 – WindSentinel with excess ice build-up on bow railing being removed by crew.

Another solution for this issue can be sensing the wind direction upstream of the wind turbine using LIDAR technology. NREL (National Renewable Energy Laboratory) has performed a field test of such kind of technology.

Overall it can be reported that the WindSentinel performed very well in severe weather conditions including seas up to 30 feet and winds in excess of 70 miles per hour. However the buoy safety rail equipment proved to be detrimental to operating in winter icing conditions and presented limitations detrimental to the survival of the equipment, Figure 14. The exposed above deck instrumentation and superstructure will need to be modified in order for the WindSentinel to operate in severe winter conditions.

Appendices

Appendix A

Laser Wind Sensor Performance Validation with an Existing Gage

Charles Standridge -- Padnos College of Engineering and Computing
David Zeitler -- Statistics Department
Erik Nordman -- Biology Department
T. Arnold Boezaart -- Michigan Alternative and Renewable Energy Center
Grand Valley State University

Jim Edmonson
Edmonson and Associates

Yeni Nieves
INC Research

T. J. Turnage
NOAA National Weather Service

Reo Phillips
Graham Howe
AXYS Technologies Inc.

Guy Meadows
Michigan Technological University

Aline Cotel
Frank Marsik
Neel Desai
University of Michigan, Ann Arbor

February 2013
The following article has been submitted to the Journal of Renewable and Sustainable Energy

Acknowledgement and Disclaimer

Acknowledgements: "This material is based upon work supported by the Department of Energy; Grand Valley State University; Michigan Public Service Commission; We Energies; Sierra Club of the Great Lakes; Grand Valley State University; Michigan State University, Michigan Natural Features Inventory; and the University of Michigan, under Award Number DE-EE0000294. And the following organizations for technical support: National Oceanic and Atmospheric Administration/Great Lakes Environmental Research Laboratory; National Data Buoy Center; Pacific Northwest National Laboratory; United States Coast Guard; United States Army Corp of Engineers; Michigan Department of Natural Resources; and West Michigan Energy Partners."

Abstract

A new approach to laser wind sensor measurement validation is described and demonstrated. The new approach relies on the paired-t statistical method to generate a time series of differences between two sets of measurements. This series of differences is studied to help identify and explain time intervals of operationally significant differences, which is not possible with the traditional approach of relying on the squared coefficient of variation as the primary metric. The new approach includes estimating a confidence interval for the mean difference and establishing a level of meaningful difference for the mean difference, and partitioning the data set based on wind speed.

To demonstrate the utility of the new approach, measurements made by a laser wind sensor mounted on a floating buoy are compared first with those made by a second laser wind sensor mounted on a nearby small island for which the co-efficient of variation is high (> 99%). It was found that time intervals when high differences in wind speed occurred corresponded to high differences in wind direction supporting a hypothesis that the two laser wind sensor units are not always observing the same wind resource. Furthermore, the average difference for the 100m range gate is positive, statistically signficant (α=0.01) and slightly larger than the precision of the gages, 0.1m/s. One possible cause of this difference is that the surface roughness over land is slowing the wind at 100m slightly.

A second comparison was made with previously existing cup anemometers mounted on a metrological mast located on-shore. The cup anemometers are about 8m lower than the center of the lowest range gate on the laser wind sensor. The data was partitioned into three sets: not windy (average wind speed at the cup anemometers $\leq$ 6.7m/s) windy but no enhanced turbulence (average wind speed at the cup anemometers > 6.7m/s), and windy with enhanced turbulence. Periods of enhanced turbulence are associated with the passage of a cold frontal boundary.

The paired-t analysis for the not windy data set showed a difference in the average wind speeds of -0.096m/s, less in absolute value than the precision of the gages. The negative sign indicates slower wind speed over land as well as at a lower height, which is expected. Similar results were obtained for the windy with no enhanced turbulence data set. In addition, the average difference was not statistically significant (α=0.01).

The windy with enhanced turbulence data set showed significant differences between the buoy mounted laser wind sensor and the on-shore mast mounted cup anemometers. The sign of the average difference depended on the direction of the winds in the periods of enhanced turbulence. Mean turbulent kinetic energy was measured to be greater when air flow into Muskegon Lake was predominantly from over land versus when air flow was predominantly from Lake Michigan. The higher mean turbulent kinetic energy for flow originating over land would likely be due to greater surface roughness experienced by the overland flow.

Overall, the value of the new approach in obtaining validation evidence has been demonstrated. In this case, validation evidence is obtained in periods of no enhanced turbulence. Differences in wind speed

during periods of enhanced turbulence are isolated in time, studied and are correlated in time with differences in wind direction.

1.0 Introduction

The focus of wind project developers has expanded from land-based wind farms to include off-shore sites, with increasing interest toward constructing taller turbines in deeper waters. One critical, pre-requisite step in each project is an assessment of available wind resources. For decades, meteorological ("met") masts with cup anemometers have been relied upon to record wind speed and wind vanes to record direction. However, the use of such met masts may not be feasible in deep water locations or to reach the hub height of taller turbines.

While met masts are relatively easy to install on terrestrial sites, installation at offshore locations can be prohibitively difficult as well as publically and politically controversial. Offshore met towers range in price from $2.5 million for installation in relatively shallow water (e.g. Cape Wind, Massachusetts) to more than $10 million in deeper water up to 30m (e.g. FINO 1, Germany) (Wissemann, 2008). Met towers in water in excess of 30m may not be cost effective. Fixed met masts cannot be easily moved to support other projects. In many cases, a fixed platform requires permits and/or bottomland leases from regulatory authorities. Obtaining such permits can be a lengthy process. Once a met tower is installed, it is difficult to change the heights at which the cup anemometers operate.

The wind resources at hub height are often approximated through the use of mathematical and statistical models (Bagiorgas et al. 2012; Veigas and Iglesias 2012). Following Lu et al. (2002), the estimation of the variation of wind speed with height is obtained using a power law relationship with which the wind speed (V) at hub height (Z) is estimated from the wind speed (V_0) measured at some reference height (Z_0), usually between 3m and 10m.

$$\frac{V}{V_0} = \left(\frac{Z}{Z_0}\right)^{a} \quad (1)$$

Lu et al. (2002) note that the exponent, α, varies with height, time of day, season, nature of the terrain, wind speeds, and temperature. While a value of one-seventh is typically used, the value can be estimated for a given flow condition if the wind speed is known at two heights. The value obtained from these two measurements can then be applied to estimate the wind speed at a third level, in this case the hub height.

Alternatively, in its report Large Scale Offshore Wind Power in the United States, the National Renewable Energy Laboratory noted a need for tools that can measure wind speeds at multiple locations and determine wind shear profiles up to hub height. The report authors also identified a need for stable buoy platforms to support the aforementioned assessment tools (Musial and Ram 2010).

To address this issue, a number of remote sensing technologies have emerged as potential alternatives to met tower mounted cup anemometers such as light detection and ranging (LiDAR), sound detection

and ranging (SoDAR) and airborne synthetic aperture radar (SAR) sensors (Hasanger et al. 2008). LiDAR and SoDAR operate similarly in that a signal (light or sound of a particular frequency) is emitted by the unit, the signal reflects off dust particles in the atmosphere, and the sensor captures and records the return signal. As the signal reflects off the moving dust particles, its frequency decreases (the Doppler effect). As wind speeds increase, so do the speeds of atmospheric particles. A large decrease in signal frequency is associated with faster wind speed (Hasanger et al. 2008).

The data collected by cup anemometers has long been trusted. However, there is comparatively little experience with the use of remote sensing technologies particularly in an offshore location. Thus, validation is a particularly critical step in the wind resource data collection process when such a device is used offshore. Validation has to do with gathering evidence that the collected data, such as wind speed and direction at various heights above the water surface, can be relied upon in computing power and energy potential as well as for decision making regard project economic viability (Sargent, 2012). One common form of validation evidence is comparison to a trusted gage such as a previously calibrated and tested cup anemometer posted on a met tower nearby or a second remote sensing unit operated in parallel.

There are several reports of such validation activities regarding the comparison of laser wind sensor units (LWS) with cup anemometers mounded on met masts in onshore and offshore settings. Danish researchers reported R^2 values of 0.99 for heights ranging from 60m to 116.5m and all wind speeds (Kindler et al. 2009). Hasanger et al. (2011) reported results of a validation experiment at the Horns Rev, Denmark. LWS measurements were compared to three met masts at 63m and found a high level of agreement (R^2 = 0.97-0.98). The measurement bias ranged from 0.12-0.15m/s. LWS. Cup anemometer measurements from the FINO platform (Westerhellweg et al. 2010) also showed a high level of agreement (R^2 = 0.99) and a bias of -0.15 m/s to 0.08 m/s at heights from 70m to more than 100m. These and other studies lead to the conclusion that remote sensing of wind speeds using LWS produces results indistinguishable from those of a traditional met tower.

Mounting an LWS unit on a floating platform introduces wave motion that could affect wind measurement and thus requires compensation. A National Renewable Energy Laboratory report made the following suggestion.

> To gain enough confidence for these systems to replace the conventional met mast, a large amount of experience with commercial projects at sea will be needed. This will require, in turn, close cooperation among private technology companies, offshore developers and operators, and government R&D programs at the US Department of Energy (DOE) and BOEM [Bureau of Ocean Energy Management], both in terms of taking the data and verifying the results. Once a reliable and proven track record has been established, the improved accuracy for wind and energy production measurements will remove a significant amount of risk from developers (Musial and Ram, 2010).

Pichugina et al. (2012) were among the first to document the use of shipboard LWS sensors with motion compensation. Their preliminary error propagation model suggested a wind speed precision of less than 0.10m/s for 15-minute averaged data. The authors noted that "work is needed, perhaps involving comparisons with lidars or tall towers mounted on a fixed offshore platform, to establish how closely the shipboard HRDL [LiDAR] system approximates the high precision that is obtainable during land based observations" (Pichugina et al. 2012, p. 334).

Jaynes (2011) as well as AXYS Technologies (2010) describe a study that addresses this issue: compensation for dynamic motion with 6 degrees of freedom for a LWS mounted on a floating platform including translation in two directions and heave of the platform as well as roll, pitch, and yaw of the LWS. The data was gathered from two identical LWS units. One unit was mounted on a small island 688 meters from the other unit which was mounted on a floating platform in the Juan de Fuca Strait between the Olympic Peninsula and Vancouver Island. Data was gathered for a one month period: October 20, 2009 to November 20, 2009. The data included wind speed and direction at 100, 150 and 200 meters; wave height and direction; air and water temperature; and barometric pressure. Results showed a 99% coefficient of variation (R^2) for wind speed at each height between the two gages. Since motion compensation is the only difference between the two measurement sites, validation evidence for the motion compensation algorithm is obtained.

All of the prior LWS validation studies referenced above use R^2 as the primary measure of correspondence between two gages. The weakness of this approach is that periods of time when differences in measurements between the two gages existed are not identified and thus no explanatory information regarding such differences is provided.

Furthermore, all of the studies report well-designed experiments with two gages premised to measure the same wind. This is an ideal that might not always be possible due to the cost, permitting, and logistics of acquiring and co-locating two gages, particularly if one is a met tower with cup anemometers. Of particular interest is the situation where one of the gages is an LWS mounted on a floating platform acquired to measure off-shore wind a significant distance from any land and where cost constraints require comparison to an existing gage located on the shoreline. Given the view of validation as the process of building confidence that the data gathered by the LWS can be used for power estimation and other decision making, using R^2 as the primary metric seems insufficient for this case.

This paper describes an approach to validation for the situation where an LWS mounted on a floating platform is compared to existing cup anemometers mounted on a land-based met tower. The strategy is to examine the difference in measurements between the two gages over time to identify intervals when the measurements were equivalent and to provide explanatory information for the intervals when the measurements were not equivalent. The strategy is implemented using the paired-t statistical method, with time being the common element. This approach is illustrated for an LWS on a floating platform acquired for collecting wind resource information in Lake Michigan with measurement

comparisons made to existing cup anemometers mounted on a met tower located on the shoreline of Muskegon Lake.

First the approach is introduced by extending the study reported by Jaynes (2011) and AXYS Technologies (2010) discussed above to show its value even between two gages premised to measure equivalent wind with a high R^2 reported.

2.0 Approach Introduction and Extension of the Juan de Fuca Strait Study

Each of the two LWS units in this study observed wind speed and direction at 100m, 150m, and 200m each second. Ten minute averages were computed. Only the 10-minute averages consisting of at least 300 valid one-second observations out of a possible 600 were included in the analysis. This is the current industry defacto standard for aggregating one-second observations. The LWS unit referred to as the Land Station is on a small island. The other referred to as the Wind Sentinel is mounted on the flowing platform or buoy.

The fundamental equation of the paired-t statistical method generates the time series of differences in the 10-minutes averages observed by the LWS units for each of the three heights:

$$\text{difference}_t = \text{Wind Sentinel}_t - \text{Land Station}_t \quad (2)$$

Given the definition of a valid 10-minute average, a valid difference is one for which both 10-minute averages are valid. Applying this definition resulted in 3022 differences at each of the three heights out of a possible 4464, 67.7%. The average difference is Student's t-distributed with degrees of freedom of one less than the number of valid differences.

An average difference of less than 0.1m/s, the precision of each gage, is considered operationally insignificant for our purposes. This value is the smallest non-zero measurement made by either a LWS or a cup anemometer. In other words, the hypothesis is the difference between the mean wind speed measured one gage and the mean wind speed measured by a second gage is equal to the precision of a gage.

The coefficient of variation (c) is also of interest:

$$c = \frac{s}{\bar{x}} \quad (3)$$

where s is the standard deviation of the differences and $\bar{x}$ is the average difference.

With respect to the difference series, the larger the value of c the better, which results when the standard deviation is larger than the mean. The standard deviation corresponds to the random variation in the differences while the mean corresponds to real differences. Thus, the larger the values of c, the more the difference is due to random variation in wind speed as opposed to real differences in measured values.

Another way to interpret c arises from realizing that it is the reciprocal of the signal-to-noise ratio. Thus, the larger the value of c, the more noise (random variation) and less signal (actual differences), which is the desired condition.

First consider a plot of the differences shown in Figure 1. Note that wsd100 represents the wind speed difference between the instruments for the 100 meter range gate, wsd150 represents the wind speed difference for 150 meter range gate, and wsd200 represents the wind speed difference for the 200 meter range gate.

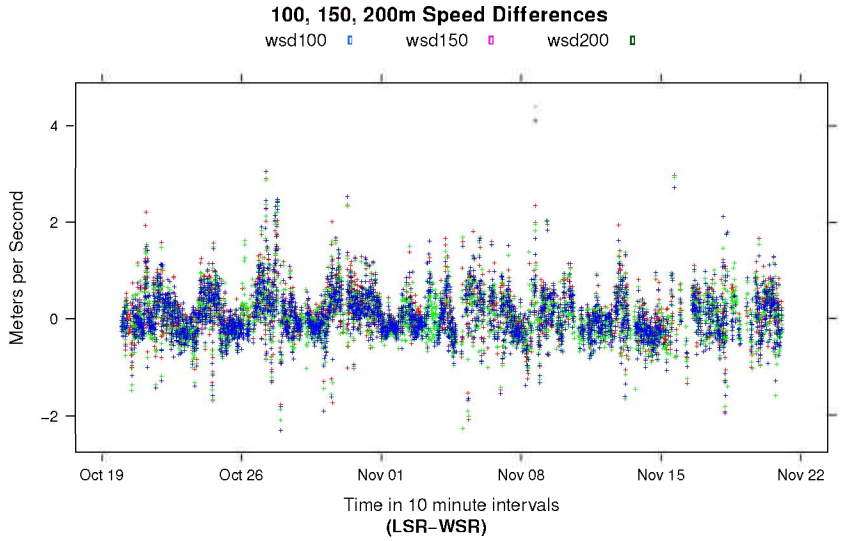

Figure 1: Speed Differences for Each Range Gate

Note despite the R^2 values of at least 99% at each range gate height that differences often exceeding 2m/s and occasionally 4m/s are observed. An explanation for these differences must be sought. In this regard, consider the plot of wind direction difference, expressed in degrees with north equal zero, shown in Figure 2.

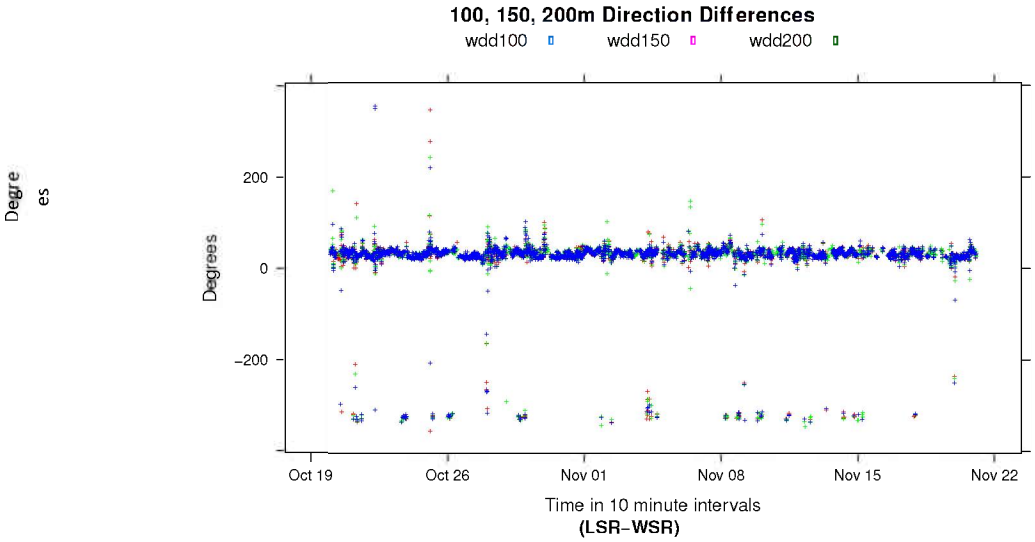

Figure 2: Direction Differences for Each Range Gate

The information shown in Figure 2 indicates that direction differences are of the same magnitude for each height and that large differences for speed and direction occur at the same points in time. Thus, it appears that differences in speed are correlated to differences in wind direction. This is consistent with the hypothesis that the wind at the two LWS units, which are 688 meters apart, is not always the same or in other words the two LWS are not always observing the same wind. Note that the differences are in isolated time periods. Thus, it is unlikely that these differences are due to causes such as instrument calibration error or poor buoy motion correction.

A statistical summary of the wind speed difference series for each range gate is shown in Table 1.

Table 1: Statistical Summary of Wind Speed Difference Series

Range Gate Height (m)	Mean Difference (m/s)	Standard Deviation (m/s)	Coefficient of variation	Number of differences (n)	99% Confidence Interval	
					Lower Bound	Upper Bound
100	0.13	0.48	3.7	3022	0.11	0.15
150	0.076	0.48	6.4	3022	0.053	0.099
200	0.074	0.48	6.5	3022	0.052	0.096

The results for the 150m and 200m range gates are virtually identical. The mean difference, as well as the 99% confidence interval for the mean difference, are less than 0.1m/s the smallest operationally significant value. The coefficient of variation is much larger than 1, indicating that difference series is comprised mostly of random variation.

Conversely for the 100m range gate, the mean difference, as well as the 99% confidence interval, are greater than 0.1m/s. The standard deviation is the same as for the other two range gates and thus the coefficient of variation is smaller.

The graphs shown in Figures 1 and 2 as well as the summary data shown in Table 1 provide the basis for insights into differences between the wind measurements made by the two gages. Such differences are not apparent when the time series of differences is not examined that is when R^2 is the primary measure of comparison. Points in time when high differences in wind speed occur correspond to high differences in wind direction suggesting that the two LWS units are not always observing the same wind resource. The average difference for the 150m and 200m ranges gates is less than the smallest operationally significant difference of 0.1m/s but the average difference for the 100m range gate is positive and slightly larger than 0.1m/s. One possible cause of this difference is that the surface roughness over land is slowing the wind at 100m slightly, while having a limited effect at 150m and 200m.

Thus, the benefits of examining the difference series of wind speeds between two gages is shown even for the case where the coefficient of determination between the two wind speed measurements is high.

3.0 Comparison of Floating Platform Mounted LWS and Met Mast Measurements

A WindSentinel buoy, including a LWS unit, was acquired in September 2011 and deployed in Muskegon Lake from 7 October 2011 through 3 November 2011. (This LWS unit is not one of the two LWS units used in the Juan de Fuca Strait Study.) The buoy was positioned 423.8m (calculated at http://jan.ucc.nau.edu/~cvm/latlongdist.html) offshore from a 50m onshore met mast at the east end of the lake. The location of each sensor was as follows:

Sensor	Site	Coordinates	Elevation (AMSL)	Sensor height above lake level
Laser sensor	Muskegon Lake	43° 14’ 55” N; 86° 14’ 55” W	176 m	57.85 m
Met mast	Open field	43° 14’ 46” N; 86° 14' 41” W	178 m	50.5 m

The LWS unit has a range gate centered at 55m, but is mounted on the buoy an additional 2.85m above the lake level. The corrected LWS lens height is 57.85m above the surface of Muskegon Lake. The onshore met mast contains two anemometers at 48.5m above ground with one anemometer facing northwest and the other southeast. The maximum wind speed of the two anemometers was used. Using the maximum, as opposed to the average, eliminates any erroneous data due to either A) one anemometer entering a failure mode; or B) differences in speed measurements due to differences in wind direction. The met mast site is 2.0m above the lake level. This puts the anemometers an effective 50.5m above Muskegon Lake.

The LWS unit and the anemometers were measuring wind speeds at slightly different heights and at locations 423.8m apart. The anemometers were on the edge of a large land mass and the LWS unit was over water. Thus, it is reasonable to hypothesize that some of the time each was measuring a different wind resource.

Figure 3: Location of Met Mast and LWS unit in Muskegon Lake

3.1 Wind Observations and Dataset Partitioning

One-second (1 Hz) wind observations were collected. Ten-minute average wind speeds were computed for non-overlapping periods from the one-second observations. As in the Juan de Fuca Strait Study, only 10-minute averages consisting of at least 300 one-second observations were considered valid.
The time series of differences is generated using Equation 4.

$$\text{difference}_t = \text{met mast}_t - \text{LWS}_t. \quad (4)$$

Recall that met mast_t is the maximum of the wind speed averages for the two anemometers. A valid difference is one for which both the met mast and LWS averages are valid. A missing observation is one for which either the met mast or the LWS average was not recorded.

Table 2 shows the number of observations by classification.

Table 2: Number of Observations by Classification

Classification	Number of Observations
Total number of observation periods	3849
Number of missing observations	385
Number of non-missing observations	3464
Percent of non-missing observations	90.0%
Number of invalid observations	270
Number of valid observations	3194
Percent of valid, non-missing observations	92.2%
Number of outliers	1
Number of observations used in study	3193
Number of observations used in study / Number of observation periods	83.0%

The laser sensor reported about 10% of the observations as missing. There was one extremely large wind speed value that could not be explained and was thus considered an outlier. Thus, 83.0% of the 10-minute averages were considered useable for analysis, well above the industry standard of 60% to 70%.

A graph of the 3193 pairs of 10-minute averages used in the study is shown in Figure 4. The observations made by the two devices track each other well. Some differences are noted at higher wind speeds. The blue line is data from LWS #8 (hws55) and the purple line is the data from the MET tower anemometers (max48).

A correlation graph is given in Figure 5. In this graph, differences at higher wind speeds are more easily seen. The correlation coefficient is 90.15%. The red line represents perfect (100%) correlation and the black points represent the estimated correlation.

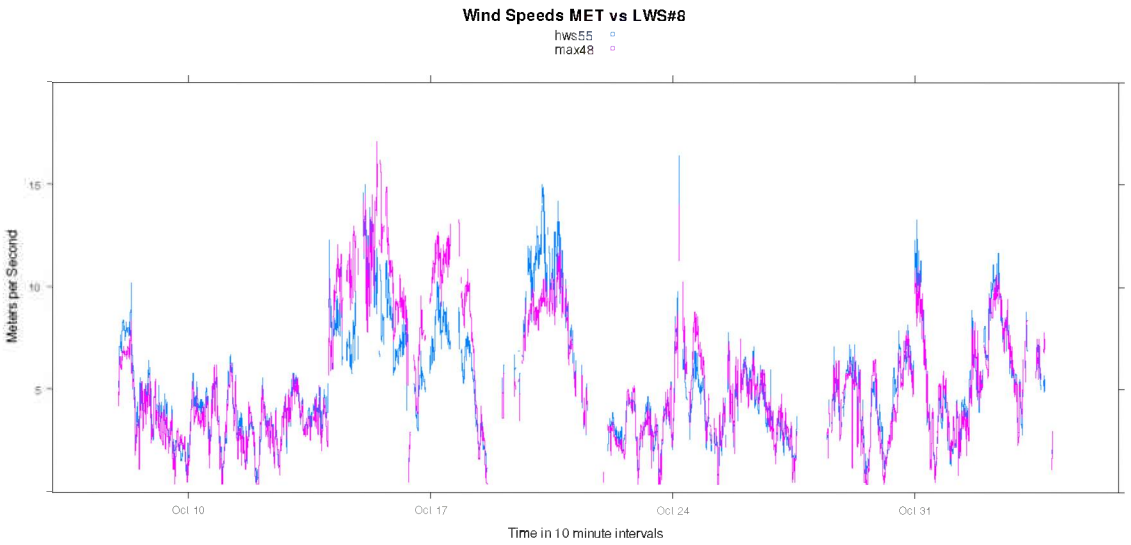

Figure 4: 10-Minute Average Pairs from Each Gage

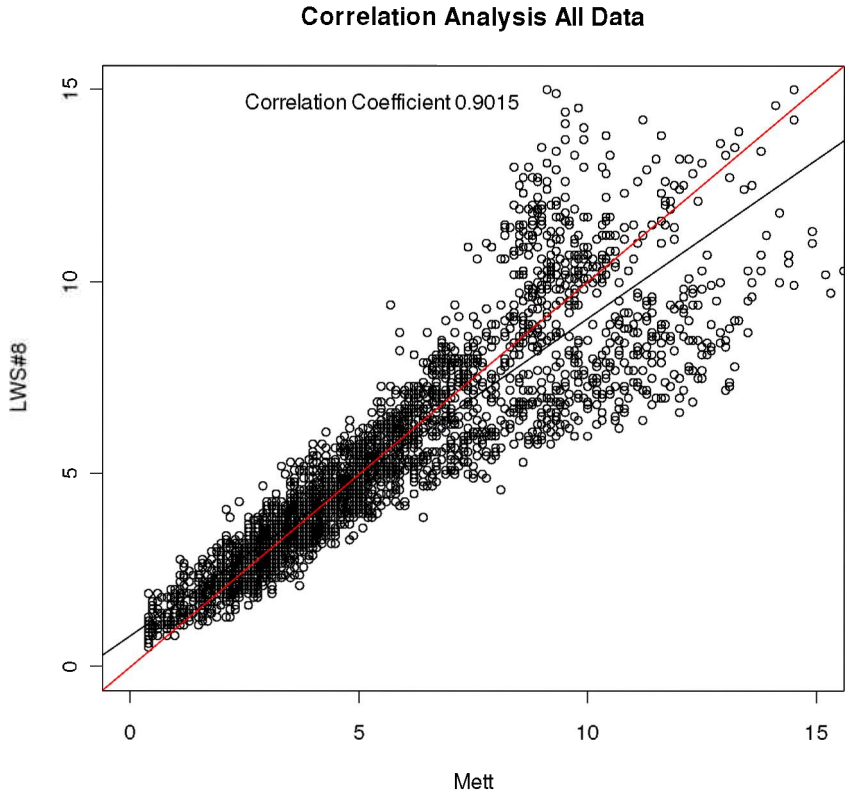

Figure 5: 10-Minute Average Pairs Correlation Plot

As seen in Figure 5, the correlation between the wind speeds measured by the two gages lessens dramatically at about 6.7m/s or 15mph. Thus, the dataset was partitioned into two subsets based on the wind speed measured by the anemometers on the met mast: ≤ 6.7m/s and > 6.7m/s. This was done

using a windowing technique with window size of one hour. If average wind speed for the current point in time and the next 5 points in time for the 10-minute averages was > 6.7m/s, then all six 10-minute averages in the window were assigned to the > 6.7m/s dataset. The next 10-minute average considered is the one immediately following those in the window. Otherwise, the current 10-minute average is assigned to the ≤ 6.7m/s data set and the next 10-minute average in time sequence is considered. Table 3 shows the number of observations in each data set resulting from this partitioning.

Table 3: Number of Observations in Dataset

Classification	**Number of Observations**
Number of observations used in study	3193
Number of observations ≤ 6.7m/s	2149
Number of observations > 6. m/s	1044
% of observations ≤ 6.7m/s	67.3%
% of observations > 6.7m/s	32.7%

3.2 Analysis of the <6.7m/s Dataset

Table 4 summarizes the results of the paired-t analysis for the hypothesis that the mean difference is zero with the alternative hypothesis that the mean difference is not zero.

Table 4: Paired-t Analysis for the ≤ 6.7m/s Data Set

Data Set	Mean Difference (m/s)	Standard Deviation (m/s)	Coefficient of Variation	R^2	Number of Differences (n)	99% Confidence Interval	
						Lower Bound	Upper Bound
≤ 6.7m/s	-0.096	0.58	-6.1	91.2%	2149	-0.13	-0.064

The magnitude of the mean difference is slightly less than 0.1m/s. Thus, this difference is not operationally significant, even though it is statistically significant (α=0.01) as the 99% confidence interval for the mean difference does not contain zero. Furthermore, the magnitude of the coefficient of variation is much greater than 1 indicating that differences in the observations made by the two data sets can be viewed as random variation. Thus, validation evidence for the LWS is obtained for wind speeds less than or equal to 6.7m/s.

In addition, the sign of the difference is negative indicating that the cup anemometer reading is slower. This is consistent with the idea that wind speed over a rougher surface (land) should be less. Furthermore, some difference in mean wind speed, as well as correlation less than in the Juan de Fuca Strait study, is expected due to the difference in heights above Muskegon Lake of the two gages.

3.3 Analysis of the > 6.7m/s dataset (no enhanced turbulence)

The analysis of the > 6.7m/s dataset was performed in two parts: observations that were windy but not during periods of enhanced turbulence, and observations during three periods of enhanced turbulence. Table 5 shows the paired t-analysis for the > 6.7m/s no enhanced turbulence dataset.

Table 5: Paired-t Analysis for the > 6.7m/s No Enhanced Turbulence Data Set

Data Set	Mean Difference (m/s)	Standard Deviation (m/s)	Coefficient of Variation	R^2	Number of Differences (n)	99% Confidence Interval	
						Lower Bound	Upper Bound
> 6.7 m/s no enhanced turbulence	-0.028	1.1	-39	65%	416	-0.17	0.11

The magnitude of the mean difference is less 0.1m/s. This difference is neither operationally significant nor statistically significant (α=0.01) as the 99% confidence interval for the true mean difference contains zero. Again, the coefficient of variation is much greater than 1 indicating that the mean difference is due to random variation. Thus, validation evidence is obtained for wind speeds greater than 6.7m/s and no enhanced turbulence.

The correlation coefficient of 65% is due to a few large differences seen at high wind speeds (Figure 5) as would be expected.

3.4 Analysis of the > 6.7 m/s dataset (enhanced turbulence periods)

Table 6 shows the time periods during which enhanced turbulence was observed.

Table 6: Enhanced Turbulence Period Time Blocks

Day Start	Time Start (UTC)	Day End	Time End (UTC)	Comments
10/14	1:30	10/16	9:10	Period 1
10/16	16:00	10/18	7:00	Period 2
10/19	16:30	10/21	3:40	Period 3

Table 7 shows the paired t-analysis for the > 6.7m/s enhanced turbulence dataset by period.

Table 7: Paired-t Analysis for the > 6.7m/s No Enhanced Turbulence Data Set

Data Set	Mean Difference (m/s)	Standard Deviation (m/s)	Coefficient of Variation	R^2	Number of Differences (n)	99% Confidence Interval	
						Lower Bound	Upper Bound
> 6.7m/s Period 1	1.8	1.9	1.1	64%	262	1.5	2.1
> 6.7m/s Period 2	2.8	0.88	0.32	88%	174	2.6	3.0
> 6.7m/s Period 3	-1.6	1.5	0.98	61%	191	-1.8	-1.3

Mean differences in measurements between buoy-mounted LWS unit and the mast-mounted cup anemometers during periods of enhanced turbulence are both operationally significant, of the order of 2m/s, and statistically significant (α=0.01). The results for all three such periods are consistent: a significantly lower level of agreement between the two gages.

Some insight into the differences is in order as follows.

1. Comparison of these results with those from other studies in not possible as most LWS unit validation studies exclude observations made under enhanced turbulence conditions (Peña et al. 2009, Kindler et al. 2009).
2. The sign of the mean difference is consistent with the direction of the wind during the enhanced turbulence periods. The wind direction is as follows: Period 1 -- from the northwest, over water; Period 2 from the west, over water; and Period 3 from the

northeast, over land. Thus, wind direction from over water indicates higher wind speed on land and vice versa.

3. The surface roughness over land (met mast) is greater than the surface roughness over water (LWS). Thus some difference in wind speed is expected, which may be more pronounced during enhanced turbulence.

An analysis of the one second observations provides support for items 2 and 3. Mean Turbulent Kinetic Energy (TKE) was measured to be greater when air flow into Muskegon Lake was predominantly from over land versus when air flow was predominantly from Lake Michigan. The higher mean TKE for flow originating over land would likely be due to greater surface roughness experienced by the overland flow. During the period on Oct 19th with wind direction from Land toward Sea, the TKE fluctuations are much higher than for an equivalent magnitude wind with direction from Sea to Land (Oct 16th). During the Land to Sea period, the spikes in the TKE are on the order of 5 times that of the Sea to Land period.

Thus, the observed difference in wind speed between the two gages during periods of enhanced turbulence seems reasonable.

4.0 Summary

A new approach to the validation of an LWS unit mounted on a floating platform with existing cup anemometers mounted on a land-based met tower nearby is described and applied. The two gages are not at the same height.

The new approach involves generating the time-series of differences between the 10-minute averages of one-second observations made by each gage. Using the statistical paired-t method, the coefficient of variation, and related graphs, the new approach improves upon the methods used in previous studies that relied on the coefficient of determination (R^2) as the primary measure of comparison. The new approach focuses on studying the time-series of differences to identify times of agreement between the instruments as well as to isolate and explain time periods when the gages appear to be measuring different wind.

To show the value of the new approach, a previously reported validation study with high R^2 = 99% is extended. The study compared two LWS units: one on a small island and the other mounted on a floating platform. The high R^2 value provided validation evidence for the motion compensation algorithm associated with the LWS unit on the floating platform. The additional value of the new approach was shown by identifying that large absolute values in the time-series of wind speed differences occurred in the same time periods as large differences in wind direction, supporting the hypothesis that during these time period the gages were observing different wind.

The validation study of a different LWS unit mounted on a floating platform in Muskegon Lake with cup anemometers mounted on a met tower on the lake shore nearby was conducted using the new method. The data was partitioned into three sets: not windy (average wind speed at the cup anemometers ≤

6.7m/s), windy but no enhanced turbulence (average wind speed at the cup anemometers > 6.7m/s), and windy with enhanced turbulence (again, average wind speed at the cup anemometers > 6.7m/s).

The paired-t analysis for the not windy data set showed a difference in the average wind speeds of -0.096m/s, less in absolute value than the 0.1m/s the smallest value either gage will measure. The negative sign indicates slower wind speed over land as well as at a lower height, which is expected. Furthermore, the magnitude of the coefficient of variation (6.1) is much greater than 1 indicating that differences in the observations made by the two data sets can be viewed as random variation. Thus, validation evidence for the LWS unit is obtained.

Similar results were obtained for the windy with no enhanced turbulence data set. In addition, the average difference was not statistically significant (α=0.01).

The windy with enhanced turbulence data set showed significant differences between the two gages. The sign of the average difference depends on the direction of the winds. Mean TKE was measured to be greater when flow was predominantly from over land versus when flow was predominantly from Lake Michigan. The higher mean TKE for flow originating over land would likely be due to greater surface roughness experienced by the overland flow. Thus, there is a plausible foundation for the observed difference in average wind speed during enhanced turbulence.

Overall, validation evidence is obtained in the absence of enhanced turbulence. In addition, differences in wind speed during enhanced turbulence can be isolated in time, studied and explained.

Bibliography

AXYS Technologies. 2012. NOMAD buoy data sheet. Web site. Available at http://www.axystechnologies.com/Portals/0/Brochures/AXYS%20NOMAD%20Buoy.pdf. Accessed 15 May 2012.

AXYS Technologies Inc. (2010). Wind Sentinel™: Field Test Data Summary. AXYS Technologies, Sydney, BC.

Bagiorgas, H. S., Mihalakakou, G., Rehman, S., and Al-Hadhrami, L.M. 2012. Wind power potential assessment for seven buoys data collection stations in Aegean Sea using Weibull distribution function. *Journal of Renewable and Sustainable Energy* 4, 013119 (2012); doi: 10.1063/1.3688030. Available at http://dx.doi.org/10.1063/1.3688030.

Catch the Wind, Inc. 2010. Vindicator optical wind sensor: product overview. Web site. Available at http://www.catchthewindinc.com/node/293/specs. Accessed 15 May 2012.

Hasanger, C. M. Badger, A. Peña, J. Badger, I. Antoniou, M. Nielsen, P. Astrup, M. Courtney, and T. Mikkelsen. Advances in offshore wind resource estimation. In *Advances in Wind Energy Conversion Technology*, S. Matthew and G. Philip (eds.), 85-106.

Hasanger, C., A. Peña, M. Christiansen, P. Astrup, M. Nielsen, F. Monaldo, D. Thompson, and P. Nielsen. 2008. Remote sensing observation used in offshore wind energy. *IEEE Journal of Selected Topics in Applied Earth Observations and Remote Sensing* 1(1): 67-79.

Jaynes, D. M. 2011. Investigating the efficacy of floating lidar motion compensation algorithms for offshore wind resource assessment applications. European Wind Energy Conference.

Kindler, D., M. Courtney, and A. Oldroyd. 2009. Testing and calibration of various LiDAR remote sensing devices for a 2 year offshore wind measurement campaign. European Wind Energy Conference report. Available at http://www.norsewind.eu/public/downloads/EWEC2009_LiDAR_Validation.pdf. Accessed 15 May 2012.

Lu, L., H. Yang, and J. Burnett. 2002. Investigation on wind power potential on Hong Kong islands—an analysis of wind power and wind turbine characteristics. Renewable Energy 27: 1–12.

Musial, W. and B. Ram. 2010. Large-scale offshore wind power in the United States: Assessment of opportunities and barriers. National Renewable Energy Laboratory Technical Report. NREL/TP-500-40745. 221 pp.

Peña, A., C. Hasanger, S. Gryning, M. Courtney, I. Antoniou, T. Mikkelsen. 2009. Offshore wind profiling using light detection and ranging measurements. Wind Energy 12: 105-124.

Pichugina, Y., R. Banta, W. Brewer, S. Sandberg, and R.l Hardesty. 2012. Doppler lidar–based wind-profile measurement system for offshore wind-energy and other marine boundary layer applications. *Journal of Applied Meteorology and Climatology*. 51, 327-249.

Sargent, R. G. 2012. Verification and validation of simulation models. *Journal of Simulation*, advance online publication. doi:10.1057/jos.2012.20.

Veigas, M. and Iglesias, G. 2012. Evaluation of the wind resource and power performance of a turbine in Tenerife. *Journal of Renewable and Sustainable Energy* 4, 053106 (2012); doi: 10.1063/1.4754155. Available at http://dx.doi.org/10.1063/1.4754155.

Westerhellweg, A., B. Canadillas, A. Beeken, and T. Neumann. 2010. One year of LiDAR measurements at FINO1-Platform: Comparison and verification to met-mast data. 10th German Wind Energy Conference DEWEK 2010. Available at http://www.dewi.de/dewi/fileadmin/pdf/publications/Publikations/S01_3.pdf. Accessed 15 May 2012.

Wissemann, C. 2009. IOOS Offshore Wind energy Meeting presentation. Rutgers University, 2 February 2009. Available at http://marine.rutgers.edu/cool/coolresults/2009/ioos_020209/. Accessed 15 May 2012.

Appendix B

Data Summary and Analysis

2012 Season

Acknowledgement and Disclaimer

Acknowledgements: "This material is based upon work supported by the Department of Energy; Grand Valley State University; Michigan Public Service Commission; We Energies; Sierra Club of the Great Lakes; Grand Valley State University; Michigan State University, Michigan Natural Features Inventory; and the University of Michigan, under Award Number DE-EE0000294. And the following organizations for technical support: National Oceanic and Atmospheric Administration/Great Lakes Environmental Research Laboratory; National Data Buoy Center; Pacific Northwest National Laboratory; United States Coast Guard; United States Army Corp of Engineers; Michigan Department of Natural Resources; and West Michigan Energy Partners."

2012 Season Data

This report summarizes the data collected by the Laser Wind Sensor (LWS) OADS Vindicator #8, mounted on an AXYS NOMAD WindSentinel with collection information as follows.

Location:	Lake Michigan – Mid-lake Plateau (4320.5100N 8707.2057W)
Date:	May 8 through December 17, 2012 (UTC)
Range Gates 1-6:	75, 90, 105, 125, 150, 175 meters
Cup Anemometer:	3 meters mounted on the buoy
Observations:	10-minute averages of wind speed and wind direction stored onboard the buoy
Quantities of Primary Interest:	Average wind speed, variation in wind speed, and distribution of wind direction
Independent Variables:	Range gate height, month, and location (versus 2011)
Number of Observations:	224 days at 6 observations per hour = 32256 observations
Missing Observations:	35 – (7/9 at 12:30-13:50; 7/24 at 11:10; 8/28 at 14:00 – 15:40; 10/23 at 18:40-18:50; 10/30 at 16:40; 11/8 at 13:10-13:20 and 14:00-15:20)
Good Observations:	32221 (99.9%)
Notes:	All high resolution 1 second data for all wind speeds is stored onboard the buoy and can be used for further detailed post processing as required. Missing observations are those not reported by LWS #8.

Wind Speed by Height

In this section, wind speed is compared across the six range gate heights. The average wind speed and variation in the wind speed as measured by the coefficient of variation are of interest.

Summary statistics for wind speed by range gate and for the cup anemometer are shown in the following tables. Good observations are 10-minute averages consisting of at least 300 one-second observations.

Table 1: Horizontal Wind Speed (meters per second) Statistics by Range Gate

Statistic	N001S007 P006 Cup Anemometer	N001S009 P083 75m	N001S009 P084 90m	N001S009 P085 105m	N001S009 P086 125m	N001S009 P087 150m	N001S009 P088 175m
Good Obs.	32216	30076	30951	30882	29265	21101	12226
% of Total (32256)	99.9	93.2	96.0	95.7	90.7	65.4	37.9
Average	6.2	8.7	8.9	9.0	8.9	9.2	9.5
Std. Dev.	3.1	4.7	4.8	4.8	4.9	5.2	5.0
Coeff. of Variation	0.50	0.54	0.54	0.53	0.55	0.57	0.53
Minimum	0.0	0.2	0.2	0.2	0.2	0.2	0.3
Quartile 1	4.0	5.1	5.3	5.4	5.1	5.2	5.7
Median	5.9	8.0	8.3	8.4	8.2	8.4	8.8
Quartile 3	8.2	11.6	11.9	12.0	11.9	12.4	12.5
Maximum	19.3	28.3	28.7	29.2	29.8	30.2	31.5
99% CI– Lower Bound	6.2	8.6	8.8	8.9	8.8	9.1	9.4
99% CI Upper Bound	6.2	8.8	9.0	9.1	9.0	9.3	9.6

Table 2: Wind Speed Frequencies by Range Gate – Percent of Time in Each Wind Speed Range

Wind Speed Range (m/s)	N001S007 P006 Cup Anemometer	N001S009 P083 75m	N001S009 P084 90m	N001S009 P085 105m	N001S009 P086 125m	N001S009 P087 150m	N001S009 P088 175m
0-4	24.8	16.1	14.7	14.4	15.5	15.8	11.5
4-8	48.6	33.6	32.3	32.0	32.8	30.8	31.1
8-12	22.4	27.0	28.3	28.5	27.1	26.5	29.5
12-16	3.7	15.0	15.9	15.9	15.1	15.9	17.6
16-20	0.6	6.0	6.2	6.4	6.4	7.4	7.0
20-24	0	2.0	2.2	2.3	2.5	2.7	2.0
24-28	0	0.2	0.4	0.4	0.5	0.8	1.0
28-32	0	0	0	0	0.1	0.1	0

Table 3 contains the summary statistics shown in table 1 for the subset of times when every range gate had a good observation that is there were 300 one-second observations for each range gate. The abbreviation CI stands for confidence interval.

Table 3: Horizontal Wind Speed (meters per second) Statistics by Range Gate – All Range Gates with Good Observations (12154/32256= 37.7%)

Statistic	N001S009 P083 75m	N001S009 P084 90m	N001S009 P085 105m	N001S009 P086 125m	N001S009 P087 150m	N001S009 P088 175m
Average	10.3	10.4	10.5	10.5	10.4	9.5
Std. Dev.	4.9	5.0	5.0	5.1	5.2	5.0
Coeff. of Variation	0.48	0.48	0.48	0.49	0.50	0.53
	0.2	0.2	0.2	0.2	0.2	0.3

Minimum						
Quartile 1	6.7	6.8	6.8	6.8	6.5	5.7
Median	9.7	9.9	9.9	10.0	9.7	8.8
Quartile 3	13.6	13.8	13.9	14.0	13.9	12.5
Maximum	27.3	28.4	29.2	29.8	30.2	31.5
99% CI– Lower Bound	10.2	10.3	10.4	10.4	10.3	9.4
99% CI Upper Bound	10.4	10.5	10.6	10.6	10.5	9.6

Table 4 shows the 99% confidence intervals for the mean difference in average wind speed between adjacent range gates, for example between the range gates centered at 175 meters and 150 meters. The difference is higher range gate – lower range gate. The confidence intervals are computed using the paired t method. An observation time is included in the difference if the number of observations for each of the two range gates was at least 300.

Table 4: Horizontal Wind Speed – Average Difference by Pairs of Adjacent Range Gates

Statistic	90m-75m	105m-90m	125m-105m	150m-125m	175m – 150m
Good Obs.	30050	30848	29251	21074	12199
% of Total (32256)	93.2	95.6	90.7	65.3	37.8
Average	0.26	0.076	-0.13	-0.43	-0.92
99% CI– Lower Bound	0.25	0.07	-0.14	-0.44	-0.95
99% CI Upper Bound	0.27	0.08	-0.12	-0.41	-0.88

Table 5 shows the energy generated for each range gate. The amount of energy generated depends on the turbine employed, in this case the Gamesa Elioca G58 850kW. The energy estimate was computed assuming that the turbine will always face the wind.

Table 5: Energy (kWh/time unit) by Range Gate

	All data		Every Range Gate with Good Obs.	
Range Gate	Average Power (MW)	Average Daily Energy (MWh)	Average Power (MW)	Average Daily Energy (MWh)
1	0.414	9.95	0.522	12.54

2	0.429	10.30	0.525	12.60
3	0.431	10.35	0.525	12.59
4	0.418	10.04	0.520	12.48
5	0.426	10.23	0.505	12.11
6	0.425	10.20	0.455	10.93
Buoy Cup	0.248	5.96	0.248	5.96

Discussion points:

Wind speed:

5. The variation in wind speed is approximately the same for each range gate height as shown by the coefficient of variation values in tables 1 and 3.
6. The average wind speed is approximately 50% higher at the range gate heights than on the buoy deck as shown in table 1.
7. The average wind speed in table 1 generally increases with height. However, the number of observations tends to decrease with height.
8. Given #3, a better comparison of average wind speed is given for those 10 minute intervals where all averages contain 300 or more 1-second observations. These results are shown in table 3. A comparison of average wind speed between adjacent range gate heights where each average in the pair contains 300 or more 1-second observations is shown in table 4. These results indicate that average wind speed increases between 75m and 105m; levels off and perhaps begins to decrease between 105m and 125m; and continues to decrease up 175m. All differences are statistically significant ($\alpha = 0.01$).
9. The results don't support the idea that the higher the wind turbine is mounted the faster the wind speed and the thus the more energy that is harvested.

LWS Performance

4. Overall, the LWS made observations for 99.9% of all 10 minute intervals.
5. The number of good observations decreases with height above 90m. Since the LWS relies on detecting particle movement in the airflow, this may be due to a lack of such particles at the mid-lake plateau as height increases that is cleaner air. In addition, there is less mixing of the air layers in the mid-lake versus near shore resulting in less movement of particulate matter.
6. The average wind speed for each range gate shown in table 3 is higher than the corresponding average in table 1, except for 175m where the two averages are the same. This indicates that

observations at 175m are only made at higher wind speeds, which is consistent with reaching the outer observation limits of the LWS.

Wind Speed by Month

Tables 6a through 6g show wind speed statistics by month, one table for each range gate and one for the cup anemometer on the buoy deck.

Table 6a: Horizontal Wind Speed (meters per second) Statistics by Month at 75m

Statistic	May	June	July	August	Sept.	October	Nov.	Dec.
Good Obs.	3358	4257	4242	4230	3829	3835	3943	2382
% of Total	97.2	98.5	95.0	91.8	88.6	85.9	91.2	97.3
Average	9.9	9.7	7.0	6.9	7.7	10.7	8.7	9.7
Std. Dev.	5.3	5.0	3.7	4.0	3.9	5.4	4.7	4.0
Coeff. of Variation	0.54	0.52	0.53	0.58	0.51	0.5	0.54	0.41
Min	0.3	0.3	0.2	0.3	0.3	0.3	0.2	0.4
1st Quart.	5.5	5.7	4.3	3.7	4.9	6.8	5.4	6.8
Median	9.5	9.1	6.2	6.0	7.5	10.1	8.0	9.6
3rd Quart.	13.6	13.1	9.5	9.8	9.9	14.4	10.8	12.4
Max	28.3	24.6	20	18.2	23.6	25.7	24.7	23
99% CI– Low Bnd.	9.7	9.5	6.9	6.7	7.5	10.5	8.5	9.5
99% CI Up Bnd.	10.1	9.9	7.1	7.1	7.9	10.9	8.9	9.9

Table 6b: Horizontal Wind Speed (meters per second) Statistics by Month at 90m

Statistic	May	June	July	August	Sept.	October	Nov.	Dec.
Good Obs.	3401	4277	4257	4245	4112	4097	4145	2417
% of Total	98.4	99.0	95.3	92.2	95.1	91.7	95.9	98.7
Average	10.1	9.9	7.2	7.1	8.1	11.1	8.8	9.9
Std. Dev.	5.3	4.9	3.8	4.1	3.9	5.4	4.7	4
Coeff. of Variation	0.52	0.49	0.53	0.58	0.48	0.49	0.53	0.4
Min	0.4	0.3	0.2	0.4	0.5	0.3	0.2	0.4
1st Quart.	5.8	6.0	4.4	3.8	5.3	7.3	5.6	6.9
Median	9.6	9.5	6.4	6.1	7.9	10.5	8.2	9.9
3rd Quart.	13.8	13.2	9.6	10	10.3	14.7	10.8	12.7
Max	28.7	25.3	20.4	18.5	23.9	26.2	25.7	23
99% CI– Low Bnd.	9.9	9.7	7.0	6.9	7.9	10.9	8.6	9.7
99% CI Up Bnd.	10.3	10.1	7.4	7.3	8.3	11.3	9.0	10.1

Table 6c: Horizontal Wind Speed (meters per second) Statistics by Month at 105m

Statistic	May	June	July	August	Sept.	October	Nov.	Dec.
Good Obs.	3385	4274	4255	4244	4120	4084	4131	2389
% of Total	97.9	98.9	95.3	92.1	95.3	91.4	95.6	97.6
Average	10.1	10.0	7.2	7.2	8.2	11.2	9.0	10.1
Std. Dev.	5.4	5.0	3.8	4.2	3.9	5.5	4.8	4.1

Coeff. of Variation	0.53	0.5	0.53	0.58	0.48	0.49	0.53	0.41
Min	0.5	0.5	0.4	0.3	0.2	0.4	0.2	0.4
1st Quart.	5.8	6.1	4.4	3.8	5.4	7.3	5.6	7.1
Median	9.7	9.4	6.4	6.1	8	10.6	8.3	10
3rd Quart.	13.8	13.2	9.7	10.2	10.4	14.8	11	12.8
Max	29.2	25.4	21	19.2	23.9	26.7	26.7	23.4
99% CI– Low Bnd.	9.9	9.8	7.0	7.0	8.0	11.0	8.8	9.9
99% CI Up Bnd.	10.3	10.2	7.4	7.4	8.4	11.4	9.2	10.3

Table 6d: Horizontal Wind Speed (meters per second) Statistics by Month at 125m

Statistic	May	June	July	August	Sept.	October	Nov.	Dec.
Good Obs.	3113	4152	4217	4215	3773	3623	3875	2297
% of Total	90.1	96.1	94.4	91.5	87.3	81.1	89.6	93.8
Average	10.1	9.9	7.1	7.1	8.0	11.0	9.0	10
Std. Dev.	5.5	5.1	3.9	4.2	4.0	5.7	5.0	4.1
Coeff. of Variation	0.54	0.52	0.55	0.59	0.5	0.52	0.56	0.41
Min	0.4	0.4	0.3	0.2	0.3	0.3	0.2	0.5
1st Quart.	5.7	5.8	4.3	3.7	5.0	6.9	5.6	7.0
Median	9.8	9.2	6.3	6.0	7.7	10.4	8.3	9.8
3rd Quart.	13.8	13.4	9.6	10.2	10.2	15	11.1	12.7
Max	29.8	25.7	21.9	19.8	24	27.1	27.8	23.8
99% CI– Low Bnd.	9.8	9.7	6.9	6.9	7.8	10.8	8.8	9.8
99% CI Up Bnd.	10.4	10.1	7.3	7.3	8.2	11.2	9.2	10.2

Table 6e: Horizontal Wind Speed (meters per second) Statistics by Month at 150m

Statistic	May	June	July	August	Sept.	October	Nov.	Dec.
Good Obs.	1889	2602	3550	2987	2543	2498	3178	1854
% of Total	54.7	60.2	79.5	64.9	58.8	55.9	73.5	75.7
Average	11.7	11.2	7.1	7.0	8.0	11.5	9.0	9.9
Std. Dev.	5.7	5.1	4.0	4.3	4.4	5.8	5.3	4.1

Coeff. of Variation	0.49	0.46	0.56	0.61	0.55	0.5	0.59	0.41
Min	0.5	1.0	0.3	0.5	0.4	0.5	0.2	1.0
1st Quart.	7.2	7.5	4.1	3.6	4.5	6.8	5.6	6.9
Median	11.7	11.0	6.3	5.7	7.6	11.3	8.0	9.7
3rd Quart.	15.5	14.6	9.4	10.1	10.4	15.7	10.4	12.5
Max	30.2	25.1	23.4	19.6	24.2	27.3	29.9	24.3
99% CI– Low Bnd.	11.4	10.9	6.9	6.8	7.8	11.2	8.8	9.7
99% CI Up Bnd.	12	11.5	7.3	7.2	8.2	11.8	9.2	10.1

Table 6f: Horizontal Wind Speed (meters per second) Statistics by Month at 175m

Statistic	May	June	July	August	Sept.	October	Nov.	Dec.
Good Obs.	1215	1207	1845	1466	1176	1629	2306	1382
% of Total	35.2	27.9	41.3	31.8	27.2	36.5	53.3	56.5
Average	12.1	11.3	7.5	8.5	8.2	11.5	8.6	9.3
Std. Dev.	5.0	4.1	3.8	4.6	4.4	5.7	5.3	4.2
Coeff. of Variation	0.41	0.36	0.51	0.54	0.54	0.5	0.62	0.45
Min	0.7	0.6	0.6	0.4	0.6	1.1	0.3	0.4
1st Quart.	9.0	8.5	4.6	4.6	4.9	7.1	5.4	6.3
Median	11.9	11.2	7.0	7.9	8.0	11.0	7.55	8.8
3rd Quart.	14.9	13.7	9.9	12.1	10.8	15.2	10	11.9
Max	30.9	22.2	23.8	19.4	21.2	26.9	31.5	23.0
99% CI– Low Bnd.	11.7	11.0	7.3	8.2	7.9	11.1	8.3	9.0
99% CI Up Bnd.	12.5	11.6	7.7	8.8	8.5	11.9	8.9	9.6

Table 6g: Horizontal Wind Speed (meters per second) Statistics by Month on Buoy Deck

Statistic	May	June	July	August	Sept.	October	Nov.	Dec.
Good Obs.	3456	4323	4453	4453	4320	4459	4307	2448
% of Total	100	100	99.8	99.8	100	99.9	99.7	100
Average	4.9	5.1	4.8	5.4	6.9	8.3	7.0	7.8
Std. Dev.	2.1	2.3	2.3	2.7	2.9	3.8	3.1	2.6

Coeff. of Variation	0.43	0.45	0.48	0.5	0.42	0.46	0.44	0.33
Min	0.3	0.2	0.2	0.5	0.4	0	0	0.7
1st Quart.	3.4	3.3	3.2	3.5	4.8	5.4	4.8	5.9
Median	4.9	4.9	4.6	5.1	7.1	8.2	6.8	7.7
3rd Quart.	6.5	6.6	6.1	6.6	8.8	10.9	9.1	9.9
Max	19.1	14.1	15.0	14.8	17.0	19.3	16.8	14.4
99% CI– Low Bnd.	4.8	5.0	4.7	5.3	6.8	8.2	6.9	7.7
99% CI Up Bnd.	5.0	5.2	4.9	5.5	7.0	8.4	7.1	7.9

Tables 7a through 7g show the 99% confidence intervals for the mean difference in average wind speed between the same range gate for adjacent months. The difference is later month – earlier month such as August values – July values. Homogeneity of variance is assumed.

Table 7a: Horizontal Wind Speed – Average Difference by Adjacent Months – 75m

Statistic	June - May	July – June	August – July	Sept. - August	October – Sept.	Nov. - October	December – Nov.
Average Difference	-0.2	-2.7	-0.1	0.8	3.0	-2.0	1.0
Pooled Std. Dev.	5.1	4.4	3.9	4.0	4.7	5.1	4.4
99% CI– Low Bnd.	-0.5	-2.9	-0.3	0.6	2.7	-2.3	0.7
99% CI Up Bnd.	0.1	-2.5	0.1	1.0	3.3	-1.7	1.3

Table 7b: Horizontal Wind Speed – Average Difference by Adjacent Months – 90m

Statistic	June - May	July – June	August – July	Sept. - August	October – Sept.	Nov. - October	December – Nov.
Average Difference	-0.2	-2.7	-0.1	1.0	3.0	-2.3	1.1
Pooled Std. Dev.	5.1	4.4	4.0	4.0	4.7	5.1	4.5
99% CI– Low Bnd.	-0.5	-2.9	-0.3	0.8	2.7	-2.6	0.8
99% CI Up Bnd.	0.1	-2.5	0.1	1.2	3.3	-2.0	1.4

Table 7c: Horizontal Wind Speed – Average Difference by Adjacent Months – 105m

Statistic	June - May	July – June	August – July	Sept. - August	October – Sept.	Nov. - October	December – Nov.

Average Difference	-0.1	-2.8	0.0	1.0	3.0	-2.2	1.1
Pooled Std. Dev.	5.2	4.4	4.0	4.1	4.8	5.2	4.6
99% CI– Low Bnd.	-0.4	-3.0	-0.2	0.8	2.7	-2.5	0.8
99% CI Up Bnd.	0.2	-2.6	0.2	1.2	3.3	-1.9	1.4

Table 7d: Horizontal Wind Speed – Average Difference by Adjacent Months – 125m

Statistic	June - May	July – June	August – July	Sept. - August	October – Sept.	Nov. - October	December – Nov.
Average Difference	-0.2	-2.8	0.0	0.9	3.0	-2.0	1.0
Pooled Std. Dev.	5.3	4.5	4.1	4.1	4.9	5.3	4.7
99% CI Low Bnd.	-0.5	-3.1	-0.2	0.7	2.7	-2.3	0.7
99% CI Up Bnd.	0.1	-2.5	0.2	1.1	3.3	-1.7	1.3

Table 7e: Horizontal Wind Speed – Average Difference by Adjacent Months – 150m

Statistic	June - May	July – June	August – July	Sept. - August	October – Sept.	Nov. - October	December – Nov.
Average Difference	-0.5	-4.1	-0.1	1.0	3.5	-2.5	0.9
Pooled Std. Dev.	5.4	4.5	4.1	4.3	5.1	5.5	4.9
99% CI Low Bnd.	-0.9	-4.4	-0.4	0.7	3.1	-2.9	0.5
99% CI Up Bnd.	-0.1	-3.8	0.2	1.3	3.9	-2.1	1.3

Table 7f: Horizontal Wind Speed – Average Difference by Adjacent Months – 175m

Statistic	June - May	July – June	August – July	Sept. - August	October – Sept.	Nov. - October	December – Nov.
Average Difference	-0.8	-3.8	1.0	-0.3	3.3	-2.9	0.7
Pooled	4.6	3.9	4.2	4.5	5.2	5.5	4.9

Std. Dev.							
99% CI Low Bnd.	-1.3	-4.2	0.6	-0.8	2.8	-3.4	0.3
99% CI Up Bnd.	-0.3	-3.4	1.4	0.2	3.8	-2.4	1.1

Table 7g: Horizontal Wind Speed – Average Difference by Adjacent Months – Buoy Deck

Statistic	June - May	July – June	August – July	Sept. - August	October – Sept.	Nov. - October	December – Nov.
Average Difference	0.2	-0.3	0.6	1.5	1.4	-1.3	0.8
Pooled Std. Dev.	2.2	2.3	2.5	2.8	3.4	3.5	2.9
99% CI Low Bnd.	0.1	-0.4	0.5	1.3	1.2	-1.5	0.6
99% CI Up Bnd.	0.3	-0.2	0.7	1.7	1.6	-1.1	1.0

Discussion points:

9. For each of the heights, the largest average wind speed is in October due to the residual effects of a hurricane in the Atlantic Ocean.
10. The general pattern in average wind speed is decline from May through August and increase from September through December, disregarding the October value as discussed in point one. This pattern is also seen in the median values.
11. The difference in average wind speeds for May and June is not statistically significant ($\alpha = 0.01$) for heights: 75m, 90m, 105m, and 125m but is statistically significant for heights 150m and 175m.
12. The difference in average wind speeds for June and July is statistically significant ($\alpha = 0.01$) for all heights.
13. The difference in average wind speeds for July and August is not statistically significant ($\alpha = 0.01$) for height 175m but is statistically significant for heights 75m, 90m, 105m, 125m and 150m.
14. The difference in average wind speeds for August and September is not statistically significant ($\alpha = 0.01$) for height 175m but is statistically significant for heights 75m, 90m, 105m, 125m and 150m.

15. The difference in average wind speeds for November and December is statistically significant (α = 0.01) for all heights.
16. The average wind speed pattern based on points 3 through 7 is level average wind speed in May and June, a large drop in average wind speed in July from June, level average wind speed in July and August, and increasing average wind speed starting in September with the average returning to May levels by December.

Wind Direction by Height

The wind rose graphs show the wind speed by direction as well as the percent of time the wind was blowing in each direction. The percent of time the wind was coming from a particular direction is shown by the inner and outer circles. For range gate one, the inner circle represents the wind coming from a particular direction 4% of the time and the outer circle 9% of the time.

Note that for each height, the dominate wind direction is SSW.

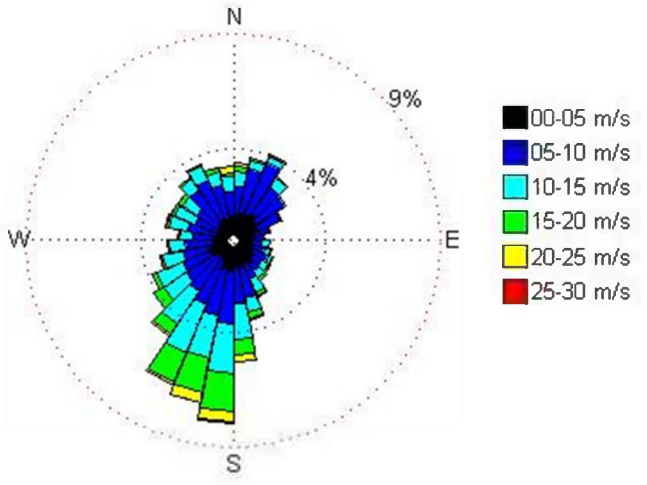

Range Gate 1: Average Wind Speed and Percent Time by Direction

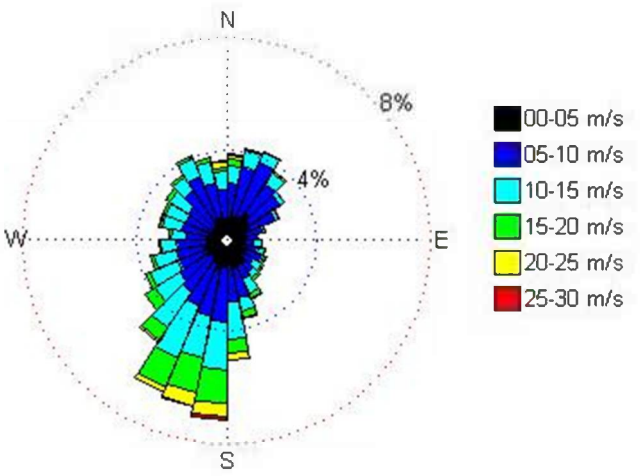

Range Gate 2: Average Wind Speed and Percent Time by Direction

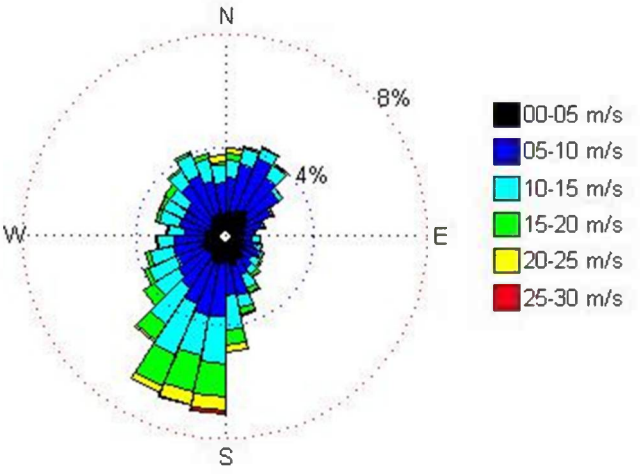

Range Gate 3: Average Wind Speed and Percent Time by Direction

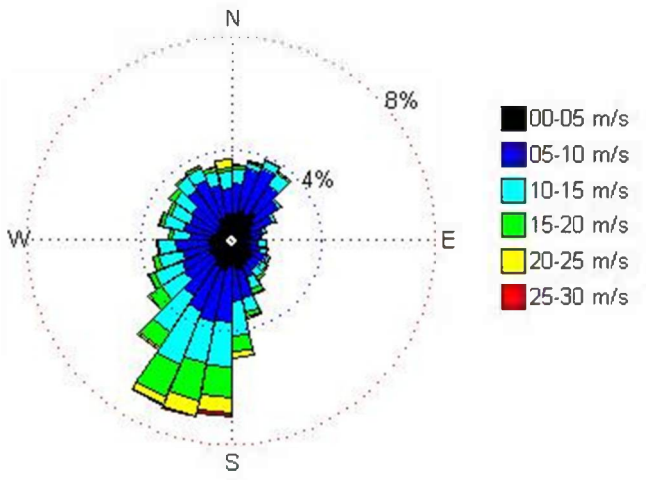

Range Gate 4: Average Wind Speed and Percent Time by Direction

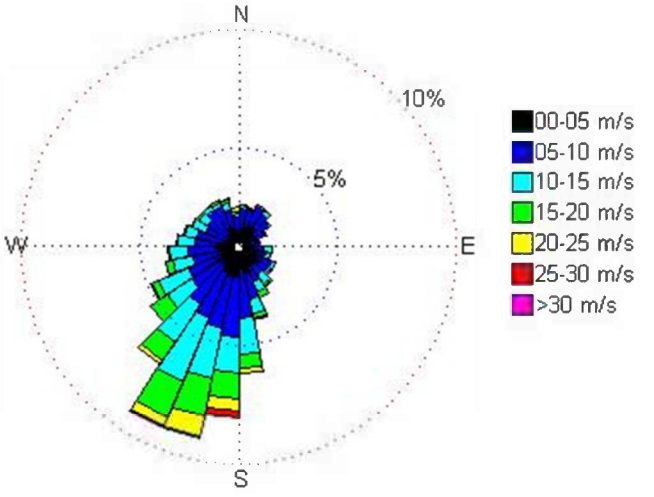

Range Gate 5: Average Wind Speed and Percent Time by Direction

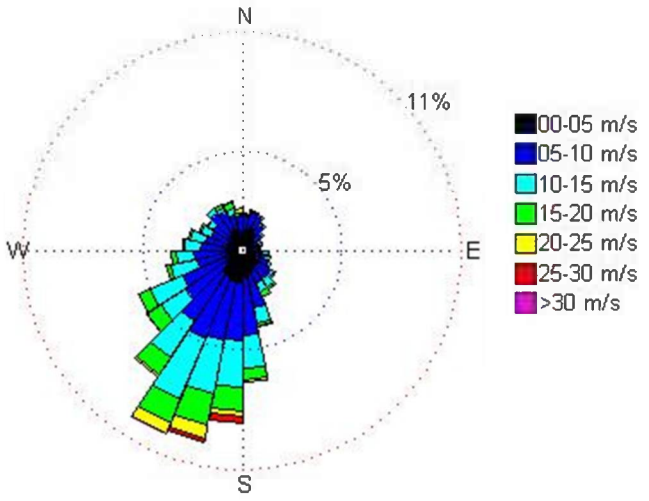

Range Gate 6: Average Wind Speed and Percent Time by Direction

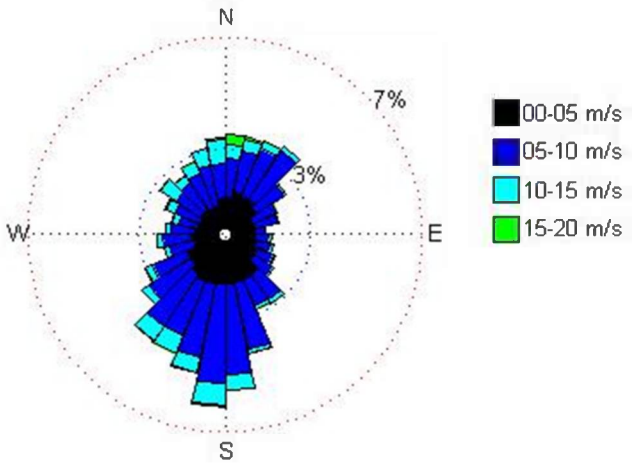

Buoy Cup Anemometer: Average Wind Speed and Percent Time by Direction

Wind Direction by Month

Table 8 shows the wind direction by month for each height. The percent of time the wind direction was in the range SSE (135 degrees) to SSW (225 degrees) as well as the percent of time the wind direction was in the range NNW (315 degrees) to NNE(45 degrees) is shown. These wind direction is in one of these two directions a majority of the time.

Table 8: Horizontal Wind Direction by Month – Percent of Time Values

		May	June	July	August	Sept.	Oct.	Nov.	Dec.
75m	**SSE-SSW**	40.8	40.8	34.2	41.8	25.6	40.6	44.3	32.2
	NNW-NNE	28.0	24.1	27.9	20.6	30.6	30.6	21.3	22.3
90m	**SSE-SSW**	40.5	43.1	37.0	41.4	24.3	38.5	42.3	31.3
	NNW-NNE	29.0	24.4	27.6	20.7	32.0	33.2	24.5	22.7
105m	**SSE-SSW**	40.9	43.0	34.0	41.5	24.0	38.0	42.7	31.7
	NNW-NNE	29.0	24.4	28.2	21.0	32.1	33.4	24.5	22.9
125m	**SSE-SSW**	44.6	42.4	34.2	41.8	25.6	41.3	45.2	32.1
	NNW-NNE	27.1	23.5	28.1	21.5	29.5	28.8	20.3	22.4
150m	**SSE-SSW**	60.4	54.6	38.7	50.4	33.7	54.2	53.3	35.0
	NNW-NNE	9.1	12.7	23.0	10.9	21.0	17.3	12.8	18.9
175m	**SSE-SSW**	70.5	57.0	38.5	54.9	37.6	57.4	46.1	32.0
	NNW-	4.5	9.6	15.5	8.8	18.7	14.6	11.2	18.1

	NNE								
Buoy Deck	**SSE-SSW**	43.2	39.1	36.8	41.1	21.7	37.2	40.1	32.0
	NNW-NNE	29.0	20.7	27.7	20.1	33.3	35.8	26.4	22.6

Discussion Points:

6. The predominant wind direction from May through December is SSE-SSW, except for September when the predominant wind direction is NNW-NNE. This is true for heights 75m through 125m and the buoy deck. For these heights, the percent of good observations exceeded 90%.
7. For the heights where the percent of good observations was less than 90%, 150m and 175m, the predominant wind direction is SSE-SSW in September as well. As was discussed in the section on average wind speed by height, this may have to do with the performance of the LWS.

Wind Speed by Location / Year

In this section, the data collected from November 8 through December 17, 2012 at the mid-lake plateau are compared to data from the same days collected in 2011 at the initial deployment near Muskegon. The results are shown in table 9. Homogeneity of variance is assumed. Note that two variables are confounded regarding the comparison:

- Location (mid-lake plateau versus near Muskegon)
- Year (2011 versus 2012)

Table 9: Comparison of 2011 and 2012 Data

Statistic	**N001S009 P083 75m**	**N001S009 P084 90m**	**N001S009 P085 105m**	**N001S009 P086 125m**	**N001S009 P087 150m**	**N001S009 P088 175m**
2011						
Good Obs.	3679	3834	4336	4577	4204	3742
% of Total (5760)	61.0%	63.6%	71.9%	75.9%	69.7%	62.1%

Average	9.1	9.3	9.5	9.6	9.9	10.1
2012						
Good Obs.	4719	4763	4728	4625	3992	2945
% of Total (5760)	81.9%	82.7%	82.1%	80.3%	69.3%	51.1%
Average	9.1	9.4	9.5	9.5	9.2	8.5
Compare						
Average Difference	0.0073	0.11	0.040	-0.16	-0.71	-1.6
Pooled Std. Dev.	4.1	4.2	4.2	4.4	4.5	4.5
99% CI– Lower Bound	-0.22	-0.12	-0.19	-0.39	-0.97	-1.9
99% CI Upper Bound	0.24	0.34	0.27	0.08	-0.45	-1.3

Discussion points:

1. The difference in average wind speed at range gate heights 75m, 90m, 105m, and 125m is not statistically significant ($\alpha = 0.01$).
2. The average difference at heights 150m and 175m is statistically significant ($\alpha = 0.01$).
3. The average wind speed at 150m and 175m is decreasing with height in 2012 and increasing in 2011.

Appendix C

Lake Michigan Wind Assessment Project

Data Summary and Analysis Comparing

2013 and 2012 Offshore Wind Assessment Seasons

April 2014

Executive Summary

A laser wind sensor mounted on a floating platform in Lake Michigan was used to measure wind speed and direction at six heights: 75, 90, 105, 125, 150, 175 meters. The laser sensor was located in 2012 at the mid-lake plateau (4320.5100N, 8707.2057W) from May 8 through December 17 and in 2013 near Muskegon (4316.542N, 8630.347W) from April 28 through December 20. A comparison of wind speed and direction with respect to location is of interest. However, buoy location is a confounding variable in comparing data by year. This was addressed by examining data from surface level buoys in both 2012 and 2013 that are located near the mid-Lake plateau and near-Muskegon.

Data from both lake-based surface level buoys showed slower average wind speeds in 2013 than in 2012. The differences between years, which are statistically significant ($\alpha = 0.01$), were 0.38m/s near the mid-Lake plateau and 0.25m/s near Muskegon.

With regard to location, the average wind speed is slower near Muskegon than in near the mid-Lake plateau for each height. The average difference generally decreases with height from 0.72m/s to 0.20m/s. All differences are statistically significant ($\alpha = 0.01$). The average differences range from approximately 9% to 2% the average wind speeds. Considering the data from the surface level buoys as well, it can be concluded that the average wind speed differences are maximum differences due to location alone. Thus, the data support the idea that 90% to 95% of the wind energy available at the mid-Lake plateau is available at the near Muskegon location.

With regard to laser wind sensor performance, the LWS made observations for over 99.6% of all 10 minute intervals. For heights 125m, 150m, and 175m, the percent of good ten minute averages is greater at the near Muskegon location than at the mid-lake location. Since the LWS relies on detecting particle movement in the airflow, this may be due to a lack of such particles at the mid-lake plateau versus near shore as height increases. In addition, there is less mixing of the air layers in the mid-lake versus near shore resulting in less movement of particulate matter.

There is little difference in wind direction between the two locations from NNE to SSE and from SSW to NNW for range gate heights 75m through 125m. There is some difference at range gate heights 150m and 175m, where the percent of good observations is lower indicating the observations are made more often when the wind is blowing in one direction than another. Wind direction could correlate in this regard with wind speed.

2013 and 2012 Season Data

This report summarizes the data collected by the Laser Wind Sensor (LWS) OADS Vindicator #8, mounted on an AXYS NOMAD WindSentinel with collection information as follows.

Location:	**2013 --** Lake Michigan – Near Muskegon (4316.542N, 8630.347W)
	2012 -- Lake Michigan – Mid-lake Plateau (4320.5100N 8707.2057W)
Date:	**2013 --** April 28 through December 20, 2013 (UTC)
	2012 -- May 8 through December 17, 2012 (UTC)
Range Gates 1-6:	75, 90, 105, 125, 150, 175 meters
Cup Anemometer:	3 meters mounted on the buoy
Observations:	10-minute averages of wind speed and wind direction stored onboard the buoy
Quantities of Primary Interest:	Average wind speed, variation in wind speed, and distribution of wind direction
Independent Variables:	Range gate height, month, and location
Number of Observations:	**2013** -- 237 days at 6 observations per hour = 34128 observations
	2012 -- 224 days at 6 observations per hour = 32256 observations
Missing Observations:	**2013** --124 – (4/29/2013: 15:20; 7/5 at 0:30, 1:40-2:20; 7/16 at 15:50, 20:00, 20:20-20:40; 7/18 at 13:00-14:00, 14:30-14:40, 15:00-15:10, 15:40, 16:10-16:40; 10/1, 1730 to 1800 & 1840 to 1900 & 2130 to 2140; 10/2, 1420 to 1500 & 1920 to 1930; 10/29, 1820 to 2010; 10/31, 1430 to 1630; 11/5, 18:40 – 19:10; 11/18, 1:00-9:20)
	2012 -- 35 – (7/9 at 12:30-13:50; 7/24 at 11:10; 8/28 at 14:00 – 15:40; 10/23 at 18:40-18:50; 10/30 at 16:40; 11/8 at 13:10-13:20 and 14:00-15:20)
Good Observations:	**2013** -- 34004 (99.636%)
	2012 -- 32221 (99.891%)
	Missing observations are those not reported by LWS #8.

Differences in Wind Speed (2013 versus 2012)

The difference in wind speed measurements from 2013 and 2012 can be divided into the difference due to years and the difference due to location. These cannot be distinguished based on the data collected by LWS #8 only. Thus, data for each year was obtained from three surface level buoys as shown in table 1.

Table 1 – Location of Surface Level Buoys

Station ID	Owner	Location	Site Elevation above Sea Level (m)	Anemometer Height above Site Elevation (m)
45007	National Data Buoy Center	42.674 N 87.026 W	176.4	4
45161	Great Lakes Environmental Research Laboratory	43.178 N 86.361 W	176	2
MKG	Great Lakes Environmental Research Laboratory	43.228 N 86.339 W	179.1	6.1

Station ID 45007 corresponds to the mid-lake plateau site used for the buoy in 2012. Station ID 45161 corresponds to the near Muskegon site for the LWS unit used in 2013. Station ID MKG is on the lake shore near Muskegon.

The buoys collect data as follows:

- 45007 – Six 10 minutes averages per hour as well as 1 average per hour from April 1 through November 30 for both years
- 45161 – 1 average per hour for both years but from July 6 to October 25 in 2012 and from April 18 to November 30 in 2013
- MKG – From April 1 through November 30 in both years, 1 average per hour in 2012 and four 15 minute averages in 2013

Table 2 shows wind speed summary statistics for each buoy for 2012 and table 3 shows the same information for 2013. Table 4 gives an analysis of the difference in the average wind speed for the two years with homogeneity of variance assumed.

Table 2: Horizontal Wind Speed (meters per second) Statistics by Buoy for 2012

Statistic	Station 45007 -- Mid Lake 10 min averages 4/1 – 11/30	Station 45007 -- Mid Lake 1 hour averages 4/1 - 11/30	Station 45161 -- Off Muskegon 1 hour averages 7/6 – 10/25	Station MKGM4 -- Muskegon Shoreline 1 hour averages 4/1 – 11/30
Possible Obs.	35136	5856	2688	5856
Total Obs.	34843	5828	2409	5572
% Total Obs.	99.17	99.52	89.62	95.15
Good Obs.	34554			
% Good Obs.	99.17			
Average	5.8	5.8	5.1	5.6
Std. Dev.	3.0	3.1	2.6	3.1
Coefficient of Variation	0.52	0.53	0.51	0.55
Minimum	0	0	0	0
Quartile 1	3.7	3.7	3.0	3.1
Median	5.5	5.5	4.8	5.1
Quartile 3	7.7	7.7	6.9	7.7
Maximum	19.4	19.4	13.0	18.5
99% CI– Lower Bound	5.76	5.7	5.0	5.5
99% CI Upper Bound	5.84	5.9	5.2	5.7

Table 3: Horizontal Wind Speed (meters per second) Statistics by Buoy for 2013

Statistic	Station 45007 -- Mid Lake 10 min averages 4/1 – 11/30	Station 45007 -- Mid Lake 1 hour averages 4/1 - 11/30	Station 45161 -- Off Muskegon – 1 hour averages 4/18 – 11/30	Station MKGM4 -- Muskegon Shoreline 15 min averages 4/1 – 11/30
Possible Obs.	35136	5856	5448	23424
Total Obs.	34778	5817	4478	22430
% Total Obs.	98.98	99.33	82.20	95.76
Good Obs.	34423			
% of Total	98.98			
Average	5.5	5.5	4.8	5.5
Std. Dev.	3.1	3.1	2.7	3.1
Coefficient of Variation	0.56	0.56	0.56	0.56
Minimum	0	0	0	0
Quartile 1	3.1	3.1	2.9	3.1
Median	5.1	5.1	4.4	4.6
Quartile 3	7.4	7.4	6.4	7.2
Maximum	20.8	17.5	14.3	23.7
99% CI– Lower Bound	5.46	5.4	4.7	5.45
99% CI Upper Bound	5.54	5.6	4.9	5.55

Table 4: Horizontal Wind Speed (meters per second) Comparison of 2012 and 2013

Statistic	Station 45007 -- Mid Lake 10 min averages	Station 45007 -- Mid Lake 1 hour averages	Station 45161 -- Off Muskegon – 1 hour averages	Station MKGM4 -- Muskegon Shoreline 1 hour and 15 min averages
Average Difference (2012-2013)	0.38	0.38	0.25	0.12
Pooled Std. Dev.	3.1	3.1	2.6	3.1
99% CI– Lower Bound	0.32	0.23	0.08	-0.01
99% CI Upper Bound	0.44	0.52	0.42	0.24

Notes:

1. The two buoys in Lake Michigan show slower average wind speeds in to 2013 than in 2012, which are statistically significant ($\alpha = 0.01$).
2. The land based buoy shows a lower average wind speed difference than the buoys in Lake Michigan, which is not statistically significant ($\alpha = 0.01$).

Table 5 shows wind speed summary statistics for range gate for 2012 and table 6 shows the same information for 2013. Table 7 gives an analysis of the difference in the average wind speed for the two years with homogeneity of variance assumed. The averages and standard deviations used for the computations whose results are shown in Table 7 use data from May 8 through December 17 in each of the two years.

Table 5: Horizontal Wind Speed (meters per second) Statistics by Range Gate for 2012

Statistic	N001S007 P006 Cup Anemometer	N001S009 P083 75m	N001S009 P084 90m	N001S009 P085 105m	N001S009 P086 125m	N001S009 P087 150m	N001S009 P088 175m
Good Obs.	32216	30076	30951	30882	29265	21101	12226
% of Total (32256)	99.9	93.2	96.0	95.7	90.7	65.4	37.9
Average	6.2	8.7	8.9	9.0	8.9	9.2	9.5
Std. Dev.	3.1	4.7	4.8	4.8	4.9	5.2	5.0
Coeff. of Variation	0.50	0.54	0.54	0.53	0.55	0.57	0.53
Minimum	0.0	0.2	0.2	0.2	0.2	0.2	0.3
Quartile 1	4.0	5.1	5.3	5.4	5.1	5.2	5.7
Median	5.9	8.0	8.3	8.4	8.2	8.4	8.8
Quartile 3	8.2	11.6	11.9	12.0	11.9	12.4	12.5
Maximum	19.3	28.3	28.7	29.2	29.8	30.2	31.5
99% CI– Lower Bound	6.2	8.6	8.8	8.9	8.8	9.1	9.4
99% CI Upper Bound	6.2	8.8	9.0	9.1	9.0	9.3	9.6

Table 6: Horizontal Wind Speed (meters per second) Statistics by Range Gate for 2013

Statistic	N001S007 P006 Cup Anemometer	N001S009 P083 75m	N001S009 P084 90m	N001S009 P085 105m	N001S009 P086 125m	N001S009 P087 150m	N001S009 P088 175m
Good Obs.	33899	25806	29532	32394	32731	30482	23050
% of Total (34128)	99.3	75.6	86.5	94.9	95.9	89.3	67.5
Average	5.9	8.0	8.2	8.5	8.7	8.8	9.2
Std. Dev.	3.2	4.3	4.3	4.4	4.4	4.4	4.3
Coeff. of Variation	0.54	0.54	0.52	0.52	0.51	0.50	0.47
Minimum	0	0.2	0.2	0.1	0.2	0.2	0.3
Quartile 1	3.5	4.9	5.1	5.3	5.4	5.6	6.1
Median	5.4	7.3	7.6	7.9	8.2	8.3	8.7
Quartile 3	7.8	10.4	10.7	11.1	11.3	11.4	11.7
Maximum	19.6	80.9	49.7	57.0	53.6	56.4	33.3
99% CI– Lower Bound	5.9	7.9	8.1	8.4	8.6	8.7	9.1
99% CI Upper Bound	5.9	8.1	8.3	8.6	8.8	8.9	9.3

Table 7: Comparison of 2012 and 2013 Data

Statistic	N001S007 P006 Cup Anemometer	N001S009 P083 75m	N001S009 P084 90m	N001S009 P085 105m	N001S009 P086 125m	N001S009 P087 150m	N001S009 P088 175m
Average Difference (2012-2013)	0.27	0.72	0.71	0.53	0.23	0.36	0.20
Pooled Std. Dev.	0.31	4.6	4.5	4.6	4.6	4.7	4.5
99% CI– Lower Bound	0.21	0.62	0.62	0.44	0.13	0.25	0.07
99% CI Upper Bound	0.34	0.82	0.81	0.63	0.33	0.47	0.33

Notes:

Wind Speed

1. For the six range gates:
    a. All differences in the average wind speeds are statistically significant ($\alpha = 0.01$).
    b. The average differences are less than 10% of the average wind speed.
    c. The average differences decrease with height in general except for 105m to 125m and 125m to 150m.
    d. The positive difference indicates a slower wind speed in 2013 near Muskegon than in 2012 at the mid-lake plateau.
2. For the cup anemometer, the average wind speed difference is statistically significant ($\alpha = 0.01$), less than 10% of the average wind speed, and slower in 2013 than 2012.

3. Based on the data from the surface level buoys, it can be concluded that the average wind speed in 2013 is less than the average wind speed in 2012 at the mid-lake LWS location and at the near Muskegon LWS location. Thus, it can be concluded that the average differences shown in Table 7 are the maximum difference due to location alone. That is, the average wind speed at the mid-lake location is no more than 10% greater than average wind speed at the near Muskegon location and likely less.

LWS Performance

7. Overall, the LWS made observations for 99.5% of all 10 minute intervals.
8. For heights 125m, 150m, and 175m, the percent of good ten minute averages is greater at the near Muskegon location than at the mid-lake location. Since the LWS relies on detecting particle movement in the airflow, this may be due to a lack of such particles at the mid-lake plateau versus near shore as height increases. In addition, there is less mixing of the air layers in the mid-lake versus near shore resulting in less movement of particulate matter.

Differences in Wind Speed (2013 versus 2012) – Storm Data Removed

Wind speeds in Lake Michigan were affected by storms in October 2012 due to hurricane Sandy and in November 2013. The effect of the storms was removed from the analysis of wind differences by repeating the analyses presented in Tables 2-7 with the data from October 2012 and November 2013 removed. The results are shown in Tables 8-13.

Table 8: Horizontal Wind Speed (meters per second) Statistics by Buoy for 2012 -- No October Data

Statistic	Station 45007 -- Mid Lake 10 min averages 4/1 – 11/30	Station 45007 -- Mid Lake 1 hour averages 4/1 - 11/30	Station 45161 -- Off Muskegon 1 hour averages 7/6 – 9/30	Station MKGM4 -- Muskegon Shoreline 1 hour averages 4/1 – 11/30
Possible Obs.	30672	5112	2088	5112
Total Obs.	30422	5088	1869	4864
% Total Obs.	99.19	99.53	89.51	95.15
Good Obs.	30174			
% Good Obs.	99.18			
Average	5.5	5.5	4.7	5.4
Std. Dev.	2.8	2.8	2.3	2.8
Coefficient of Variation	0.50	0.51	0.49	0.52
Minimum	0	0	0	0
Quartile 1	3.5	3.5	2.8	3.1
Median	5.2	5.2	4.4	4.6
Quartile 3	7.1	7.2	6.3	7.2
Maximum	17.2	16.7	12.9	18.5

99% CI– Lower Bound	5.42	5.4	4.6	5.3
99% CI Upper Bound	5.50	5.6	4.8	5.5

Table 8: Horizontal Wind Speed (meters per second) Statistics by Buoy for 2013 -- No November Data

Statistic	Station 45007 -- Mid Lake 10 min averages 4/1 – 10/31	Station 45007 -- Mid Lake 1 hour averages 4/1 - 10/31	Station 45161 -- Off Muskegon 1 hour averages 4/18 – 10/31	Station MKGM4 -- Muskegon Shoreline 1 hour averages 4/1 – 10/31
Possible Obs.	30672	5112	4728	20544
Total Obs.	30492	5102	3878	19951
% Total Obs.	99.41	99.80	82.02	97.11
Good Obs.	30313			
% Good Obs.	99.41			
Average	4.9	4.9	4.3	5.1
Std. Dev.	2.7	2.7	2.3	2.8
Coefficient of Variation	0.55	0.55	0.53	0.55
Minimum	0	0	0	0
Quartile 1	2.9	2.9	2.6	3.1
Median	4.6	4.6	4.1	4.6
Quartile 3	6.6	6.6	5.7	6.7
Maximum	18	17.5	14.3	21.6
99% CI– Lower Bound	4.87	4.8	4.2	5.05
99% CI Upper Bound	4.95	5.0	4.4	5.15

Table 9: Horizontal Wind Speed (meters per second) Comparison of 2012 (No October Data) and 2013 (No November Data)

Statistic	Station 45007 -- Mid Lake 10 min averages	Station 45007 -- Mid Lake 1 hour averages	Station 45161 -- Off Muskegon – 1 hour averages	Station MKGM4 -- Muskegon Shoreline 1 hour and 15 min averages
Average Difference (2012-2013)	0.55	0.54	0.31	0.25
Pooled Std. Dev.	2.7	2.7	2.3	2.8
99% CI– Lower Bound	0.50	0.40	0.14	0.14
99% CI Upper Bound	0.61	0.68	0.48	0.37

Notes:

1. The two buoys in Lake Michigan show slower average wind speeds in to 2013 than in 2012, which are statistically significant ($\alpha = 0.01$).
2. The land based buoy shows a lower average wind speed difference than the buoys in Lake Michigan, which is statistically significant ($\alpha = 0.01$).
3. The average difference with storms shown in Table 4 is less than the average difference without storms shown in Table 9.

Table 10: Horizontal Wind Speed (meters per second) Statistics by Range Gate for 2012 – No October Data

Statistic	N001S007 P006 Cup Anemometer	N001S009 P083 75m	N001S009 P084 90m	N001S009 P085 105m	N001S009 P086 125m	N001S009 P087 150m	N001S009 P088 175m
Good Obs.	27757	26241	26854	26798	25642	18603	10597
% of Total (27792)	99.87	94.42	96.62	96.42	92.26	66.94	38.13
Average	5.9	8.4	8.6	8.7	8.6	8.9	9.1
Std. Dev.	2.8	4.6	4.6	4.6	4.7	5.0	4.7
Coeff. of Variation	0.48	0.54	0.53	0.53	0.55	0.57	0.52
Minimum	0	0.2	0.2	0.2	0.2	0.2	0.3
Quartile 1	3.8	4.9	5.1	5.2	5	5	5.6
Median	5.6	7.7	8	8.1	7.9	8.2	8.5
Quartile 3	7.7	11.2	11.5	11.5	11.5	11.8	12.1
Maximum	19.1	28.3	28.7	29.2	29.8	30.2	31.5
99% CI– Lower Bound	5.85	8.3	8.5	8.6	8.5	8.8	9.0
99% CI Upper Bound	5.94	8.5	8.7	8.8	8.7	9.0	9.2

Table 11: Horizontal Wind Speed (meters per second) Statistics by Range Gate for 2013 – No November Data

Statistic	N001S007 P006 Cup Anemometer	N001S009 P083 75m	N001S009 P084 90m	N001S009 P085 105m	N001S009 P086 125m	N001S009 P087 150m	N001S009 P088 175m
Good Obs.	27765	20987	24008	26386	26707	24763	18420
% of Total (27816)	99.39	75.13	85.94	94.45	95.60	88.64	65.93
Average	5.4	7.5	7.8	8.0	8.2	8.3	8.8
Std. Dev.	2.8	4.2	4.1	4.2	4.2	4.2	4.1
Coeff. of Variation	0.52	0.56	0.52	0.52	0.51	0.50	0.46
Minimum	0	0.2	0.2	0.1	0.2	0.2	0.3
Quartile 1	3.3	4.6	4.8	5	5.1	5.3	5.9
Median	5	6.9	7.2	7.5	7.8	7.9	8.4
Quartile 3	7.1	9.7	10	10.4	10.6	10.8	11.2
Maximum	19.4	80.9	49.7	57	53.6	56.4	27.6
99% CI– Lower Bound	5.34	7.46	7.69	7.96	8.14	8.27	8.7
99% CI Upper Bound	5.43	7.61	7.82	8.09	8.27	8.42	8.9

Table 12: Comparison of 2012 (No October Data) and 2013 (No November Data)

Statistic	N001S007 P006 Cup Anemometer	N001S009 P083 75m	N001S009 P084 90m	N001S009 P085 105m	N001S009 P086 125m	N001S009 P087 150m	N001S009 P088 175m
Average Difference (2012-2013)	0.51	0.85	0.85	0.65	0.39	0.51	0.32
Pooled Std. Dev.	0.28	4.4	4.3	4.4	4.5	4.6	4.4
99% CI– Lower Bound	0.45	0.75	0.75	0.56	0.29	0.39	0.18
99% CI Upper Bound	0.57	0.96	0.95	0.75	0.49	0.62	0.45

Notes:

Wind Speed

1. For the six range gates:
    a. All differences in the average wind speeds are statistically significant ($\alpha = 0.01$).
    b. The average differences are less than 12% of the average wind speed.
    c. The average differences decrease with height in general except for 125m to 150m.
    d. The positive difference indicates a slower wind speed in 2013 near Muskegon than in 2012 at the mid-lake plateau.
2. For the cup anemometer, the average wind speed difference is statistically significant ($\alpha = 0.01$), less than 10% of the average wind speed, and slower in 2013 than 2012.
3. Based on the data from the surface level buoys, it can be concluded that the average wind speed in 2013 is less than the average wind speed in 2012 at the mid-lake LWS location and at

the near Muskegon LWS location. Thus, it can be concluded that the average differences shown in Table 12 are the maximum difference due to location alone. That is, the average wind speed at the mid-lake location is no more than 12% greater than average wind speed at the near Muskegon location and likely less.

4. Based on the statistics in tables 4 and 9, the difference in average wind speed near the lake surface when no storms are present is slightly greater than when storms are present. The average differences shown in Table 12 are slightly larger than those shown in Table 7. This further supports the conclusion that the average differences shown in Tables 7 and 12 are the maximum differences due to location alone.

LWS Performance

1. For heights 125m, 150m, and 175m, the percent of good ten minute averages is greater at the near Muskegon location than at the mid-lake location. Since the LWS relies on detecting particle movement in the airflow, this may be due to a lack of such particles at the mid-lake plateau versus near shore as height increases. In addition, there is less mixing of the air layers in the mid-lake versus near shore resulting in less movement of particulate matter.

Differences in Wind Direction (2013 versus 2012)

The following tables compare wind directions for 2012 and 2013.

Table 13: Horizontal Wind Direction by Range Gate for 2012 and 2013 -- Percent of Time

Statistic	N001S007 P006 Cup Anemometer	N001S009 P083 75m	N001S009 P084 90m	N001S009 P085 105m	N001S009 P086 125m	N001S009 P087 150m	N001S009 P088 175m
0 -180							
2012	45.9	38.8	38.6	38.1	36.5	32.0	28.5
2013	45.7	40.7	40.5	40.1	39.6	39.7	38.1
180-360							
2012	54.0	61.2	61.3	61.7	63.3	68.0	71.5
2013	54.4	59.2	59.5	60.0	60.4	60.4	61.7
0-90							
2012	22.9	20.4	21.0	20.9	19.1	12.0	7.2
2013	17.5	13.8	15.8	17.4	17.5	16.7	12.9
90-180							
2012	23.0	18.4	17.6	17.2	17.4	20.0	21.3
2013	28.2	26.9	24.7	22.7	22.1	23.0	25.2
180-270							
2012	33.6	38.7	38.1	38.4	40.3	49.7	54.7
2013	26.1	36.1	34.2	32.4	32.4	33.9	38.9

270-360							
2012	20.4	22.5	23.2	23.3	23.0	18.3	16.8
2013	28.3	23.1	25.3	27.6	28.0	26.5	22.8

Table 14: Horizontal Wind Direction by Range Gate for 2012 (No October Data) and 2013 (No October Data) -- Percent of Time

Statistic	N001S007 P006 Cup Anemometer	N001S009 P083 75m	N001S009 P084 90m	N001S009 P085 105m	N001S009 P086 125m	N001S009 P087 150m	N001S009 P088 175m
0 -180							
2012	46.3	40.2	40.0	39.5	38.2	33.0	29.2
2013	48.2	42.4	42.3	42.0	41.7	41.7	39.7
180-360							
2012	53.7	59.8	60.0	60.6	61.8	67.1	70.8
2013	51.8	57.6	57.7	58.0	58.5	58.3	60.3
0-90							
2012	23.2	21.6	22.0	21.9	20.5	12.7	7.9
2013	18.7	17.1	18.8	19.0	18.1	13.8	18.7
90-180							
2012	23.0	18.6	18.0	17.6	17.7	20.3	21.3
2013	29.5	25.2	23.2	22.7	23.6	25.9	29.5
180-270							
2012	34.7	38.9	38.4	38.8	40.3	49.1	54.7
2013	24.8	33.8	32.0	32.0	33.4	38.4	24.8
270-360							
2012	19.0	20.9	21.6	21.8	21.5	18.0	16.1

2013	27.0	23.9	26.0	26.5	24.9	21.9	27.0

Notes:

1. When all data is considered (Table 13), there is little difference in wind direction between 2012 and 2013 from NNE to SSE and from SSW to NNW on the buoy deck and range gate heights 75m through 125m. There is some difference at range gate heights 150m and 175m, where the percent of good observations is lower indicating the observations are made more often when the wind is blowing in one direction than another. Wind direction could correlate in this regard with wind speed.
2. Again when all data is considered (Table 13), difference is wind direction between 2012 and 2013 is seen at all heights between north to east, east to south, south to west, and west to north with possible exception of south to west and west to north for 75m range gate.
3. When the storm data is eliminated (Table 14), the same difference as in points 1 and 2 are seen.

Acknowledgement and Disclaimer

Acknowledgements: "This material is based upon work supported by the Department of Energy; Grand Valley State University; Michigan Public Service Commission; We Energies; Sierra Club of the Great Lakes; Grand Valley State University; Michigan State University, Michigan Natural Features Inventory; and the University of Michigan, under Award Number DE-EE0000294. And the following organizations for technical support: National Oceanic and Atmospheric Administration/Great Lakes Environmental Research Laboratory; National Data Buoy Center; Pacific Northwest National Laboratory; United States Coast Guard; United States Army Corp of Engineers; Michigan Department of Natural Resources; and West Michigan Energy Partners."

Appendix D

Wind Energy Assessment using a Wind Turbine with Dynamic Yaw Control

Md Nahid Pervez

A Thesis Submitted to the Graduate Faculty of

GRAND VALLEY STATE UNIVERSITY

In

Partial Fulfillment of the Requirements
For the Degree of
Master of Science in Engineering
School of Engineering

April 2013

Acknowledgement and Disclaimer

Acknowledgements: "This material is based upon work supported by the Department of Energy; Grand Valley State University; Michigan Public Service Commission; We Energies; Sierra Club of the Great Lakes; Grand Valley State University; Michigan State University, Michigan Natural Features Inventory; and the University of Michigan, under Award Number DE-EE0000294. And the following organizations for technical support: National Oceanic and Atmospheric Administration/Great Lakes Environmental Research Laboratory; National Data Buoy Center; Pacific Northwest National Laboratory; United States Coast Guard; United States Army Corp of Engineers; Michigan Department of Natural Resources; and West Michigan Energy Partners."

Dedication

This thesis is dedicated to my parents. There is no word that can describe their contribution to my life and success.

Acknowledgement

This research is supported by the Lake Michigan Wind Energy Assessment Project by Michigan Alternative and Renewable Energy Center (MAREC). I express my gratitude to School of Engineering, Grand Valley State University for supporting my studies. I thank Bhakthavathsala Penumalli and Steven Taylor for helping me with the cumbersome wind data management. I also thank Dr. M. M. Azizur Rahman, Dr. Charles Standridge, Mr. Arn Boezaart and Dr. David Zeitler for their valuable inputs in the research. Finally I want to thank my thesis supervisor Dr. Mehmet Sözen for his guidance throughout this research.

Abstract

The goal of this project was to analyze the wind energy potential over Lake Michigan. For this purpose, a dynamic model of a utility-scale wind turbine was developed to estimate the potential electrical energy that could be generated. The dynamic model was supported by wind data collected by an unmanned buoy based Laser Wind Sensor data acquisition system that has been deployed in Lake Michigan since October, 2011. Data summarization tools were also developed to help profile the wind resource based on the collected data.

Table of Contents

List of Figures

List of Tables

Chapter 1

1.1 Introduction

The current energy crisis and the adverse effects of global warming are pushing us towards alternative and renewable energy sources. Among all the alternative energy sources wind energy has been the one that has attracted significant attention of scientists, engineers and energy policy makers. This is mainly because of its success in several European countries. These countries have utilized both onshore and offshore wind potential. In the United States efforts have been directed to both onshore and offshore wind technology advancement. It is projected that by 2020 the United States can meet 20% of its electrical energy demand by wind energy [1].

This recent emphasis on the wind energy has made the government and privately owned energy companies look for potential locations for wind farms. Since a wind farm requires a lot of land resources, not only onshore but also offshore wind farms seem quite attractive to wind farm developers because of the low land cost. Moreover, the wind on the offshore location has very low turbulence. That is very favorable for wind turbine performance. However, the cost of developing the base and maintenance of turbines on an offshore location is very high.

Assessing the wind energy potential of a location is an extensive and time consuming process. It requires a collaborative effort of different organizations and mutual sharing of expertise. The preliminary work is to collect the wind data at different altitudes. Analyzing wind data for different altitudes give a better picture of the wind profile of that location. Moreover, reliable high altitude data help to assess the wind potential more accurately. Present utility-scale wind turbines have a hub height of 50 m to 100 m. Typically at onshore locations the wind data are collected by setting up a MET tower and equipping it with wind speed and wind direction sensors. The MET tower height should be high enough to collect the real-time hub height data. However for offshore locations measuring and collecting high altitude wind data by installing a MET tower is quite troublesome and expensive. This is because of the high installation cost of establishing the foundation of the MET tower. In some of the offshore locations the installation of the MET tower is not permitted by state or federal law.

If MET tower is not an option the wind data can be collected by a small tower and then data can be extrapolated by using the power law relationship between wind speed and altitude. This is just an estimation process and the accuracy of this method varies from location to location. However, the present state of the art LIDAR technology can also be used to collect the wind data. In this technology there is no need of high towers. Therefore, this technology can operate even in marine environment.

The collected data then has to be processed and analyzed to estimate the wind energy that can be harnessed from that location. Several methodologies are available at present to analyze the wind data to estimate the energy that can be harnessed. However due to the intermittent and uncertain nature of wind it is very difficult to estimate the energy accurately. The current estimation methodologies employ gross simplifying assumptions and could consider more parameters of the utility-scale wind turbine to estimate the amount of wind energy that can be harnessed more accurately. In most cases the wind

farms on average can generate 25% of total generation capacity. As a result by design the wind farm has to be oversized to be able to meet the demand of energy. This implies a large installation cost which is detrimental to the popularity of this technology.

Michigan Alternative and Renewable Energy Center (MAREC) is a research and technology development entity of Grand Valley State University. MAREC is currently conducting a research project entitled, "Lake Michigan Wind Energy Assessment Project" in collaboration with University of Michigan, and Michigan State University. The primary purpose of this project, as the title suggests, is to conduct an assessment of wind energy potential over Lake Michigan. In this project wind data was collected from Lake Michigan (offshore location) with the help of an unmanned buoy named "Wind Sentinel" equipped with a LIDAR (light detection and ranging) sensor. It was the first time the LIDAR sensor was used on a marine environment in an unmanned buoy. The wind data were collected at a frequency of 1 Hz.

The data collected by the Wind Sentinel were used to estimate the potential wind energy that can be harnessed from Lake Michigan. To improve the accuracy of the estimation of wind energy a novel methodology to estimate the potential wind energy that can be converted into electricity was developed in this study. This method was capable of considering the effect of dynamic yaw movement of the wind turbine. The data sets collected by the Wind Sentinel required some pre-processing in order to eliminate the issues they had such as missing data and missing time stamps. A data pre-processing module was developed to perform the pre-processing task.

A parametric study was also performed to analyze the effect of the frequency of the data set on the energy estimate. This study required data sets averaged over different time periods. An averaging module to generate data sets averaged over 30 seconds, 1 minute, 2 minutes, 5 minutes, and 10 minutes was developed.

For representation of wind data a representation module capable of generating the typical wind regime representing techniques: wind roses and frequency distributions was also developed in this study.

1.2 Background

Great Lakes region is a great location for offshore wind energy generation. Several studies have been conducted on this area for wind energy assessment. An example is the Wisconsin Focus on Energy on Lake Michigan Offshore Wind Resource [2].

MAREC acquired an unmanned buoy system named Wind Sentinel that is capable of collecting meteorological data in marine environment on a moving platform. It has a state-of-the-art LIDAR sensor along with other sensors such as bird and bat sensors. This system was made by AXYS Technologies, Inc, Sydney, British Columbia, Canada. It is a stand-alone system capable of acquiring wind data at altitudes up to 175 m, at six different altitudes at a frequency of 1 Hz. It eliminates the necessity of putting a MET tower in an offshore location. This reduces the cost of data collection and the developer or research team does not have to go through the legal issues to acquire the permit to put up a MET tower on offshore location.

The most important feature of this data acquisition system is the LIDAR wind data collecting device. With the help of this technology it is now possible to sense the real time wind data at a height of 150 m or above. Previously one had to rely on the empirical models to estimate the wind speed at that height. This real time data is very useful for validating the existing models of boundary layer theory and also can be used to create a boundary layer model over a marine environment.

Two major studies were performed with the data collected from the Wind Sentinel. One was the validation of the LIDAR technology on a moving platform in a marine environment. The technology was new and had never been tested on a floating platform in a lake or sea. The other study was the wind energy potential assessment over the Lake Michigan. For this, the Wind Sentinel has been deployed since October 2011 in different parts of the lake at different times and collected valuable wind data. At regular intervals the collected data were retrieved from the buoy for further analysis.

1.3 Literature review

Estimation of the potential for electrical energy generation from wind at a location is quite complex and prone to non-precise estimation due to the uncertain nature of the winds. It is very hard to capture all the sources that affect the energy output by any model. The possible changes of the wind regimes at a particular location could be daily and seasonal variations. Moreover, this variation can never be predicted accurately as there are so many parameters that affect the speed, direction and turbulence in prevailing winds. As a result, the estimation of wind energy potential will always have a margin of error. Moreover, the energy output is also largely dependent on the wind energy conversion systems (WECS) such as different types of wind turbines. Different wind turbines will have different energy outputs over the same period of operation at a given location based on the turbine characteristics. For this reason the term 'wind power density' is widely used as a non-turbine-specific parameter. It refers to the available wind power per unit area for that location and can be found by the following equation.

$$P_{avail} = \frac{1}{2}\rho v^3 \tag{1}$$

where, P_{avail} is the available power in the prevailing wind in W/m^2, ρ is the density of the wind in kg/m^3, and v is the wind speed in m/s.

The term wind power density fails to provide any information about the energy that can be harnessed from that location. Researchers have been trying to develop mathematical models for assessing the performance of the wind turbines for quite a long time and significant improvements have been seen in this area. Generally the WECS such as wind turbines have a conversion factor that can be a constant value or a function of wind speed. By using this conversion factor the energy that can be harnessed can be estimated. In the case of wind turbine, this conversion factor is called the power coefficient.

A pure analytical approach is the starting point for the estimation of energy output by a generic wind turbine model. This approach is helpful for understanding the physics of flow of air through a wind turbine. Almost all of the pure analytical models deal with a generic wind turbine model. Some analytical models include Betz analysis, Gluert model, GGS model, and One two three equation [3].

However, in siting analysis of a wind farm these generic models fail to provide an accurate turbine specific estimation of the wind energy that can be harnessed. To eliminate this problem another technique is widely used. This technique uses the power curve of the utility-scale wind turbine and statistical wind data from the location of interest and estimates the energy output of the turbine. Several estimation processes based on this approach are available. These include Kiranoudis model, Polynomial modeling, Random number generation, and INL wind energy analysis model.

These models are described in the following section along with the assumptions they employ and their shortcomings.

1.3.1 Betz analysis

Albert Betz, a German physicist, proposed a theoretical approach [3] to estimate the ideal power coefficient of a wind turbine. A simplified diagram showing the model parameters can be found in Figure 1.1.

By using this model, the maximum theoretically possible power output by an ideal wind turbine can be found by the following equation

$$P_{max} = \frac{16}{27} \frac{1}{2} \rho A v^3 \tag{2}$$

where, P_{max} is the maximum power output, ρ is the density of the wind, A is the area of the rotor, and v is the prevailing wind speed.

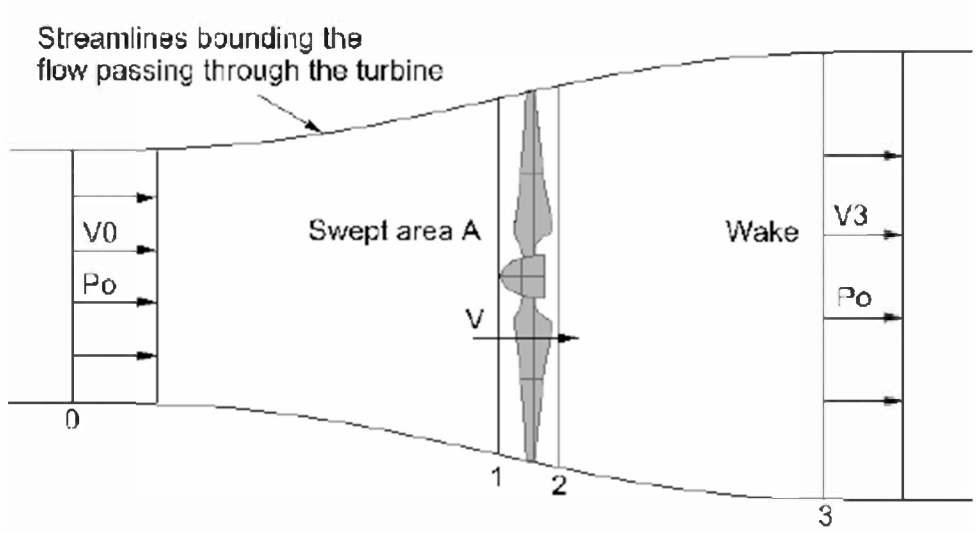

Figure 1.1 Betz model

The wind power density can also be found by rearranging the Equation (2).

$$\frac{P_{max}}{A} = \frac{16}{27} \frac{1}{2} \rho v^3 \tag{3}$$

where, $\frac{P_{max}}{A}$ is the maximum power density for ideal wind turbine.

From Equation (3) and Equation (1) it can be found that

$$\frac{P_{max}}{A} = \frac{16}{27} \quad P_{avail} \tag{4}$$

Equation (4) presents the theoretical maximum power coefficient as $\frac{16}{27}$ or 0.593. This means that, even with ideal wind turbine at most only 59.3% of the available wind power can be harnessed. This model also assumes the power coefficient to be a function of axial induction factor. Axial induction factor is the fractional decrease in wind velocity between the free stream and rotor plane and can be expressed by the equation:

$$a = \frac{V_0 - V}{V_0} \tag{5}$$

where, V_0 is the upstream velocity and V is the downstream velocity of the turbine.

The functional relationship between the power coefficient and the axial induction factor can be observed from Figure 1.2 [4].

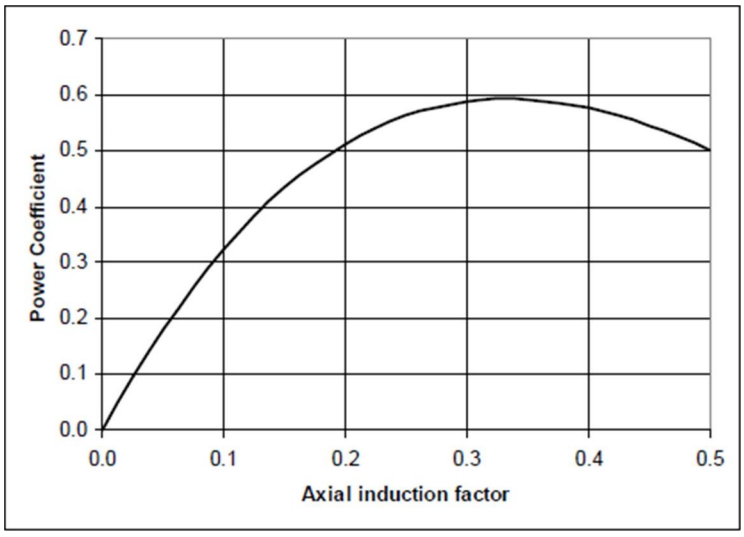

Figure 1.2 Power coefficient by Betz model as a function of axial induction factor

The major assumptions of this model are:

1. The rotor does not possess a hub; this is an ideal rotor, with an infinite number of blades which have no drag. Any resulting drag would only lower this idealized value.

2. The flow into and out of the rotor is axial. This is a control volume analysis, and to construct a solution the control volume must contain all flow going in and out. Failure to account for that flow would violate the conservation equations.
3. The flow is incompressible and inviscid. The flow is isothermal.

By analyzing the assumptions it can be stated that, the model is a very simplistic approach to a complex and unpredictable system. However, this model sets up the maximum theoretical limit for the power coefficient and gives a general idea about how much energy can be generated from any potential wind farm site. A real wind turbine never achieves this limit because of the following reasons [4]:

1. Rotation in the wake caused by the reaction with the spinning rotor.
2. A non-uniform pressure distribution in the turbine plane. The turbine plane is a virtual plane created by the turbine blades.
3. Aerodynamic drag due to viscous effects.
4. Energy loss due to vortices at the blade tips.

1.3.2 One two three equation

Carlin [6] proposed a mathematical model for estimating the generated energy by a WECS. The wind regime is modeled as a Rayleigh distribution and the average power output of a WECS is found by Equation (6). The hourly averaged wind speed, v_{ave}, is based on the Rayleigh distribution model. The annual energy, E_{ann} , can be found by Equation (7) which he called the one two three equation.

$$P_{ave} = \frac{\rho}{\rho_0}\left(\frac{2}{3}D\right)^2 v_{ave}^3 \tag{6}$$

$$E_{ann} = 8760\frac{\rho}{\rho_0}\left(\frac{2}{3}D\right)^2 v_{ave}^3 \tag{7}$$

where, P_{ave} is the available power in the prevailing wind in watts, ρ is density of the wind at that temperature in kg/m^3, ρ_0 is the density of the wind at standard temperature and pressure (STP) condition in kg/m^3, D is the diameter of the wind turbine in use in m, v_{ave} is the wind speed in m/s, and E_{ann} is the annual energy in joules.

Several assumptions were made to simplify the mathematical model in this technique. The major assumptions were [6]:

1. The rotor and power train have no inertia and are therefore at all times in equilibrium with the local wind both in rotational speed and in yaw alignment. There is neither friction nor any other mechanical loss.
2. The local wind speed probability density is given by the Rayleigh density expression. It is also assumed that a single number is sufficient to describe the instantaneous wind at the rotor disk.

3. The power coefficient of the turbine will be $C_p = {}^{16}/_{27}$, which is the classical Betz limit.

Although the accuracy of this method is not so high, it is widely accepted for its simplicity. An important issue is that the power coefficient is assumed to be the classical Betz limit which is not possible in real cases as stated before. However, only three parameters are needed for the estimation. That makes this method easy to apply.

1.3.3 Kiranoudis model

Kiranoudis proposed a method [7] of estimating the energy output of a wind turbine. In this method the power coefficient of a WECS is assumed to be a function of wind speed which is true for every WECS. The relation is found by the following Equation (8).

$$C_p = C_{pr} e^{\frac{(\ln v - \ln v_r)^2}{2(\ln s)^2}} \tag{8}$$

Here, the turbine characteristics are the nominal power coefficient, C_{pr}, the rated wind speed, v_r, and a parameter expressing the operating range of wind speed, s. The annual energy, E_{ann}, can be expressed as:

$$E_{ann} = 8760 \frac{\rho}{\rho_0} \frac{P_r}{v_r^3} \left(\int_0^{v_f} e^{\frac{(\ln v - \ln v_r)^2}{2(\ln s)^2}} \right) v^3 f(v) dv \tag{9}$$

The nominal power coefficient, C_{pr}, is the maximum value of power coefficient, C_p, for a given wind speed value representing the nominal performance of the turbine.

The assumptions for this model are:

1. The wind speed pattern can be modeled as Weibull distribution.
2. The power coefficient of the turbine is a function of wind speed.
3. The turbine rotor will face the wind direction normally at any instant.

This model needs six input parameters for estimating the energy output. That makes it hard to apply in energy estimation process. However this model has a considerably higher accuracy than the One two three equation [8].

1.3.4 Polynomial modeling

In Polynomial method [10-12], wind turbine power curve is approximated by a polynomial like the following equation.

$$P(v) = \begin{cases} 0 & v < v_c \; or \; v > v_f \\ P_r & v_r < v < v_f \\ (v^m - v_c^m)/(v_r^m - v_c^m) & v_c \leq v \leq v_r \end{cases} \tag{10}$$

where, $P(v)$ is the power output of the turbine in kW, P_r is the rated power output of the turbine , v_c , v_r , v_f are the cut-in speed, rated speed and the cut-out speed of the wind turbine respectively, and m is the order of the polynomial. In most of the cases the value is assumed to be 1 or 2.

The annual energy, E_{ann}, can be found by Equation (7).

$$E_{ann} = 8760 \frac{\rho}{\rho_0} \left(\int_{v_c}^{v_r} \frac{v^m - v_c^m}{v_r^m - v_c^m} f(v)dv + \int_{v_r}^{v_f} f(v)dv \right) \quad (11)$$

where, $f(v)$ is the Weibull distribution function, v_c , v_r , v_f are the cut-in speed, rated speed and the cut-out speed of the wind turbine respectively.

This model has higher accuracy of estimating the energy for pitch controlled wind turbines [8]. A wind turbine can have three types of control and the power curve varies for each case. Figure 1.3 shows the typical power curve shape for pitch control, stall control and yaw control wind turbine.

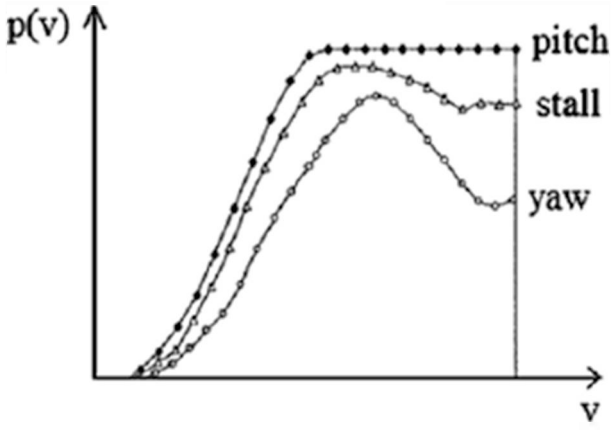

Figure 1.3 Typical power curves of modern utility-scale turbines

Nowadays mostly the pitch control turbine is used for its steady power output (rated power) for a range of wind speed.

As in previous estimation techniques this method has an assumption that the turbine has no inertia or mechanical resistance that prevents yaw rotation, i.e., the turbine rotor will face the wind perpendicularly at any instant.

1.3.5 Random number generation

In random number generation method [8], hourly wind speed values during a period of year are synthesized by means of generation of 8760 random numbers based on the Weibull distribution. For this the parameters of Weibull distribution have to be known a priori. The annual energy output, E_{ann}, can be estimated by the following equation.

$$E_{ann} = \frac{\rho}{\rho_0} \sum_{i=1}^{8760} P(v_i) * \Delta t \quad (12)$$

where, $P(v_i)$ is the available power in the prevailing wind in watts in a time averaged period (wind data such as wind speed, wind direction are not a continuous stream of data; rather a time averaged value of wind speed and direction is generally stored), Δt is length of the time step of data in seconds, ρ is the density of the wind at that temperature in kg/m^3, ρ_0 is the density of the wind at standard temperature and pressure (STP) condition in kg/m^3.

The density of the wind has to be known in this method. The result is also dependent on the random number generation technique [8]. Moreover, the power curve of the turbine has to be known.

The assumptions employed in this method are:

1. The wind regime follows the Weibull distribution.
2. The wind turbine rotor faces the wind perpendicularly at any instant.

1.3.6 INL wind energy

INL (Idaho National Lab) has a wind energy program [12] based on MS Excel® for estimating wind energy based on the statistical data available for any location. In this method, the power curve of the wind turbine has to be known. The energy can be found by the following equation

$$E = \sum_{i=1}^{t} P(v_i) \times \Delta t \tag{13}$$

where, $P(v_i)$ is the available power in the prevailing wind in watts in a time averaged period, Δt is length of the time period in seconds and E is the energy of the entire time duration of interest.

The accuracy of this method depends on the frequency of available data. The advantage of this method is that the wind regime does not have to follow any statistical distribution. However, this method also assumes that the turbine will face the prevailing wind perpendicularly at all times.

1.4 Limitations of current estimation techniques

Detailed literature review suggested some possible approaches to estimate the electrical energy that can be harnessed from wind energy of a location. However, every approach had their advantages and limitations. Since a utility-scale wind farm requires a comprehensive estimate of the energy, the turbine specific approach is always preferred.

Most of the turbine specific energy estimation techniques except the Kiranoudis method mentioned in the literature review section, utilized the power curve of the turbine used to estimate the energy output of that turbine placed at that location. They all assumed that the rotor and power train have no inertia and are, therefore, at all times in equilibrium with the local wind both in rotational speed and in yaw alignment. In addition, they assumed that there is neither friction nor any other mechanical loss.

However, in reality, utility-scale wind turbines have a large inertia, and the yaw rotation of the turbine is limited to 0.3 ~ 5 deg/sec [10] in order to minimize the gyroscopic effect. The wind direction may change continuously. However, the utility-scale wind turbines do not change their yaw orientation continuously

to match the wind direction. It is normally done at a regular or variable time interval in order to increase the life of the yaw bearing and other mechanical components [10]. The reasons for this are to eliminate the controller complicacy and to save the bearing and other mechanical components from wearing out quickly. This leads to a possibility of the turbine to be misaligned with the prevailing wind. A turbine controller takes the decision to yaw the turbine by sensing the wind direction and then finding the misalignment. The wind direction sensed by the sensor is already past the turbine. Therefore, the turbine will align itself with the wind that has already passed through the turbine. While doing that the wind direction has already changed. This means that the turbine may always have some misalignment with the prevailing wind. This misalignment is termed as yaw error of the turbine.

Yaw error reduces the power output of the turbine. Assuming the wind direction vector and the vector normal to the face of the rotor are at an angle θ, the active velocity becomes $u = v\cos\theta$. Thus the power equation becomes

$$P = \frac{1}{2}\rho C_p A v^3 cos^3\theta \tag{14}$$

From this equation it can be seen that for $\theta = 20^o$ the power output decreases by 17%.

A dynamic mathematical model of the yaw control of a utility-scale turbine can be developed to consider the effects of yaw error on the power output of the turbine. If the yaw error is considered in the estimation process the results would be more accurate than the other methods available at present.

While considering the yaw error some other questions also needed be answered. For example, what is the effect of yaw rate on the energy output of the turbine? And how frequently should the turbine align itself with the prevailing wind direction? To answer these questions some terms such as 'Time step' and 'Delay time' are needed to be defined now as they will be used frequently from this point on.

Time step: The frequency of the data set that will be the input of the dynamic model.

Delay time: The time period in between two consecutive changes in the orientation of the turbine.

Chapter 2

2.1 Methodology

Based on the literature review, the major steps of the research were identified. The primary goal was to develop a dynamic yaw control model of wind turbine to assess the energy that can be harnessed from any location. The statistical wind data were fed to the dynamic model to estimate the output energy by any specific turbine. The data had to be quality controlled and continuous. The missing data points had to be noted as 'NaN' value to work with MATLAB coding.

The data collected from the Wind Sentinel was at 1 Hz frequency. These data were managed and stored by the Watchman-500 (an AXYS data acquisition and storing system) on the buoy in a flash card. The data were physically retrieved by pulling out the data card from the buoy every 6 weeks. Watchman-500 also generated a 10 minute averaged data set and transmitted the data through cellular network, the Iridium satellite network. During the project when the buoy was within the cellular data network it transmitted 10 minute averaged data sets at a frequency of 10 minutes. While the buoy was in mid-lake position, the data were transmitted every hour via satellite to reduce the cost of transmission of data. The transmitted data were the 10 minute averaged values of wind data at the moment of transmission.

In theory the 1 Hz data would have a continuous stream of 86400 data points per day. However, in practice the data set did not have 86400 data points and a large number of data as well as the time stamps were missing. The missing data were denoted by character 'Â' by the Watchman system. This 1 sec data were not usable in MATLAB code due to discontinuity of time stamp and the special character in the data set. Moreover, it was not a wise decision to feed the 1 Hz data into the MATLAB code. Generally the utility-scale turbines have a large moment of inertia, which makes them slow responding systems. The turbine cannot respond to the quick fluctuations of wind speed due to the turbulence in wind. These reasons discouraged the use of 1 Hz data in the dynamic model.

Therefore, the data set had to be preprocessed to create the time stamps for the missing time stamps and replace the missing values denoted by 'Â' characters with 'NaN' character. The data set also had to be averaged over a longer time frame to feed into the MATLAB code and it also had to be quality controlled. To address these issues a separate data preprocessing tool was developed.

To present the wind pattern over the location of interest a wind data representation tool was developed. This module generated the wind rose and frequency distribution based on the processed wind data set collected by the Wind Sentinel system.

To compare the results with other models of wind energy estimation, separate modules capable of estimating wind energy by using the same data set were developed as well. These modules assessed the wind potential based on several methods described in the literature review and finally compared the findings to the dynamic yaw control model.

Just to give an idea of how much data had to be processed, each day had a data set with 86401 rows and 146 columns. In total 395 days of data had to be processed. The total size of data collected was

approximately $20\ GB$. Processing these large scale data sets required large computing power. The computing facilities of the Padnos College of Engineering and Computing were used for this project, namely the Tesla machine was capable of handling such large scale data and calculation steps. This machine was used extensively in the current study.

The following steps were followed to complete this study:

1. Development of a dynamic yaw control model of a utility-scale turbine to estimate wind energy.
2. Development of a data preprocessing tool to refine the raw data to feed in the dynamic model.
3. Development of post processing tools to represent the wind pattern over the location of interest.
4. Development of computational modules to estimate the wind energy using other methods stated in literature review for comparison.

These steps required their own methodology to develop. Brief description of the methodology of each step is presented in the following section.

2.1.1 Energy estimation with dynamic yaw control model

For energy estimation the INL wind analysis program was taken as a starting point. It was considered as the base dynamic model of the turbine. The energy estimating module took in the wind data – wind speed and wind direction. Then the corresponding power output by the turbine at that specific wind speed was sought out from the power curve. The power curves obtained from the INL wind analysis program were not continuous function of wind speed; rather they provided sets of discrete power outputs corresponding to the wind speeds. The resolution of the wind speed in that power curve was 0.01 mph. All the wind speed values were rounded to two significant digits.

In the case of INL wind analysis program the energy per time step was found by multiplying the power output at that time step found from the power curve of the turbine with the time step of the input wind data. The effect of the yaw error was not considered in that program. The dynamic model developed in this study considered yaw error of the turbine while estimating the energy.

An important factor to keep in mind is that if the yaw error is not more than a threshold value, the turbine does not change its orientation in modern utility-scale wind turbines. A possible reason for this is the amount of energy needed to rotate these large turbines is more than the turbine can generate by aligning itself with the wind. Another reason for this is that this way the mechanical components of the turbine, such as the bearings, will experience less wear and tear as they go through less working strain. This threshold value is different for different operating region of a turbine. The operating regions of a pitch-controlled turbine are presented in Figure 2.1.

From Figure 2.1 it can be seen that Region 1 and Region 4 do not generate any power. During these regions the yaw brake is enabled to protect the valuable turbine components. Region 2 is the maximum power coefficient mode of a turbine. In this region the turbine tries to extract as much energy as

possible from the wind. The accepted yaw error window is very small (approximately 8°) in this region in order to reduce the losses [11]. Region 3 is the maximum power output mode. Here the turbine operates to generate the maximum power – rated power of that turbine. The yaw error allowance is slightly greater (approximately 18°) in this region.

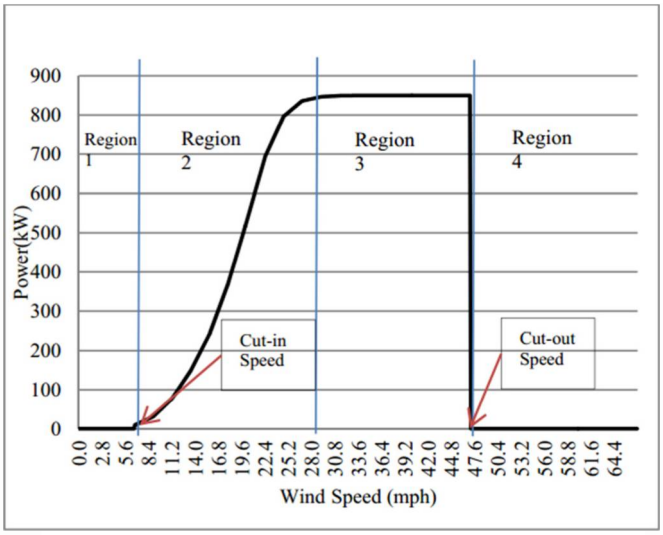

Figure 2.1 Different operating regions of a pitch controlled wind turbine (Gamesa Eolica G58-850kW)

In order to include the effect of yaw error, several new parameters had to be known – the yaw rate, the wind direction, the turbine orientation at that time step, the threshold values of the accepted yaw error and the time period in between two consecutive changes in the orientation of that turbine (delay time). In the dynamic model, while calculating energy generation within a single time step (the time resolution of input data) these parameters were all considered.

Among these parameters, yaw rate and time period between two consecutive changes in turbine orientation (delay time) were not dependent on the wind speed but the threshold value of accepted yaw error was dependent on the wind speed. An algorithm for dynamic yaw control taking these points into account was developed and presented by the flow chart in Figure 2.2. In this figure *fixed value 1* and *fixed value 2* are the allowed yaw errors in Region 2 and Region 3 respectively.

Based on this control model the turbine orientation was calculated at any instant. For a time step, the wind direction was assumed to be fixed. Therefore, for a given time step, the yaw error was found at a fixed time interval for the turbine. By using this yaw error and the wind speed for that time step the active speed (normal component of speed on the wind turbine blade) for the turbine was found by Equation (15).

$$active\ speed = prevailing\ wind\ speed * cosine\ of\ yaw\ error \tag{15}$$

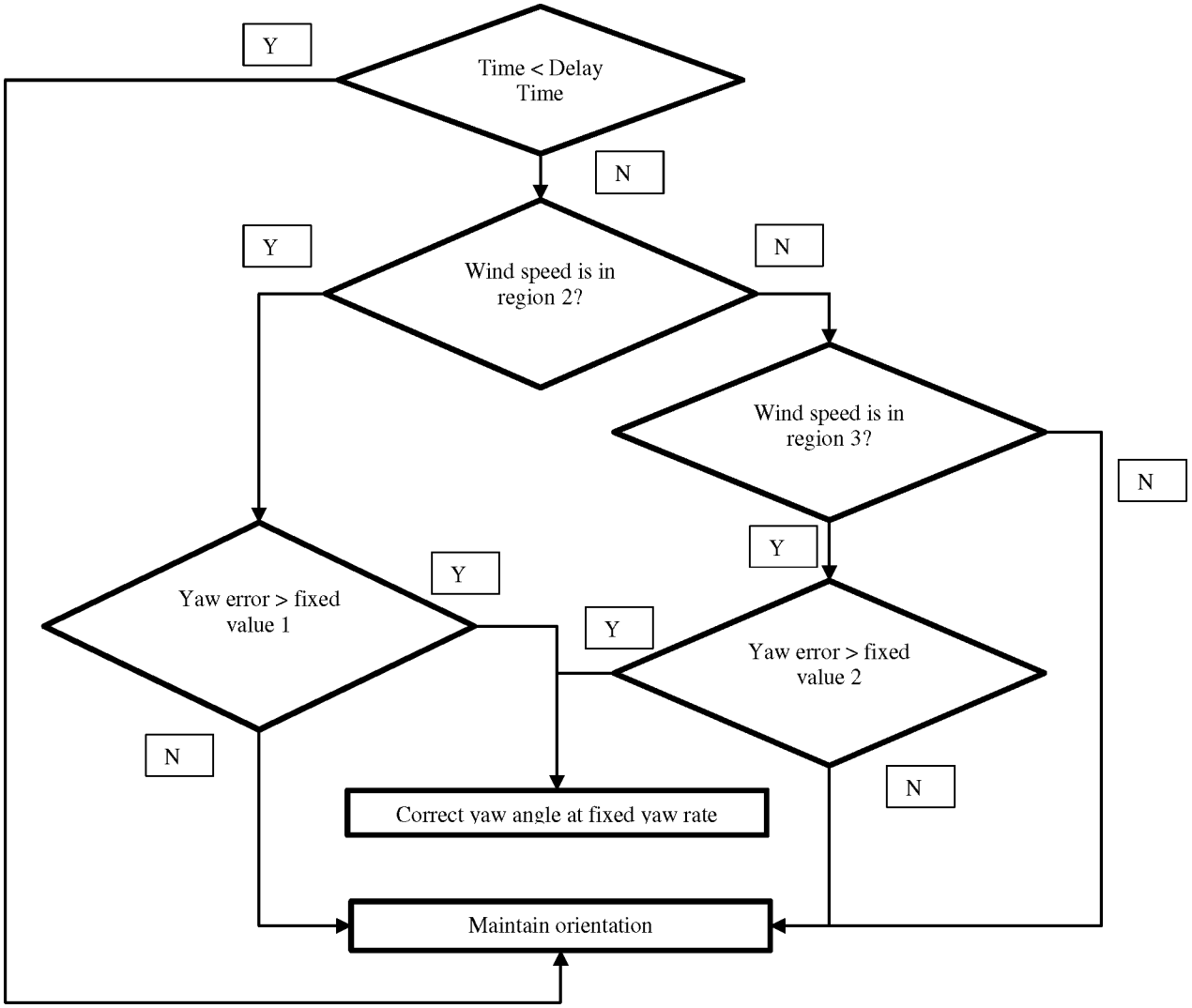

Figure 2.2 Yaw control module flow chart

The power output for that active speed was sought out from the power curve and used as the power output for that time interval. The total energy output was found by integrating the power output as in Equation (14). A flow chart outlining the energy estimation process from the dynamic control model is presented in Figure 2.3.

Based on the control algorithm presented in Figure 2.3 a MATLAB code was developed. The detailed MATLAB code is attached in Appendix A.1 for further understandings and future reference.

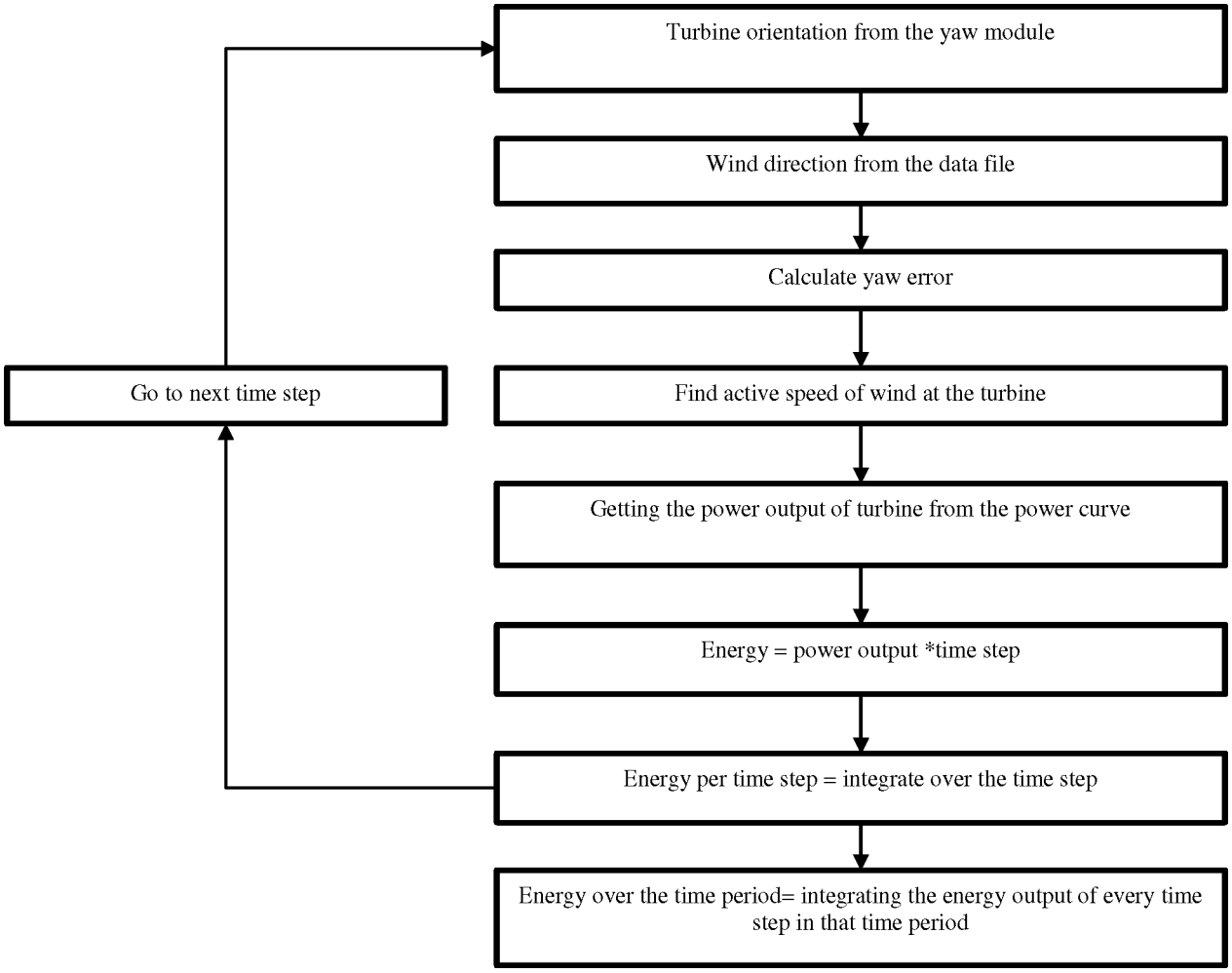

Figure 2.3 Energy estimation process flowchart

2.1.2 Energy estimation by other models

2.1.2.1 Wind energy density

First the power density of the prevailing wind was calculated by using Equation (1). For doing that the density of the air at the height of the data had to be known but the data set did not have the density of the wind at the height of measurement. The density was modeled according to the U.S. standard atmosphere model 1976 version [16]. The model parameters are:

Sea level standard atmospheric pressure p_0= 101.325 kPa
Sea level standard temperature T_0= 288.15 K
Earth-surface gravitational acceleration g= 9.80665 m/s^2.
Temperature lapse rate L= 0.0065 K/m
Ideal (universal) gas constant R = 8.31447 $J/(mol \cdot K)$
Molar mass of dry air M = 0.0289644 kg/mol

The highest altitude of wind data was 175 m which was within the troposphere of the earth's atmosphere (17 km) so the temperature at that altitude was found by using Equation (16).

$$T = T_s - Lh \tag{16}$$

where, T_s is the temperature at water surface measured by the buoy in K, L is the temperature lapse rate inside troposphere in K/m, and h is the altitude of interest in m.

Then the pressure at that altitude was found by the following Equation (17).

$$p = p_0(1 - \frac{Lh}{T_s})^{\frac{gM}{RL}} \tag{17}$$

where, p_0 is the pressure at sea level in kPa, L is the temperature lapse rate inside troposphere in K/m, h is the altitude of the data set in m, T_s is the temperature at the water surface in K, g is the earth-surface gravitational acceleration in m/s^2, M is the molar mass of dry air in kg/mol, and R is the universal gas constant in $J/(mol.K)$.

By using the pressure and temperature at the given height the density of the air was found by Equation (18).

$$\rho = \frac{pM}{RT} \tag{18}$$

where, ρ is the molar density of air in kg/mol, p is the pressure in kPa, M is the molar mass of dry air in kg/mol, R is the universal gas constant in $J/(mol.K)$, and T is the temperature in K.

By using the density of air at the height of the data set the power density of wind was found. The averaged power density of wind per month was used to simplify the calculation. The available energy density of wind was found by multiplying the time step for the data set with the power density of wind found in Equation (1). The MATLAB code for this process is presented in Appendix A.2.1.

2.1.2.2 Betz analysis

Wind energy by the Betz analysis was easily found by using Equation (4). The available wind energy density was calculated by the methodology presented in section ***2.1.2.1***. The energy estimated by Betz analysis is 59.3% of the available wind energy density.

2.1.2.3 One two three equation

Electrical energy that can be generated from the available wind energy can be estimated by using this method with the help of Equation (7). The average density was found from the buoy data set and then extrapolated using the US standard atmospheric model [16]. The energy was normalized by dividing by the density of air at standard temperature and pressure. The MATLAB code for this method is attached in the Appendix A.2.1.

2.1.2.4 Polynomial modeling

In this method the power curve of the wind turbine was modeled with the help of Equation (11). The order of the polynomial,m, was assumed to be 2. Then the power output by the turbine was determined by using the power curve model equation. The energy was found by multiplying the power output with the time step of data. Then integrating over the entire time period the total energy was found. The MATLAB code of this module can be found in Appendix A.2.2.

2.1.2.5 Random number generation

For this method the Weibull parameters of the wind regime had to be determined. Then it was used to determine the wind energy by using generating random values of wind speed. This method is useful for a site where the long term statistical wind data are available. This site did not have long term statistical wind data to estimate energy by random number generation. Therefore, the energy that can be harnessed from the available wind energy could not be estimated by this method.

2.1.2.6 INL wind energy

Energy can be estimated by the simple approach of finding the power output of the turbine at any specific wind speed from the power curve and then multiplying it with the time period of data. For this a discrete set of wind power curves were needed. The power curves were collected from the INL wind energy software. The MATLAB code is presented in Appendix A.2.3.

2.1.3 Data preprocessing

The dynamic control model needed a continuous stream of data with proper time stamps. The number of data points should be 86400 per day for 1 sec data set. The data preprocessing module took in the raw unrefined data set. In MATLAB a continuous set of time stamps was created to compare with the time stamps of the raw data file. By doing this the missing time stamps were found and were filled in according to the time stamps created in the program.

The missing data points were denoted by 'NaN' values to make them compatible with MATLAB. Then the refined data set were saved as comma separated values in daily data. The steps are presented as a form of flow chart in Figure 2.4.

Based on the flow chart a MATLAB script was developed to refine the raw data. The MATLAB code is presented in Appendix A.3 for reference.

As stated earlier it is not desirable to feed in the 1 sec data into the dynamic model. Therefore, the data set had to be average to different time steps. Four averaging time periods were considered, i.e., 30 sec, 1 min, 2 min, 5 min and 10 min. During averaging the data was checked for quality. If the number of samples was less than 50% of the number of data points in ideal case in the averaging time period the averaged value was considered as invalid and was omitted from the averaged data set. Then the data set was stored in the comma separated value (CSV) format. The associated data set had the average wind speed and average wind direction per time step.

Wind speed is a scalar quantity and can be averaged using normal averaging formula. However, the wind direction is a vector quantity. Therefore, averaging the wind direction is not a simple straight forward procedure. The average angle in a time averaged period can be found by Equations (19), (20) and (21)

$$sine = \sum \sin(\theta_i) \tag{19}$$

$$cosine = \sum \cos(\theta_i) \tag{20}$$

$$\theta = \arctan(sine/cosine) \tag{21}$$

In MATLAB the sign convention is different than that of the input wind data file. Therefore, the angle was converted before any calculation and similarly again converted to normal notation which is 0° due north, 90° due east, 180° due south and 270° due west. The overall procedure is presented in a flow chart format in Figure 2.5.

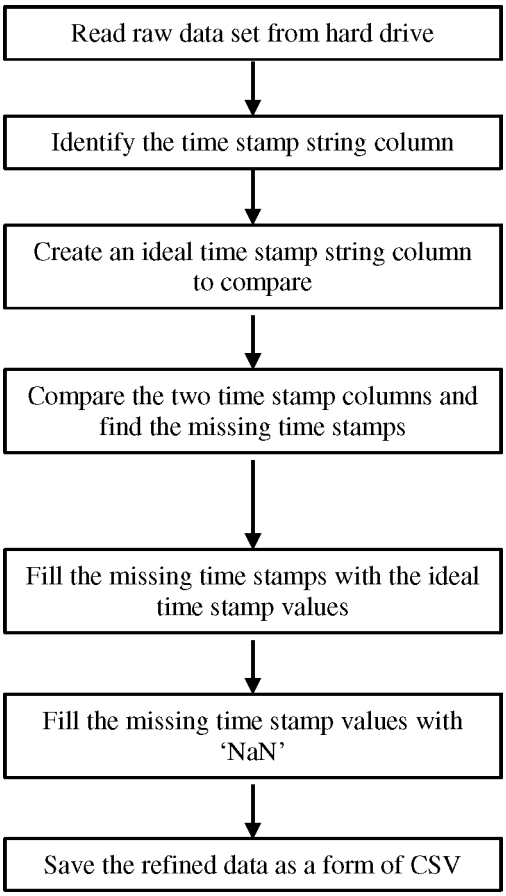

Figure 2.4 Data processing module flow chart

With the help of this flow chart presented in Figure 2.5, a separate MATLAB code was developed. The code can be found in Appendix A.4.

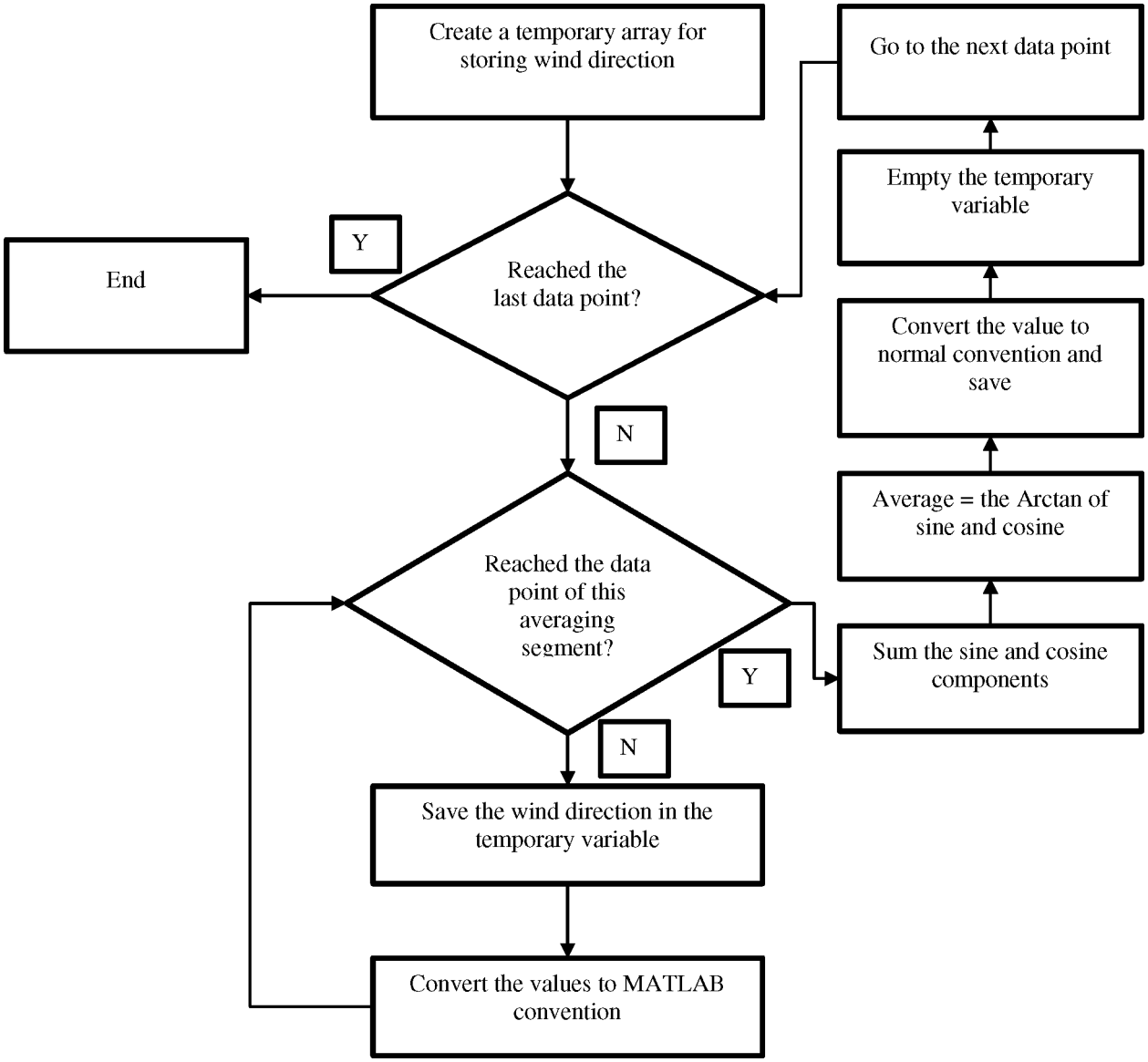

Figure 2.5 Averaging module flowchart

2.1.4 Representation of the results

Wind data representation is different than any other representation as the wind velocity is a vector quantity. In most of the reports and technical papers a special type of graph is used. It is called the wind rose. The wind rose is the graphical representation of the average wind speed or average duration of wind in any particular range of direction. It is essentially a bin sorting process or histogram where the bin criterion is the wind direction.

Therefore, in order to generate the wind rose for representation, the wind data were sorted in different bins. That means, in a certain direction range the average wind speed or averaged duration of wind blowing in that range was sorted out from the data file. Then the wind speed was averaged and assigned

for that particular range. Duration of time wind blowing in that direction as a percentage of total time of the data set was also calculated. The scheme for this sorting and averaging is presented in a flow chart format in Figure 2.6. However, the built-in function of MATLAB to generate wind rose was unable to represent the result. Therefore, Microsoft Excel was used as a plotting solution. Radar type plot was used to represent the data calculated by MATLAB. The MATLAB code for this module is attached in Appendix A.5.

Another form of representing wind data is the frequency distribution. It is the averaged wind speed and duration of time of wind blowing in a particular range of wind speed. It is similar to the wind rose but the bin criterion is the wind speed.

Similar to wind rose, a sorting scheme was adapted and also a MATLAB code was developed. However, in this case the built-in MATLAB plotting solution was sufficient enough to represent the results. The algorithm for this process can be found in Figure 2.7 and the MATLAB code is presented in Appendix A.6.

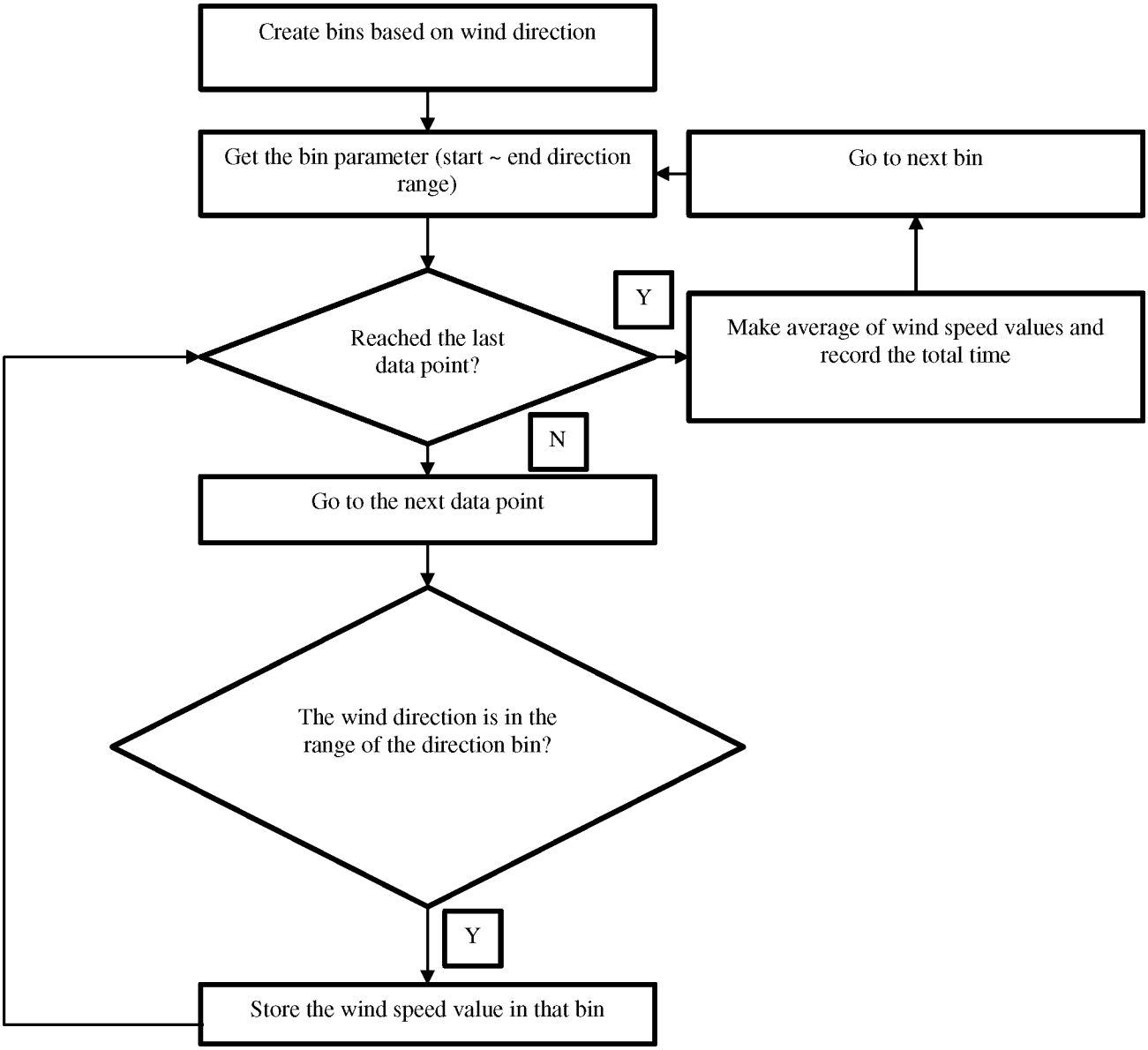

Figure 2.6 Wind rose generating flow chart

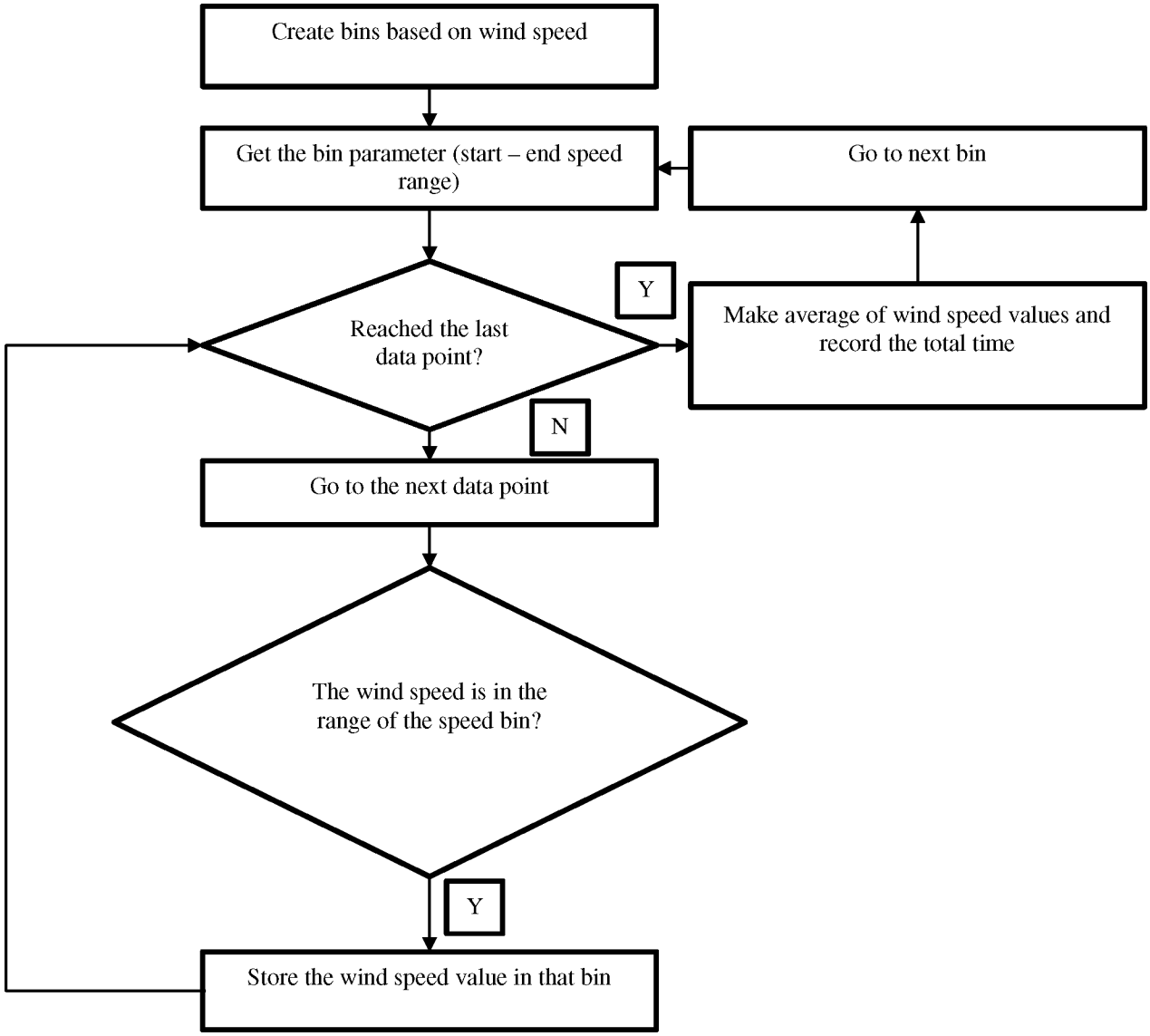

Figure 2.7 Frequency distribution generating flow chart

Chapter 3

3.1 Energy estimation by the dynamic control model

3.1.1 Validation of the dynamic model

For validating the developed model the codes were organized in such a way that the dynamic model can be deactivated or activated for total energy estimation. If the dynamic model is deactivated during the calculation, the model assumes that the turbine will face the wind direction at any instant similar to the other estimation techniques. As the base model is similar to the INL wind energy model, for the same data sets the results should be very close for both cases. To test this, a sample data set collected from INL website was used. The metadata of the data file: Site: Idaho [17]; Latitude: 43.7058°N; Site Number: 1041; Longitude: 111.731°E; Site Description: Louise Twitchell site; Turbine model: Games Eolica G58-850 kW; Project Code: Idaho; Project Description: Idaho Wind; Location Description: Near Archer, ID; Site Elevation: 5360 ft; Start time: 6/22/2006 19:50; End time: 2/4/2007 18:00; Hours in file: 5446.33 hours; Time Zone: GMT-7. The results are presented in Table 3.1 and the results are similar as expected.

Table 3.1 Comparative results of the INL wind energy and MATLAB code developed

INL wind energy	MATLAB code	Difference
956,875.69 kWh	956,875.90 kWh	0.0005%

Figures 3.1 and Figure 3.2 show a comparative analysis of the percentage of total time and percentage of total energy in different direction bins obtained from the two codes. The results are very close, verifying the accuracy of the MATLAB code developed.

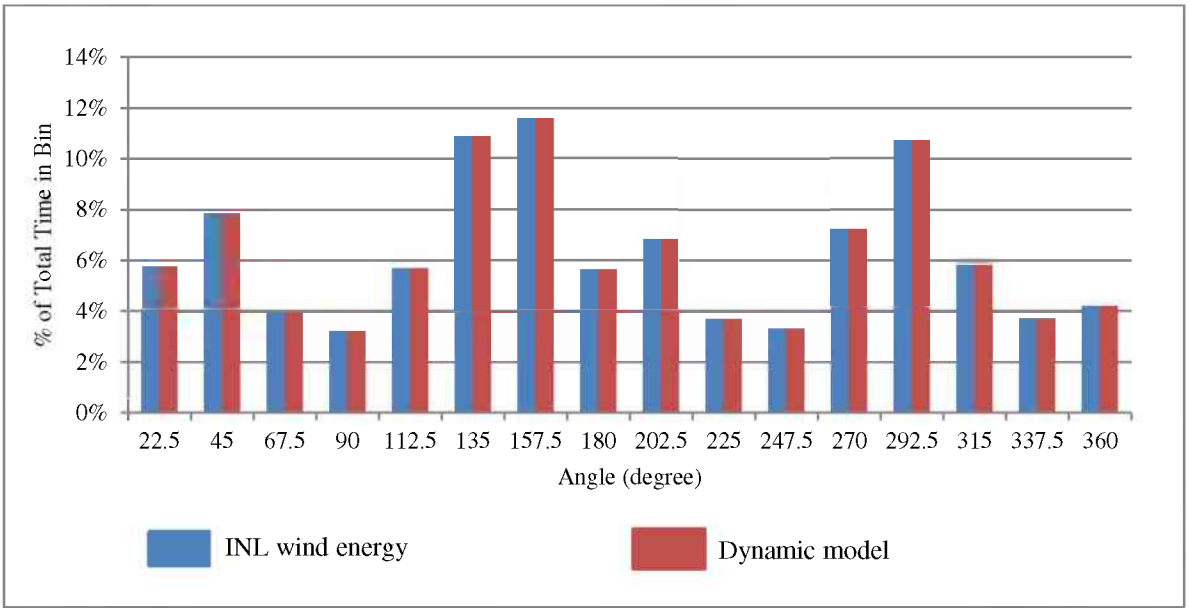

Figure 3.1 Comparative results of percentage of total time in every direction bin

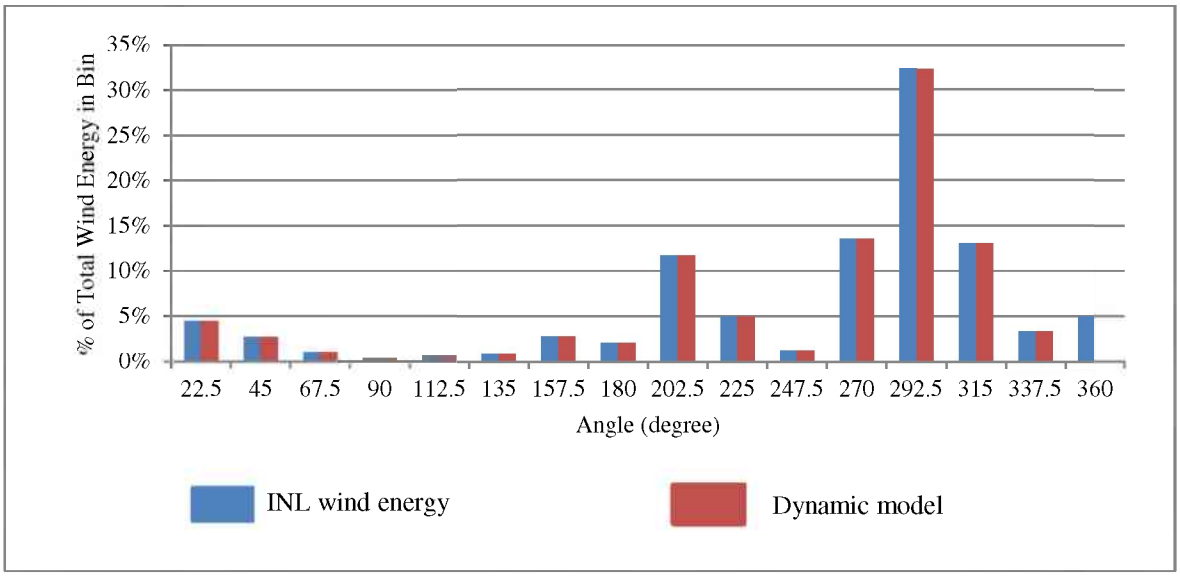

Figure 3.2 Comparative results of Percentage of total energy in every direction bin

Figures 3.3 and Figure 3.4 depict a comparative analysis of the results from two codes with respect to the total energy generation and relative frequency in different speed bins. Again, as may be seen these results are very close.

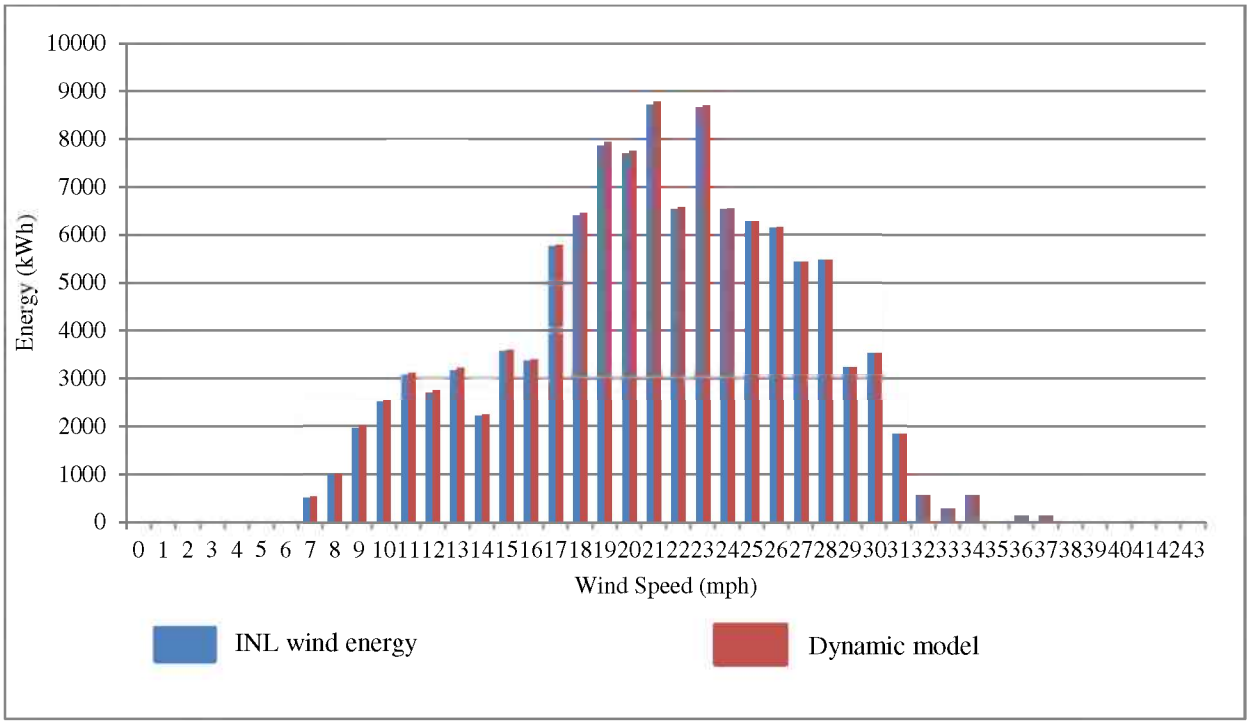

Figure 3.3 Comparative results of energy at different speed bins

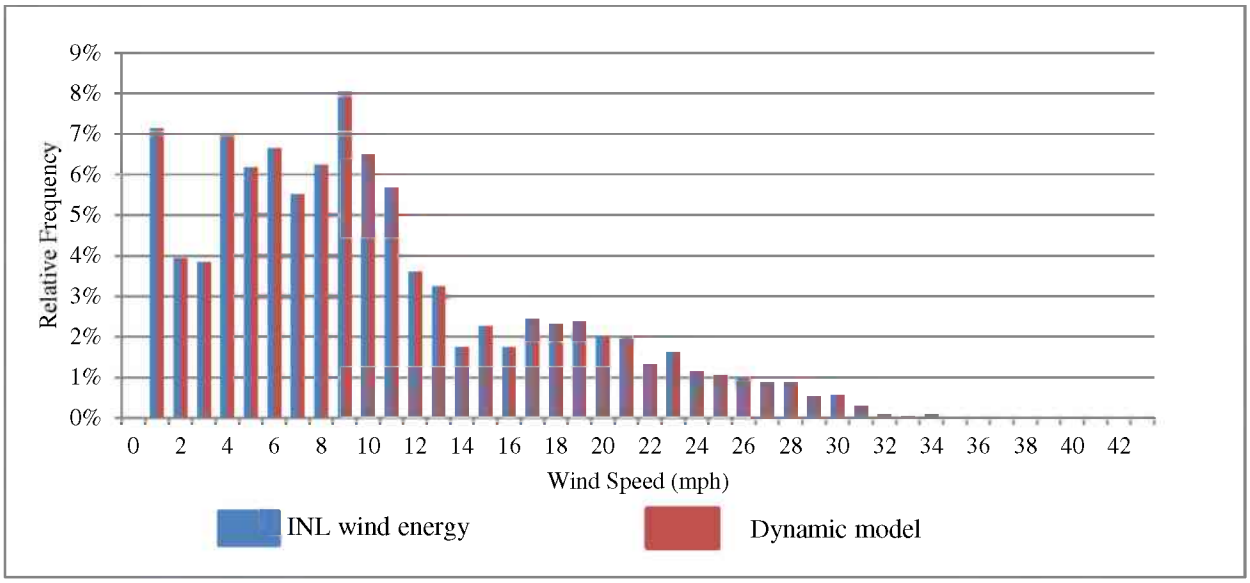

Figure 3.4 Comparative results of the frequency distribution of wind

In the speed bins, the difference between the total energy generations in each bin from the two codes was generally below 2.5% with the exception of the bin of 7 mph where the difference was approximately 3.5%. The direction bins show relatively lower differences, with the highest difference being 0.09%.

The base model without the dynamic yaw misalignment correction generates similar results as other estimation techniques confirming the validity of the model.

3.1.2 Time line of data set

At different stages of the project, the buoy was deployed at different locations. The range gates (RG) of the Wind Sentinel were varied for different locations. The timeline, locations and altitudes of the buoy are presented below:

Table 3.2 Time line of the buoy location

Time frame	Location	Duration
October 7, 2011 to November 3, 2011	Lake Muskegon	28 days
November 8, 2011 to December 30, 2011	Lake Michigan (near shore)	53 days
January 5, 2012 to May 7, 2012	NOAA field station (Muskegon)	124 days
May 7, 2012 to December 15, 2012	Mid-lake plateau of Lake Michigan	223 days

Table 3.3 Altitudes of different range gates at different deployments

Location	Altitudes (m)

	RG1	RG2	RG3	RG4	RG5	RG6
Lake Muskegon	55	60	75	90	110	120
Lake Michigan (near shore)	55	60	75	90	110	120
NOAA field station (Muskegon)	55	60	75	90	110	120
Mid-lake plateau of Lake Michigan	75	90	105	125	150	175

The results of longest deployment (mid-lake plateau) and range gate 1 are presented here. The other deployment results are attached in Appendix B for further reading.

3.1.3 Effect of yaw rate and delay time

The dynamic control model required two important parameters, yaw rate and delay time, to estimate the energy that can be harnessed. The effect of yaw rate on the energy output can be observed from Figure 3.5. The figure presents the estimated energy at a hub height of 75 m (RG1) for mid-lake deployment. The data sets were averaged over 1 minute time step.

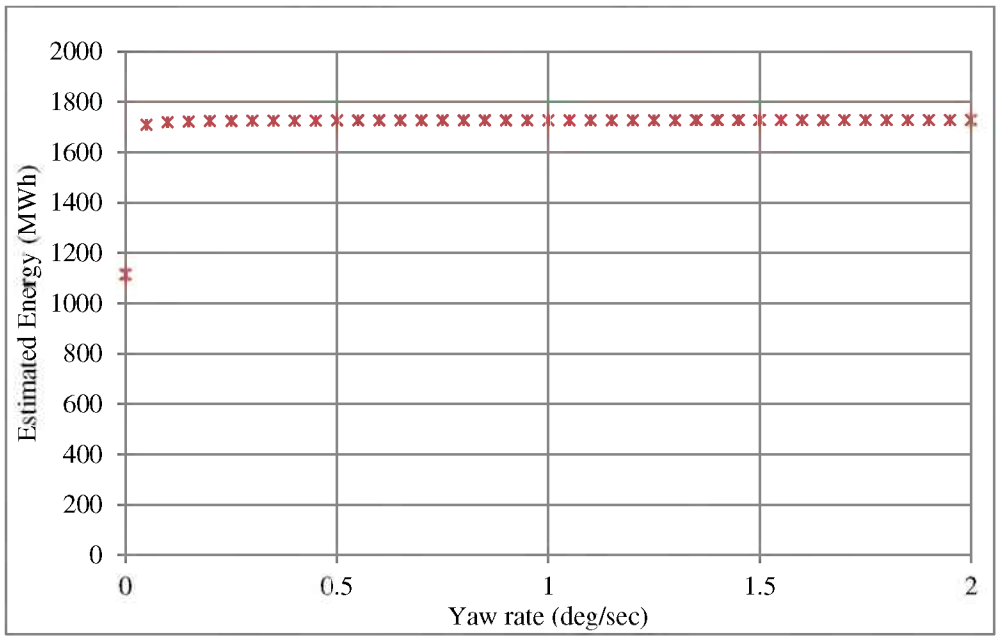

Figure 3.5 Effect of yaw rate on estimated energy

A close up look of the very slow yaw rate can be seen in Figure 3.6. This figure shows that the energy output increases with the increase of yaw rate. However, the relation between the energy output and the yaw rate is dependent on the turbine model and wind data.

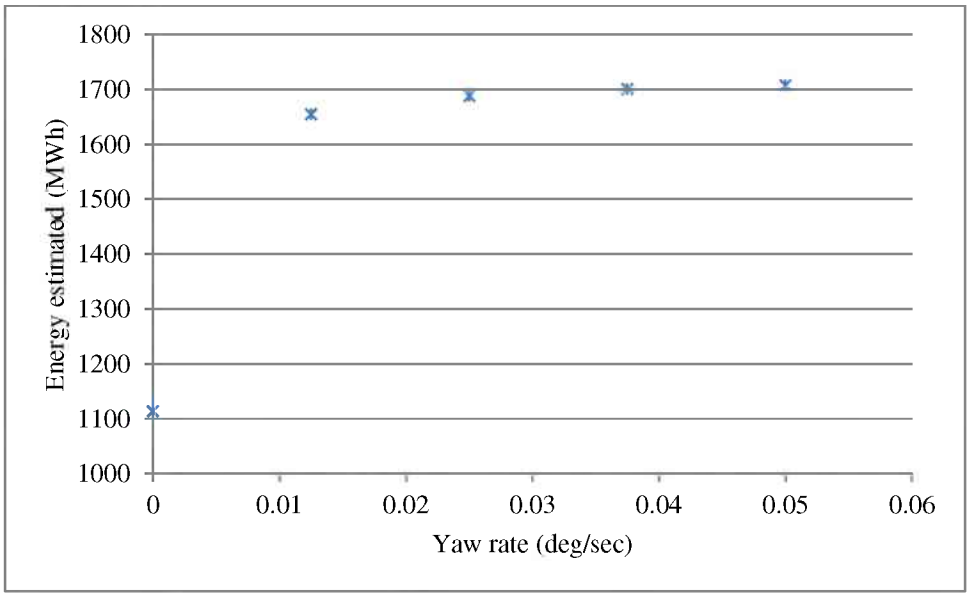

Figure 3.6 Estimated energy at slow yaw rate for Gamesa Eolica G52-850kW

The turbine model used for the analysis was Gamesa Eolica G52-850kW. The associated power curve of the turbine can be found in Figure 3.7.

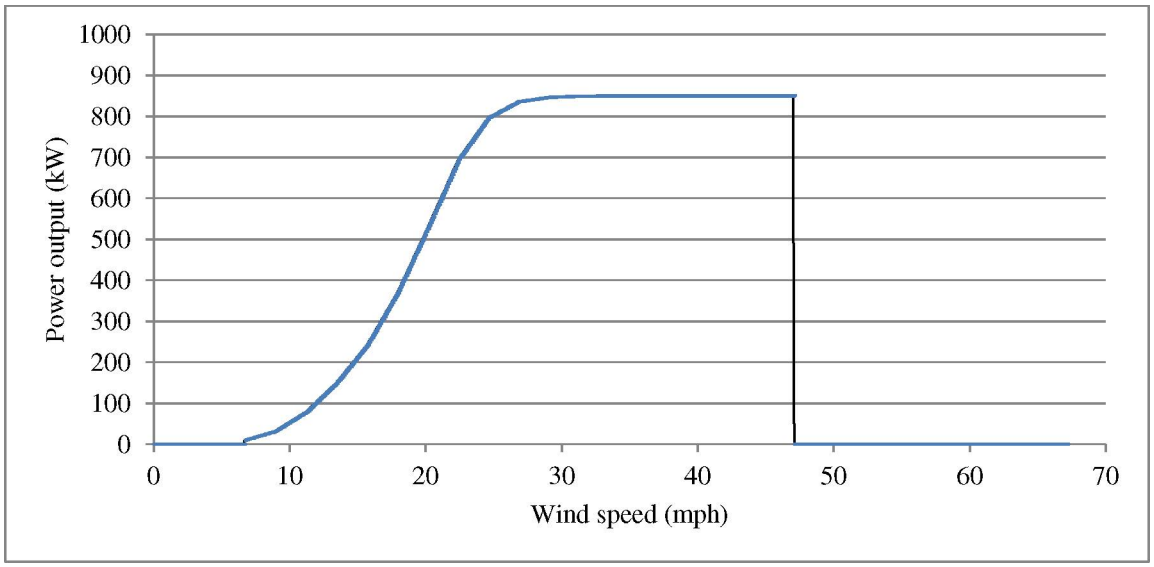

Figure 3.7 Power curve of Gamesa Eolica G52 850kW [13]

The turbine parameters are (estimated from the power curve):

Cut in speed: 8.9 mph
Cutout speed: 47 mph
Rated speed: 31.3 mph
Region 2 threshold of yaw error (assumed from a generalized estimation found in [11]): 8°

Region 3 threshold of yaw error (assumed from a generalized estimation found in [11]): 18°
In this study the yaw rate was varied from 0 deg/sec to 2 deg/sec at an increment of 0.05 deg/sec. It can be observed that the energy output increased with the increase of yaw rate. However, the increase is sharp from yaw rate of 0 deg/sec (no yaw movement) to 0.05 deg/sec. After that, the rate of increase decreases dramatically.

This is because the fast yawing turbine will align itself with the prevailing wind much faster that slow yawing turbine. This results a higher energy output. However, one thing that has to be considered is that the turbine first senses the wind direction and then tries to align itself with the wind direction but the wind direction may change by the time the turbine aligns. Therefore, the turbine may always be subject to yaw error as it is aligning itself with the wind that already passed the turbine. Nevertheless, higher yaw rate would help the turbine to align much faster that the slower one.

Now let us observe the effect of the delay time on the energy output from Figure 3.8. The energy output of the turbine at a yaw rate of 0.05 deg/sec at different delay times is presented here. As seen from the figure this phenomenon is quite unpredictable and solely depends on the instantaneous wind direction. The energy output varies with the delay time but not in any orderly fashion and the highest energy yield is at the minimum delay time (in this case 1 min = 60 sec). An optimized value can be suggested to reduce the wear on the turbine components by knowing the corresponding parameters such fatigue life of design, endurance limit of the materials, etc.

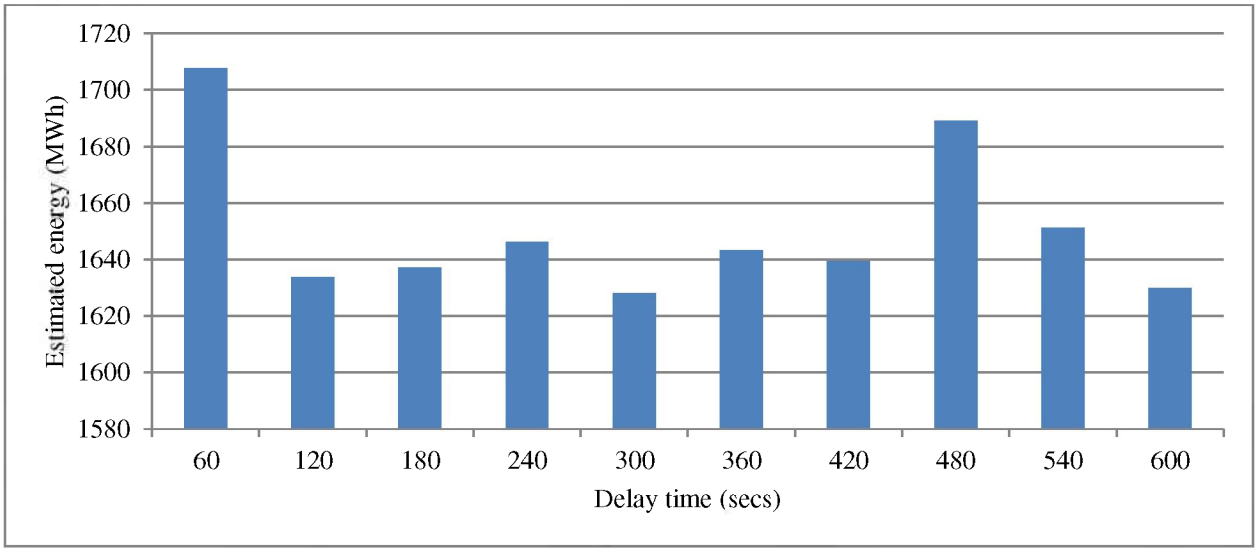

Figure 3.8 Effect of delay time on estimated energy

In the case of the delay time it is not easy to predict the variation in energy output with the change of delay time. First it is to be noticed that, the minimum delay time cannot be lower than the time step of the data. However, the delay time does not have a maximum limit. Typically it can be expected that, at longer delay time the turbine will be at yaw error for longer time if the wind direction changes within that delay time. It might happen that the direction did not change significantly during that time span. Then the energy output will not vary that much. On the other hand it might also happen that the shorter

delay time may result in larger yaw error over the time because the controller takes decision by sensing the instantaneous wind direction.

For example consider Table 3.4 of wind data (wind speed in mph, wind direction in due north). In this table T.O. stands for turbine orientation due north, and A.Y.E. stands for absolute yaw error in degree. The turbine will change its orientation if the yaw error is more than 8˚. Let us assume that the yaw rate is large enough to compensate the yaw errors within a single time step for this example. From the table it can be seen that, even for shorter delay time of 5 min the average yaw error is greater than the longer delay time. The reason for this is that the yaw correction decision taken by the controller is based on the wind data at that instant. This leads the turbine to be in greater yaw error for the coming delay time. Since the energy output is a function of yaw error the energy output will vary according to the error. Also, the error affects the energy output through a cosine function relation (as in Equation (14)). Therefore, both the positive and negative error of same magnitude affects the energy output by same amount.

Table 3.4 A hypothetical case of wind data, turbine orientation and average yaw error

Time stamp	Wind Speed (mph)	Wind direction (due north)	Delay time 1 min		Delay time 5 min		Delay time 10 min	
			T.O.	A.Y.E.	T.O.	A.Y.E.	T.O.	A.Y.E.
12:00AM	8.9	160	150	10	150	10	150	10
12:01AM	9	170	160	10	150	20	150	20
12:02AM	10.1	166	170	4	150	16	150	16
12:03AM	10.4	161	170	9	150	11	150	11
12:04AM	11.1	170	161	9	150	20	150	20
12:05AM	9.2	189	170	19	150	39	150	39
12:06AM	8.8	160	189	13	189	29	150	10
12:07AM	9.1	160	189	29	189	29	150	10
12:08AM	10.1	180	160	20	189	20	150	30
12:09AM	11.1	160	180	20	189	20	150	10
12:10AM	9.5	166	160	6	189	23	150	16
Average yaw error				16.55		21.54		17.46

Another important phenomenon can be observed from Table 3.4 that even at the minimum delay time which is the time step of the data (in this example, 1 min) the turbine is never aligned with the prevailing wind. The reason for this is that the turbine controller takes decision based on the past time step. Therefore, it is theoretically not possible to truly align the turbine at every instant with the prevailing wind without measuring the wind direction at upstream of the wind turbine or predicting the wind direction up ahead. Even predicting the wind speed for a small time period is very difficult as the wind is unpredictable by nature.

It can be deduced that the effect of delay time on the energy output is random. However, it can be stated that the maximum energy output will be on the minimum delay time. Anything higher than the minimum delay time will result a lower energy output.

Moreover, it should be considered that both yaw rate and delay time dictate the energy output. Therefore, the energy output varies as their combinations change. The results of different energy output at different combinations of yaw rate and delay time are presented in Table 3.5.

Table 3.5 Energy output (MWh) at different yaw rate and delay time for Gamesa Eolica G52 850kW (mid-lake deployment, RG1, 1 min data set)

Yaw Rate (deg/sec)	**Delay Time (sec)**									
	60	120	180	240	300	360	420	480	540	600
0	1113.37	1073.65	1082.55	1085.48	1078.75	1083.21	1084.09	1109.55	1088.61	1079.35
0.05	1707.73	1633.82	1637.15	1646.24	1628.18	1643.24	1639.33	1689.08	1651.24	1629.88
0.1	1718.53	1648.22	1650.63	1661.01	1642.93	1652.28	1650.36	1700.15	1663.71	1639.13
0.15	1721.22	1654.12	1656.88	1663.38	1645.68	1657.75	1653.04	1702.78	1668.12	1642.84
0.2	1723.14	1657.98	1659.94	1667.81	1650.14	1661.00	1655.17	1705.75	1671.48	1645.51
0.25	1724.04	1660.60	1663.13	1669.32	1653.74	1663.28	1656.70	1707.31	1678.32	1648.17
0.3	1724.53	1662.47	1666.74	1672.04	1655.85	1665.20	1657.24	1708.31	1681.35	1649.82
0.35	1724.83	1664.25	1669.49	1672.61	1657.74	1666.60	1658.20	1709.18	1682.91	1650.90
0.4	1725.12	1665.67	1670.87	1673.84	1659.78	1668.17	1658.92	1710.20	1685.58	1652.91
0.45	1725.35	1666.90	1672.21	1674.86	1661.38	1668.84	1659.79	1710.49	1689.33	1654.29
0.5	1725.51	1667.97	1673.37	1675.72	1662.76	1669.50	1659.76	1710.95	1690.49	1655.31
0.55	1725.59	1668.87	1674.75	1676.51	1663.88	1670.15	1660.36	1711.19	1691.05	1655.90
0.6	1725.66	1669.64	1675.85	1677.32	1664.55	1671.59	1660.92	1711.44	1691.81	1656.72
0.65	1725.76	1670.38	1676.55	1677.67	1665.29	1675.57	1661.32	1711.81	1692.04	1657.18
0.7	1725.85	1670.88	1678.34	1677.81	1666.87	1676.82	1662.01	1712.10	1692.25	1657.40
0.75	1725.95	1671.24	1681.32	1677.93	1669.31	1677.24	1662.03	1712.38	1691.98	1657.33
0.8	1726.01	1671.68	1682.98	1678.11	1671.28	1677.47	1662.61	1712.59	1692.28	1657.87

Yaw Rate (deg/sec)	Delay Time (sec)									
	60	120	180	240	300	360	420	480	540	600
0.85	1726.06	1672.16	1683.68	1678.36	1671.76	1677.73	1662.40	1712.56	1692.17	1657.57
0.9	1726.10	1672.54	1683.77	1678.72	1671.74	1677.65	1662.41	1712.78	1692.09	1657.71
0.95	1726.11	1672.85	1683.97	1678.81	1672.42	1677.59	1662.84	1713.01	1691.97	1657.84
1	1726.16	1673.19	1684.74	1678.75	1673.07	1677.87	1662.71	1712.61	1691.64	1657.51
1.05	1726.24	1673.50	1685.19	1679.21	1673.18	1677.68	1662.81	1712.91	1692.08	1657.62
1.1	1726.31	1673.85	1686.52	1679.20	1672.60	1677.23	1662.91	1712.88	1691.98	1657.21
1.15	1726.35	1674.28	1687.61	1679.35	1671.90	1676.38	1663.18	1712.54	1690.91	1656.63
1.2	1726.40	1674.76	1688.07	1679.61	1671.77	1676.69	1662.67	1712.03	1690.28	1656.45
1.25	1726.49	1675.23	1688.18	1679.80	1672.80	1677.70	1662.90	1712.38	1691.57	1657.60
1.3	1726.61	1675.71	1688.74	1680.00	1673.48	1678.46	1663.28	1712.66	1692.15	1658.38
1.35	1726.74	1676.07	1688.89	1680.21	1673.54	1678.63	1663.63	1712.85	1692.62	1658.74
1.4	1726.82	1676.35	1689.08	1680.30	1673.63	1678.18	1663.69	1712.86	1692.43	1658.24
1.45	1726.84	1676.71	1689.08	1680.28	1673.48	1677.02	1663.38	1712.54	1691.75	1656.70
1.5	1726.88	1677.06	1688.38	1679.82	1670.44	1674.48	1662.07	1712.23	1688.17	1654.58
1.55	1726.73	1677.31	1688.37	1679.80	1669.40	1673.49	1661.92	1712.31	1687.70	1653.58
1.6	1726.78	1677.67	1688.65	1679.95	1669.71	1673.54	1662.13	1712.47	1687.47	1654.07
1.65	1726.87	1678.05	1689.06	1680.18	1670.36	1674.16	1662.63	1712.50	1688.27	1654.83
1.7	1726.99	1678.46	1689.35	1680.40	1671.27	1674.99	1662.94	1712.77	1688.96	1655.67
1.75	1727.11	1678.85	1689.67	1680.96	1672.21	1675.84	1663.61	1713.01	1690.24	1656.81
1.8	1727.22	1679.24	1689.92	1681.29	1673.32	1677.00	1664.23	1713.28	1691.30	1657.80
1.85	1727.30	1679.62	1690.25	1681.63	1674.31	1678.00	1664.72	1713.47	1692.37	1658.68

Yaw Rate (deg/sec)	Delay Time (sec)									
	60	120	180	240	300	360	420	480	540	600
1.9	1727.35	1679.89	1690.39	1681.81	1675.17	1678.55	1664.92	1713.54	1692.64	1658.80
1.95	1727.39	1680.15	1690.41	1681.77	1675.68	1679.03	1664.90	1712.97	1692.66	1658.93
2	1727.39	1680.43	1690.37	1681.58	1675.35	1678.62	1664.69	1712.13	1691.68	1658.48

The results of other deployment and other range gates are presented in Appendix B.1, B.2, and B.3.

3.1.4 Comparison with INL wind energy model

Now let us compare the energy output difference between the INL wind energy model and the dynamic model of this study. Figure 3.9 shows the energy estimated by the INL wind energy in comparison to the dynamic model developed. In both cases the same turbine model Gamesa Eolica G52-850kW was used.

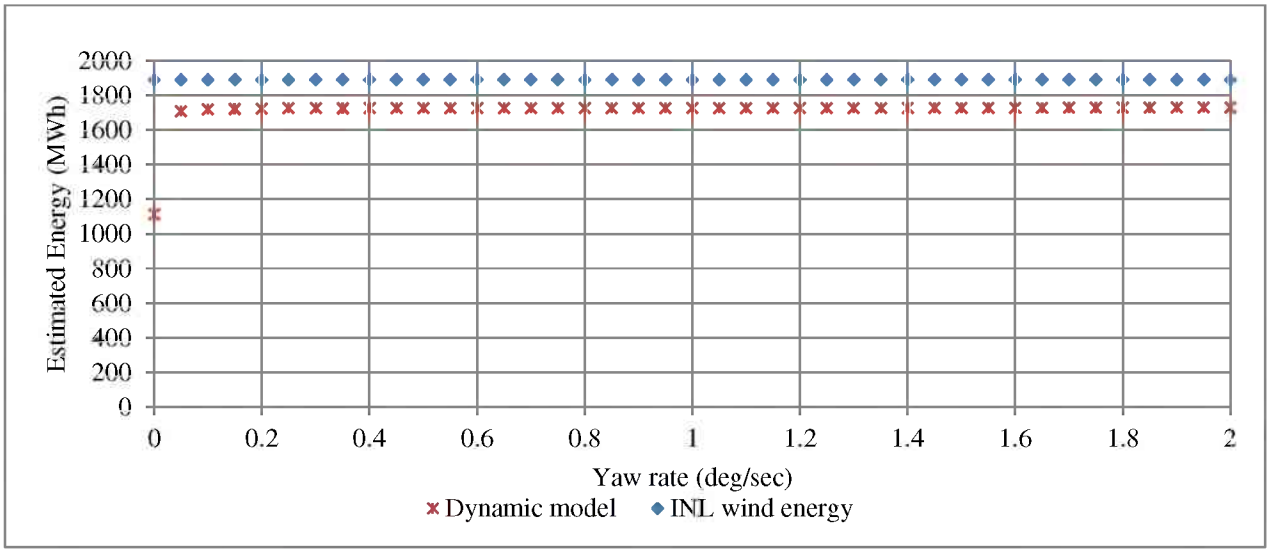

Figure 3.9 Comparison of energy estimate by INL wind energy and dynamic model

It can be seen from Figure 3.9 that the INL wind energy program overestimates the energy by 7% for this time period. This is due to the basic assumption of the INL wind energy program, which states that the turbine is aligned with the prevailing wind at any instant.

3.1.5 Comparison with other models

A comparison of the estimated energy with other energy estimation methods can be found in Figure 3.10. The available energy in the wind during that time period is also presented in the figure.

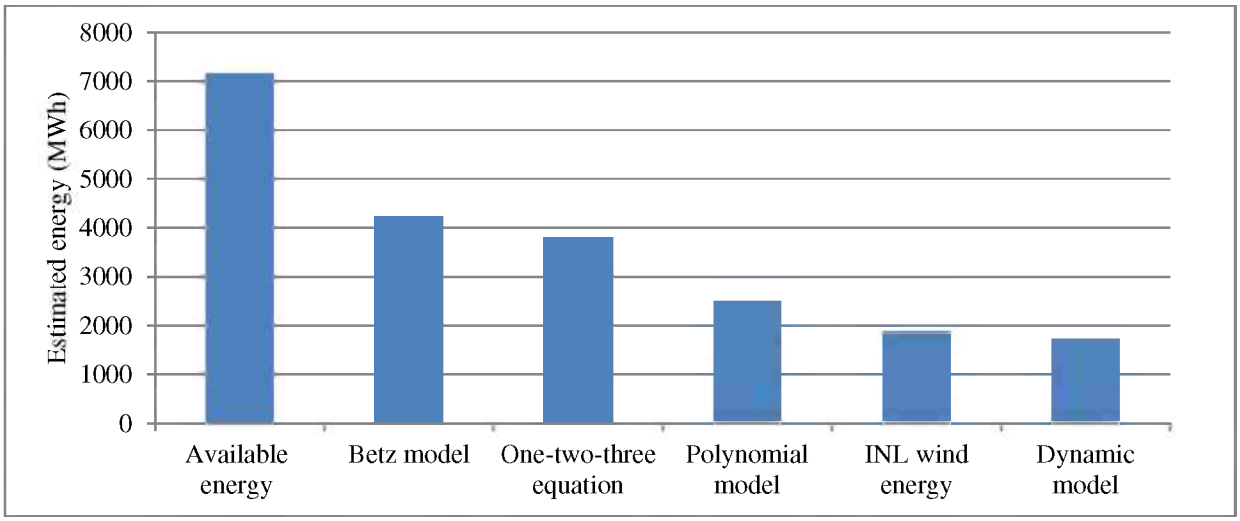

Figure 3.10 Estimated energy by different models

In Figure 3.10 the one-two-three equation, polynomial model, INL wind energy, and dynamic model are turbine specific energy estimates. It can be seen from the figure that by Gamesa Eolica G52-850kW only 24% of the available wind energy can be harnessed (estimation based on the dynamic model). Similarly for INL wind energy model the energy that can be harnessed from wind is 26% and by polynomial model it is 35%. The other range gates and other deployment results can be found in Appendix B.1, B.2 and B.3.

3.1.6 Effect of turbine model

Other turbine options were explored to observe the energy output. The wind frequency distribution for this time period is presented in Figure 3.11. From the frequency distribution we can see that most of the time the wind has a speed of 5 mph ~ 27 mph. Therefore, a turbine with high power output in this range would be a good fit for this location.

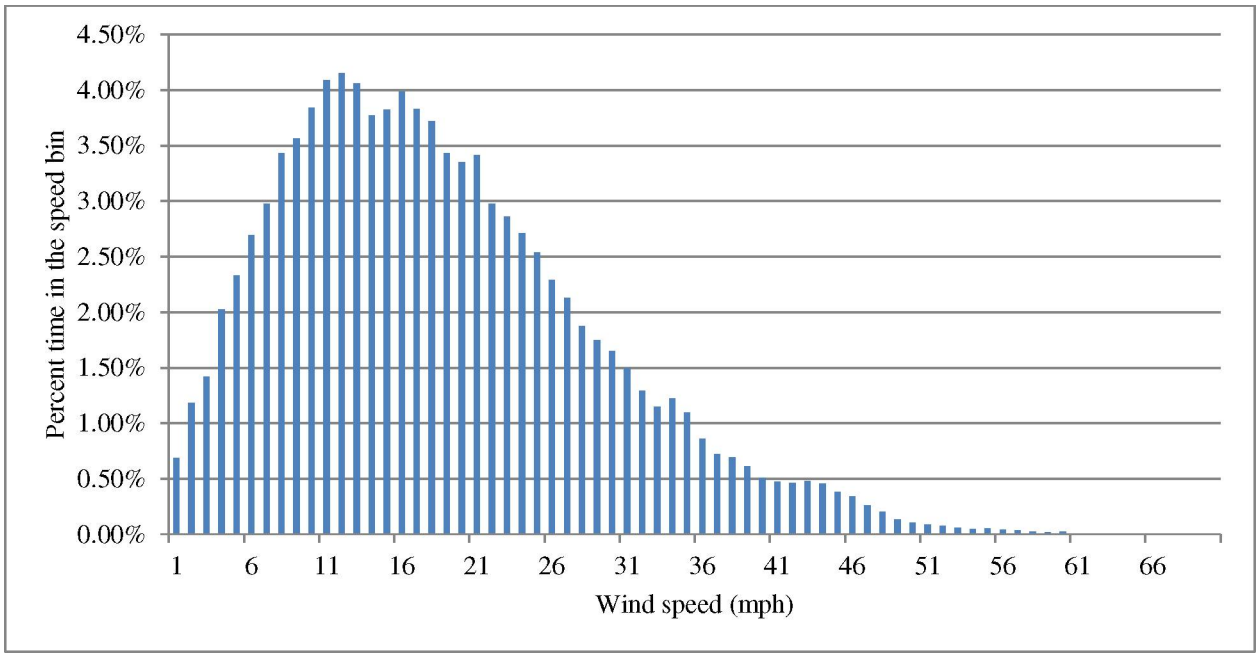

Figure 3.11 Frequency distribution of wind

The explored turbine model was Lagerwey LW72-2000kW. This turbine had a broader operating range. The power curve of this turbine is presented in Figure 3.12. The turbine parameters for the dynamic model are:

Cut in speed: 5 mph
Cutout speed: 57 mph
Rated speed: 33 mph
Region 2 threshold of yaw error (assumed from a generalized estimation found in [11]): 8°
Region 3 threshold of yaw error (assumed from a generalized estimation found in [11]): 18°

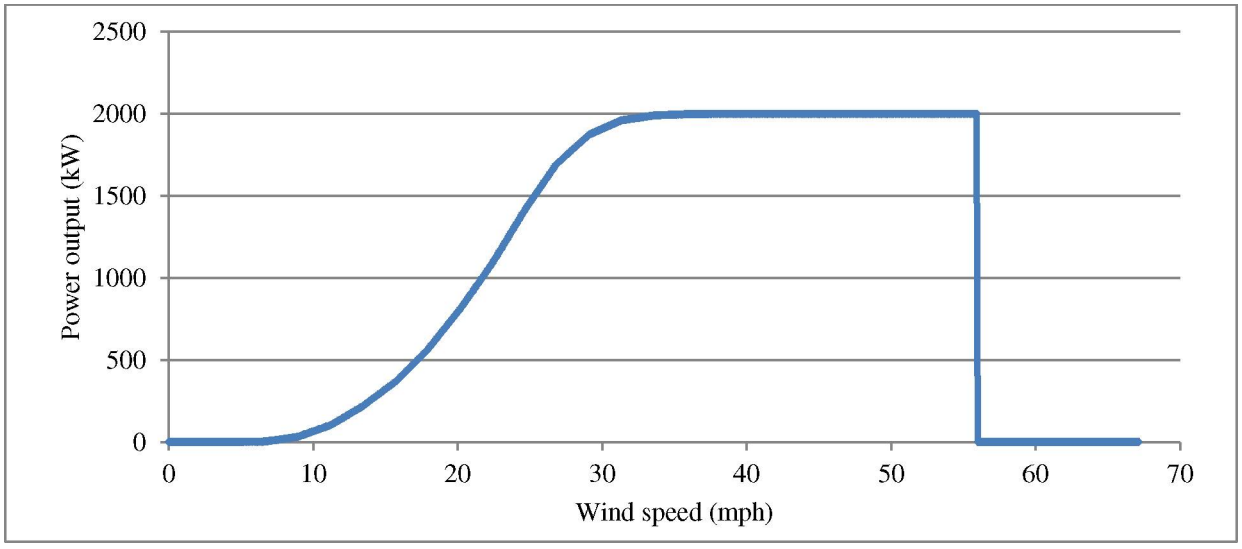

Figure 3.12 Power curve of Lagerwey LW72-2000kW [13]

The energy estimated by different models using Lagerwey LW72-2000kW and Gamesa Eolica G52-850kW can be found in Figure 3.13. The energy output was doubled after using this turbine model. However, the Lagerwey LW72-2000kW turbine is able to harness approximately 26% of the available wind energy as opposed to 24% for Gamesa Eolica G52-850 kW.

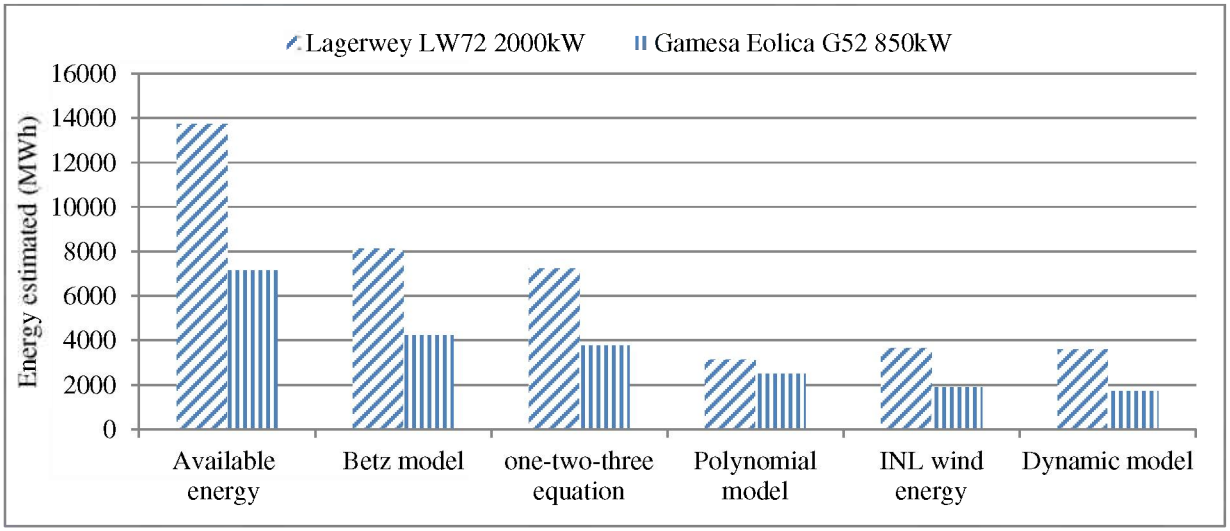

Figure 3.13 Energy estimated by different wind turbine model

3.1.7 Other range gate results

The results of the dynamic model for RG2, RG3, RG4 for mid-lake deployment at a delay time of 1 min are presented in Figure 3.14. The turbine model is Gamesa Eolica G52 850kW. The time period is the mid-lake plateau deployment. RG5 and RG6 were set at altitudes of 150 m and 175 m respectively during mid-lake deployment of the buoy. They were set to test the capabilities of the vindicator sensor but significant amount of data could not be collected by these two range gates. Therefore, no analysis was performed on these.

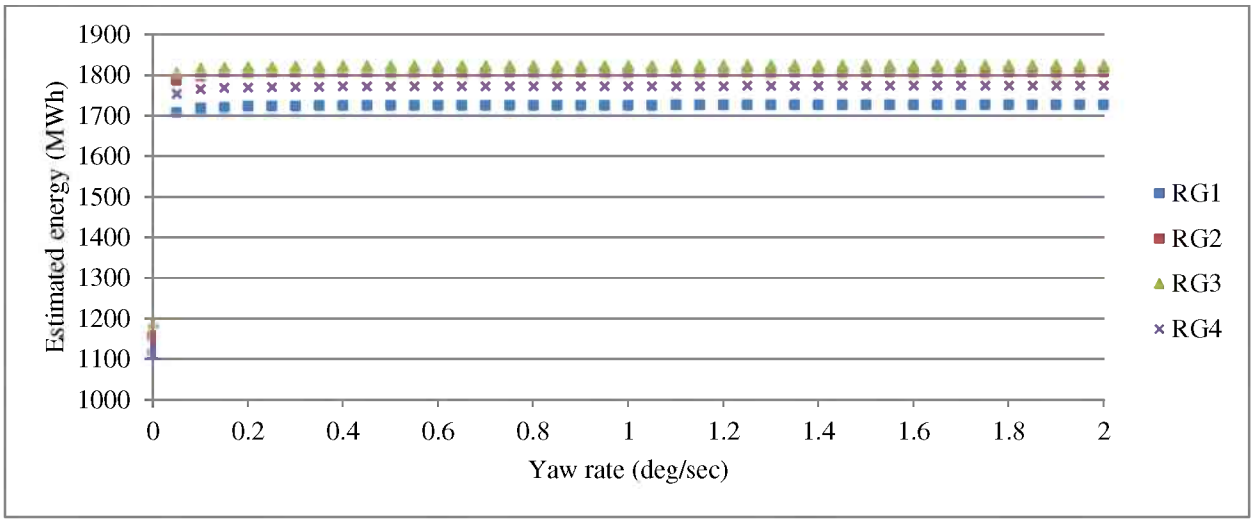

Figure 3.14 Energy estimated at different range gate

It can be seen that the energy estimated increased as the altitude increased. However, the increase was not that significant. The reason for this was that at higher altitudes (75m~125m) the wind speed did not increase that much in this region. The energy output at RG4 was also lower than other range gates. Because the wind speed slowed down at RG4 as seen from Table 3.6. The average wind speeds of the mid-lake deployment for the range gates are presented in Table 3.6. Other deployment results are presented in Appendix B.

Table 3.6 Average wind speeds at different range gates

Range Gate	Altitude(m)	Wind speed (mph)
RG1	75	19.07
RG2	90	19.64
RG3	105	19.83
RG4	125	19.55
RG5	150	18.56
RG6	175	19.07

3.1.8 Effect of time step of data set

A similar study was performed with the 30 sec, 2 min, 5min and 10 min averaged data set. The time frame and the turbine model were similar to the 1 min analysis. The results can be found in Figure 3.15. Theoretically shorter time averaged data set will have more accurate estimation. As we see from the figure the energy estimated varied only less than 2 % with the change of different averaged time.

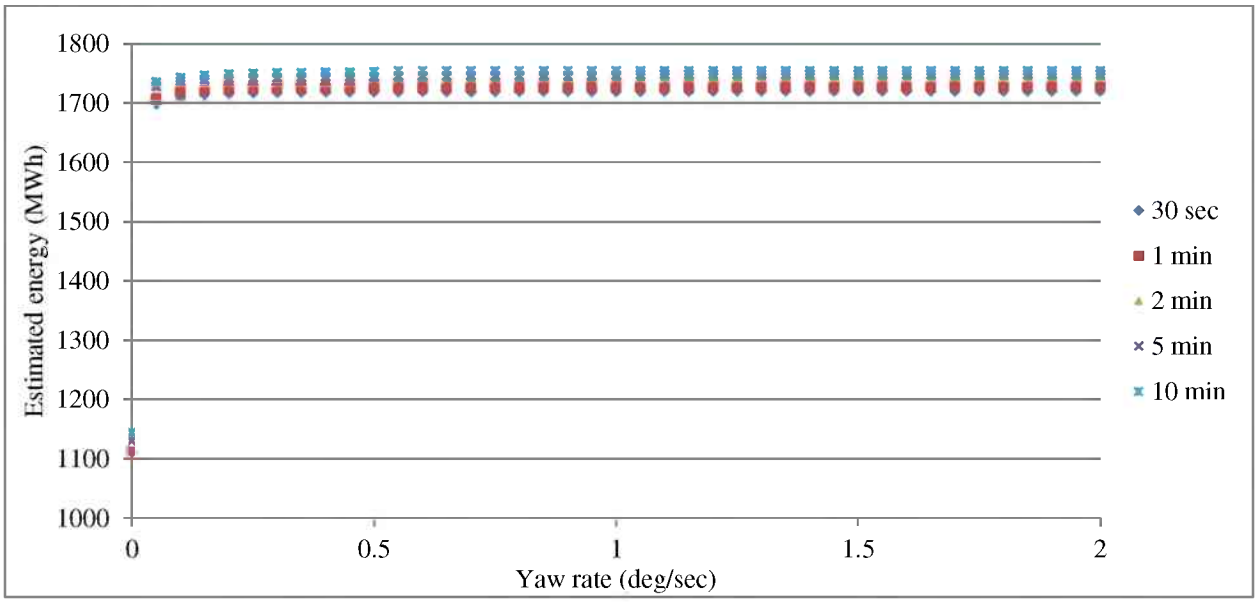

Figure 3.15 Comparison of estimated energy with different time averaged data set

The reason of this increased energy can be explained. At same yaw rate the time taken for the turbine to align itself with the prevailing wind is same for all. Therefore, the yaw error remains minimum for the rest of the delay time. In longer time step the duration of this minimum yaw rate region is longer than shorter time period which results in overestimation in the case of longer time period.

3.1.9 Capacity factor

The capacity factor of a wind farm is the ratio of its actual output over a period of time, to its potential output if it were possible for it to operate at full nameplate capacity during operational time.

The capacity factor is generally calculated over a year to include the seasonal variations on the wind. It is normally presented for the total plant. Therefore, the capacity factor reported on one individual turbine and for a partial wind data for the location can be misleading. It can, however, easily be calculated from the results by the following formula.

$$Capacity\ factor = \frac{Energy\ generated\ by\ the\ turbine}{\begin{matrix}Energy\ generated\ by\ the\ turbine\ if\ it \\ operates\ at\ rated\ capacity\ for\ the\ entire\ time\ period\end{matrix}} \quad (22)$$

The capacity factors of a single Gamesa Eolica G52 850kW during this time period at different altitudes are presented in Table 3.7. The other deployment results are presented in Appendix B.1.

Table 3.7 Capacity factor at different range gate for Gamesa Eolica G52 850kW

Range Gate	Altitude (m)	Energy output (MWh)	Nameplate capacity (kW)	Capacity factor
RG1	75	1707.732224	850	37.9%
RG2	90	1786.540252	850	39.3%

Range Gate	Altitude (m)	Energy output (MWh)	Nameplate capacity (kW)	Capacity factor
RG3	105	1805.26632	850	39.7%
RG4	125	1754.083151	850	38.5%

3.1.10 Other deployments

Similar analysis was performed for other locations. For other locations the same turbine model: Gamesa Eolica G52-850kW was used. The detailed results are presented in Appendix B.

3.2 Data representation

3.2.1 Wind rose

The two major data representation techniques that were used in this study were the wind rose and the frequency distribution. Both are a kind of representation of data segregated in bins. If the data set is the wind speed or wind direction segregated by the bin parameter of prevailing wind direction then it is called the wind rose. If the data set is wind speed segregated by the bin parameter of wind speed it is called the frequency distribution.

The wind rose is the graphical representation of the average wind speed or average duration of wind in any particular range of direction. Therefore, two types of wind rose were generated for the data set: the average wind speed in every direction bin and the duration of wind in any direction bin. The bin size was 10 degrees. For computation, a MATLAB script was developed based on the algorithm presented in Methodology. To generate the wind roses MS Excel® was used using the data calculated by MATLAB. The plot type was radar type plot available in MS Excel.

The wind roses of mid-lake deployment can be found in Figure 3.16 and Figure 3.17. 10 min averaged data sets were used to generate these wind roses. The data was collected at a height of 75 m. The wind roses at a height of 90 m for other deployments can be found in Appendix B.2, B.3, and B.4.

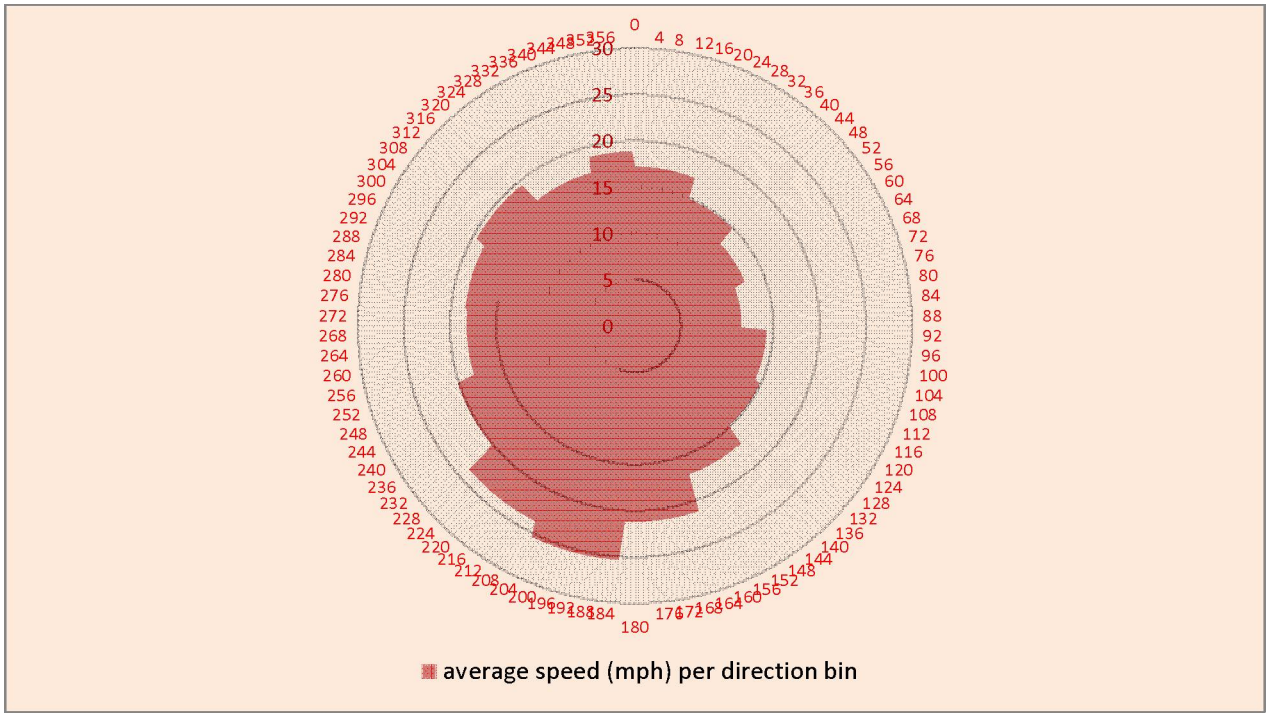

Figure 3.16 Wind rose of averaged speed per direction bin

The wind rose is helpful to determine the predominant wind direction of that location during the time period. The seasonal changes in wind direction and wind speed of a location can be found by comparing the wind roses of different seasons.

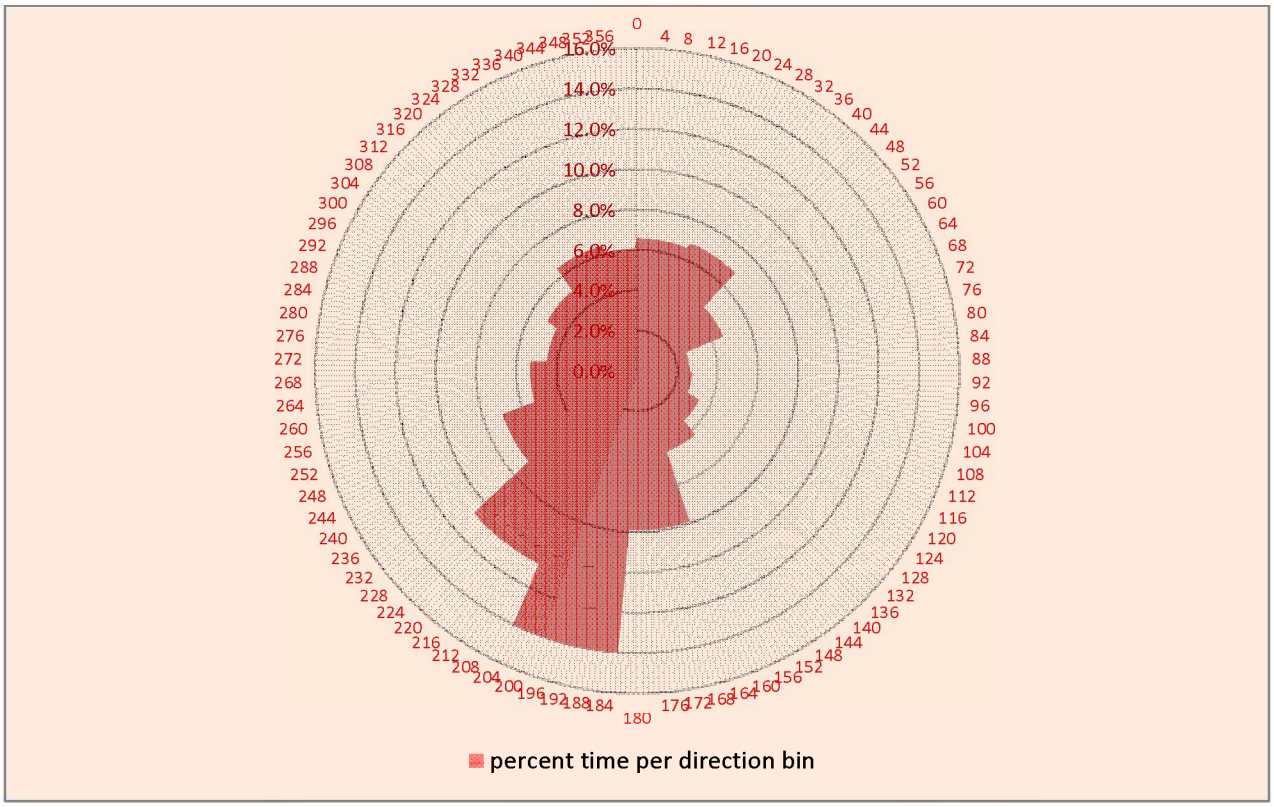

Figure 3.17 Wind rose of fraction time per direction bin

3.2.2 Frequency distribution

Frequency distribution is also calculated by a MATLAB script based on the algorithm presented in Figure 2.7. Unlike the wind rose this plot is more helpful for longer time period of data. The frequency distribution of the RG1 data during the mid-lake deployment is shown in Figure 3.18.

Some interesting information can be found Figure 3.18. First, the typical wind frequency curve follows Weibull or Rayleigh distribution curve. Frequency distribution provides a qualitative result of the data. By knowing the distribution parameters for that location the wind regime can also be predicted for long range energy mapping. However, to estimate the Weibull parameters of that location more than 1~5 years of wind data set is required to remove any seasonal bias. Due to the lack of data these parameters could not be estimated.

Another important feature of frequency distribution is that it shows the wind speeds at which the wind blows most of the time at that location. Therefore, while choosing a turbine for a given location this information can be very helpful as we have seen before. The turbine should have an operating speed which matches the wind speed at which the wind blows most of the time. This way the turbine can harness most of the energy from that location.

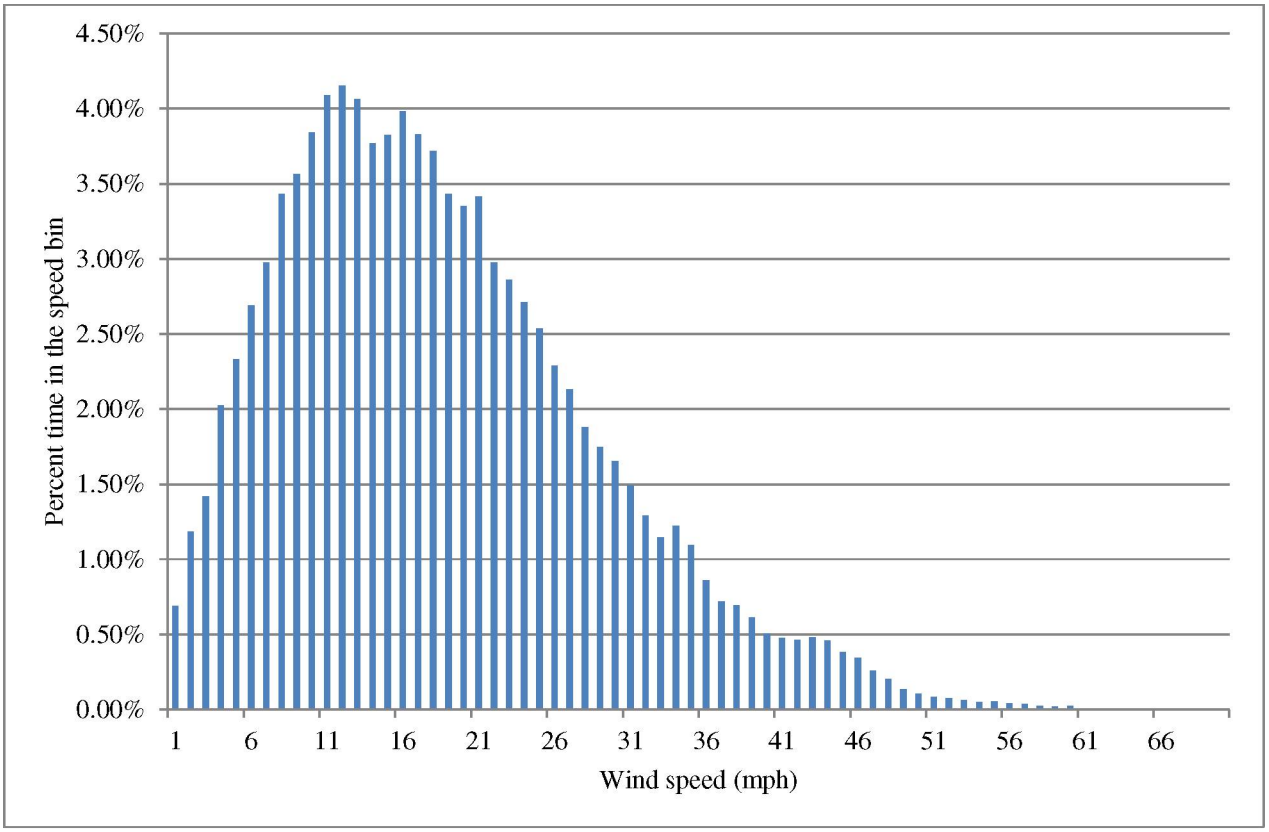

Figure 3.18 Frequency distribution of RG 1

3.3 Data Preprocessing

3.3.1 1 Hz data set

A sample unrefined data set can be found in Table 3.8. The problems with the data set are also marked in the figure.

Table 3.8 Unrefined data set example

DataDBID	DataTimeStamp	ModbusNodelD	SerialNumber	...	WindSpeedHor3MinRG1	WindSpeedHor10MinRG1	WindDirHorRG1	WindDirHor3MinRG1	...
...	...	...	...	...	...	...	...	...	...
1768a1...	1:28:02 PM	1	8	...	4	-4.4	0	0	...
d6068c...	1:28:09 PM	1	8	...	2	-4.8	0	0	...
12695...	1:28:10 PM	1	8	...	1.5	Â	0	0	...

Unnecessary columns

Missing time stamps

Unrecognized character

DataDBID	DataTimeStamp	ModbusNodeID	SerialNumber	…	WindSpeedHor3MinRG1	WindSpeedHor10MinRG1	WindDirHorRG1	WindDirHor3MinRG1	…
17d8c…	1:28:11 PM	1	8	…	Â	-6.6	0	0	…
…	…	…	…	…	…	…	…	…	…

From the unrefined data table the problems were identified as:

1. Unnecessary columns: These were deleted in the refined 1 Hz data set.
2. Missing time stamps: The missing time stamps were filled with NaN values to work with MATLAB codes.
3. The unrecognized characters were replaced by NaN values also.

A refined 1 Hz data set is presented in Table 3.9.

Table 3.9 Refined 1 Hz data example

DataTimeStamp	ModbusNodeID	SerialNumber	…	WindSpeedHor3MinRG1	WindSpeedHor10MinRG1	WindDirHorRG1	WindDirHor3MinRG1	…
…	…	…	…	…	…	…	…	…
1:28:02 PM	1	8	…	4	-4.4	0	0	…
1:28:03 PM	NaN	NaN	…	NaN	NaN	NaN	NaN	…
1:28:04 PM	NaN	NaN	…	NaN	NaN	NaN	NaN	…
1:28:05 PM	NaN	NaN	…	NaN	NaN	NaN	NaN	…
1:28:06 PM	NaN	NaN	…	NaN	NaN	NaN	NaN	…
1:28:07 PM	NaN	NaN	…	NaN	NaN	NaN	NaN	…
1:28:08 PM	NaN	NaN	…	NaN	NaN	NaN	NaN	…
1:28:09 PM	1	8	…	2	-4.8	0	0	…
1:28:10 PM	1	8	…	1.5	NaN	0	0	…
1:28:11	1	8	…	NaN	-6.6	0	0	…

DataTime Stamp	Modbu sNodel D	SerialN umber	...	WindSpeedHo r3MinRG1	WindSpeedHor 10MinRG1	WindDirH orRG1	WindDirHor3 MinRG1	...
PM								
...	...	...	...	...	...	...	...	...

3.3.2 Time averaged data set

The refined 1 Hz data set then used to generate the time averaged data set. Data were averaged over 30 sec, 1 min, 2 min, 5 min, and 10 min time period. A sample output of the averaged data set can be found in Table 3.10. The standard deviations were also calculated for any possible future work with this data set.

Table 3.10 Time averaged data set example (30 sec)

DataTimeStamp	RG1 Speed	RG1 Direction	RG2 Speed	...	RG1wind speed Standard deviation	RG1wind direction Standard deviation	RG2wind speed Standard deviation	...
...	...	...		...	...	...	...	...
1:28:00 PM	NaN	NaN	NaN	...	NaN	NaN	NaN	...
1:28:30 PM	8	163	8.2	...	0.002	0.005	0.002	...
1:29:00 PM	8.2	165	8.4	...	0.004	0.004	0.003	...
1:29:30 PM	8.3	159	8.5	...	0.054	0.024	0.004	...
1:30:00 PM	6.7	168	6.6	...	0.126	0.095	0.097	...
1:30:30 PM	NaN	NaN	NaN	...	NaN	NaN	NaN	...
1:31:00 PM	3	140	3.1	...	NaN	NaN	NaN	...
1:28:09 PM	2.6	138	2.8	...	0.003	0.005	0.004	...
1:28:10 PM	4.1	163	4.36	...	0.004	0.002	0.003	...
1:28:11 PM	1	154	1.1	...	0.008	0.004	0.006	...
...	...	...		...	...	...	...	...

Chapter 4

4.1 Conclusion

This project was conducted to assess the wind potential over Lake Michigan. The wind data were collected at 1 Hz frequency at six different altitudes within the range of 55m-175m at different locations over the entire project period. The data were collected by state-of-art LIDAR sensor mounted on an unmanned buoy named Wind Sentinel that was developed by AXYS Technologies, Inc., Sydney, British Columbia, Canada.

A thorough literature review was performed to develop an accurate methodology to analyze the collected wind data and assess the wind potential over Lake Michigan. From the literature review it was found that the publicly available estimation techniques overestimate the energy output because of not considering the effect of yaw error and dynamic yaw motion in the estimation process. Therefore, a dynamic mathematical model capable of considering the yaw error and dynamic yaw motion in the estimation technique was developed.

This model required a quality controlled continuous stream of daily data set. However, the collected data were at 1 Hz frequency and had some issues such as missing data and time stamps, unnecessary columns, and unrecognized characters in the data set. A refining module for this unrefined data set was developed to address these issues. An averaging module was also developed to average the data set over 30 sec, 1 min, 2 min, 5 min, and 10 min to observe the effect of data set frequency on the energy output. To represent the dominant wind direction and time duration of wind blowing in different wind directions, a wind rose generating model was developed. A wind frequency generating module was also developed.

The dynamic model was developed in such a way that the effect of yaw control can be included or disregarded in the calculation. If the yaw error is disregarded then the results should be same as the INL wind energy model. The dynamic model was validated by comparing a test data set results with the INL wind energy model. For validation process the effect of yaw error was not considered and the dynamic model generated same results as the INL wind energy model with the same data set which confirms the validity of the MATLAB code developed.

The effect of the two important parameters of the dynamic model, yaw rate and delay time, on the energy output was analyzed. The results suggested that the turbine generated more energy if the yaw rate of the turbine increased. Up to 0.05 deg/sec yaw rate the energy increased sharply. Later the increase was not that significant. The effect of delay time was quite unpredictable. The only conclusion that can be drawn is that the turbine generated highest energy at the minimum delay time which is equal to the time step of the data set.

The findings of the dynamic model were then compared with the INL wind energy model. The INL wind energy model overestimated the output energy. The amount of overestimate depends on the time frame of data as the energy is dependent on the time frame of the data set. For the mid-lake

deployment the INL energy model overestimated the output energy by 7% at 75 m altitude. The reason for this was that the INL energy did not consider the yaw misalignment in the energy estimation. The dynamic model results were also compared with the other estimation techniques. The results showed that the turbine used for calculation (Gamesa Eolica G52-850 kW) could harness about 24% of the available wind energy during the mid-lake deployment at 75 m of hub height. The other locations and hub height results were also very close to this.

The dynamic model was a turbine specific estimation technique like INL wind energy model, polynomial model, and one two three equation model. To observe the effect of turbine model on the estimated output energy another turbine, Lagerwey LW72-2000 kW, was used. The energy output was doubled by using this turbine because the turbine was larger in size and had higher rated power output. However, the turbine harnessed about 26% of the available wind energy. The effect of the time step of the data set was also analyzed by using different time averaged data set. The results showed that longer time averaged data sets overestimated energy by small amounts.

The capacity factors of the turbine used in dynamic model (Gamesa Eolica G58-850 kW) were also calculated. The capacity factor varied from 35%~40% for different altitudes and different deployment locations. Note that, the capacity factor calculated was only for one turbine. A wind farm consists of a large of number of wind turbines. Some of those wind turbines may have a lower capacity factor than the other turbines in that wind farm due to maintenance and unavailability of wind resource. While calculating the capacity factor of the entire wind farm the capacity factors of individual turbines are averaged. Therefore, for entire wind farm the capacity factor is generally lower than the capacity factor of an individual turbine. The wind roses provided a good representation of the prevailing wind direction and wind speed. The frequency distributions for different deployments and different altitudes were also generated.

The dynamic yaw control model predicted that the potential energy output from the Gamesa Eolica G58-850 kW would be about 7% lower than the prediction of the INL wind energy model for the mid-lake deployment of the Wind Sentinel. Of course it does not take into account the power that goes into the dynamic control of the turbine.

4.2 Suggested future work

As seen from the results and discussion section it is not possible to truly align the turbine with the prevailing wind. This results in a loss in energy output. A possible solution for this can be the prediction of the wind direction by utilizing the previous wind direction pattern. A time series can be formed to estimate the wind direction for the coming few seconds. Several mathematical estimation techniques can be used such as artificial neural networking (ANN), machine learning approach, etc. Another solution can be sensing the wind direction upstream of the wind turbine using LIDAR technology. NREL (National Renewable Energy Laboratory) has performed a field test of such kind of technology [18].

The estimated energy by different turbines can be used to perform a cost analysis. By knowing the installation and running cost of different turbine models a cost analysis can be performed to find the best cost effective turbine for any location.

References

[1] 20% wind energy by 2030, Increasing Wind Energy's Contribution to U. S. Electricity Supply', Energy Efficiency and Renewable Energy, U. S. Department of Energy, July 2008.

[2] Owen. R., Final Report to Wisconsin Focus on Energy on Lake Michigan Offshore Wind Resource Assessment, 2004. Retrieved from http://www.focusonenergy.com/files /document_management_system/renewables/lakemichiganwindresource_finalreport.pdf

[3] Betz, A. Introduction to the Theory of Flow Machines. (D. G. Randall, Trans.) Oxford: Pergamon Press, 1966.

[4] Hartwanger, D., Horvat, A., 3D Modelling of a Wind Turbine Using CFD, NAMFEMS UK Conference 2008 "Engineering Simulation: Effective Use and Best Practice", Cheltenham, United Kingdom, June 10-11, 2008.

[5] Gorban, A. N., Limits of the wind turbine efficiency for free fluid flow, Journal of Energy Resources Technology, 2001, Vol. 123, pp. 311-317.

[6] White, F.M., Fluid Mechanics, 2nd Edition, McGraw-Hill, Singapore, 1988.

[7] Carlin P.W., Analytic expressions for maximum wind turbine, average power in a Rayleigh wind regime, Proc. 1997 ASME/AIAA wind Symposium, pp. 255–263.

[8] Kiranoudis C.T., Voros N.G., Maroulis Z.B., Short-cut design of wind farms. Energy Policy 2001, pp. 567–578.

[9] Jafarian M., Ranjabar A.M., Fuzzy modeling techniques and artificial neural networks to estimate annual energy output of a wind turbine, Renewable Energy 35; 2010, pp. 2008–2014.

[10] Pallabazzer R., Provisional estimation of the energy output of wind generators. Renewable Energy 29, 2004, pp. 413–20.

[11] Torres J.L., Prieto E., Garcia A., De Blas M., Ramirez F., De Francisco A., Effects of the model selected for the power curve on the site effectiveness and the capacity factor of a pitch regulated wind turbine. Solar Energy 74, No. 2, 2003, pp. 93–102.

[12] Powel W.R., An analytical expression for average output power of wind machine. Solar Energy 26, No. 1, 1981, pp. 77–80.

[13] https://inlportal.inl.gov/portal/server.pt?open=512&objID=424&PageID=3993&cached=true&mode=2&userID=1829 last access date: 15/12/2011

[14] Manwell J.F., McGowan J.G., and Rogers A.L., Wind Energy Explained: Theory, Design and Application, John Wiley & Sons, New York, NY, 2002

[15] Mamidipudi P., Dakin E., Hopkins A., Belen F. Leishman J., Yaw Control The Forgotten Control Problem, March, 2011.

[16] http://ntrs.nasa.gov/archive/nasa/casi.ntrs.nasa.gov/19770009539_1977009539.pdf

[17] http://www.inl.gov/wind/idaho/data/idaho_state/update/twitchell/ last access date: 15/12/2011.

[18] Scholbrock A., Fleming P., Fingersh L, Wright A., Schlipf D., Haizman F., Belen F., "Field Testing LIDAR Based Feed-Forward Controls on the NREL Controls Advanced Research Turbine", 51st AIAA Aerospace Meeting, Grapevine, Texas, 2013.

Appendix A

A.1 Dynamic model

```
%last updated on 17 March 2013 %% final version 2.5

clear;
clc;
close all;
clear all;
% turbine parameters and importing the turbine data
rgn2_spd=8.9;%mph
rgn2_thrsold=8;
rgn3_spd=31.3;%mph
rgn3_thrsold=18;
cut_out=47;
[trbn_data trbn_text]=xlsread('turbine_data.xlsx');
turbine=17;
trbn_power=trbn_data(:,turbine+1);
trbn_speed=trbn_data(:,1);
% for different delay time the data was calculated
for freq=30:30:300
      % saving the results
    freq_s=num2str(freq);
      dtd=['30 sec yaw rate results for 30 sec (lake shore): ',freq_s,'
secs.txt'];
      diary(dtd)
      diary on
      disp(freq)
    data_freq=30;

    sumcounter=0;
    f_sumcounter=0;
      % for different yaw rate the results are calculated
      for yaw_rate_per_sec=0:.05:2
            disp(yaw_rate_per_sec)
            yaw_rate=yaw_rate_per_sec*data_freq;% will be changed in
different data set
            dt_freq=data_freq; % data frequency
            ratio=freq/dt_freq;
            reply='y';
            if isempty(reply)
                  reply='y';
            end
            if reply=='y'
                  dynamic_decision=1;
            else
                  dynamic_decision=2;
            end
            daily_energy=zeros(500,1);
            wind_data_length=86400/dt_freq;
```

```
          loop_counter=1;
          for file_name=734811:734868
               file_date=datestr(file_name,29); % ISO format date
               import_file=['GVSU-Vindicator-30-sec-
',file_date,'.csv'];
               dir_data=dir;
               dir_index=[dir_data.isdir];
               file_list={dir_data(~dir_index).name};
               decision=strcmp(import_file,file_list);
               decision=sum(decision);
               if decision==1
                    str=['Importing file: ',import_file];
                    file=importdata(import_file);
                    dynamic_trbn_direction=zeros((86400/dt_freq),6);
                    % if dynamic model activated
                    if dynamic_decision==1
                         c=3; % wind direction column
                         for i=1:6
                              dynamic_trbn_direction(1,i)=file(1,c);
%initial value
                              c=c+2;
                         end
                         for c=2:2:12
                              for i=1:(86400/dt_freq)
                              file(i,c)=file(i,c)*2.2369;
%conversion to mph
                              end
                         end
                         n=1;
                         for c=2:2:12
                              j=1;
                              k=1;
                              l=1;
                              for i=2:ratio:(86400/dt_freq)


                                   if file(i,c)<=rgn2_spd ||
file(i,c)>cut_out || isnan(file(i,c)) % region 1 and 4
                                  for l=i:i+ratio

dynamic_trbn_direction(l,n)=dynamic_trbn_direction(l-1,n); % no change
in turbine orientation
                                  end
                                   elseif (file(i,c)>=rgn2_spd &&
file(i,c)<rgn3_spd)||(file(i,c)>rgn3_spd && file(i,c)<=cut_out) %
region 2 & 3
                                  if file(i,c)>=rgn2_spd &&
file(i,c)<rgn3_spd
                                      thrsold=rgn2_thrsold;
                                  else
                                      thrsold=rgn3_thrsold;
                                  end
```

```
                                        error=file(i-1,c+1)-
dynamic_trbn_direction(i-1,n); %checking yaw error
                                        if abs(error)<thrsold
                                    for l=i:i+ratio

dynamic_trbn_direction(l,n)=dynamic_trbn_direction(l-1,n); % if yaw
error is less than accepted value then no change in turbine
orientation
                                    end
                                        elseif abs(error)>=thrsold
% activated yaw rotation
                                             if error<0 % for
clock wise rotation
                                        sign=1;
                                    else
                                        sign=2;
                                    end
                                    m=1;
                                    % step 1
                                    if yaw_rate>abs(error)

dynamic_trbn_direction(i,n)=file(i-1,c+1); % if yaw movement is larger
than error then the turbine will stop at the angle of wind direction
                                    else

dynamic_trbn_direction(i,n)=dynamic_trbn_direction(i-1,n)+(-
1)^sign*yaw_rate;
                                    end
                                    % step 2
                                    if ratio==2
                                        error=file(i,c+1)-
dynamic_trbn_direction(i,n);
                                        if yaw_rate>abs(error)

dynamic_trbn_direction(i+1,n)=file(i,c+1); % if yaw movement is larger
than error then the turbine will stop at the angle of wind direction
                                        else

dynamic_trbn_direction(i+1,n)=dynamic_trbn_direction(i,n)+(-
1)^sign*yaw_rate;
                                        end
                                    end
                                    if ratio>2

                                       error=file(i,c+1)-
dynamic_trbn_direction(i,n);


limiter=floor(abs(error/yaw_rate));% how many time steps is needed for
the correction of yaw
```

```
                                        if limiter>=ratio ||
isnan(limiter) || isinf(limiter)
                                            limiter=ratio-2;
                                        end
                                         if limiter>=1 &&
isinf(limiter)==0 && i<=86400/dt_freq
                                             for l=i+1:i+limiter

dynamic_trbn_direction(l,n)=dynamic_trbn_direction(l-1,n)+(-
1)^sign*yaw_rate*m;

dynamic_trbn_direction(l,n)=error_correction(dynamic_trbn_direction(l,
n));
                                             end
                                         end
                                    end
                                    %step 3
                                    if ratio>2
                                      for l=i+limiter+1:i+ratio-1

dynamic_trbn_direction(l,n)=dynamic_trbn_direction(l-1,n);

dynamic_trbn_direction(l,n)=error_correction(dynamic_trbn_direction(l,
n));
                                      end
                                    end

                                end
                                m=1;
                            end
                            j=j+1;
                        end
                        n=n+1;
                        end
                            %toc
                            if
length(dynamic_trbn_direction)>(86400/dt_freq) % deleting the end
values
                                for i=1:(length(dynamic_trbn_direction)-
(86400/dt_freq))

dynamic_trbn_direction(length(dynamic_trbn_direction),:)=[];
                                end
                            end
                            % if dynamic model not activated
                        elseif dynamic_decision==2
                            for c=2:2:12
                                for i=1:(86400/dt_freq)
                                file(i,c)=file(i,c)*2.2369; %conversion to
mph
                                end
                            end
```

```
                        cl=1;
                        for c=3:2:14
                            for r=1:(86400/dt_freq)

dynamic_trbn_direction(r,cl)=file(r,c);
                            end
                            cl=cl+1;
                        end
                    end
                      % yaw error
                      d=zeros((86400/dt_freq),6);
                      s=zeros((86400/dt_freq),6);
                      cl=1;

                      for c=2:2:13
                            for i=1:(86400/dt_freq)
                                  s(i,cl)=file(i,c);% wind speed mph
                                  d(i,cl)=file(i,c+1); % wind direction
                            end
                      cl=cl+1;
                      end
                      for c=1:6
                            for i=1:(86400/dt_freq)
                                  if d(i,c) == 90
                                        d(i,c)=NaN;
                                  end
                            end
                      end
                            error=d-dynamic_trbn_direction;
                %nancounter
                nancounter=isnan(s);
                sumcounter=sum(nancounter);
                      energy=zeros((86400/dt_freq),6);
                      for c=1:6
                            for i=1:(86400/dt_freq)
                                  s(i,c)=s(i,c)*cosd(error(i,c)); %
resolved wind speed
                                  for j=1:length(trbn_data)
                                        if
(round(s(i,c)*10)/10)==trbn_data(j,1) % finding the value in turbine
file

      energy(i,c)=trbn_data(j,turbine+1)*data_freq;
                                        end
                                  end
                            end
                      end
                      for i=1:6

      daily_energy(loop_counter,i)=sum(energy(:,i))/(3600000);

                      end
```

```
                end
                loop_counter=loop_counter+1;
            end
            %fprintf('\n')
            for i=1:6
                total_energy=sum(daily_energy(:,i));
                fprintf('Total_energy_for_the_time_period:_RG%d: %f
MWh\n',i,total_energy)
        end
        f_sumcounter=f_sumcounter+sumcounter;
           fprintf('\n')
      end
      diary off
end
```

A.2 Other models

A.1.1 Other models

```
% Unit of energy: MWh

clear;
clc;
close all;
freq=30;
density=1.155;
power=zeros((86400/freq),6);
energy=zeros(6,1);
total_energy=zeros(6,1);
avg_spd=zeros(6,1);
avg_array=[];
loop_counter=1;
dtd='Other model results diff turbine.txt';
diary(dtd)
diary on
%disp('Import the Wind data file.....');
for file_name=734811:734868
    file_date=datestr(file_name,29); % ISO format date
    import_file=['GVSU-Vindicator-30-sec-',file_date,'.csv'];
    dir_data=dir;
    dir_index=[dir_data.isdir];
    file_list={dir_data(~dir_index).name};
    decision=strcmp(import_file,file_list);
    decision=sum(decision);
    if decision==1
        str=['Importing file: ',import_file];
        %disp(str)
        tic
        file=importdata(import_file);
```

```
        %toc
        j=1;
        for c=2:2:12
            for i=1:(86400/freq)
                power(i,j)=file(i,c).^3.*0.5.*density; % W
            end
            j=j+1;
        end
        i=1;
        for c=2:2:12
            avg_spd(i)=nanmean(file(:,c)); % m/s
            i=i+1;
        end
        for i=1:6

energy(i)=nansum(power(:,i)).*freq./3600./1000./1000.*pi*58^2/4;
%MWh/m2
        end
        total_energy=total_energy+energy;
        avg_array=[avg_array avg_spd];
        loop_counter=loop_counter+1;
    end
end
% average wind speed
fprintf('Average wind speed:\n');
avg_spd=nanmean(avg_array,2);
for i=1:6
    fprintf('RG%d Average speed: %.3f m/s \n',i,(avg_spd(i))); %energy
is multiplied by area of LW58-850
end
fprintf('\n');
% energy available for G52-850
fprintf('Energy available:\n');
for i=1:6
    fprintf('RG%d Energy (for G58-850): %.3f MWh
\n',i,(total_energy(i))); %energy is multiplied by area of LW58-850
end
fprintf('\n');
% betz analysis
betz_energy=total_energy.*0.593;
fprintf('Betz model:\n');
for i=1:6
    fprintf('RG%d Energy (for G58-850): %.3f MWh
\n',i,(betz_energy(i))); %energy is multiplied by area of G58-850
end
fprintf('\n');
% one-two-three equation
fprintf('Energy generation (one-two-three equation model):\n');
one_two_three=(density/1.18)*(2*58/3)^2.*(avg_spd).^3; %in W
one_two_three=one_two_three./1000000*(60/3600); % in MWh/min
one_two_three=one_two_three.*24.*60.*(loop_counter-1);
for i=1:6
```

```
    fprintf('RG%d Energy (for LW58-850) : %.3f MWh
\n',i,one_two_three(i)); %energy is multiplied by area of G52-850
end
diary off
```

A.1.2 Polynomial model

```
% Unit of energy: MWh
clear;
clc;
close all;
freq=60;
density=1.155;
power=zeros((86400/freq),6);
energy=zeros(6,1);
total_energy=zeros(6,1);
avg_spd=zeros(6,1);
avg_array=[];
loop_counter=0;
diary('Polynomial results NOAA.txt')
diary on
%disp('Import the Wind data file.....');
for file_name=734873:734967
    file_date=datestr(file_name,29); % ISO format date
    import_file=['GVSU-Vindicator-1-min-',file_date,'.csv'];
    dir_data=dir;
    dir_index=[dir_data.isdir];
    file_list={dir_data(~dir_index).name};
    decision=strcmp(import_file,file_list);
    decision=sum(decision);
    if decision==1
        str=['Importing file: ',import_file];
        %disp(str)
        tic
        file=importdata(import_file);
        %toc
        j=1;
        for c=2:2:12
            for i=1:(86400/freq)
                power(i,j)=power_function(file(i,c)); % kW
            end
            j=j+1;
        end
        for i=1:6
            energy(i)=nansum(power(:,i))*60/1000/3600; %MWh/m2
        end
        total_energy=total_energy+energy;
    end
end
fprintf('polynomial model:\n');
for i=1:6
```

```
    fprintf('RG%d Energy (for G58-850): %.3f MWh
\n',i,(total_energy(i))); %energy is multiplied by area of G58-850
end
fprintf('\n');
diary off
```

```
function
power_output=power_function_inl(wind_speed,wind_set_values,turbine_pow
er)
% remember! output is in kW

wind_speed=round(wind_speed*2.2369*10)/10; %conversion to mph
row=find(wind_set_values==wind_speed);
power_output=turbine_power(row);
if isempty(row)
    power_output=0;
end
```

A.1.3 INL wind energy

```
% Unit of energy: MWh
clear;
clc;
close all;
freq=60;
density=1.155;
power=zeros((86400/freq),6);
energy=zeros(6,1);
total_energy=zeros(6,1);
avg_spd=zeros(6,1);
avg_array=[];
loop_counter=0;
[trbn_data trbn_text]=xlsread('turbine_data.xlsx');
turbine=17;
trbn_power=trbn_data(:,turbine+1);
trbn_speed=trbn_data(:,1);
disp('Import the Wind data file.....');
diary on
diary('INL results for 1 min.txt')
for file_name=734997:735240
    file_date=datestr(file_name,29); % ISO format date
    import_file=['GVSU-Vindicator-1-min-',file_date,'.csv'];
    dir_data=dir;
    dir_index=[dir_data.isdir];
    file_list={dir_data(~dir_index).name};
    decision=strcmp(import_file,file_list);
    decision=sum(decision);
    if decision==1
        str=['Importing file: ',import_file];
        disp(str)
        tic
```

```
        file=importdata(import_file);
        toc
        j=1;
        for c=2:2:12
            for i=1:(86400/freq)

power(i,j)=power_function_inl(file(i,c),trbn_speed,trbn_power); % kW
            end
            j=j+1;
        end
        for i=1:6
            energy(i)=nansum(power(:,i))*60/1000/3600; %MWh/m2
        end
        total_energy=total_energy+energy;
    end
end
fprintf('INL wind energy:\n');
for i=1:6
    fprintf('RG%d Energy (for G52-850kW): %.3f MWh
\n',i,(total_energy(i)));
end
fprintf('\n');
diary off
```

```
function power_output=power_function(wind_speed)
% remember! output is in kW

cut_in=8.9;% mph
rated_speed=18;% mph
cut_out=47;% mph
rated_power=850; % in kW
m=2;
wind_speed=wind_speed*2.2369; %conversion to mph
if wind_speed<cut_in || wind_speed>cut_out
    power_output=0;
elseif wind_speed>rated_speed && wind_speed<cut_out
    power_output=rated_power;
elseif wind_speed>=cut_in && wind_speed<=rated_speed
    power_output=(wind_speed^m-cut_in^m)/(rated_speed^m-
cut_in^m)*rated_power;
elseif isnan(wind_speed)
    power_output=0;
end
```

A.2 One second refining module

```
%% One second data refining module
clear all;
clc;
close all;
```

```
% file progress graphics handler
h=waitbar(0,'Files Processing...');
step=0;
steps=395; %number of daily data files

% logging of the results
dt=date;
dtd=['Log-w1.1-',dt,'.txt'];
diary(dtd)
diary on

% data file processing in range
for file_name=734783:735224
     % importing the unrefined raw data file
    file_date_s=datestr(file_name,29); % ISO format date
    import_file=[file_date_s,'.csv'];
    check_file=['GVSU-Vindicator-Refined-',file_date_s,'.csv'];
    file_date=file_name;
     % looking for the data file in the directory and checking for the
file is already prcessed or not
    dir_data=dir;
    dir_index=[dir_data.isdir];
    file_list={dir_data(~dir_index).name};
    decision=strcmp(import_file,file_list);
    decision1=strcmp(check_file,file_list);
    decision=sum(decision);
    decision1=sum(decision1);
    str=['Importing file: ',import_file];
    disp(str)

    if decision==1 && decision1~=1
        %% Importing the unrefined 1 sec data
        file=importdata(import_file,',',1);
        date=file.textdata(:,2); % Time stamp
        date(1)=[]; % deleting the column header
        st_date=file_date; % initial date

        % Creating a time stamp
        date_stamp=linspace(st_date,(st_date+1-1.1574e-005),86400); %
creating the time stamp (numerical value)
        date_stamp_s=datestr(date_stamp,31); % converting the
numerical time stamp
        date_stamp_s=cellstr(date_stamp_s); % converting the HH:MM:SS
strings array to cell array to make them queriable
        date_stamp_s=strtrim(date_stamp_s); % Trimming the white space
from the front and back from the string values

        % Data assign
           limit=size(file.data,2);
        column_n=zeros(86400,limit); % creating new array for storing
the refined data
```

```
        length_of_data=length(date);
        sttr=date(length_of_data);

           % checking the last time stamp for check
        dsp=['Last time stamp is',sttr];
        disp('For checking purpose:')
        disp(dsp)

        % Comparing the time stamps and adding NaN values in missing
time stamps
        for i=1:86400
                find1=strcmp(date_stamp_s(i),date); % comparing the
time stamp from data file with the created time stamp
                k=find(find1>0);
                      if isempty(k)==0
                                column_n(i,:)=file.data(k,:);
                      else % adding NaN values if the time stamp is
missing
                                column_n(i,:)=NaN;
                      end
           end

        % Output
        day_of_data=st_date;
        date_f=datenum(day_of_data);
        date_data=datestr(date_f,1);
        date_f=file_date;
        date_stamp_f=linspace(date_f,(date_f+1-1.1574e-005),86400)';
        file_date=date_f;
        file_date=datenum(file_date);
        filename=['GVSU-Vindicator-Refined-',file_date_s,'.csv'];
        answer=[date_stamp_f column_n];
        csvwrite(filename,answer); % writing a csv file for the
refined data set
        str=[import_file,': File Processed Successfully !'];
        disp (str)
    else
           str=[import_file,': File not found !'];
           disp(str)
    end
    step=step+1;
    waitbar(step/steps)
end
close(h)
diary off
```

A.3 Averaging module

```
% file progress graphics handler
h=waitbar(0,'Files Processing...');
step=0;
steps=441;
```

```
% logging of the results
dt=date;
dtd=['Average-Log-5-min-',dt,'.txt'];
diary(dtd)
diary on

% data file processing in range
for file_name=734783:735224

     % importing the 1 Hz file
    file_date=datestr(file_name,29); % ISO format date
    import_file=['GVSU-Vindicator-Refined-',file_date,'.csv'];
    check=['GVSU-Vindicator-5-min-',file_date,'.csv'];
    dir_data=dir;
    dir_index=[dir_data.isdir];
    file_list={dir_data(~dir_index).name};
    decision=strcmp(import_file,file_list);

     % looking for the data file in the directory and checking for the
file is already prcessed or not
    decision1=strcmp(check,file_list);
    decision=sum(decision);
    decision1=sum(decision1);
    str=['Importing file: ',import_file];
    disp(str)
    if decision==1 && decision1~=1
           file=importdata(import_file);
           counter=1;
           pivot=300; % the averaging time in seconds
           temp=zeros(pivot,1);
           x=1;
           number=86400/pivot; % number of data points per day
           avg=zeros(number,6); % average value
           std=zeros(number,6); % standard deviation value
           limit=size(file,2);
        column=[];
        y=1;
            for i=2:8:limit
                column(:,y)=file(:,i); % taking in the wind speed and
other data
                y=y+2;
            end
        y=2;
            for i=5:8:limit
                column(:,y)=file(:,i); % taking in the wind speed and
other data
            end
        for y=2:2:12
            for i=1:86400
                if column(i,y)<0
                    column(i,y)=column(i,y)+360;
```

```
                end
            end
        end
        column_n=zeros(86400,12); % creating new array for storing the
refined data
        length_of_data=length(date);
        nansin=[];
        nancos=[];
           %% Calculation
           for c=1:2:11
                x=1;
                for i=1:86400
                     if counter<=pivot
                          temp(counter)=column(i,c); % creating a
temporary block of data for calculation
                          counter=counter+1;
                          if counter>pivot
                               if sum(isnan(temp))<(pivot/2) %
checking for availablity of 50% sample size
                                    avg(x,c)=nanmean(temp);
                                    std(x,c)=nanstd(temp);
                                    x=x+1;
                                    counter=1;
                               else
                                    avg(x,c)=NaN;
                                    std(x,c)=NaN;
                                    x=x+1;
                                    counter=1;
                               end
                          end
                     end
                end
           end
           for c=2:2:12
                x=1;
                for i=1:86400
                     if counter<=pivot
                          temp(counter)=column(i,c); % creating a
temporary block of data for calculation
                          counter=counter+1;
                          if counter>pivot
                               if sum(isnan(temp))<(pivot/2) %
checking for availablity of 50% sample size
                                    nansin=nansum(sin(temp*pi/180));
                                    nancos=nansum(cos(temp*pi/180));

     avg(x,c)=atan2(nansin,nancos)*180/pi;
                                    nan_check=isnan(avg(x,c));
                                    if nan_check==1
                                         avg(x,c)=NaN;
                                    else
```

```
                                                    if avg(x,c)>=0 &&
avg(x,c)<=90
                                                        avg(x,c)=90-avg(x,c);
                                                        elseif avg(x,c)>90 &&
avg(x,c)<=180
                                                        avg(x,c)=360-
(avg(x,c)-90);
                                                        elseif avg(x,c)<0 &&
avg(x,c)>=-180

      avg(x,c)=abs(avg(x,c))+90;
                                                    end
                                               end
                                               std(x,c)=nanstd(temp);
                                               x=x+1;
                                               counter=1;
                                          else
                                               avg(x,c)=NaN;
                                               std(x,c)=NaN;
                                               x=x+1;
                                               counter=1;
                                          end
                                     end
                                end
                           end
                      end
         date_f=file_name; % excel time format
         date_stamp_f=linspace(date_f,(date_f+1-1.1574e-
005*pivot),86400/pivot)';
         filename=['GVSU-Vindicator-5-min-',file_date,'.csv'];
         answer=[date_stamp_f avg std];
         csvwrite(filename,answer); % writing a csv file for the
refined data set
         str=[import_file,': File Processed Successfully !'];
         disp (str)
      else
           str=[import_file,': File not found !'];
           disp(str)
    end
    step=step+1;
    waitbar(step/steps)
end
close(h)
diary off
```

A.4 Wind rose

```
clear;
clc;
close all;
```

```
file=uiimport;
%trbn(:,2)=csvread('powercurves.csv',2,17,[2,17,673,17]);
%trbn(:,1)=csvread('powercurves.csv',2,0,[2,0,673,0]);
res=600; % data frequency in seconds
tme=zeros(16,1);
sum_energy=zeros(16,1);
spd_clmn=1;
dir_clmn=spd_clmn+6;
db=22.5;
last_data_point=length(file.data(:,spd_clmn));
direction_bin=0:22.5:360;
tmp=[];
bin_avg=zeros(16,1);
bin_counter=zeros(16,1);
%% converting the wind speed in mph unit
for i=1:last_data_point
    file.data(i,spd_clmn)=file.data(i,spd_clmn)*2.23693629;
end
for dir_bin_number=1:16
    for i=1:last_data_point
        if file.data(i,dir_clmn)>=direction_bin(dir_bin_number) &&
file.data(i,dir_clmn)<=direction_bin(dir_bin_number+1)
            tmp=[tmp file.data(i,spd_clmn)];
            bin_counter(dir_bin_number)=bin_counter(dir_bin_number)+1;
        end
        tmp(1)=NaN;
        bin_avg(dir_bin_number)=nanmean(tmp);
    end
    tmp=[];
end
bin_counter;
bin_avg;
counter=0;
x=1;
rose_avg=zeros(360,1);
for i=1:360
    rose_avg(i)=bin_avg(x);
    rose_count(i)=bin_counter(x);
    counter=counter+1;
    if counter==23
        x=x+1;
        counter=0;
    end
end
rose_time_percent=rose_count'./last_data_point;
```

A.5 Frequency distribution

```
% frequency distribution
clear;
```

```
clc;
close all;
freq=60;
histogram=zeros(70,6);
final_histogram=zeros(70,6);
percentile=zeros(70,6);
total_time=zeros(1,6);
dtd='frequency distribution';
diary(dtd)
diary on
for file_name=734873:734967
    file_date=datestr(file_name,29); % ISO format date
    import_file=['GVSU-Vindicator-1-min-',file_date,'.csv'];
    dir_data=dir;
    dir_index=[dir_data.isdir];
    file_list={dir_data(~dir_index).name};
    decision=strcmp(import_file,file_list);
    decision=sum(decision);
    if decision==1
        file=importdata(import_file);
        i=1;
        for c=2:2:12
            temp=file(:,c)*2.2369;
            temp(isnan(temp))=[];
            histogram(:,i)=histc(temp,1:70);
            i=i+1;
        end
        final_histogram=final_histogram+histogram;
    end
end
for i=1:6
    total_time(i)=nansum(final_histogram(:,i));
    percentile(:,i)=final_histogram(:,i)./total_time(i);
end
csvwrite('frequency distribution percentile of time midlake
locaiton.txt',percentile);
bar(percentile(:,1));
```

Appendix B

B.1 Lake Muskegon deployment results

Table B.1 Summary of results of different range gates

Appendix B R ange Gate	Appendix C Al titude (m)	Appendix D A verage wind speed (mph)	Appendix E Ener gy output (MWh)	Appendix F Ca pacity factor
Appendix G R G1	Appendix H 55	Appendix I 12 .69	Appendix J 79.1 98585	Appendix K 13 .9%
Appendix L R G2	Appendix M 60	Appendix N 13 .22	Appendix O 87.5 30522	Appendix P 15 .3%
Appendix Q R G3	Appendix R 75	Appendix S 14 .38	Appendix T 106. 80838	Appendix U 18 .7%
Appendix V R G4	Appendix W 90	Appendix X 15 .33	Appendix Y 122. 574758	Appendix Z 21 .5%
Appendix AA R G5	Appendix BB 11 0	Appendix CC 15 .92	Appendix DD 135. 333345	Appendix EE 23 .7%
Appendix FF R G6	Appendix GG 12 0	Appendix HH 16 .03	Appendix II 135. 945984	Appendix JJ 23 .8%

Table B.2 Energy (MWh) estimated by dynamic model for RG1 (30 sec averaged data set)

Yaw Rate (deg/sec)	Delay Time (secs)																			
	30	60	90	120	150	180	210	240	270	300	330	360	390	420	450	480	510	540	570	600
0	43.2	40.4	40.4	40.5	40.4	40.4	40.4	40.5	40.4	40.4	42.5	41.1	42.5	41.0	40.5	42.9	42.7	42.3	42.5	41.0
0.05	76.6	72.7	71.5	72.2	72.4	72.1	71.5	72.2	72.4	72.4	72.7	71.2	73.2	73.8	72.0	74.1	74.4	70.5	71.2	70.5
0.1	76.8	73.3	72.7	74.1	72.0	71.8	72.7	74.1	72.0	71.0	74.7	72.2	73.6	75.1	70.7	74.8	73.9	71.0	72.8	72.5
0.15	77.0	73.7	73.1	74.2	72.7	72.0	73.1	74.2	72.7	73.1	73.1	72.1	74.4	73.7	72.2	73.6	72.8	71.5	73.0	71.9
0.2	77.3	74.0	72.8	72.7	72.7	71.7	72.8	72.7	72.7	72.5	73.6	72.4	73.2	74.5	72.3	73.6	73.6	72.0	72.9	73.5
0.25	77.3	73.8	73.1	73.2	72.5	71.2	73.1	73.2	72.5	73.7	73.9	72.4	74.3	73.3	71.9	73.5	74.1	72.2	73.2	73.5
0.3	77.6	73.8	72.0	73.2	72.6	71.9	72.0	73.2	72.6	73.1	73.6	72.7	74.4	73.2	71.9	73.8	74.4	72.0	73.6	74.4
0.35	77.7	73.8	71.7	71.4	72.6	72.1	71.7	71.4	72.6	73.2	73.8	72.7	74.3	74.0	72.4	73.8	74.3	72.3	72.7	73.1
0.4	77.8	73.8	71.0	71.5	72.6	72.1	71.0	71.5	72.6	72.5	73.4	72.6	74.7	73.9	72.9	74.4	74.5	72.4	73.0	72.9
0.45	77.7	73.8	71.2	72.1	71.9	72.2	71.2	72.1	71.9	73.2	73.7	73.4	74.5	73.7	72.4	73.9	74.0	72.4	72.7	73.0
0.5	77.7	74.0	70.7	72.1	72.1	71.9	70.7	72.1	72.1	73.1	73.2	73.6	75.0	73.8	72.8	73.8	74.1	72.7	72.9	73.2
0.55	77.6	74.1	71.3	71.6	72.4	72.4	71.3	71.6	72.4	73.7	73.6	73.2	74.6	74.0	73.3	74.2	73.8	72.4	73.2	74.0
0.6	77.6	74.2	71.0	71.8	72.1	72.5	71.0	71.8	72.1	74.2	73.7	73.4	74.5	73.8	73.1	74.4	74.2	72.6	73.6	74.0
0.65	77.5	74.3	71.6	71.6	72.6	72.4	71.6	71.6	72.6	73.8	73.4	73.2	74.9	73.9	73.1	74.1	74.4	72.8	73.5	73.8
0.7	77.5	74.4	71.0	71.8	72.8	73.0	71.0	71.8	72.8	74.0	73.7	73.3	75.1	74.5	73.8	74.4	74.6	72.7	73.6	73.9
0.75	77.6	74.6	71.7	71.9	72.7	72.9	71.7	71.9	72.7	73.8	73.9	73.1	74.6	74.2	73.9	74.3	74.7	73.3	73.9	73.9
0.8	77.6	74.6	72.0	72.2	72.9	72.8	72.0	72.2	72.9	73.8	74.3	73.2	75.1	74.5	74.0	74.6	74.8	73.5	74.1	74.0
0.85	77.7	74.6	72.0	72.5	73.0	72.8	72.0	72.5	73.0	73.7	74.0	73.3	75.2	74.7	74.3	74.7	75.0	73.4	73.9	74.3
0.9	77.7	74.7	71.8	72.5	72.8	72.7	71.8	72.5	72.8	73.6	73.8	73.4	75.3	74.9	74.2	74.8	75.1	73.5	74.3	74.4
0.95	77.7	74.8	72.1	72.6	73.1	72.8	72.1	72.6	73.1	74.0	74.3	73.6	75.5	74.7	74.4	75.1	75.0	73.6	74.3	74.2
1	77.7	75.0	72.2	72.9	73.4	72.8	72.2	72.9	73.4	74.2	74.3	73.8	75.4	75.0	74.5	74.8	74.8	73.4	74.2	74.2
1.05	77.8	75.2	72.2	73.2	73.4	72.9	72.2	73.2	73.4	74.3	74.6	73.9	75.3	75.1	74.4	74.8	74.9	73.6	74.3	74.3
1.1	77.8	75.2	72.3	73.2	73.5	73.2	72.3	73.2	73.5	74.7	74.6	74.0	75.5	75.0	74.8	74.7	75.3	73.7	74.2	74.3
1.15	77.8	75.2	72.4	73.3	73.5	73.2	72.4	73.3	73.5	74.5	74.8	74.0	75.2	74.9	74.3	74.9	75.0	73.6	74.2	74.5
1.2	77.8	75.2	72.3	73.4	73.6	73.7	72.3	73.4	73.6	74.9	74.7	73.9	75.3	75.2	74.5	74.8	74.9	73.8	74.1	74.8

Yaw Rate (deg/sec)	Delay Time (secs)																			
	30	60	90	120	150	180	210	240	270	300	330	360	390	420	450	480	510	540	570	600
1.25	77.8	75.3	72.4	73.4	73.8	73.6	72.4	73.4	73.8	74.6	74.6	74.0	75.4	75.1	74.5	75.1	75.0	73.7	74.3	74.7
1.3	77.8	75.4	72.3	73.5	73.8	73.8	72.3	73.5	73.8	74.6	74.6	74.1	75.5	75.0	74.4	75.0	75.0	73.6	74.1	74.7
1.35	77.8	75.5	72.8	73.7	73.9	73.8	72.8	73.7	73.9	74.9	74.5	74.0	75.5	75.2	75.0	75.2	74.8	73.7	73.9	75.1
1.4	77.8	75.5	72.9	73.9	74.1	73.6	72.9	73.9	74.1	74.6	74.7	74.0	75.9	75.3	74.5	75.4	75.1	73.3	73.9	74.8
1.45	77.7	75.5	72.9	73.7	74.1	73.7	72.9	73.7	74.1	74.6	74.7	73.9	75.4	75.1	74.2	75.2	75.0	73.5	73.9	74.5
1.5	77.8	75.5	73.2	73.9	74.1	73.4	73.2	73.9	74.1	74.8	74.8	74.1	75.9	75.4	74.6	74.9	74.9	73.8	74.0	75.2
1.55	77.8	75.6	73.1	73.9	73.9	73.6	73.1	73.9	73.9	75.0	75.0	74.1	75.8	75.4	75.2	75.4	75.0	74.0	73.9	75.1
1.6	77.7	75.6	73.2	74.0	74.3	73.7	73.2	74.0	74.3	75.0	74.9	74.0	75.8	75.5	74.8	75.4	75.2	74.0	74.1	74.9
1.65	77.7	75.8	73.1	73.9	74.5	73.8	73.1	73.9	74.5	74.9	75.0	73.9	75.5	75.2	74.3	75.2	74.9	73.6	73.6	74.8
1.7	77.7	75.9	73.2	74.2	74.5	73.6	73.2	74.2	74.5	74.8	74.9	74.3	75.5	75.4	74.4	75.3	75.1	73.6	73.5	74.9
1.75	77.7	75.9	73.3	74.3	74.4	73.6	73.3	74.3	74.4	75.0	74.9	74.4	75.7	75.6	74.6	75.4	75.2	73.7	73.7	74.9
1.8	77.7	76.0	73.3	74.3	74.3	73.6	73.3	74.3	74.3	74.9	75.0	74.5	75.9	75.6	75.2	75.7	75.3	74.1	74.1	74.9
1.85	77.7	76.0	73.2	74.3	74.3	73.7	73.2	74.3	74.3	74.8	74.9	74.3	75.7	75.2	75.2	75.7	75.5	74.1	73.9	75.1
1.9	77.7	76.0	73.2	74.3	74.5	73.8	73.2	74.3	74.5	74.7	74.7	73.8	75.6	74.8	74.1	75.3	75.1	73.5	73.8	74.5
1.95	77.7	76.0	73.2	74.1	74.4	73.7	73.2	74.1	74.4	74.5	74.6	74.0	75.2	74.6	73.8	74.7	75.0	73.1	73.3	74.2
2	77.7	76.0	73.3	74.1	74.3	73.9	73.3	74.1	74.3	74.7	74.6	73.9	75.4	74.7	74.1	74.6	74.9	73.5	73.2	74.6

Table B.3 Energy (MWh) estimated by dynamic model for RG2 (30 sec averaged data set)

Yaw Rate (deg/sec)	Delay Time (secs)																			
	30	60	90	120	150	180	210	240	270	300	330	360	390	420	450	480	510	540	570	600
0	58.3	52.9	52.8	52.9	52.8	52.8	52.8	52.9	52.8	52.9	57.4	53.7	57.3	53.6	52.9	57.7	57.5	56.8	57.1	53.6
0.05	86.4	81.3	79.4	79.9	80.7	79.9	79.4	79.9	80.7	79.8	81.5	80.4	81.3	79.7	81.5	81.9	81.0	77.8	78.4	78.5
0.1	86.1	81.9	80.7	81.9	81.5	79.5	80.7	81.9	81.5	79.0	81.3	79.9	80.5	83.4	80.2	81.4	80.0	79.4	81.8	79.9
0.15	85.8	81.9	80.9	82.7	81.1	80.3	80.9	82.7	81.1	80.1	80.5	80.6	81.7	82.8	79.6	81.8	80.8	80.0	80.8	80.0
0.2	85.7	81.9	80.6	82.0	80.4	80.7	80.6	82.0	80.4	80.6	82.0	80.7	82.5	81.4	79.3	80.9	82.2	80.8	81.0	80.7
0.25	85.7	82.2	80.4	81.1	80.1	78.6	80.4	81.1	80.1	81.6	81.5	80.3	82.3	81.6	80.2	82.4	82.0	80.4	80.9	81.0
0.3	85.8	82.1	80.7	80.5	81.0	80.1	80.7	80.5	81.0	81.3	81.8	80.6	83.1	81.6	80.1	82.1	81.8	80.7	80.9	82.1
0.35	85.9	82.1	79.8	80.1	80.7	79.1	79.8	80.1	80.7	81.3	81.7	80.3	82.4	82.0	80.3	82.2	82.3	80.2	80.8	81.0
0.4	86.0	82.2	80.0	80.5	80.3	79.6	80.0	80.5	80.3	81.1	82.1	80.3	83.1	81.7	80.8	82.4	82.2	80.3	80.6	81.4
0.45	86.0	82.3	79.9	79.9	80.1	79.6	79.9	79.9	80.1	81.5	82.2	80.9	82.9	82.4	80.5	82.5	82.1	80.0	81.0	81.1
0.5	86.1	82.4	79.8	80.1	80.5	80.5	79.8	80.1	80.5	81.5	82.1	81.4	83.0	82.2	80.7	82.1	82.3	80.8	80.7	81.4
0.55	86.1	82.5	80.1	80.6	79.9	80.9	80.1	80.6	79.9	81.7	81.9	81.2	82.9	81.8	81.0	82.5	82.4	80.5	81.4	81.9
0.6	86.2	82.5	79.6	80.8	79.9	80.3	79.6	80.8	79.9	82.2	81.5	81.4	83.2	82.3	80.9	82.6	82.3	80.4	81.4	81.6
0.65	86.2	82.8	79.2	80.8	80.7	80.9	79.2	80.8	80.7	82.0	82.0	81.2	83.3	82.3	81.1	82.3	82.5	80.8	81.6	81.7
0.7	86.4	82.9	79.7	80.7	80.7	80.5	79.7	80.7	80.7	82.1	81.8	81.3	83.6	82.4	81.7	82.7	82.8	81.2	81.6	81.8
0.75	86.4	82.9	79.8	80.8	80.8	81.0	79.8	80.8	80.8	82.0	81.9	81.6	83.8	82.3	81.9	82.9	82.9	81.2	81.5	82.1
0.8	86.5	83.0	80.0	80.6	81.2	81.2	80.0	80.6	81.2	81.9	82.4	81.8	84.0	82.7	82.1	83.3	83.0	81.5	81.8	81.9
0.85	86.5	83.1	79.9	81.0	81.1	81.5	79.9	81.0	81.1	82.0	82.4	81.4	84.4	83.0	82.5	83.3	83.1	81.8	81.7	81.9
0.9	86.5	83.3	80.1	81.2	81.2	81.4	80.1	81.2	81.2	82.0	82.2	81.6	84.2	83.5	82.4	83.6	83.0	81.6	81.8	82.1
0.95	86.6	83.4	80.3	81.4	81.7	81.1	80.3	81.4	81.7	82.2	82.4	81.8	84.4	83.3	82.3	83.6	83.1	81.6	81.9	82.2
1	86.6	83.6	80.4	81.7	81.9	81.5	80.4	81.7	81.9	82.3	82.5	82.1	84.4	83.2	82.5	83.6	83.2	81.9	81.9	82.4
1.05	86.6	83.6	80.4	81.8	81.7	81.3	80.4	81.8	81.7	82.4	83.0	82.1	84.3	83.3	82.4	83.6	83.0	81.6	82.0	82.3
1.1	86.6	83.8	80.6	81.9	82.1	81.4	80.6	81.9	82.1	82.5	83.1	82.3	84.4	83.1	82.5	83.6	83.3	82.0	82.0	82.3
1.15	86.6	83.9	80.6	82.0	82.0	81.5	80.6	82.0	82.0	82.9	83.3	82.0	84.2	83.7	82.5	83.7	83.0	81.7	82.1	82.5
1.2	86.6	84.0	80.6	81.9	82.2	81.8	80.6	81.9	82.2	82.9	83.1	82.3	84.6	83.8	82.6	83.7	83.1	82.0	82.1	82.8

Yaw Rate (deg/sec)	Delay Time (secs)																			
	30	60	90	120	150	180	210	240	270	300	330	360	390	420	450	480	510	540	570	600
1.25	86.6	84.0	80.5	81.9	82.1	81.8	80.5	81.9	82.1	82.6	83.1	82.1	84.4	83.6	82.5	84.1	83.3	81.9	82.4	82.5
1.3	86.7	84.1	80.7	82.2	82.0	81.9	80.7	82.2	82.0	82.9	83.0	82.4	84.4	83.7	82.6	83.6	82.9	81.7	82.1	82.4
1.35	86.7	84.1	80.9	82.2	82.1	81.9	80.9	82.2	82.1	83.0	83.0	82.2	84.5	83.7	82.8	84.0	83.0	81.9	82.1	82.4
1.4	86.6	84.2	81.1	82.3	82.6	81.7	81.1	82.3	82.6	82.7	83.1	82.4	84.4	83.8	82.6	84.0	83.0	82.0	82.5	82.4
1.45	86.6	84.2	81.1	82.4	82.4	81.9	81.1	82.4	82.4	82.8	83.1	82.3	84.2	83.6	82.3	84.0	82.8	81.6	82.2	82.6
1.5	86.6	84.3	81.2	82.6	82.6	81.8	81.2	82.6	82.6	83.0	83.3	82.5	84.5	83.8	82.8	84.1	83.0	81.9	81.9	83.2
1.55	86.6	84.4	81.3	82.6	82.5	81.7	81.3	82.6	82.5	83.4	83.2	82.6	84.7	83.8	83.4	84.2	83.0	82.1	82.2	83.1
1.6	86.6	84.5	81.4	82.6	82.7	81.8	81.4	82.6	82.7	83.2	83.4	82.5	84.3	83.9	82.9	84.3	83.0	82.4	82.0	83.1
1.65	86.6	84.5	81.3	82.7	82.9	82.0	81.3	82.7	82.9	83.3	83.5	82.5	84.4	83.5	82.5	84.0	83.5	81.7	81.6	82.7
1.7	86.7	84.6	81.3	82.5	83.0	81.8	81.3	82.5	83.0	83.0	83.2	82.6	84.4	83.8	82.4	84.0	83.5	81.9	81.6	82.9
1.75	86.7	84.6	81.6	82.6	82.8	81.8	81.6	82.6	82.8	83.2	83.5	82.7	84.5	83.9	82.8	84.3	83.9	81.8	82.0	83.3
1.8	86.6	84.7	81.7	82.7	82.9	81.8	81.7	82.7	82.9	83.4	83.5	82.8	84.5	83.9	83.1	84.2	83.9	82.1	82.4	83.0
1.85	86.7	84.8	81.6	82.6	82.6	81.9	81.6	82.6	82.6	83.2	83.1	82.8	84.5	83.9	83.4	84.1	83.7	82.4	82.1	83.2
1.9	86.6	84.7	81.6	82.7	82.7	82.0	81.6	82.7	82.7	83.1	83.2	82.1	84.5	83.4	82.9	84.0	83.4	81.4	81.9	82.7
1.95	86.6	84.7	81.7	82.6	82.7	82.0	81.7	82.6	82.7	83.0	83.0	82.2	84.1	83.1	82.0	83.6	83.4	81.3	81.5	82.4
2	86.7	84.8	81.6	82.5	82.7	82.1	81.6	82.5	82.7	82.9	82.8	82.1	84.2	83.0	82.0	83.6	83.4	81.6	81.7	82.6

Table B.4 Energy (MWh) estimated by dynamic model for RG3 (30 sec averaged data set)

Yaw Rate (deg/sec)	Delay Time (secs)																			
	30	60	90	120	150	180	210	240	270	300	330	360	390	420	450	480	510	540	570	600
0	71.9	65.1	65.1	65.2	65.1	65.2	65.1	65.2	65.1	65.2	70.6	66.5	70.5	66.4	65.3	71.1	70.8	69.9	70.3	66.3
0.05	105.3	98.5	97.7	97.9	98.7	98.4	97.7	97.9	98.7	98.1	98.8	98.6	99.8	101.2	100.0	100.2	99.1	95.7	96.8	96.4
0.1	105.2	99.4	99.0	99.7	99.0	98.8	99.0	99.7	99.0	98.0	98.9	97.9	100.6	99.4	99.6	100.5	99.7	97.4	99.3	98.1
0.15	105.2	99.9	99.1	101.3	98.8	98.8	99.1	101.3	98.8	98.3	99.7	98.2	99.9	98.8	99.6	100.1	100.8	97.8	99.4	99.2
0.2	105.0	100.5	99.1	99.3	98.6	96.7	99.1	99.3	98.6	100.0	99.5	99.3	100.0	99.8	100.0	100.1	99.7	97.7	98.9	99.4
0.25	105.1	100.6	99.1	99.7	98.3	98.1	99.1	99.7	98.3	99.3	99.8	99.1	100.3	100.5	98.3	101.1	100.6	97.6	99.0	100.1
0.3	105.5	101.0	98.6	99.1	97.8	98.7	98.6	99.1	97.8	99.7	99.5	99.6	101.6	100.5	98.8	101.2	101.1	98.3	99.4	100.7
0.35	105.7	101.3	98.8	98.4	98.8	98.0	98.8	98.4	98.8	100.4	99.8	99.1	101.4	100.9	98.9	101.0	101.0	98.3	99.6	100.3
0.4	106.0	101.4	98.2	99.5	98.2	98.8	98.2	99.5	98.2	99.2	99.9	99.7	101.6	100.8	99.9	102.0	100.9	97.7	99.4	99.9
0.45	106.1	101.5	98.0	98.0	98.8	98.2	98.0	98.0	98.8	99.9	99.8	99.3	101.8	101.0	99.0	101.0	100.8	97.9	98.9	99.5
0.5	106.1	101.5	98.1	98.2	98.6	99.2	98.1	98.2	98.6	100.0	100.2	99.8	101.8	101.4	98.6	101.2	100.9	98.2	98.8	100.5
0.55	106.0	101.3	97.8	98.5	98.7	98.9	97.8	98.5	98.7	100.5	100.3	99.6	101.7	101.1	99.3	101.3	100.8	97.6	99.6	100.0
0.6	105.9	101.3	98.1	97.8	98.2	98.7	98.1	97.8	98.2	101.1	100.6	99.5	101.8	101.3	99.5	101.3	101.4	98.1	99.9	100.7
0.65	105.8	101.4	98.5	98.1	98.4	98.6	98.5	98.1	98.4	100.8	100.4	100.0	101.9	101.5	99.5	101.0	101.3	98.4	99.7	100.4
0.7	105.7	101.5	98.4	98.8	99.0	98.8	98.4	98.8	99.0	100.9	100.1	100.0	102.3	100.8	99.7	101.9	101.5	98.1	100.2	100.5
0.75	105.7	101.6	97.9	98.9	99.1	98.7	97.9	98.9	99.1	101.7	100.4	100.1	102.1	101.3	100.2	102.5	101.3	98.5	100.3	100.6
0.8	105.6	101.7	98.4	99.0	99.2	99.2	98.4	99.0	99.2	101.7	100.6	100.2	102.5	101.8	100.5	102.3	102.1	98.7	100.4	100.7
0.85	105.5	101.6	98.5	99.4	99.6	99.5	98.5	99.4	99.6	101.2	101.4	100.3	102.3	102.3	100.9	102.6	101.7	99.0	100.4	100.6
0.9	105.6	101.8	98.9	99.8	99.7	99.7	98.9	99.8	99.7	101.3	100.9	100.6	102.6	101.9	100.7	102.7	101.3	99.3	100.1	100.8
0.95	105.6	101.9	99.0	99.6	99.8	99.7	99.0	99.6	99.8	101.3	101.7	100.5	103.0	102.2	101.1	102.9	101.6	99.0	100.5	101.3
1	105.7	102.2	98.9	99.7	100.3	100.1	98.9	99.7	100.3	101.1	101.4	100.8	103.1	102.2	101.1	102.7	101.9	99.5	101.0	101.1
1.05	105.7	102.2	99.0	100.1	100.2	100.0	99.0	100.1	100.2	101.5	101.6	100.9	103.2	102.5	101.0	103.0	102.1	99.5	100.4	100.7
1.1	105.8	102.2	98.7	100.3	100.2	100.0	98.7	100.3	100.2	101.3	101.7	101.0	103.2	103.4	101.1	102.8	101.9	99.7	100.6	101.0
1.15	105.8	102.2	99.2	100.4	100.4	100.0	99.2	100.4	100.4	101.5	101.7	101.1	103.1	102.7	101.1	103.0	102.0	99.4	100.6	100.8
1.2	105.9	102.3	99.2	100.8	100.5	100.2	99.2	100.8	100.5	101.8	101.7	101.3	103.4	102.7	101.2	103.2	102.0	99.7	100.9	101.1

Yaw Rate (deg/sec)	Delay Time (secs)																			
	30	60	90	120	150	180	210	240	270	300	330	360	390	420	450	480	510	540	570	600
1.25	105.9	102.4	99.8	100.5	100.7	100.3	99.8	100.5	100.7	102.1	101.8	101.2	103.4	102.9	101.2	103.1	101.9	99.3	101.1	101.5
1.3	106.0	102.4	99.6	100.6	100.7	100.3	99.6	100.6	100.7	101.8	102.1	101.2	103.5	102.6	101.0	103.2	101.6	99.3	100.5	100.9
1.35	106.0	102.5	100.1	100.8	100.7	100.2	100.1	100.8	100.7	101.7	101.8	101.4	103.4	103.1	100.9	103.0	101.6	99.3	101.0	100.9
1.4	106.0	102.6	100.4	101.0	100.7	100.0	100.4	101.0	100.7	101.9	101.8	101.4	103.4	103.1	101.2	103.2	101.7	99.1	100.8	101.4
1.45	106.0	102.6	100.2	101.3	100.9	100.1	100.2	101.3	100.9	101.7	102.0	101.2	103.5	102.7	101.2	103.1	101.5	99.1	100.3	101.4
1.5	106.0	102.6	100.5	101.4	101.1	100.4	100.5	101.4	101.1	102.0	102.0	101.4	103.7	103.1	100.8	103.2	101.6	99.4	100.5	101.8
1.55	105.9	102.8	100.5	101.3	100.9	100.4	100.5	101.3	100.9	102.4	102.1	101.6	103.6	103.2	101.2	103.2	101.9	99.7	100.7	101.5
1.6	105.9	102.8	100.6	101.5	101.2	100.4	100.6	101.5	101.2	102.6	102.1	101.5	103.4	102.9	101.3	103.1	102.3	99.7	100.6	101.8
1.65	105.9	102.9	100.5	101.4	101.1	100.6	100.5	101.4	101.1	102.1	102.2	101.3	103.4	102.8	100.9	103.3	101.4	99.3	100.1	101.5
1.7	105.9	103.0	100.7	101.5	100.9	100.7	100.7	101.5	100.9	102.0	102.0	101.3	103.2	103.2	101.0	103.2	101.9	99.5	100.3	101.9
1.75	105.9	103.0	101.0	101.6	101.1	100.7	101.0	101.6	101.1	102.5	102.3	101.7	103.6	103.2	101.2	103.1	102.3	99.7	100.5	102.1
1.8	105.9	103.1	101.0	101.5	101.3	100.8	101.0	101.5	101.3	102.3	102.3	101.9	103.5	103.0	101.5	103.2	102.2	100.2	101.0	101.7
1.85	105.9	103.2	100.9	101.3	101.1	100.9	100.9	101.3	101.1	102.2	102.2	101.6	103.6	102.7	101.7	103.4	102.3	99.6	100.8	101.6
1.9	106.0	103.3	100.9	101.5	101.1	100.9	100.9	101.5	101.1	102.3	102.1	101.3	103.6	102.8	101.8	102.6	101.9	99.2	100.3	101.8
1.95	105.9	103.3	101.0	101.5	101.0	100.7	101.0	101.5	101.0	101.7	101.7	101.0	103.0	102.1	100.9	102.8	101.8	98.8	99.5	101.3
2	106.0	103.3	101.0	101.5	101.1	100.6	101.0	101.5	101.1	101.7	101.7	101.2	103.0	102.5	101.1	102.8	102.0	98.8	99.8	100.9

Table B.5 Energy (MWh) estimated by dynamic model for RG4 (30 sec averaged data set)

Yaw Rate (deg/sec)	Delay Time (secs)																			
	30	60	90	120	150	180	210	240	270	300	330	360	390	420	450	480	510	540	570	600
0	81.0	73.7	73.7	73.7	73.6	73.8	73.7	73.7	73.6	73.7	79.6	75.2	79.4	75.1	74.0	80.1	79.8	78.8	79.2	75.0
0.05	121.9	114.1	113.6	112.5	113.6	113.3	113.6	112.5	113.6	112.7	114.0	112.9	114.2	112.8	111.2	115.8	115.4	114.4	113.9	111.1
0.1	121.4	114.4	114.8	114.4	115.2	113.7	114.8	114.4	115.2	112.4	113.2	113.1	116.4	114.1	112.3	114.4	114.0	115.3	113.6	110.6
0.15	120.9	114.2	114.8	114.6	111.9	113.5	114.8	114.6	111.9	111.8	115.6	114.4	115.1	113.7	114.1	114.3	114.9	112.6	112.6	111.7
0.2	120.5	114.3	114.5	114.8	113.9	112.3	114.5	114.8	113.9	111.9	114.6	113.3	114.6	114.2	113.2	114.5	114.3	113.5	113.8	113.8
0.25	120.4	114.8	113.5	114.2	112.1	113.4	113.5	114.2	112.1	112.4	114.1	114.4	114.9	114.8	112.5	116.0	114.3	112.8	113.5	113.1
0.3	120.5	115.1	112.8	114.0	112.2	112.9	112.8	114.0	112.2	113.5	114.7	114.1	115.1	115.2	113.2	115.0	114.4	112.9	114.2	114.3
0.35	120.4	115.3	111.4	113.6	111.2	113.2	111.4	113.6	111.2	113.4	113.8	114.0	115.9	115.3	114.0	116.6	114.6	113.0	114.6	114.2
0.4	120.5	115.6	112.6	113.2	112.5	112.4	112.6	113.2	112.5	113.6	114.0	114.5	114.8	115.1	114.3	116.4	114.6	112.4	114.2	113.8
0.45	120.6	115.6	111.6	113.3	111.8	112.1	111.6	113.3	111.8	113.9	114.4	114.0	115.4	115.4	113.5	115.9	114.4	112.3	114.2	114.3
0.5	120.7	115.5	111.9	113.0	113.1	112.9	111.9	113.0	113.1	114.2	113.7	115.1	115.4	115.6	113.7	115.4	114.7	112.4	113.6	114.3
0.55	120.7	115.6	111.9	112.9	112.8	112.7	111.9	112.9	112.8	115.0	114.5	114.6	115.8	115.5	114.0	116.0	114.6	111.9	113.7	114.4
0.6	120.6	115.6	112.3	112.4	113.0	113.2	112.3	112.4	113.0	114.8	114.5	114.3	116.1	115.2	114.2	115.7	114.8	112.7	114.5	114.6
0.65	120.6	115.6	112.7	113.2	113.3	113.2	112.7	113.2	113.3	114.8	114.4	114.7	116.1	115.4	113.4	115.9	115.0	112.9	114.8	114.7
0.7	120.6	115.6	112.2	113.4	113.3	113.2	112.2	113.4	113.3	115.0	114.6	114.8	116.0	115.2	114.2	116.6	115.6	112.7	114.6	115.2
0.75	120.5	115.7	112.5	113.6	113.8	114.0	112.5	113.6	113.8	115.0	114.6	114.6	116.3	116.0	114.9	116.5	115.6	113.0	114.8	115.1
0.8	120.5	115.8	112.5	114.5	114.1	113.8	112.5	114.5	114.1	114.8	114.7	114.6	116.5	116.2	115.1	117.0	115.4	113.4	115.1	115.2
0.85	120.4	115.9	112.6	114.7	114.3	113.7	112.6	114.7	114.3	115.4	114.6	114.6	116.9	116.4	115.5	117.0	115.2	113.3	115.2	115.1
0.9	120.4	116.0	112.3	114.3	114.0	113.7	112.3	114.3	114.0	115.5	114.9	114.9	116.7	116.5	115.6	117.1	115.2	113.7	115.3	115.1
0.95	120.4	116.1	113.0	114.6	114.3	114.0	113.0	114.6	114.3	116.2	115.0	115.1	117.1	116.4	115.9	117.0	115.3	113.8	115.7	116.0
1	120.4	116.2	113.1	114.7	114.6	114.3	113.1	114.7	114.6	116.4	115.0	115.0	117.3	116.8	115.9	117.3	115.6	114.0	115.4	115.6
1.05	120.4	116.3	113.1	114.8	114.8	114.7	113.1	114.8	114.8	116.2	115.1	115.4	117.2	116.8	116.0	116.9	115.7	113.9	115.7	115.7
1.1	120.5	116.5	113.5	115.1	114.7	114.6	113.5	115.1	114.7	116.1	115.7	115.4	117.4	117.0	116.0	117.3	115.7	113.9	115.3	115.8
1.15	120.5	116.7	113.6	115.2	115.0	114.5	113.6	115.2	115.0	116.8	115.7	115.6	117.7	117.0	115.9	117.3	116.0	114.2	115.5	115.6
1.2	120.5	116.8	113.8	115.5	115.0	114.1	113.8	115.5	115.0	116.6	116.0	115.5	117.6	117.5	115.9	117.1	116.2	114.1	115.4	115.6

Yaw Rate (deg/sec)	Delay Time (secs)																			
	30	60	90	120	150	180	210	240	270	300	330	360	390	420	450	480	510	540	570	600
1.25	120.6	116.8	113.7	115.4	114.7	114.5	113.7	115.4	114.7	116.7	116.2	115.8	117.7	116.9	116.2	117.5	116.3	114.3	115.6	115.9
1.3	120.6	116.9	113.5	115.5	115.2	114.5	113.5	115.5	115.2	116.9	116.1	115.9	117.6	117.2	115.5	117.5	115.9	114.3	115.3	115.8
1.35	120.6	117.1	113.8	115.5	115.1	114.5	113.8	115.5	115.1	117.1	116.1	115.9	118.0	117.6	115.9	117.5	116.0	114.4	115.7	115.4
1.4	120.6	117.1	113.8	115.7	115.1	114.6	113.8	115.7	115.1	116.9	116.2	116.4	118.1	117.1	116.0	117.7	115.9	114.3	115.6	116.4
1.45	120.6	117.1	113.9	116.0	115.1	114.9	113.9	116.0	115.1	117.1	116.4	115.8	118.0	117.2	115.9	117.8	115.7	114.0	115.2	115.7
1.5	120.6	117.2	114.3	116.0	115.3	114.8	114.3	116.0	115.3	117.0	116.0	115.9	118.0	117.5	115.6	117.4	115.6	114.5	115.3	116.3
1.55	120.6	117.3	114.5	115.9	115.3	114.9	114.5	115.9	115.3	117.4	116.5	116.0	118.2	117.8	115.6	117.7	116.0	114.8	115.9	116.2
1.6	120.7	117.3	114.6	116.0	115.5	114.8	114.6	116.0	115.5	117.1	116.3	116.1	118.1	117.2	116.0	117.7	116.1	114.4	115.8	116.4
1.65	120.7	117.4	114.6	116.2	115.7	114.9	114.6	116.2	115.7	117.1	116.5	115.8	118.0	117.3	116.3	117.7	115.9	114.4	115.6	116.1
1.7	120.7	117.4	114.8	116.2	115.6	115.1	114.8	116.2	115.6	117.0	116.1	115.5	118.0	117.4	116.0	117.6	115.9	114.7	115.3	116.4
1.75	120.7	117.5	115.1	116.2	115.8	115.2	115.1	116.2	115.8	117.1	116.4	115.7	118.2	117.7	115.9	117.9	116.0	114.5	115.5	116.2
1.8	120.7	117.6	115.3	116.1	115.5	115.2	115.3	116.1	115.5	117.3	116.4	115.8	118.3	117.7	116.1	118.0	116.2	114.8	115.8	116.3
1.85	120.7	117.7	115.2	116.1	115.5	115.3	115.2	116.1	115.5	117.0	116.6	116.3	118.0	117.4	116.4	118.2	116.1	114.4	115.9	116.4
1.9	120.8	117.9	114.9	116.2	115.4	115.1	114.9	116.2	115.4	116.7	116.1	115.7	118.0	117.0	116.3	117.6	115.6	114.0	115.7	115.6
1.95	120.7	117.9	114.7	116.1	115.3	114.9	114.7	116.1	115.3	116.6	115.9	115.7	117.7	116.8	115.8	117.3	115.5	113.7	115.1	115.6
2	120.8	118.0	114.7	116.2	115.4	115.2	114.7	116.2	115.4	116.8	115.9	115.6	117.3	117.1	116.1	117.0	115.6	113.6	114.6	115.5

Table B.6 Energy (MWh) estimated by dynamic model for RG5 (30 sec averaged data set)

Yaw Rate (deg/sec)	Delay Time (secs)																			
	30	60	90	120	150	180	210	240	270	300	330	360	390	420	450	480	510	540	570	600
0	85.1	77.9	77.8	78.0	77.8	77.9	77.8	78.0	77.8	78.0	83.8	79.4	83.6	79.3	78.2	84.3	84.0	83.0	83.4	79.1
0.05	132.2	125.2	123.7	122.5	123.7	124.7	123.7	122.5	123.7	125.3	125.2	121.1	127.2	124.8	124.4	123.7	123.5	122.1	121.9	121.3
0.1	133.0	126.2	125.0	122.3	126.2	123.0	125.0	122.3	126.2	123.9	124.3	120.6	125.7	123.6	122.5	124.7	124.4	122.2	122.4	121.9
0.15	132.8	126.0	125.1	122.4	124.2	123.0	125.1	122.4	124.2	124.0	123.7	121.1	125.5	123.4	122.6	125.0	123.5	121.6	123.0	122.0
0.2	132.6	125.7	122.0	121.8	123.1	121.5	122.0	121.8	123.1	124.9	123.3	122.5	125.3	122.8	121.6	125.6	123.9	120.8	123.3	122.5
0.25	132.6	125.8	123.0	122.2	122.3	120.8	123.0	122.2	122.3	124.2	123.4	122.7	125.3	123.4	122.9	125.3	124.1	122.6	123.5	123.2
0.3	132.4	125.5	122.2	122.2	121.6	121.6	122.2	122.2	121.6	122.9	124.8	122.9	125.3	122.9	123.7	124.8	124.6	122.1	123.8	123.6
0.35	132.2	125.2	120.9	122.7	121.7	122.2	120.9	122.7	121.7	122.7	124.5	123.2	125.1	123.8	123.2	125.5	124.7	122.9	123.7	122.6
0.4	132.0	125.2	122.3	122.6	122.6	121.1	122.3	122.6	122.6	123.8	124.0	124.0	125.4	123.4	123.3	125.0	124.7	122.8	123.3	122.3
0.45	131.6	125.1	123.4	122.7	123.1	121.6	123.4	122.7	123.1	123.7	124.1	123.2	125.7	124.4	123.2	124.7	124.4	122.2	123.3	122.5
0.5	131.4	125.0	122.3	122.7	123.1	121.4	122.3	122.7	123.1	124.2	124.3	124.2	125.7	123.6	123.9	124.7	124.6	122.2	123.0	122.7
0.55	131.3	125.1	120.8	122.6	123.6	122.3	120.8	122.6	123.6	124.3	124.7	124.1	125.2	124.4	123.9	124.9	124.3	122.2	123.5	122.8
0.6	131.0	125.2	121.4	122.9	123.4	122.1	121.4	122.9	123.4	124.7	124.4	124.3	125.1	124.1	123.9	125.2	124.2	122.1	123.9	123.2
0.65	130.8	125.2	122.0	123.4	124.3	122.4	122.0	123.4	124.3	125.2	124.6	124.3	124.5	124.5	124.2	125.4	124.2	122.6	123.9	123.6
0.7	130.8	125.2	122.6	123.3	123.3	123.2	122.6	123.3	123.3	125.0	124.4	124.2	124.8	124.5	124.2	125.4	124.5	122.8	124.3	123.5
0.75	130.7	125.3	121.4	123.9	123.3	122.9	121.4	123.9	123.3	124.9	124.4	123.8	125.2	124.4	124.5	125.9	125.2	123.0	123.9	123.8
0.8	130.6	125.4	122.3	123.8	124.1	122.9	122.3	123.8	124.1	124.9	124.8	124.3	125.1	124.5	124.8	125.9	125.3	123.0	124.3	124.3
0.85	130.5	125.5	122.0	124.1	124.2	123.0	122.0	124.1	124.2	124.3	125.0	123.7	125.7	125.3	124.7	126.0	125.1	123.2	124.1	124.0
0.9	130.5	125.7	122.6	124.1	124.4	123.5	122.6	124.1	124.4	125.0	125.3	124.2	126.2	125.4	125.3	126.5	125.5	123.8	124.3	124.1
0.95	130.5	125.9	122.7	123.9	124.8	123.5	122.7	123.9	124.8	125.4	125.0	124.6	126.1	125.6	125.5	126.4	125.1	123.3	124.4	124.1
1	130.6	126.0	122.5	124.0	124.2	123.8	122.5	124.0	124.2	125.4	125.2	124.6	126.7	125.7	125.5	126.3	125.4	123.6	124.5	124.6
1.05	130.6	126.2	123.1	124.3	124.8	123.9	123.1	124.3	124.8	125.5	125.5	124.8	126.2	125.6	125.5	126.5	125.4	123.8	124.7	124.1
1.1	130.6	126.4	122.6	124.6	124.4	123.8	122.6	124.6	124.4	125.8	125.7	124.8	126.8	125.7	125.6	126.7	125.5	123.7	124.4	124.3
1.15	130.6	126.5	122.8	124.9	124.6	124.0	122.8	124.9	124.6	125.8	126.2	124.9	126.5	126.1	125.7	126.8	125.6	124.1	124.4	124.3
1.2	130.6	126.7	123.3	124.7	124.6	123.8	123.3	124.7	124.6	125.7	125.8	125.1	127.1	125.8	126.0	126.8	125.8	123.9	124.2	124.3

Yaw Rate (deg/sec)	Delay Time (secs)																			
	30	60	90	120	150	180	210	240	270	300	330	360	390	420	450	480	510	540	570	600
1.25	130.6	126.8	123.2	125.3	124.7	124.0	123.2	125.3	124.7	126.0	125.9	124.9	127.0	125.7	125.7	126.9	125.7	123.6	124.5	124.3
1.3	130.6	127.0	123.2	125.3	124.8	124.0	123.2	125.3	124.8	126.3	126.2	125.8	126.7	125.7	125.4	127.0	126.1	123.6	124.6	124.5
1.35	130.6	127.1	123.4	125.2	124.8	124.1	123.4	125.2	124.8	126.2	126.1	125.2	127.2	126.1	125.9	126.8	125.7	124.5	124.5	124.7
1.4	130.6	127.2	123.4	125.6	125.0	123.9	123.4	125.6	125.0	126.3	126.5	125.3	127.0	125.9	125.7	126.8	125.6	123.8	124.9	124.4
1.45	130.6	127.2	123.4	125.5	124.9	124.3	123.4	125.5	124.9	126.1	126.4	125.4	126.5	125.4	125.5	126.8	125.6	124.1	124.5	124.4
1.5	130.6	127.2	123.7	125.5	125.0	124.3	123.7	125.5	125.0	126.1	126.1	125.6	126.9	125.9	125.6	127.0	125.8	124.1	124.8	124.7
1.55	130.7	127.3	123.8	125.5	125.0	124.7	123.8	125.5	125.0	126.3	126.5	125.3	127.0	126.4	125.8	127.0	125.7	124.8	124.4	124.5
1.6	130.7	127.3	124.0	125.9	124.9	124.7	124.0	125.9	124.9	126.4	126.0	125.2	127.2	126.2	126.0	126.9	125.7	124.1	124.8	124.4
1.65	130.7	127.3	124.3	125.9	125.0	124.8	124.3	125.9	125.0	126.1	126.2	125.4	126.8	125.7	125.7	126.7	125.6	124.1	124.6	124.6
1.7	130.7	127.4	124.2	125.7	125.2	124.7	124.2	125.7	125.2	126.1	126.3	125.6	127.0	125.9	125.5	127.0	125.8	123.9	124.6	123.9
1.75	130.7	127.4	124.4	125.7	125.4	124.8	124.4	125.7	125.4	126.3	126.5	125.5	127.0	126.0	125.8	127.2	126.0	124.1	125.2	124.8
1.8	130.7	127.5	124.4	125.8	125.2	124.8	124.4	125.8	125.2	126.2	126.7	125.8	127.4	126.2	125.9	127.2	125.9	125.0	125.1	124.8
1.85	130.7	127.6	124.4	126.0	125.1	124.8	124.4	126.0	125.1	126.1	126.5	125.3	127.3	126.7	125.9	127.2	125.8	124.1	125.3	124.5
1.9	130.7	127.6	124.4	126.0	125.2	124.8	124.4	126.0	125.2	126.0	126.3	125.1	126.9	125.8	125.9	126.7	125.5	123.8	124.3	124.5
1.95	130.7	127.8	124.4	125.7	125.0	124.7	124.4	125.7	125.0	126.0	125.6	125.0	126.5	125.5	125.0	126.8	125.0	123.6	123.9	123.8
2	130.7	127.8	124.3	125.9	124.9	124.8	124.3	125.9	124.9	125.8	125.5	124.9	126.4	125.2	125.2	126.8	125.0	122.8	124.0	124.6

Table B.7 Energy (MWh) estimated by dynamic model for RG6 (30 sec averaged data set)

Yaw Rate (deg/sec)	Delay Time (secs)																			
	30	60	90	120	150	180	210	240	270	300	330	360	390	420	450	480	510	540	570	600
0	84.3	77.8	77.6	77.8	77.7	77.7	77.6	77.8	77.7	77.8	82.9	78.9	83.0	78.7	77.9	83.5	83.2	82.3	82.7	78.8
0.05	133.6	127.1	125.4	125.7	125.7	125.8	125.4	125.7	125.7	124.9	124.7	124.2	125.3	125.6	125.4	124.9	126.8	123.2	122.3	120.8
0.1	134.3	128.1	127.0	126.5	124.4	125.3	127.0	126.5	124.4	126.6	123.2	122.8	125.3	124.9	124.0	125.8	124.3	122.0	124.6	122.4
0.15	134.2	128.1	126.9	125.0	123.1	121.9	126.9	125.0	123.1	125.5	124.3	125.7	123.7	126.5	125.6	125.3	126.0	122.3	124.3	123.2
0.2	134.2	127.8	126.0	123.9	123.5	121.1	126.0	123.9	123.5	124.5	123.4	124.7	125.8	124.6	124.8	126.2	126.4	122.7	124.5	124.1
0.25	134.2	127.5	125.8	124.1	123.1	121.5	125.8	124.1	123.1	125.3	124.3	124.6	126.3	125.8	125.0	126.4	127.2	122.5	124.8	124.0
0.3	134.0	127.4	125.0	123.5	123.0	121.8	125.0	123.5	123.0	124.6	124.7	125.1	125.7	124.5	124.6	126.2	126.6	123.3	124.9	124.4
0.35	133.8	127.1	125.0	124.6	123.6	122.3	125.0	124.6	123.6	124.3	125.1	125.1	125.8	124.7	125.2	127.2	126.7	123.6	125.4	123.8
0.4	133.5	127.0	123.5	124.1	124.5	122.9	123.5	124.1	124.5	124.6	125.6	125.6	125.9	125.6	125.2	126.5	126.2	124.0	124.7	123.3
0.45	133.3	126.7	123.2	124.3	124.2	122.8	123.2	124.3	124.2	125.7	125.0	125.2	126.5	125.7	124.8	126.6	126.0	124.2	124.8	124.0
0.5	133.1	126.6	122.6	124.0	123.3	123.2	122.6	124.0	123.3	125.2	125.5	125.4	126.7	125.9	124.9	126.5	126.8	123.6	125.3	123.5
0.55	133.0	126.8	123.2	124.0	123.4	123.5	123.2	124.0	123.4	126.0	126.5	125.0	126.2	125.2	124.8	126.5	126.0	124.0	125.5	124.3
0.6	132.8	126.9	123.9	124.0	122.9	123.0	123.9	124.0	122.9	125.8	126.0	124.9	126.1	125.2	125.2	126.6	125.6	123.7	125.5	124.7
0.65	132.7	127.0	123.2	124.0	123.6	123.2	123.2	124.0	123.6	126.1	126.1	125.4	126.4	126.2	125.6	127.1	126.5	124.5	125.2	125.3
0.7	132.5	127.1	123.5	124.4	124.1	123.1	123.5	124.4	124.1	125.8	125.6	125.2	126.4	126.2	125.6	127.4	126.6	124.6	125.3	124.6
0.75	132.4	127.2	123.3	125.0	124.2	123.8	123.3	125.0	124.2	126.0	125.4	125.0	125.7	125.9	125.8	127.4	126.3	124.9	125.6	124.9
0.8	132.3	127.3	124.1	125.5	124.4	123.8	124.1	125.5	124.4	125.8	126.0	124.9	126.5	126.3	126.0	127.6	126.6	124.9	125.7	125.1
0.85	132.1	127.4	123.9	125.2	124.4	124.0	123.9	125.2	124.4	125.7	126.0	125.2	126.5	126.4	126.3	127.5	126.8	124.9	125.8	125.1
0.9	132.1	127.6	123.9	125.3	124.9	123.9	123.9	125.3	124.9	125.7	125.9	125.5	127.0	126.5	126.2	128.2	127.0	125.0	125.6	124.7
0.95	132.0	127.7	124.0	125.7	125.3	124.6	124.0	125.7	125.3	126.1	126.3	125.7	127.2	126.9	126.5	127.9	126.8	125.0	125.7	125.2
1	132.0	127.9	124.0	125.6	125.1	124.5	124.0	125.6	125.1	126.1	126.7	125.7	127.6	127.2	126.4	128.0	127.3	125.0	125.7	125.2
1.05	132.0	127.8	123.8	125.9	125.5	124.8	123.8	125.9	125.5	126.4	126.6	125.7	127.5	127.0	126.8	128.4	127.0	125.2	125.7	125.4
1.1	132.0	128.0	123.6	126.1	125.7	124.8	123.6	126.1	125.7	126.7	126.8	125.9	128.1	127.0	126.8	128.4	126.8	124.7	125.4	125.3
1.15	132.0	128.2	123.9	126.1	125.9	125.4	123.9	126.1	125.9	126.7	127.0	126.1	128.0	127.1	127.0	128.3	126.8	125.3	125.3	125.8
1.2	132.0	128.5	124.1	126.6	125.7	125.5	124.1	126.6	125.7	126.9	127.1	126.1	128.5	127.1	127.6	128.9	126.9	125.1	125.8	126.0

Yaw Rate (deg/sec)	Delay Time (secs)																			
	30	60	90	120	150	180	210	240	270	300	330	360	390	420	450	480	510	540	570	600
1.25	132.0	128.6	124.3	126.6	125.6	125.3	124.3	126.6	125.6	127.4	127.2	126.3	128.1	127.0	127.4	128.8	127.4	124.8	125.9	125.6
1.3	132.0	128.6	124.8	126.5	125.8	125.4	124.8	126.5	125.8	127.3	127.2	126.4	128.2	127.1	127.3	128.7	127.1	125.0	126.0	125.5
1.35	132.1	128.7	124.6	126.5	125.9	125.1	124.6	126.5	125.9	127.3	127.3	126.5	128.1	127.3	127.6	128.9	127.4	125.2	125.8	126.3
1.4	132.0	128.9	124.8	126.9	126.0	125.3	124.8	126.9	126.0	127.4	127.2	126.3	128.1	127.0	127.3	128.8	127.6	124.8	125.9	126.1
1.45	132.0	129.0	124.9	126.6	126.2	125.2	124.9	126.6	126.2	127.3	127.3	126.2	127.9	126.9	126.7	128.5	127.3	125.4	125.4	126.0
1.5	132.0	129.0	125.3	127.0	126.2	125.4	125.3	127.0	126.2	127.3	127.4	126.1	128.3	126.9	127.5	128.7	127.3	125.3	125.8	126.0
1.55	132.0	129.0	125.2	127.1	126.4	125.3	125.2	127.1	126.4	127.4	127.4	126.2	128.5	127.3	127.3	129.1	127.5	125.8	125.6	126.0
1.6	132.0	129.1	125.4	127.2	126.2	125.7	125.4	127.2	126.2	127.5	127.6	126.2	128.3	127.6	127.6	128.9	127.6	125.2	125.9	126.2
1.65	132.0	129.2	125.2	127.3	126.3	125.9	125.2	127.3	126.3	127.8	127.6	126.4	127.9	127.2	126.9	128.4	127.0	125.6	125.8	125.8
1.7	132.0	129.2	125.6	127.3	126.5	125.6	125.6	127.3	126.5	127.8	127.1	126.0	128.1	127.3	126.8	128.5	127.4	125.1	126.1	125.9
1.75	132.0	129.2	125.7	127.4	126.6	125.7	125.7	127.4	126.6	127.6	127.3	126.3	128.2	127.3	127.5	128.8	127.9	125.5	125.8	126.1
1.8	132.0	129.3	125.8	127.4	126.3	125.7	125.8	127.4	126.3	127.6	127.3	126.5	128.6	127.3	127.2	129.2	127.9	125.4	126.1	125.8
1.85	132.0	129.3	126.0	127.4	126.5	125.9	126.0	127.4	126.5	127.7	127.3	126.4	128.8	127.9	127.5	128.7	127.4	125.5	125.9	126.3
1.9	132.0	129.5	126.0	127.5	126.6	126.0	126.0	127.5	126.6	127.3	127.2	126.6	128.1	127.3	127.0	128.5	126.7	125.0	125.6	125.6
1.95	132.0	129.5	125.9	127.2	126.4	125.6	125.9	127.2	126.4	127.4	126.5	125.9	127.9	126.5	126.4	128.2	126.6	124.5	125.2	125.0
2	132.0	129.6	125.9	127.2	126.2	125.9	125.9	127.2	126.2	127.1	126.5	126.0	128.1	126.4	126.6	128.2	126.6	124.1	125.3	125.6

Table B.8 Energy (MWh) estimated by dynamic model for RG1 (1 min averaged data set)

Yaw Rate (deg/sec)	Delay Time (secs)									
	60	120	180	240	300	360	420	480	540	600
0	46.4	44.7	45.4	45.1	45.7	45.9	45.1	46.2	45.9	45.7
0.05	79.2	75.3	75.1	75.8	76.0	75.2	75.4	75.9	73.5	76.6
0.1	79.4	77.6	74.3	76.1	73.2	76.6	76.3	76.8	75.2	75.5
0.15	79.7	77.5	76.0	73.9	75.5	75.3	75.5	76.3	76.5	75.9
0.2	79.9	77.5	75.7	74.9	75.0	74.5	75.7	76.4	77.3	75.6
0.25	79.8	77.5	75.2	74.3	75.5	74.9	75.4	77.8	76.5	75.0
0.3	79.7	77.7	74.8	74.2	75.9	74.8	76.0	77.7	76.3	75.6
0.35	79.6	77.8	75.2	75.1	76.3	75.7	75.7	77.8	77.1	75.7
0.4	79.6	77.8	75.0	75.6	76.1	75.6	75.9	78.1	77.0	75.4
0.45	79.6	77.9	76.4	75.9	75.7	76.2	75.6	78.2	77.0	75.6
0.5	79.5	78.0	76.1	76.3	76.1	76.1	76.0	77.9	77.2	75.8
0.55	79.5	78.0	76.4	76.4	76.2	76.6	75.9	78.0	76.8	75.8
0.6	79.4	78.0	76.3	76.0	76.2	76.5	76.3	77.5	77.1	76.0
0.65	79.3	78.1	76.7	76.2	76.9	76.6	75.8	78.2	77.1	76.1
0.7	79.3	78.2	76.6	76.2	76.7	76.7	75.8	77.6	77.1	76.1
0.75	79.3	78.3	76.9	76.5	77.1	76.8	76.0	78.2	77.7	76.4
0.8	79.3	78.3	77.0	76.7	77.0	77.1	76.0	77.9	77.3	76.6
0.85	79.3	78.2	77.0	76.9	77.1	77.0	76.3	78.0	77.0	76.7
0.9	79.3	78.3	77.1	77.2	76.7	77.4	76.7	78.3	77.7	76.8
0.95	79.3	78.5	77.1	77.3	77.0	77.4	76.2	78.5	77.2	76.6
1	79.4	78.6	76.8	77.1	76.7	77.4	76.6	77.8	77.5	76.1
1.05	79.5	78.6	77.1	77.1	76.8	77.7	76.5	78.1	77.4	76.4
1.1	79.5	78.6	77.3	77.2	76.7	77.8	76.8	78.3	77.6	76.3
1.15	79.5	78.7	77.5	77.0	77.1	77.7	76.5	78.4	77.4	76.3
1.2	79.6	78.7	77.6	77.3	76.6	77.5	76.4	78.2	77.0	76.3
1.25	79.6	78.8	77.6	77.3	76.9	77.5	76.1	77.8	76.8	76.6
1.3	79.7	78.9	77.8	77.3	77.0	77.6	76.3	78.0	77.1	77.0
1.35	79.8	78.9	77.9	77.3	76.8	77.9	76.4	78.2	77.6	76.9
1.4	79.8	79.1	78.0	77.4	77.0	78.0	76.5	78.3	77.4	76.8
1.45	79.8	79.0	78.1	77.5	77.3	77.9	76.5	78.2	77.6	76.4
1.5	79.8	79.0	77.9	77.6	77.1	77.4	76.5	77.5	77.1	76.4
1.55	79.9	79.0	77.7	77.3	76.9	77.5	76.4	77.8	77.0	76.4
1.6	79.9	79.0	77.7	77.5	77.0	77.5	76.4	77.8	77.3	76.6
1.65	80.0	79.1	77.7	77.5	77.1	77.4	76.4	78.2	77.5	76.5
1.7	80.2	79.1	77.8	77.7	77.3	77.5	76.5	78.4	77.6	76.9
1.75	80.3	79.2	78.0	77.8	77.6	77.8	76.8	78.7	77.9	77.2
1.8	80.4	79.3	78.2	78.1	77.9	78.1	77.1	79.0	78.6	77.4
1.85	80.5	79.4	78.5	78.3	78.1	78.3	77.3	79.2	78.5	77.8
1.9	80.5	79.4	78.4	78.2	77.9	77.9	77.4	79.4	77.6	77.8

Yaw Rate (deg/sec)	Delay Time (secs)									
	60	120	180	240	300	360	420	480	540	600
1.95	80.5	79.5	78.3	78.1	77.7	77.9	76.9	79.0	77.8	77.6
2	80.5	79.5	78.4	78.1	78.0	77.8	76.7	78.6	77.6	77.3

Table B.9 Energy (MWh) estimated by dynamic model for RG2 (1 min averaged data set)

Yaw Rate (deg/sec)	Delay Time (secs)									
	60	120	180	240	300	360	420	480	540	600
0	60.9	58.6	59.7	59.1	60.0	60.3	59.1	60.8	60.3	60.0
0.05	87.5	83.0	83.0	83.4	84.6	83.5	84.9	84.5	81.5	83.4
0.1	87.7	85.3	82.0	83.6	83.8	82.7	83.3	84.1	83.3	83.5
0.15	87.7	85.6	82.5	82.8	83.4	83.6	83.8	85.8	83.7	83.7
0.2	88.1	85.5	83.5	83.9	85.0	83.5	83.4	85.1	84.8	84.7
0.25	88.2	85.8	83.0	83.5	83.1	83.2	83.5	86.7	84.7	84.0
0.3	88.2	85.9	83.0	83.2	83.9	84.3	83.7	86.8	84.9	83.9
0.35	88.3	86.1	83.2	84.0	84.6	84.6	84.4	86.8	85.3	84.0
0.4	88.3	86.2	84.0	84.3	84.7	84.4	84.6	86.5	85.5	84.1
0.45	88.4	86.3	84.4	85.0	84.7	85.2	84.1	86.7	85.6	84.1
0.5	88.4	86.5	84.3	85.2	84.9	84.9	84.7	86.9	85.4	83.7
0.55	88.4	86.5	85.0	85.0	84.6	86.0	84.5	86.7	85.3	84.0
0.6	88.4	86.5	85.5	85.1	85.0	85.4	84.6	86.9	85.9	84.5
0.65	88.4	86.6	84.7	85.4	85.5	85.4	84.4	86.9	85.4	84.7
0.7	88.4	86.6	84.6	85.2	85.5	85.8	84.7	86.7	85.8	84.5
0.75	88.5	86.8	85.4	85.6	85.4	85.7	84.6	87.1	86.2	84.9
0.8	88.5	86.8	85.5	85.7	85.3	86.1	84.8	87.1	86.1	85.0
0.85	88.5	86.9	85.8	86.1	85.6	86.1	85.0	87.3	85.9	85.0
0.9	88.5	87.0	85.7	85.9	85.5	86.3	85.5	87.4	86.6	85.2
0.95	88.6	87.1	85.6	86.2	85.9	86.2	85.0	87.6	86.0	84.9
1	88.6	87.2	85.7	85.7	85.5	86.3	85.3	86.9	86.2	84.5
1.05	88.7	87.3	85.7	85.9	85.8	86.4	85.3	87.0	86.0	84.6
1.1	88.7	87.3	85.9	85.8	85.7	86.2	85.4	87.3	86.5	84.7
1.15	88.7	87.4	86.1	86.0	86.1	86.2	85.1	87.6	86.1	84.7
1.2	88.7	87.4	86.4	86.0	85.7	86.3	84.9	87.0	85.6	84.6
1.25	88.8	87.5	86.3	86.0	85.6	86.2	84.9	86.6	85.5	84.8
1.3	88.9	87.6	86.4	86.0	85.7	86.3	85.2	87.0	85.8	85.1
1.35	88.9	87.8	86.6	86.2	85.8	86.7	85.5	87.2	86.5	85.1
1.4	89.0	87.9	86.7	86.1	85.9	86.6	85.3	87.3	86.2	85.0
1.45	89.0	87.8	86.6	86.4	86.1	86.5	84.8	87.4	86.3	85.4
1.5	89.0	87.9	86.4	86.2	86.1	86.5	85.0	86.5	85.8	84.8
1.55	89.1	87.9	86.3	86.0	85.8	86.2	85.1	86.8	85.7	84.6
1.6	89.1	87.9	86.3	86.1	85.8	86.4	85.2	86.8	85.8	84.7
1.65	89.2	87.9	86.3	86.2	86.0	86.1	85.3	87.2	86.0	84.6

Yaw Rate (deg/sec)	Delay Time (secs)									
	60	120	180	240	300	360	420	480	540	600
1.7	89.4	88.0	86.5	86.4	86.2	86.3	85.3	87.5	86.2	84.9
1.75	89.5	88.1	86.7	86.6	86.5	86.6	85.7	87.7	86.5	85.3
1.8	89.6	88.2	87.0	87.1	86.8	87.0	86.0	87.9	87.2	85.6
1.85	89.7	88.3	87.1	87.1	87.0	87.2	86.1	88.0	87.5	86.0
1.9	89.7	88.3	87.0	87.0	86.8	86.7	86.0	88.4	86.6	86.0
1.95	89.7	88.4	87.0	86.9	86.5	86.7	85.7	87.7	86.5	85.8
2	89.7	88.4	87.1	86.9	86.8	86.8	85.2	87.4	86.2	85.5

Table B.10 Energy (MWh) estimated by dynamic model for RG3 (1 min averaged data set)

Yaw Rate (deg/sec)	Delay Time (secs)									
	60	120	180	240	300	360	420	480	540	600
0	75.4	71.9	73.4	72.7	73.9	74.3	72.9	75.0	74.4	73.9
0.05	106.8	100.5	101.7	101.3	102.1	102.0	100.8	103.6	101.2	100.5
0.1	107.0	101.9	101.6	103.8	101.3	102.3	102.8	105.3	102.9	102.8
0.15	107.4	103.2	100.8	101.2	103.9	103.3	102.0	104.2	104.0	101.9
0.2	107.8	104.0	102.2	101.4	102.7	103.4	102.6	106.1	104.4	102.8
0.25	108.2	104.3	100.4	102.0	101.9	102.4	103.0	106.3	104.5	102.6
0.3	108.2	104.4	102.5	102.2	102.8	102.9	103.1	106.1	104.6	102.2
0.35	108.2	104.7	102.2	102.9	103.3	102.6	102.7	105.2	105.2	103.1
0.4	108.2	104.9	103.0	102.9	102.9	103.0	103.9	105.7	104.4	102.9
0.45	108.1	105.2	103.1	103.1	103.3	103.1	103.4	105.9	104.7	102.8
0.5	108.1	105.5	103.4	103.5	103.5	102.9	103.9	106.1	104.9	102.5
0.55	108.1	105.5	103.6	103.8	103.7	104.6	103.7	106.2	104.6	102.8
0.6	108.1	105.6	104.1	104.0	104.0	103.8	103.5	106.1	104.6	103.2
0.65	108.1	105.6	104.4	104.1	104.4	104.0	103.8	106.2	104.2	103.7
0.7	108.0	105.7	104.3	104.2	104.4	104.6	104.0	106.1	105.0	103.1
0.75	108.0	105.8	104.5	104.3	104.6	104.0	104.0	106.5	104.9	103.5
0.8	108.0	105.8	104.8	104.7	104.4	104.7	104.2	106.5	105.0	103.8
0.85	108.0	106.0	104.7	104.8	104.6	104.8	104.2	106.5	104.9	104.1
0.9	108.0	106.1	104.8	105.0	104.4	104.8	104.5	106.4	105.2	104.1
0.95	108.1	106.2	105.1	104.9	104.6	104.8	104.4	106.6	105.6	103.8
1	108.1	106.2	104.8	104.6	104.4	104.7	104.2	106.7	104.3	103.8
1.05	108.1	106.3	104.8	104.8	104.8	104.6	104.4	106.3	104.3	103.5
1.1	108.1	106.3	105.1	104.6	104.8	104.8	104.4	106.5	104.9	103.4
1.15	108.2	106.3	105.4	104.6	105.2	104.6	104.4	106.4	104.7	103.3
1.2	108.2	106.4	105.5	104.6	104.3	104.4	104.0	106.0	104.3	103.4
1.25	108.3	106.6	105.5	104.3	104.6	104.6	104.2	105.8	104.5	103.8
1.3	108.4	106.7	105.7	104.6	104.9	105.0	104.3	106.1	104.3	104.3
1.35	108.5	106.8	106.0	104.6	105.1	105.2	104.6	106.3	104.8	103.9
1.4	108.6	106.8	105.8	104.7	105.4	105.1	104.9	106.4	105.2	103.8

Yaw Rate (deg/sec)	Delay Time (secs)									
	60	120	180	240	300	360	420	480	540	600
1.45	108.6	106.9	105.7	104.7	105.1	105.1	104.5	106.3	104.9	104.0
1.5	108.6	107.0	105.5	104.8	105.2	104.7	103.9	106.0	104.7	103.3
1.55	108.7	107.0	105.4	104.7	104.9	104.4	104.0	105.6	104.1	103.1
1.6	108.8	107.1	105.5	104.8	104.9	104.2	104.1	105.7	104.1	103.0
1.65	108.9	107.1	105.6	104.9	105.1	104.0	104.1	105.8	104.3	102.9
1.7	109.0	107.3	105.7	105.0	105.3	104.3	104.5	106.1	104.7	103.3
1.75	109.2	107.4	105.7	105.3	105.6	104.8	104.9	106.4	104.8	103.7
1.8	109.3	107.5	105.9	105.6	105.9	105.3	105.1	106.7	105.5	104.1
1.85	109.4	107.6	106.0	105.9	105.8	105.4	105.5	107.2	105.8	104.6
1.9	109.4	107.7	106.0	105.8	105.8	105.5	105.4	107.4	105.3	104.9
1.95	109.4	107.7	106.0	105.7	105.6	105.0	104.9	106.7	105.0	104.3
2	109.4	107.7	106.3	105.7	105.8	105.1	104.6	106.4	104.9	104.7

Table B.11 Energy (MWh) estimated by dynamic model for RG4 (1 min averaged data set)

Yaw Rate (deg/sec)	Delay Time (secs)									
	60	120	180	240	300	360	420	480	540	600
0	84.3	80.5	82.3	81.5	82.8	83.2	81.6	83.9	83.3	82.8
0.05	122.6	115.9	116.3	115.5	116.8	115.6	118.1	120.9	115.8	116.3
0.1	122.1	116.3	115.8	116.5	116.7	118.0	115.5	120.6	116.0	119.0
0.15	121.6	116.7	118.2	116.9	117.6	115.9	116.0	119.4	116.3	116.8
0.2	122.1	117.8	115.0	116.0	116.4	117.3	116.3	120.4	118.1	117.3
0.25	122.4	118.4	114.9	116.2	115.9	117.1	116.4	119.5	117.6	115.9
0.3	122.9	118.6	115.4	116.2	115.5	116.8	116.8	119.4	117.8	116.4
0.35	123.0	119.1	115.5	116.6	116.2	117.6	116.9	120.0	119.7	116.6
0.4	122.8	119.4	115.9	117.1	116.5	117.3	117.4	120.5	119.6	116.1
0.45	122.8	119.7	116.9	116.9	116.7	117.7	118.5	120.3	119.3	116.4
0.5	122.8	120.1	117.2	117.2	117.6	118.6	118.3	120.0	119.8	116.6
0.55	122.8	120.4	117.5	116.9	117.8	118.5	118.4	120.1	120.0	116.4
0.6	122.8	120.7	118.9	118.1	118.0	119.1	118.6	120.4	119.6	116.4
0.65	122.8	120.9	118.9	118.6	118.4	118.6	118.3	120.6	119.4	117.2
0.7	122.9	120.9	118.6	118.6	118.9	119.1	118.3	120.8	120.0	116.7
0.75	122.9	120.8	118.7	118.6	118.9	118.9	118.6	121.0	119.6	117.6
0.8	123.0	120.8	118.8	119.6	119.1	119.0	118.6	121.4	120.0	117.9
0.85	123.0	120.9	119.0	119.3	118.8	119.5	118.9	120.9	119.6	117.9
0.9	123.1	121.0	119.6	119.1	118.7	119.4	119.2	121.0	120.1	117.8
0.95	123.1	121.0	119.6	118.9	119.1	119.0	119.1	121.4	120.1	118.1
1	123.1	121.0	119.3	118.9	119.0	118.6	119.2	121.0	119.4	117.2
1.05	123.2	121.1	119.5	119.1	119.2	118.9	119.2	121.3	119.5	117.3
1.1	123.3	121.1	119.6	119.3	119.2	119.1	119.3	121.1	120.4	117.5
1.15	123.3	121.1	119.8	119.2	119.2	119.4	119.0	120.7	119.6	117.7

Yaw Rate (deg/sec)	Delay Time (secs)									
	60	120	180	240	300	360	420	480	540	600
1.2	123.4	121.2	120.0	119.2	119.5	119.0	118.9	120.6	119.1	117.0
1.25	123.5	121.4	120.2	119.1	119.0	118.8	118.6	120.9	119.5	117.2
1.3	123.6	121.5	120.6	119.1	119.4	119.1	119.0	121.1	119.8	117.3
1.35	123.7	121.7	120.9	119.4	119.5	119.0	119.4	121.1	120.0	117.4
1.4	123.7	121.8	120.9	119.5	119.7	119.1	119.4	121.1	120.2	117.6
1.45	123.7	121.8	120.8	119.5	119.6	119.4	118.6	120.6	119.2	117.5
1.5	123.7	122.0	120.4	119.4	119.5	118.8	118.4	120.0	119.3	116.6
1.55	123.8	122.0	120.4	119.5	119.3	118.3	118.5	119.9	118.9	116.6
1.6	123.9	122.1	120.4	119.6	119.4	118.3	118.7	120.1	119.1	117.0
1.65	124.0	122.2	120.4	119.7	119.5	118.3	118.9	120.3	119.3	117.4
1.7	124.2	122.3	120.6	119.9	119.5	118.6	119.3	120.7	119.8	117.6
1.75	124.3	122.4	120.9	120.3	119.8	119.1	119.7	121.1	120.2	118.1
1.8	124.4	122.5	121.0	120.6	120.0	119.5	120.1	121.6	120.8	118.2
1.85	124.5	122.5	121.3	120.8	120.2	119.8	120.1	121.7	120.9	118.2
1.9	124.5	122.6	121.0	120.7	120.5	119.9	119.4	121.9	120.1	118.3
1.95	124.5	122.6	120.9	120.5	120.0	119.5	119.0	121.5	119.4	117.9
2	124.5	122.6	121.0	120.7	119.9	119.7	118.8	121.0	119.8	118.1

Table B.12 Energy (MWh) estimated by dynamic model for RG5 (1 min averaged data set)

Yaw Rate (deg/sec)	Delay Time (secs)									
	60	120	180	240	300	360	420	480	540	600
0	88.5	84.7	86.5	85.7	87.0	87.4	85.8	88.1	87.5	87.0
0.05	135.3	128.1	127.9	125.6	128.3	128.6	127.0	129.5	125.6	126.9
0.1	135.5	128.5	127.0	127.2	127.0	128.1	125.7	129.2	127.8	125.9
0.15	134.8	127.9	127.7	124.6	127.0	126.5	127.3	128.1	127.6	125.9
0.2	134.7	128.1	125.2	125.9	125.9	128.4	127.0	129.0	127.2	125.1
0.25	134.4	128.4	124.7	125.4	124.5	126.7	126.3	129.6	128.7	125.6
0.3	134.3	128.9	124.9	126.1	125.7	127.1	125.9	129.7	128.5	126.1
0.35	134.2	129.3	125.4	126.4	126.4	128.0	125.6	129.7	128.9	126.4
0.4	133.9	129.7	126.6	126.4	126.0	127.7	127.0	130.0	129.0	126.2
0.45	133.8	130.0	126.0	127.5	126.5	128.1	127.3	129.9	129.5	126.3
0.5	133.7	130.0	126.5	128.0	127.4	128.6	127.9	129.6	129.7	126.6
0.55	133.6	130.4	127.1	128.5	127.8	129.1	128.0	129.9	129.6	126.2
0.6	133.5	130.7	127.9	128.8	127.9	129.3	127.8	130.1	129.6	127.0
0.65	133.4	130.7	127.6	128.3	128.3	128.6	127.8	130.5	129.4	126.6
0.7	133.3	130.8	127.7	128.5	128.1	128.9	127.6	130.6	129.4	126.6
0.75	133.3	130.6	128.5	129.0	128.0	128.9	127.8	130.8	129.8	127.1
0.8	133.2	130.6	128.7	129.0	128.6	129.5	127.9	131.1	129.9	127.5
0.85	133.1	130.7	128.9	129.3	128.4	129.0	127.9	131.0	129.8	127.1

Yaw Rate (deg/sec)	Delay Time (secs)									
	60	120	180	240	300	360	420	480	540	600
0.9	133.1	130.8	128.8	129.4	128.6	129.2	128.6	130.9	130.3	127.4
0.95	133.0	131.2	129.2	129.5	128.6	129.4	128.2	130.9	130.2	127.4
1	133.1	131.3	129.3	129.8	128.4	128.8	128.3	130.8	129.4	126.9
1.05	133.1	131.4	129.2	129.5	128.8	129.0	128.6	130.9	130.0	126.8
1.1	133.1	131.4	129.8	129.8	128.8	129.0	128.9	130.8	129.9	127.2
1.15	133.1	131.4	129.5	129.7	129.0	129.2	128.3	130.6	130.2	126.7
1.2	133.1	131.5	130.1	129.8	129.0	128.8	127.8	130.5	129.2	126.7
1.25	133.2	131.7	130.4	129.6	129.0	129.0	128.1	130.5	129.3	126.8
1.3	133.3	131.8	130.3	129.9	129.0	129.5	128.6	130.9	129.5	127.0
1.35	133.4	132.2	130.5	129.7	129.2	129.8	129.2	131.1	129.8	127.3
1.4	133.4	132.1	130.7	129.8	129.1	129.2	129.0	131.5	129.6	127.5
1.45	133.4	132.1	130.3	130.0	128.9	129.3	128.3	130.7	129.2	126.8
1.5	133.5	132.1	130.1	129.7	128.5	128.9	127.8	130.4	129.2	126.2
1.55	133.6	132.2	130.1	129.8	128.5	128.7	127.8	130.5	128.5	126.2
1.6	133.7	132.2	130.1	129.9	128.6	128.7	127.9	130.7	128.7	126.6
1.65	133.9	132.3	130.1	130.1	128.8	128.9	128.2	130.9	129.5	126.8
1.7	134.1	132.4	130.4	130.4	129.0	129.2	128.3	131.3	129.3	127.4
1.75	134.3	132.5	130.6	130.7	129.3	129.7	128.9	131.7	129.8	127.8
1.8	134.4	132.6	130.9	130.9	129.8	130.2	129.4	132.0	130.3	128.3
1.85	134.5	132.7	131.1	131.0	129.8	129.9	129.6	132.0	130.6	128.7
1.9	134.5	132.7	130.7	131.0	129.8	130.1	129.1	131.8	129.7	128.1
1.95	134.5	132.7	130.7	130.6	129.5	129.7	128.4	131.3	129.4	127.0
2	134.5	132.7	131.0	130.5	129.5	129.4	127.9	131.4	129.2	127.4

Table B.13 Energy (MWh) estimated by dynamic model for RG6 (1 min averaged data set)

Yaw Rate (deg/sec)	Delay Time (secs)									
	60	120	180	240	300	360	420	480	540	600
0	88.2	84.7	86.3	85.6	86.7	87.1	85.8	87.8	87.2	86.7
0.05	135.9	129.4	129.1	128.1	128.9	129.5	127.7	130.0	127.8	126.0
0.1	135.9	130.2	128.7	127.7	128.3	126.8	124.6	129.2	127.9	127.2
0.15	135.6	129.4	126.7	127.3	128.1	126.2	126.3	129.3	128.0	127.5
0.2	135.2	129.4	128.6	128.6	126.9	128.6	125.9	129.8	129.0	126.2
0.25	135.0	129.7	127.1	127.1	126.0	127.1	126.7	130.3	128.6	126.0
0.3	135.0	129.7	126.2	127.8	128.2	128.3	127.5	130.9	129.4	127.0
0.35	134.8	130.1	126.2	127.8	127.7	127.4	127.1	131.0	129.6	128.4
0.4	134.6	130.5	126.0	127.9	126.9	128.3	128.3	131.1	129.6	127.3
0.45	134.5	131.1	126.9	129.5	127.6	129.7	128.8	131.2	130.1	127.6
0.5	134.4	131.2	126.9	129.6	128.3	129.7	129.4	130.6	130.0	127.9
0.55	134.4	131.4	127.5	129.2	128.5	129.9	129.4	130.8	130.0	128.1

Yaw Rate (deg/sec)	Delay Time (secs)									
	60	120	180	240	300	360	420	480	540	600
0.6	134.4	131.7	128.5	130.0	129.3	129.9	129.1	131.1	130.2	128.2
0.65	134.3	131.7	129.6	130.4	129.5	129.7	129.2	131.5	130.1	128.4
0.7	134.2	131.7	128.9	130.2	129.2	129.6	129.3	131.4	130.3	128.1
0.75	134.1	131.7	129.6	130.5	129.2	129.6	129.4	131.7	130.5	128.2
0.8	134.1	131.8	129.8	130.5	129.3	130.1	129.8	132.0	130.8	128.6
0.85	134.1	132.0	130.2	130.8	129.4	129.9	130.3	131.9	130.9	128.2
0.9	134.0	132.0	130.6	131.2	129.7	130.0	130.5	132.5	131.4	128.6
0.95	134.0	132.4	130.7	131.4	129.6	130.2	130.3	132.0	130.8	128.3
1	134.0	132.4	130.6	131.2	129.5	130.0	130.3	131.8	130.9	127.8
1.05	134.0	132.5	130.7	131.1	129.7	130.0	130.4	132.0	130.4	127.9
1.1	134.0	132.4	130.9	131.1	130.0	130.3	130.8	132.2	131.0	128.4
1.15	134.0	132.5	130.9	131.0	129.8	130.2	130.4	132.0	130.9	127.8
1.2	134.1	132.6	131.2	131.0	129.6	130.0	130.2	131.5	130.4	127.8
1.25	134.2	132.7	131.1	131.0	129.9	130.2	130.4	132.0	130.2	127.9
1.3	134.3	132.8	131.3	131.0	130.2	130.3	130.7	132.6	130.7	128.4
1.35	134.3	133.0	131.4	131.0	130.7	130.5	131.0	132.5	130.6	129.0
1.4	134.4	133.1	131.9	130.9	130.6	130.8	130.8	132.5	131.3	128.9
1.45	134.4	133.1	131.4	131.4	130.3	130.1	130.2	132.1	130.6	128.5
1.5	134.4	133.1	131.4	131.3	129.6	130.0	129.3	131.6	129.9	127.5
1.55	134.5	133.1	130.9	130.9	129.4	129.8	129.6	131.9	129.3	127.0
1.6	134.7	133.2	131.0	131.0	129.5	129.9	129.8	132.1	129.4	127.3
1.65	134.9	133.3	131.1	131.2	129.7	130.2	130.1	132.3	129.8	127.7
1.7	135.1	133.4	131.3	131.5	130.0	130.7	130.4	132.8	130.0	128.1
1.75	135.3	133.5	131.6	131.9	130.3	131.0	131.0	133.2	130.8	128.6
1.8	135.4	133.6	132.0	132.1	130.7	131.4	131.6	133.7	131.0	129.3
1.85	135.5	133.7	132.0	132.2	130.8	131.9	131.8	133.8	131.4	129.9
1.9	135.5	133.7	131.7	132.3	130.8	131.4	131.0	133.5	131.2	129.6
1.95	135.5	133.7	131.8	131.8	130.9	130.4	130.7	132.7	131.0	128.7
2	135.5	133.8	131.8	131.9	130.8	130.4	130.3	132.3	130.5	128.6

Table B.14 Energy (MWh) estimated by dynamic model for RG1 (2 min averaged data set)

Yaw Rate (deg/sec)	Delay Time (secs)				
	120	240	360	480	600
0	56.6	55.5	56.7	55.6	56.5
0.05	80.6	78.9	79.5	77.4	79.8
0.1	80.9	79.0	78.3	75.4	79.6
0.15	81.4	80.0	78.6	77.8	78.6
0.2	81.7	80.2	80.4	78.1	79.5
0.25	81.9	80.7	80.4	80.2	79.8

Yaw Rate (deg/sec)	Delay Time (secs)				
	120	240	360	480	600
0.3	82.0	80.8	80.2	80.0	80.4
0.35	81.9	81.1	80.5	79.9	80.8
0.4	81.8	81.4	81.0	80.4	80.4
0.45	81.8	81.1	81.2	80.0	80.7
0.5	81.9	81.2	81.4	80.1	81.0
0.55	82.0	81.3	81.5	80.2	81.1
0.6	82.0	81.6	81.5	80.2	81.3
0.65	82.2	81.8	82.0	80.3	81.5
0.7	82.4	82.2	82.0	80.7	81.4
0.75	82.4	82.3	81.5	80.6	81.1
0.8	82.5	82.3	81.3	80.1	81.1
0.85	82.7	82.4	81.6	80.3	81.3
0.9	83.0	82.6	82.1	80.9	81.9
0.95	83.1	82.9	82.7	81.4	82.0
1	83.1	82.9	82.2	81.3	81.7
1.05	83.1	82.9	82.2	81.3	81.7
1.1	83.2	82.9	82.1	81.3	81.8
1.15	83.2	82.9	82.1	81.4	81.9
1.2	83.3	83.0	82.1	81.4	82.2
1.25	83.6	83.3	82.3	81.8	82.5
1.3	83.8	83.5	82.6	82.2	82.9
1.35	84.1	83.8	83.0	82.9	83.5
1.4	84.3	84.1	83.7	83.0	83.7
1.45	84.4	84.3	83.5	82.7	83.7
1.5	84.4	84.2	83.5	82.3	83.2
1.55	84.4	84.1	83.3	82.3	83.0
1.6	84.4	84.1	83.1	82.2	82.8
1.65	84.4	84.0	83.0	82.0	82.6
1.7	84.4	83.9	83.0	81.9	82.5
1.75	84.4	83.8	83.0	81.9	82.4
1.8	84.4	83.8	83.0	81.9	82.3
1.85	84.4	83.8	83.0	81.9	82.3
1.9	84.4	83.8	83.1	82.0	82.4
1.95	84.4	83.8	83.1	82.0	82.5
2	84.4	83.8	83.1	81.9	82.5

Table B.15 Energy (MWh) estimated by dynamic model for RG2 (2 min averaged data set)

Yaw Rate (deg/sec)	Delay Time (secs)				
	120	240	360	480	600
0	65.4	64.2	65.6	64.3	65.4

Yaw Rate (deg/sec)	Delay Time (secs)				
	120	240	360	480	600
0.05	89.4	86.8	87.5	85.4	86.5
0.1	89.7	87.5	88.6	84.2	87.9
0.15	90.4	88.4	87.7	86.5	87.2
0.2	90.5	88.8	89.7	87.8	89.1
0.25	90.7	89.1	89.3	87.2	89.1
0.3	90.8	89.2	89.2	88.6	89.8
0.35	90.8	89.6	89.2	88.8	89.9
0.4	90.9	90.1	89.9	89.0	89.5
0.45	91.0	90.2	90.2	88.8	89.6
0.5	91.2	89.9	90.4	88.8	90.0
0.55	91.3	89.9	90.5	88.8	89.7
0.6	91.3	90.4	90.4	88.9	90.0
0.65	91.5	90.6	91.1	89.1	89.7
0.7	91.7	91.0	91.4	89.5	90.0
0.75	91.8	91.2	90.7	89.5	89.9
0.8	91.9	91.2	90.7	88.9	89.6
0.85	92.1	91.4	91.0	89.2	89.7
0.9	92.4	91.6	91.4	89.8	90.2
0.95	92.5	91.8	91.8	90.2	90.5
1	92.5	91.9	91.3	90.2	90.5
1.05	92.6	91.8	91.3	90.3	90.1
1.1	92.6	91.8	91.2	90.2	90.1
1.15	92.6	91.8	91.3	90.3	90.2
1.2	92.7	91.9	91.4	90.3	90.8
1.25	92.9	92.2	91.7	90.7	91.1
1.3	93.2	92.4	92.0	91.2	91.5
1.35	93.5	92.7	92.4	91.8	92.1
1.4	93.7	93.1	93.0	92.0	92.6
1.45	93.8	93.3	92.9	91.6	92.2
1.5	93.8	93.2	92.8	91.1	91.9
1.55	93.8	93.2	92.6	91.1	91.5
1.6	93.8	93.1	92.4	91.0	91.5
1.65	93.8	93.0	92.3	90.9	91.3
1.7	93.8	92.9	92.2	90.8	91.1
1.75	93.8	92.9	92.2	90.7	91.0
1.8	93.8	92.8	92.3	90.7	91.0
1.85	93.8	92.8	92.3	90.8	91.0
1.9	93.8	92.8	92.4	90.9	91.1
1.95	93.8	92.8	92.4	90.8	91.2
2	93.8	92.8	92.4	90.9	91.2

Table B.16 Energy (MWh) estimated by dynamic model for RG3 (2 min averaged data set)

Yaw Rate (deg/sec)	Delay Time (secs)				
	120	240	360	480	600
0	80.1	78.2	80.2	78.3	79.9
0.05	109.4	106.8	107.7	103.4	105.6
0.1	110.1	108.1	107.6	103.1	107.0
0.15	110.6	109.3	109.0	106.0	108.9
0.2	111.0	109.6	108.7	106.7	108.7
0.25	110.9	109.8	108.2	107.7	109.4
0.3	110.8	109.9	108.2	108.0	109.7
0.35	110.9	110.2	109.7	107.5	110.2
0.4	111.0	110.5	109.4	108.2	109.7
0.45	111.2	110.7	110.2	109.1	109.8
0.5	111.2	110.5	111.1	108.9	109.7
0.55	111.4	110.7	111.4	108.8	109.7
0.6	111.5	110.8	111.3	109.1	110.1
0.65	111.7	111.2	111.7	109.0	110.4
0.7	112.0	111.5	111.3	109.1	110.1
0.75	112.1	111.6	111.1	109.3	110.0
0.8	112.2	111.6	111.2	109.1	110.1
0.85	112.5	111.8	111.5	109.4	110.4
0.9	112.8	112.0	112.0	109.9	110.9
0.95	113.0	112.2	112.2	110.6	111.0
1	113.0	112.2	112.3	110.3	110.1
1.05	113.0	112.2	112.2	110.2	110.3
1.1	113.0	112.2	112.2	110.1	110.4
1.15	113.1	112.2	112.3	110.3	110.4
1.2	113.3	112.4	112.5	110.3	111.2
1.25	113.6	112.7	112.9	110.6	111.7
1.3	113.9	113.0	113.3	110.9	112.3
1.35	114.2	113.3	113.8	111.5	112.7
1.4	114.4	113.6	114.0	111.7	113.2
1.45	114.5	114.0	113.1	111.3	112.7
1.5	114.5	113.8	113.3	111.4	112.7
1.55	114.5	113.7	112.9	111.3	112.3
1.6	114.5	113.6	112.7	111.2	112.2
1.65	114.5	113.5	112.6	111.2	112.0
1.7	114.5	113.4	112.5	111.2	111.9
1.75	114.5	113.3	112.5	111.1	111.8
1.8	114.5	113.2	112.6	111.1	111.8
1.85	114.5	113.2	112.7	111.2	111.8
1.9	114.5	113.2	112.9	111.2	111.8

Yaw Rate (deg/sec)	Delay Time (secs)				
	120	240	360	480	600
1.95	114.5	113.2	112.9	111.2	111.8
2	114.5	113.2	112.9	111.2	111.8

Table B.17 Energy (MWh) estimated by dynamic model for RG4 (2 min averaged data set)

Yaw Rate (deg/sec)	Delay Time (secs)				
	120	240	360	480	600
0	89.6	87.6	89.8	87.6	89.4
0.05	125.6	121.7	121.8	118.5	123.2
0.1	125.0	122.6	120.5	117.7	122.5
0.15	124.6	123.1	121.6	120.0	124.0
0.2	125.0	123.4	122.8	122.4	123.0
0.25	125.6	123.9	123.4	121.8	123.5
0.3	125.7	124.4	123.8	123.1	123.9
0.35	125.8	124.8	124.7	123.3	124.7
0.4	125.8	125.1	125.3	123.4	124.7
0.45	126.0	125.4	126.4	124.3	124.7
0.5	126.1	125.5	126.2	124.1	124.8
0.55	126.2	125.7	126.4	123.8	125.0
0.6	126.3	125.8	126.2	123.9	124.8
0.65	126.7	126.2	126.7	124.2	125.1
0.7	126.9	126.5	126.9	124.3	125.2
0.75	127.0	126.6	126.1	124.0	125.0
0.8	127.2	126.7	126.0	123.9	124.9
0.85	127.7	126.9	126.4	124.2	125.2
0.9	128.1	127.2	127.0	125.0	125.6
0.95	128.2	127.4	127.2	125.7	125.9
1	128.2	127.4	127.3	125.0	125.3
1.05	128.3	127.4	127.3	124.9	125.3
1.1	128.3	127.4	127.4	124.8	125.5
1.15	128.4	127.5	127.5	124.9	125.5
1.2	128.6	127.7	127.8	125.0	125.8
1.25	129.0	128.1	128.2	125.4	126.3
1.3	129.4	128.5	128.7	125.9	127.1
1.35	129.8	128.8	129.2	126.5	127.8
1.4	130.0	129.1	129.5	127.3	128.0
1.45	130.0	129.4	128.9	126.8	127.5
1.5	130.0	129.5	128.5	126.2	127.5
1.55	130.0	129.4	128.4	126.2	127.5
1.6	130.0	129.3	128.2	126.1	127.2

Yaw Rate (deg/sec)	Delay Time (secs)				
	120	240	360	480	600
1.65	130.0	129.2	128.1	126.0	127.1
1.7	130.0	129.1	128.0	126.0	127.0
1.75	130.0	129.1	127.9	126.0	126.9
1.8	130.0	129.0	128.0	126.0	126.9
1.85	130.0	129.0	128.2	126.0	126.9
1.9	130.0	129.0	128.3	126.1	126.9
1.95	130.0	129.0	128.3	126.2	126.9
2	130.0	129.0	128.3	126.2	126.9

Table B.18 Energy (MWh) estimated by dynamic model for RG5 (2 min averaged data set)

Yaw Rate (deg/sec)	Delay Time (secs)				
	120	240	360	480	600
0	94.1	92.1	94.3	92.2	93.9
0.05	137.8	132.6	132.1	131.1	129.8
0.1	136.8	132.4	130.9	130.4	133.6
0.15	136.4	133.0	130.5	130.0	134.0
0.2	136.2	133.6	131.9	131.5	134.0
0.25	136.2	134.3	133.3	131.6	133.6
0.3	136.1	134.5	133.8	133.6	133.6
0.35	136.2	134.9	133.8	133.3	134.2
0.4	136.3	135.2	134.6	134.0	134.5
0.45	136.6	135.5	135.9	134.2	134.1
0.5	136.6	135.5	135.8	134.1	134.4
0.55	136.8	135.7	136.1	134.4	134.5
0.6	136.9	136.0	136.3	134.1	134.2
0.65	137.1	136.2	136.6	134.6	134.9
0.7	137.3	136.4	136.6	134.5	135.2
0.75	137.4	136.4	136.2	134.2	134.4
0.8	137.6	136.5	135.9	134.1	134.5
0.85	138.0	136.7	136.3	134.3	135.2
0.9	138.3	137.0	136.9	134.9	136.2
0.95	138.4	137.0	137.2	135.5	136.3
1	138.4	137.1	137.5	134.6	135.5
1.05	138.4	137.1	137.5	135.0	136.2
1.1	138.5	137.1	137.5	134.8	135.4

Yaw Rate (deg/sec)	Delay Time (secs)				
	120	240	360	480	600
1.15	138.5	137.1	137.6	134.8	135.5
1.2	138.7	137.2	138.0	134.8	135.7
1.25	139.1	137.6	138.3	135.6	136.1
1.3	139.5	138.1	139.0	136.2	137.0
1.35	139.8	138.4	139.4	136.7	137.8
1.4	139.9	138.9	139.8	137.3	138.2
1.45	140.0	139.2	139.4	137.0	137.5
1.5	140.0	139.1	139.0	136.5	136.3
1.55	140.0	139.1	138.4	136.4	136.1
1.6	140.0	139.0	138.2	136.2	136.1
1.65	140.0	138.9	138.0	136.1	135.9
1.7	140.0	138.7	137.9	136.0	135.8
1.75	140.0	138.6	137.8	135.9	135.7
1.8	140.0	138.6	137.9	136.0	135.8
1.85	140.0	138.5	137.9	136.0	136.0
1.9	140.0	138.5	138.0	136.1	136.1
1.95	140.0	138.6	138.0	136.2	136.1
2	140.0	138.6	138.0	136.2	136.1

Table B.19 Energy (MWh) estimated by dynamic model for RG6 (2 min averaged data set)

Yaw Rate (deg/sec)	Delay Time (secs)				
	120	240	360	480	600
0	94.2	92.5	94.3	92.5	94.0
0.05	139.7	135.6	136.4	131.7	132.5
0.1	139.2	135.3	132.3	131.4	132.7
0.15	138.7	135.8	134.9	133.3	131.5
0.2	138.4	135.5	134.7	132.6	134.8
0.25	138.1	136.1	134.6	133.6	134.2
0.3	137.8	136.1	135.0	134.4	134.9
0.35	137.7	136.5	135.8	134.3	135.4
0.4	137.6	136.6	135.9	134.8	135.4
0.45	137.7	136.6	136.1	135.3	135.7
0.5	137.7	136.6	136.5	135.2	135.4
0.55	137.8	136.7	136.7	135.6	135.3
0.6	137.8	136.9	137.1	135.3	135.8
0.65	138.2	137.1	136.9	135.7	136.2
0.7	138.4	137.3	137.1	136.0	136.4
0.75	138.4	137.3	136.8	135.7	135.9
0.8	138.6	137.4	136.5	135.6	135.7

Yaw Rate (deg/sec)	Delay Time (secs)				
	120	240	360	480	600
0.85	138.9	137.7	136.9	135.8	136.2
0.9	139.2	138.0	137.6	136.4	136.9
0.95	139.3	138.2	138.0	136.9	137.1
1	139.3	138.3	137.8	136.0	137.1
1.05	139.4	138.3	137.8	136.4	136.9
1.1	139.4	138.2	137.9	136.3	137.0
1.15	139.5	138.3	138.0	136.3	137.0
1.2	139.7	138.5	138.3	136.2	137.2
1.25	140.0	138.8	138.9	137.0	137.9
1.3	140.4	139.3	139.5	137.7	138.5
1.35	140.7	139.6	139.8	138.0	138.9
1.4	140.9	139.8	140.1	138.1	139.6
1.45	140.9	140.1	139.8	137.9	139.3
1.5	140.9	140.0	139.4	137.7	137.7
1.55	140.9	140.0	139.2	137.5	137.8
1.6	140.9	139.9	139.0	137.3	137.7
1.65	140.9	139.8	138.8	137.2	137.5
1.7	140.9	139.7	138.7	137.1	137.4
1.75	140.9	139.6	138.6	137.1	137.4
1.8	140.9	139.5	138.7	137.1	137.4
1.85	140.9	139.5	138.8	137.2	137.5
1.9	140.9	139.5	138.8	137.3	137.6
1.95	140.9	139.5	138.9	137.3	137.6
2	140.9	139.5	138.9	137.3	137.6

Table B.20 Energy (MWh) estimated by dynamic model for RG1 (5 min averaged data set)

Yaw Rate (deg/sec)	Delay Time (secs)		Yaw Rate (deg/sec)	Delay Time (secs)	
	300	600		300	600
0	59.1	59.3	1.05	87.3	87.5
0.05	82.9	82.8	1.1	88.0	88.0
0.1	83.6	83.6	1.15	88.3	88.4
0.15	83.5	84.7	1.2	88.4	88.5
0.2	83.7	84.9	1.25	88.4	88.5
0.25	83.9	85.1	1.3	88.4	88.5
0.3	84.4	85.3	1.35	88.4	88.5
0.35	84.7	85.3	1.4	88.4	88.5
0.4	85.1	85.5	1.45	88.4	88.5
0.45	85.1	85.6	1.5	88.4	88.5
0.5	85.4	85.8	1.55	88.4	88.5
0.55	85.8	86.1	1.6	88.4	88.5

Yaw Rate (deg/sec)	Delay Time (secs)		Yaw Rate (deg/sec)	Delay Time (secs)	
	300	600		300	600
0.6	85.9	86.8	1.65	88.4	88.5
0.65	85.9	86.7	1.7	88.4	88.5
0.7	85.9	86.6	1.75	88.4	88.5
0.75	86.0	86.6	1.8	88.4	88.5
0.8	86.0	86.7	1.85	88.4	88.5
0.85	86.0	86.7	1.9	88.4	88.5
0.9	86.0	86.7	1.95	88.4	88.5
0.95	86.2	86.8	2	88.4	88.5
1	86.6	87.1			

Table B.21 Energy (MWh) estimated by dynamic model for RG2 (5 min averaged data set)

Yaw Rate (deg/sec)	Delay Time (secs)		Yaw Rate (deg/sec)	Delay Time (secs)	
	300	600		300	600
0	65.1	65.5	1.05	97.1	96.7
0.05	91.1	91.4	1.1	97.8	97.5
0.1	92.3	92.4	1.15	98.2	98.1
0.15	92.4	93.4	1.2	98.3	98.2
0.2	92.8	93.6	1.25	98.3	98.2
0.25	93.1	93.9	1.3	98.3	98.2
0.3	93.6	94.4	1.35	98.3	98.2
0.35	93.9	94.5	1.4	98.3	98.2
0.4	94.2	94.8	1.45	98.3	98.2
0.45	94.2	94.9	1.5	98.3	98.2
0.5	94.6	95.2	1.55	98.3	98.2
0.55	95.3	95.7	1.6	98.3	98.2
0.6	95.6	95.8	1.65	98.3	98.2
0.65	95.6	95.7	1.7	98.3	98.2
0.7	95.6	95.5	1.75	98.3	98.2
0.75	95.6	95.5	1.8	98.3	98.2
0.8	95.7	95.6	1.85	98.3	98.2
0.85	95.7	95.6	1.9	98.3	98.2
0.9	95.7	95.6	1.95	98.3	98.2
0.95	95.8	95.8	2	98.3	98.2
1	96.3	96.1			

Table B.22 Energy (MWh) estimated by dynamic model for RG3 (5 min averaged data set)

Yaw Rate (deg/sec)	Delay Time (secs)		Yaw Rate (deg/sec)	Delay Time (secs)	
	300	600		300	600
0	79.2	79.4	1.05	118.0	117.8
0.05	111.0	112.0	1.1	118.9	118.6
0.1	112.6	113.0	1.15	119.3	119.2
0.15	112.8	113.9	1.2	119.4	119.3
0.2	113.1	114.2	1.25	119.4	119.3
0.25	113.4	114.4	1.3	119.4	119.3
0.3	113.8	115.2	1.35	119.4	119.3
0.35	114.3	115.3	1.4	119.4	119.3
0.4	114.6	115.5	1.45	119.4	119.3
0.45	114.7	115.5	1.5	119.4	119.3
0.5	115.1	115.8	1.55	119.4	119.3
0.55	116.0	116.4	1.6	119.4	119.3
0.6	116.2	116.8	1.65	119.4	119.3
0.65	116.2	116.7	1.7	119.4	119.3
0.7	116.2	116.4	1.75	119.4	119.3
0.75	116.2	116.4	1.8	119.4	119.3
0.8	116.3	116.4	1.85	119.4	119.3
0.85	116.3	116.4	1.9	119.4	119.3
0.9	116.3	116.4	1.95	119.4	119.3
0.95	116.4	116.6	2	119.4	119.3
1	117.0	117.0			

Table B.23 Energy (MWh) estimated by dynamic model for RG4 (5 min averaged data set)

Yaw Rate (deg/sec)	Delay Time (secs)		Yaw Rate (deg/sec)	Delay Time (secs)	
	300	600		300	600
0	88.7	89.0	1.05	134.0	133.5
0.05	126.1	127.1	1.1	135.0	134.5
0.1	126.8	128.2	1.15	135.4	135.1
0.15	127.9	129.6	1.2	135.4	135.2
0.2	128.2	129.6	1.25	135.4	135.2
0.25	128.5	129.8	1.3	135.4	135.2
0.3	128.8	130.1	1.35	135.4	135.2
0.35	129.6	130.3	1.4	135.4	135.2
0.4	130.0	130.7	1.45	135.4	135.2
0.45	130.0	130.7	1.5	135.4	135.2
0.5	130.7	131.1	1.55	135.4	135.2
0.55	131.7	132.0	1.6	135.4	135.2
0.6	131.9	132.4	1.65	135.4	135.2
0.65	131.9	132.1	1.7	135.4	135.2
0.7	131.9	131.8	1.75	135.4	135.2
0.75	131.9	131.8	1.8	135.4	135.2

Yaw Rate (deg/sec)	Delay Time (secs)		Yaw Rate (deg/sec)	Delay Time (secs)	
	300	600		300	600
0.8	131.9	131.8	1.85	135.4	135.2
0.85	131.9	131.8	1.9	135.4	135.2
0.9	131.9	131.8	1.95	135.4	135.2
0.95	132.1	132.0	2	135.4	135.2
1	132.9	132.6			

Table B.24 Energy (MWh) estimated by dynamic model for RG5 (5 min averaged data set)

Yaw Rate (deg/sec)	Delay Time (secs)		Yaw Rate (deg/sec)	Delay Time (secs)	
	300	600		300	600
0	93.4	93.7	1.05	144.6	143.8
0.05	138.7	136.5	1.1	145.4	144.7
0.1	138.5	137.1	1.15	145.7	145.4
0.15	139.1	138.4	1.2	145.8	145.4
0.2	139.0	138.9	1.25	145.8	145.4
0.25	139.2	139.2	1.3	145.8	145.4
0.3	139.6	139.7	1.35	145.8	145.4
0.35	140.3	140.3	1.4	145.8	145.4
0.4	140.6	140.6	1.45	145.8	145.4
0.45	140.7	140.5	1.5	145.8	145.4
0.5	141.2	141.1	1.55	145.8	145.4
0.55	142.0	142.1	1.6	145.8	145.4
0.6	142.1	142.4	1.65	145.8	145.4
0.65	142.1	142.1	1.7	145.8	145.4
0.7	142.1	141.8	1.75	145.8	145.4
0.75	142.1	141.8	1.8	145.8	145.4
0.8	142.2	141.8	1.85	145.8	145.4
0.85	142.2	141.8	1.9	145.8	145.4
0.9	142.2	141.8	1.95	145.8	145.4
0.95	142.5	142.1	2	145.8	145.4
1	143.3	142.8			

Table B.25 Energy (MWh) estimated by dynamic model for RG6 (5 min averaged data set)

Yaw Rate (deg/sec)	Delay Time (secs)		Yaw Rate (deg/sec)	Delay Time (secs)	
	300	600		300	600
0	93.9	94.1	1.05	145.5	144.7
0.05	140.7	139.4	1.1	146.3	145.7
0.1	139.9	138.6	1.15	146.7	146.4
0.15	140.3	139.7	1.2	146.7	146.5
0.2	140.1	139.9	1.25	146.7	146.5

Yaw Rate (deg/sec)	Delay Time (secs)		Yaw Rate (deg/sec)	Delay Time (secs)	
	300	600		300	600
0.25	140.3	140.2	1.3	146.7	146.5
0.3	140.6	140.8	1.35	146.7	146.5
0.35	141.3	141.1	1.4	146.7	146.5
0.4	141.6	141.3	1.45	146.7	146.5
0.45	141.7	141.4	1.5	146.7	146.5
0.5	142.2	142.1	1.55	146.7	146.5
0.55	143.0	143.0	1.6	146.7	146.5
0.6	143.1	143.3	1.65	146.7	146.5
0.65	143.1	143.0	1.7	146.7	146.5
0.7	143.1	142.6	1.75	146.7	146.5
0.75	143.1	142.5	1.8	146.7	146.5
0.8	143.1	142.5	1.85	146.7	146.5
0.85	143.1	142.6	1.9	146.7	146.5
0.9	143.1	142.6	1.95	146.7	146.5
0.95	143.4	142.8	2	146.7	146.5
1	144.2	143.6			

Table B.26 Energy (MWh) estimated by dynamic model for RG1 (10 min averaged data set)

Yaw Rate (deg/sec)	Delay Time (secs)	Yaw Rate (deg/sec)	Delay Time (secs)
	600		600
0	58.4	1.05	88.5
0.05	82.6	1.1	88.5
0.1	83.1	1.15	88.5
0.15	83.9	1.2	88.5
0.2	84.8	1.25	88.5
0.25	85.3	1.3	88.5
0.3	86.3	1.35	88.5
0.35	86.3	1.4	88.5
0.4	86.3	1.45	88.5
0.45	86.3	1.5	88.5
0.5	86.8	1.55	88.5
0.55	88.1	1.6	88.5
0.6	88.5	1.65	88.5
0.65	88.5	1.7	88.5
0.7	88.5	1.75	88.5
0.75	88.5	1.8	88.5
0.8	88.5	1.85	88.5
0.85	88.5	1.9	88.5
0.9	88.5	1.95	88.5
0.95	88.5	2	88.5
1	88.5		

Table B.27 Energy (MWh) estimated by dynamic model for RG2 (10 min averaged data set)

Yaw Rate (deg/sec)	Delay Time (secs)	Yaw Rate (deg/sec)	Delay Time (secs)
	600		600
0	64.2	1.05	98.1
0.05	90.9	1.1	98.1
0.1	91.6	1.15	98.1
0.15	93.2	1.2	98.1
0.2	94.4	1.25	98.1
0.25	94.8	1.3	98.1
0.3	95.8	1.35	98.1
0.35	95.8	1.4	98.1
0.4	95.8	1.45	98.1
0.45	95.9	1.5	98.1
0.5	96.4	1.55	98.1
0.55	97.7	1.6	98.1
0.6	98.1	1.65	98.1
0.65	98.1	1.7	98.1
0.7	98.1	1.75	98.1
0.75	98.1	1.8	98.1
0.8	98.1	1.85	98.1
0.85	98.1	1.9	98.1
0.9	98.1	1.95	98.1
0.95	98.1	2	98.1
1	98.1		

Table B.28 Energy (MWh) estimated by dynamic model for RG3 (10 min averaged data set)

Yaw Rate (deg/sec)	Delay Time (secs)	Yaw Rate (deg/sec)	Delay Time (secs)
	600		600
0	77.8	1.05	119.6
0.05	110.9	1.1	119.6
0.1	111.8	1.15	119.6
0.15	113.8	1.2	119.6
0.2	114.9	1.25	119.6
0.25	115.5	1.3	119.6
0.3	116.7	1.35	119.6
0.35	116.8	1.4	119.6
0.4	116.8	1.45	119.6
0.45	116.8	1.5	119.6
0.5	117.5	1.55	119.6
0.55	119.2	1.6	119.6
0.6	119.6	1.65	119.6
0.65	119.6	1.7	119.6
0.7	119.6	1.75	119.6
0.75	119.6	1.8	119.6

Yaw Rate (deg/sec)	Delay Time (secs)	Yaw Rate (deg/sec)	Delay Time (secs)
	600		600
0.8	119.6	1.85	119.6
0.85	119.6	1.9	119.6
0.9	119.6	1.95	119.6
0.95	119.6	2	119.6
1	119.6		

Table B.29 Energy (MWh) estimated by dynamic model for RG4 (10 min averaged data set)

Yaw Rate (deg/sec)	Delay Time (secs)	Yaw Rate (deg/sec)	Delay Time (secs)
	600		600
0	87.3	1.05	135.9
0.05	127.5	1.1	135.9
0.1	127.6	1.15	135.9
0.15	129.5	1.2	135.9
0.2	130.7	1.25	135.9
0.25	131.4	1.3	135.9
0.3	132.7	1.35	135.9
0.35	132.7	1.4	135.9
0.4	132.7	1.45	135.9
0.45	132.8	1.5	135.9
0.5	133.7	1.55	135.9
0.55	135.5	1.6	135.9
0.6	135.9	1.65	135.9
0.65	135.9	1.7	135.9
0.7	135.9	1.75	135.9
0.75	135.9	1.8	135.9
0.8	135.9	1.85	135.9
0.85	135.9	1.9	135.9
0.9	135.9	1.95	135.9
0.95	135.9	2	135.9
1	135.9		

Table B.30 Energy (MWh) estimated by dynamic model for RG5 (10 min averaged data set)

Yaw Rate (deg/sec)	Delay Time (secs)	Yaw Rate (deg/sec)	Delay Time (secs)
	600		600
0	92.2	1.05	145.7
0.05	138.6	1.1	145.7
0.1	138.0	1.15	145.7

Yaw Rate (deg/sec)	Delay Time (secs)	Yaw Rate (deg/sec)	Delay Time (secs)
	600		600
0.15	139.2	1.2	145.7
0.2	140.2	1.25	145.7
0.25	141.0	1.3	145.7
0.3	142.1	1.35	145.7
0.35	142.1	1.4	145.7
0.4	142.2	1.45	145.7
0.45	142.4	1.5	145.7
0.5	143.4	1.55	145.7
0.55	145.4	1.6	145.7
0.6	145.7	1.65	145.7
0.65	145.7	1.7	145.7
0.7	145.7	1.75	145.7
0.75	145.7	1.8	145.7
0.8	145.7	1.85	145.7
0.85	145.7	1.9	145.7
0.9	145.7	1.95	145.7
0.95	145.7	2	145.7
1	145.7		

Table B.31 Energy (MWh) estimated by dynamic model for RG6 (10 min averaged data set)

Yaw Rate (deg/sec)	Delay Time (secs)	Yaw Rate (deg/sec)	Delay Time (secs)
	600		600
0	92.8	1.05	146.7
0.05	139.7	1.1	146.7
0.1	139.3	1.15	146.7
0.15	140.5	1.2	146.7
0.2	141.4	1.25	146.7
0.25	142.2	1.3	146.7
0.3	143.3	1.35	146.7
0.35	143.3	1.4	146.7
0.4	143.5	1.45	146.7
0.45	143.6	1.5	146.7
0.5	144.7	1.55	146.7
0.55	146.4	1.6	146.7
0.6	146.7	1.65	146.7

Yaw Rate (deg/sec)	Delay Time (secs)	Yaw Rate (deg/sec)	Delay Time (secs)
	600		600
0.65	146.7	1.7	146.7
0.7	146.7	1.75	146.7
0.75	146.7	1.8	146.7
0.8	146.7	1.85	146.7
0.85	146.7	1.9	146.7
0.9	146.7	1.95	146.7
0.95	146.7	2	146.7
1	146.7		

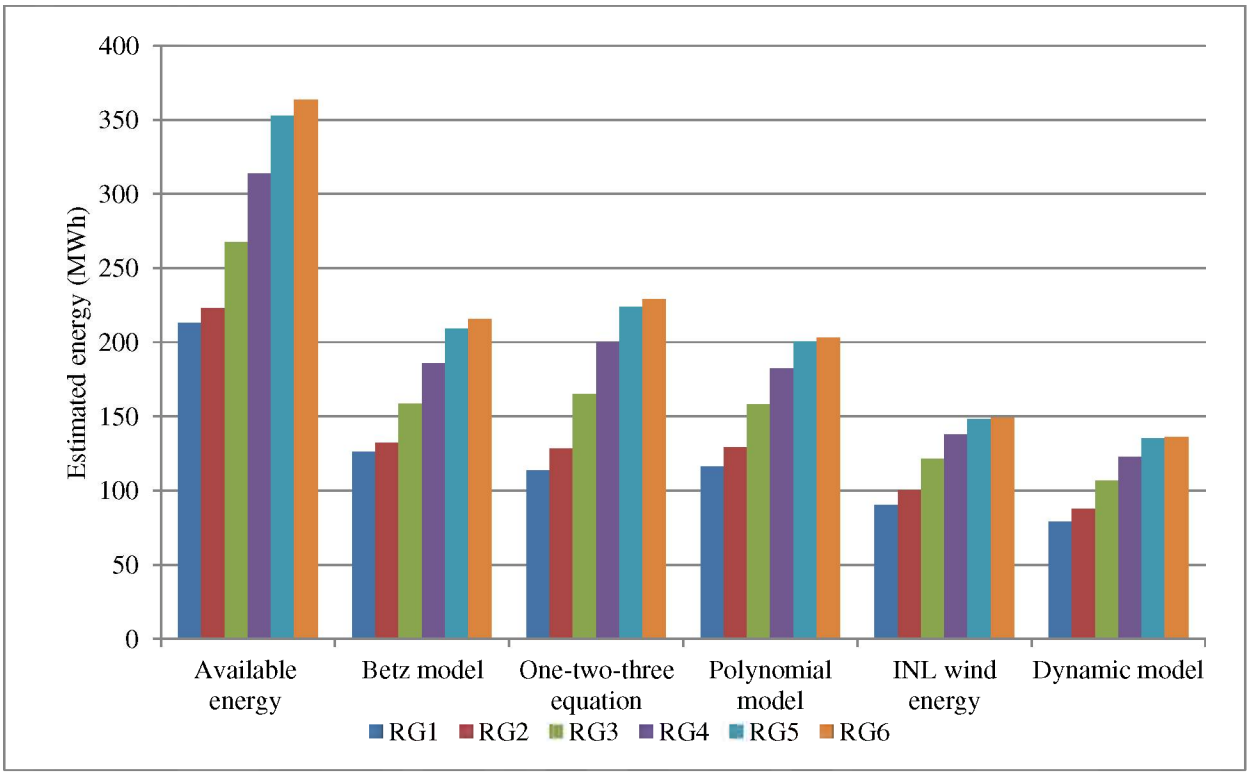

Figure B.1 Comparison of energy estimated by different models (1 min data set)

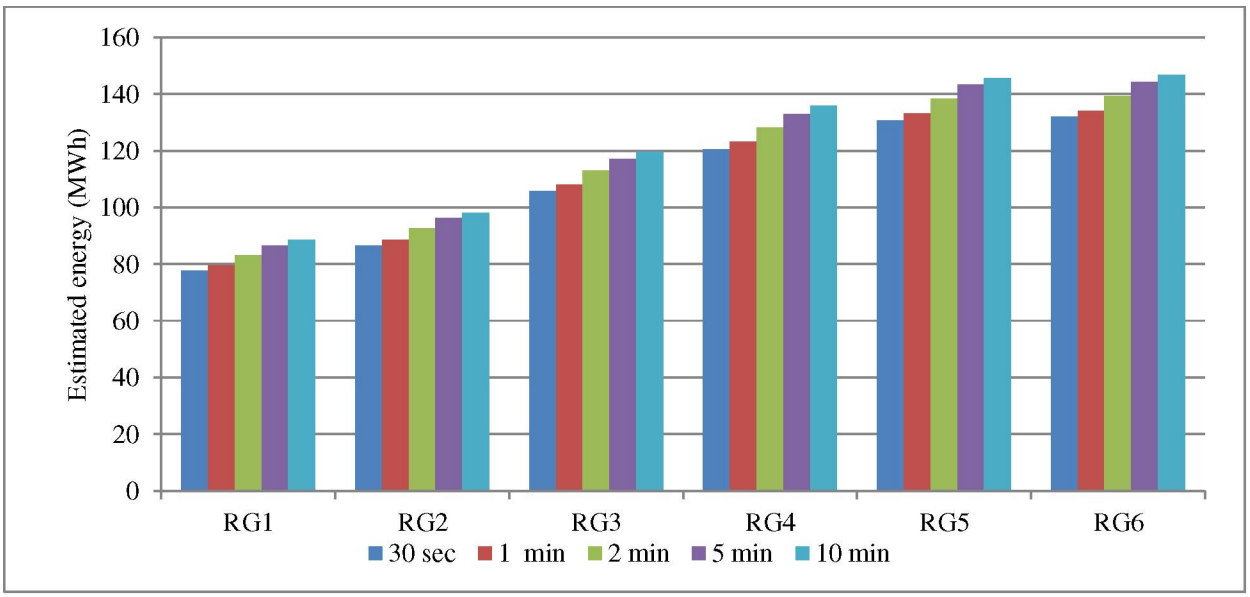

Figure B.2 Comparison of energy estimated by different frequency data sets (yaw rate 1 deg/sec)

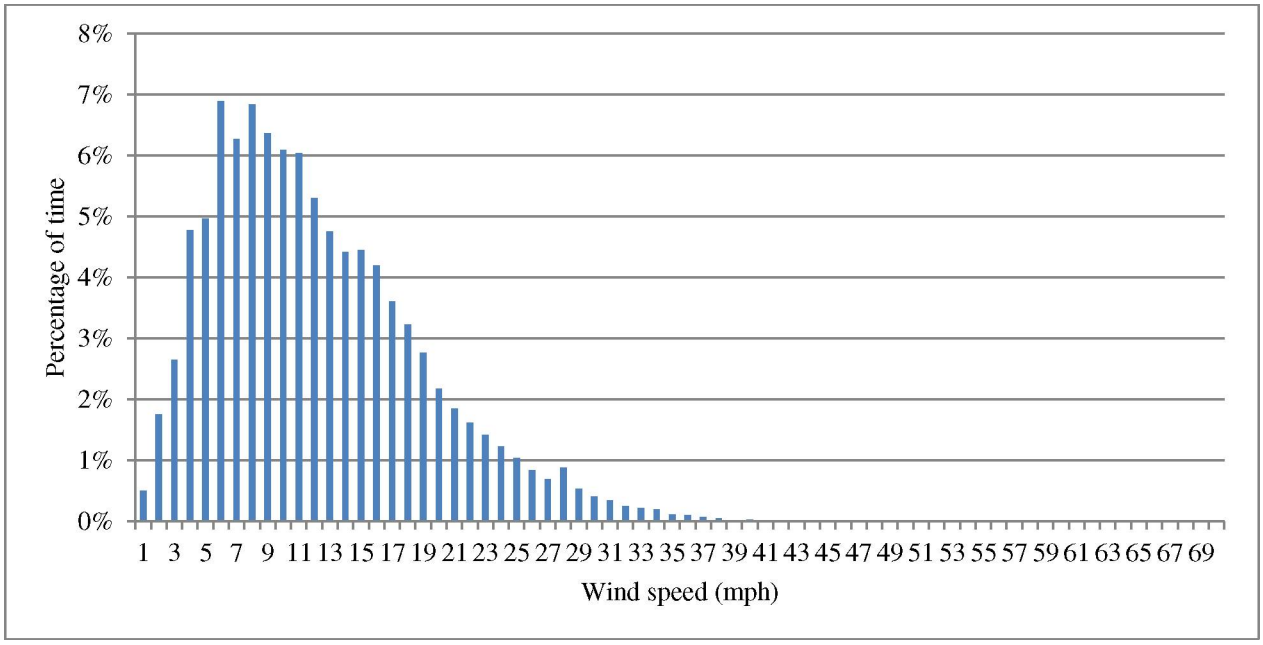

Figure B.3 Frequency distribution at RG1

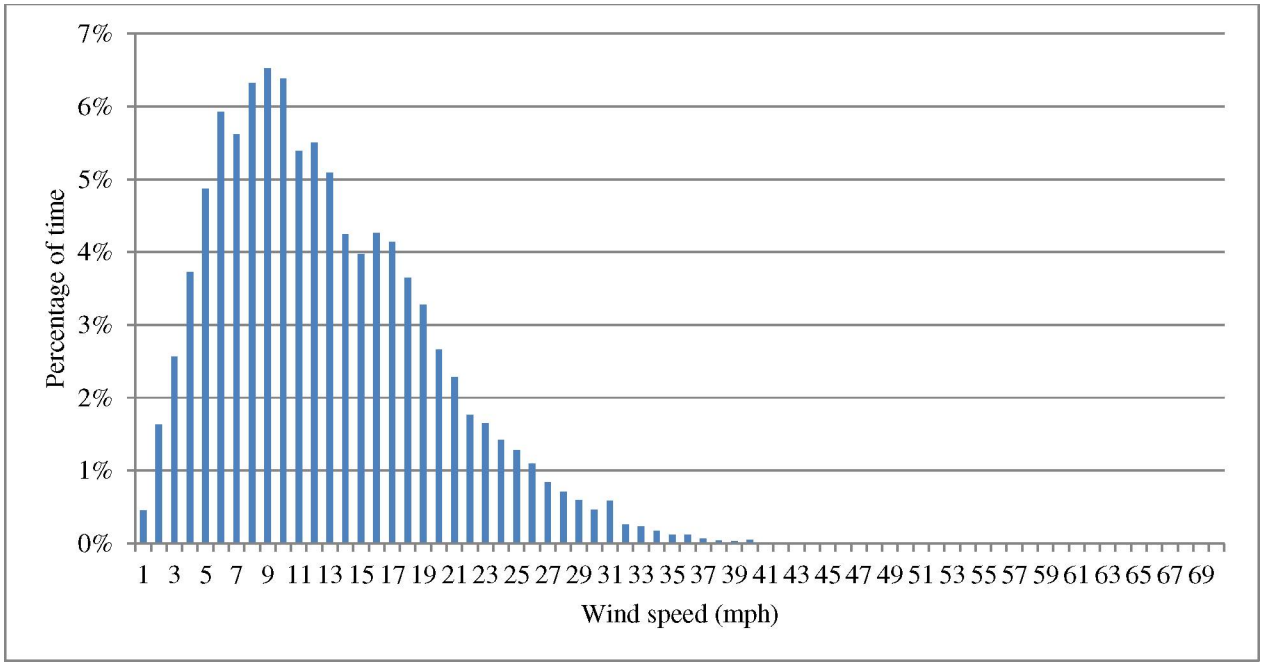

Figure B.4 Frequency distribution at RG2

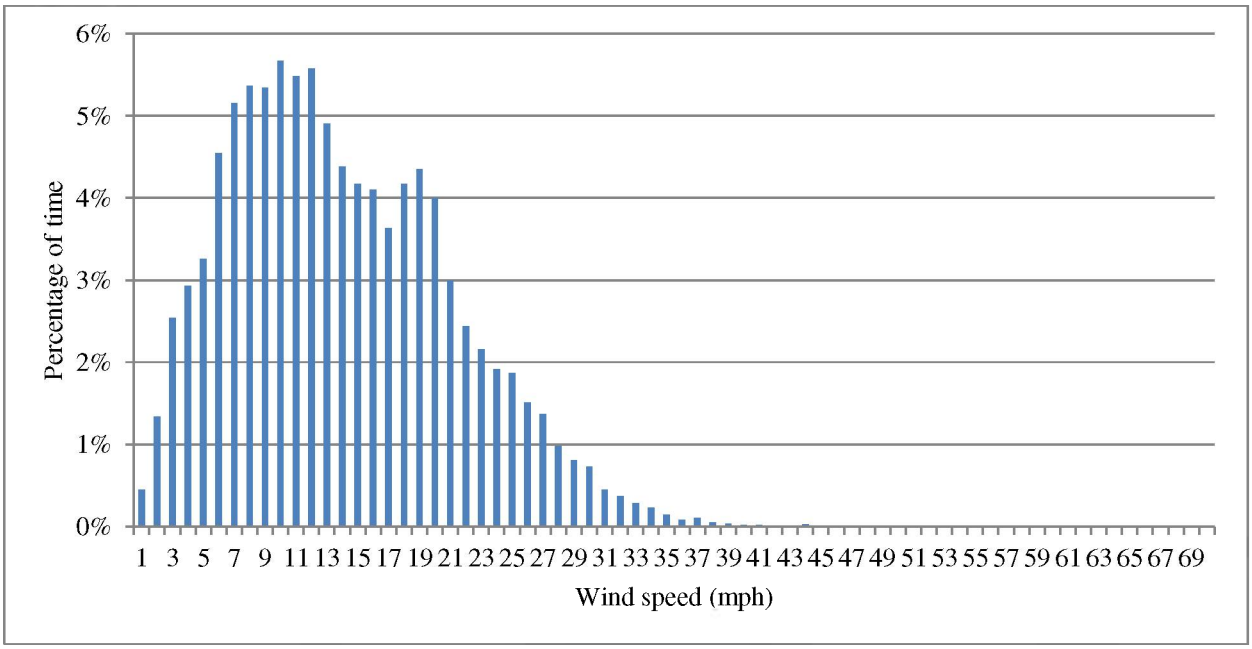

Figure B.5 Frequency distribution at RG3

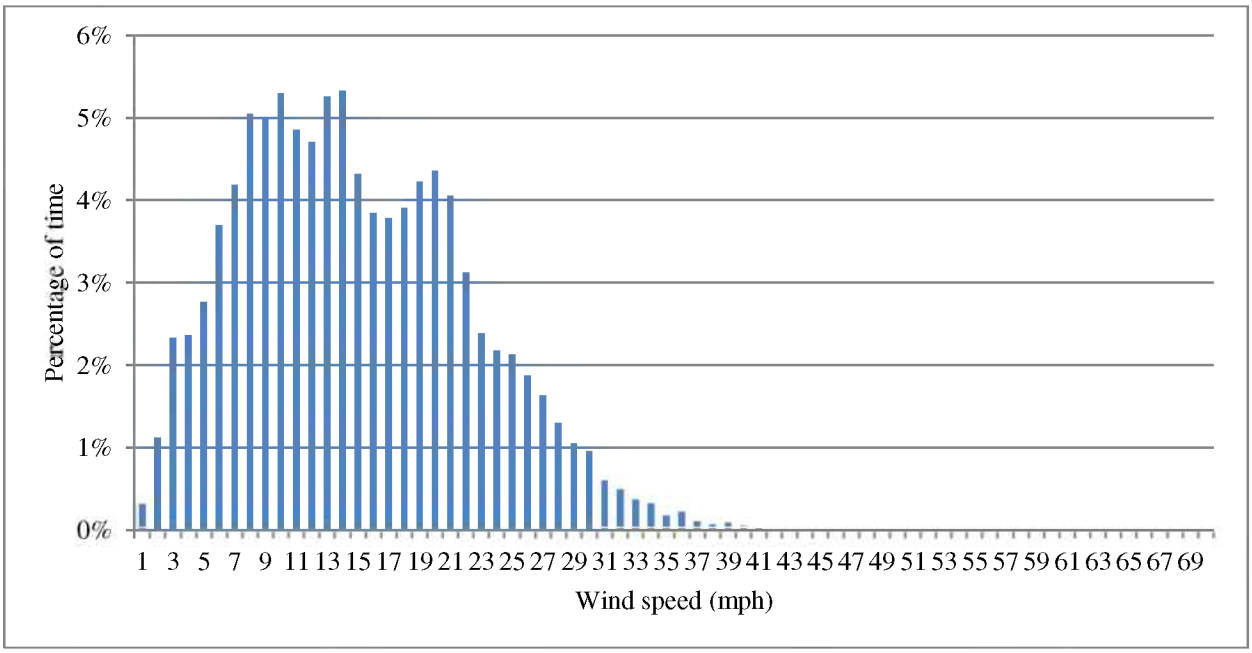

Figure B.6 Frequency distribution at RG4

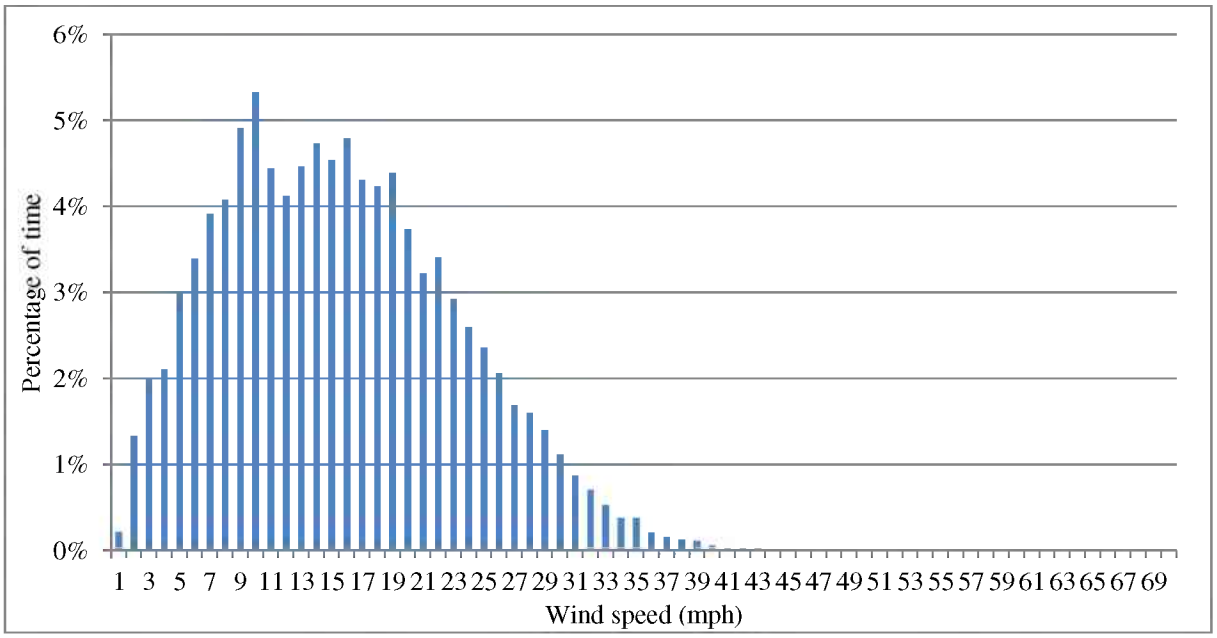

Figure B.7 Frequency distribution at RG5

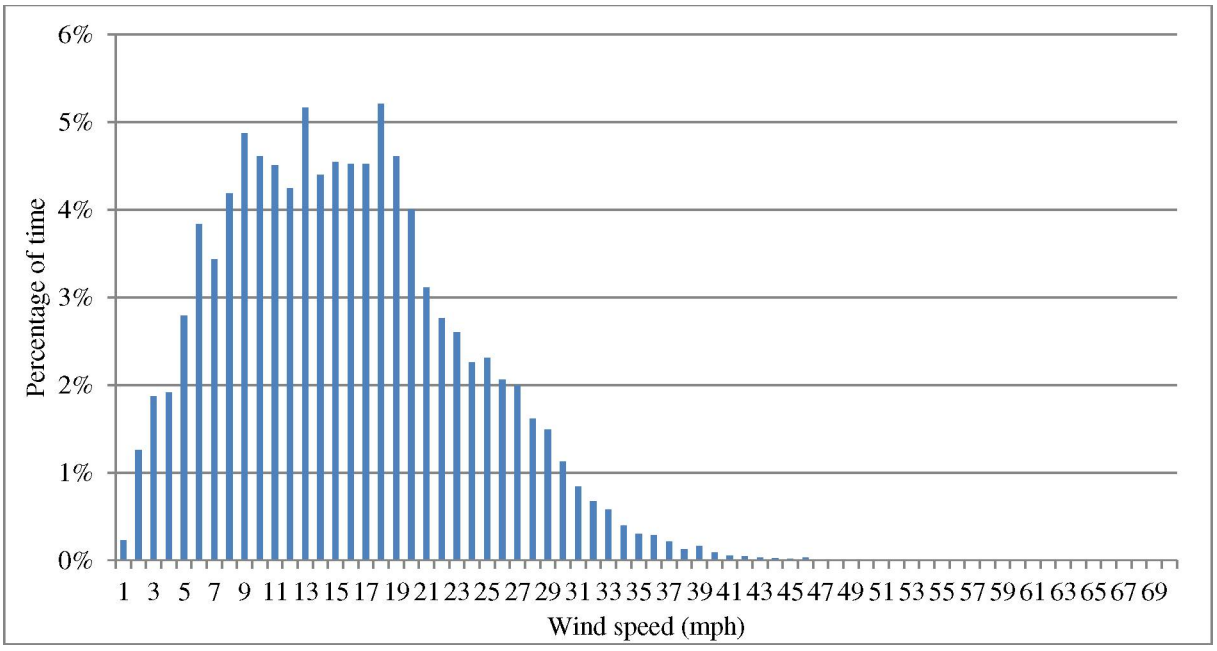

Figure B.8 Frequency distribution at RG6

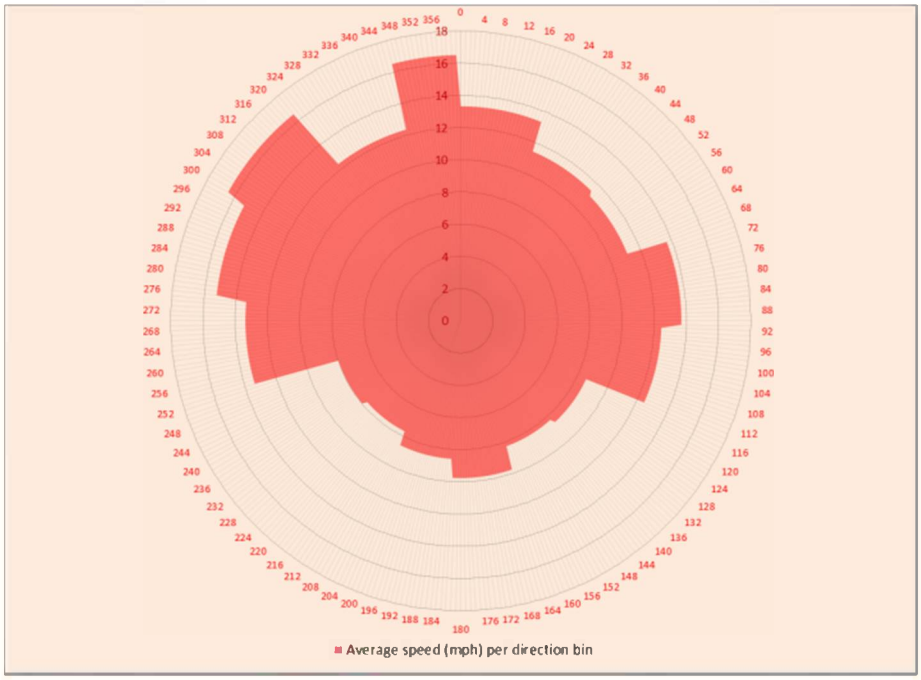

Figure B.9 Wind rose for average speed of RG1

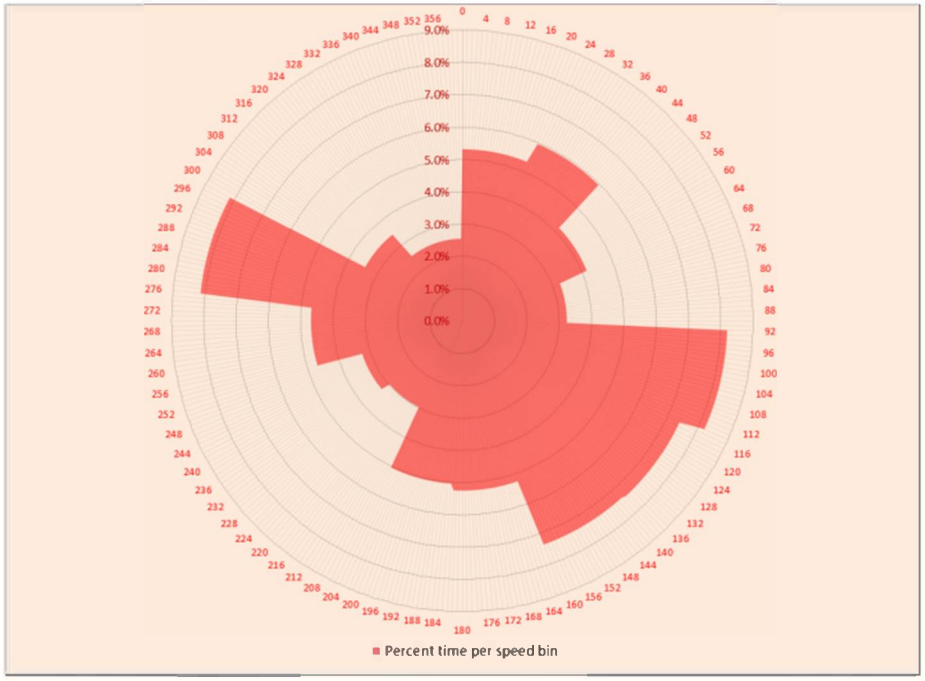

Figure B.10 Wind rose for percentage of time RG1

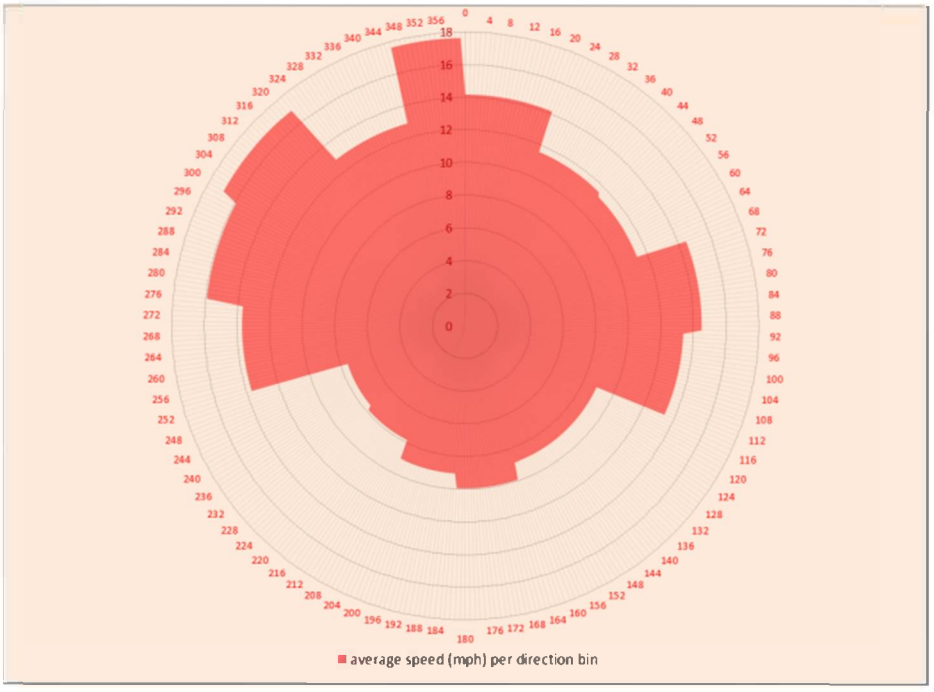

Figure B.11 Wind rose for average speed of RG2

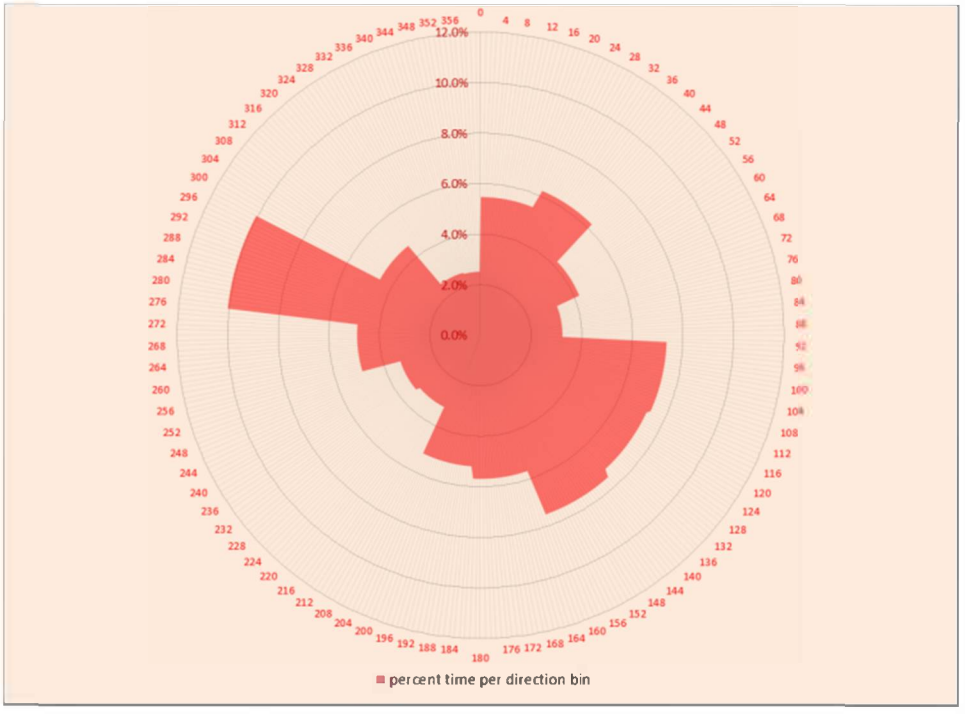

Figure B.12 Wind rose for percentage of time RG2

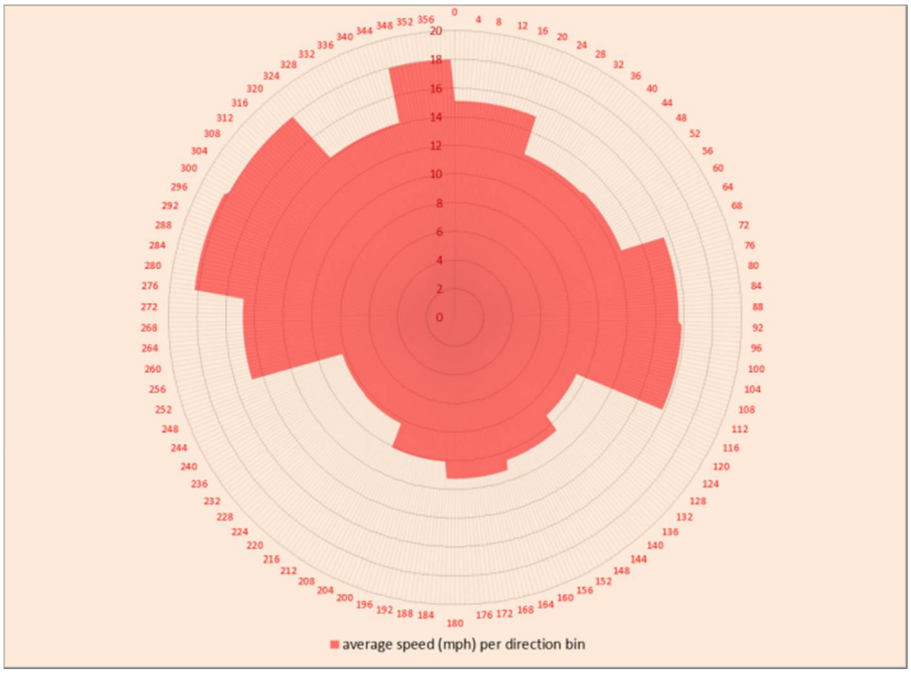

Figure B.13 Wind rose for average speed of RG3

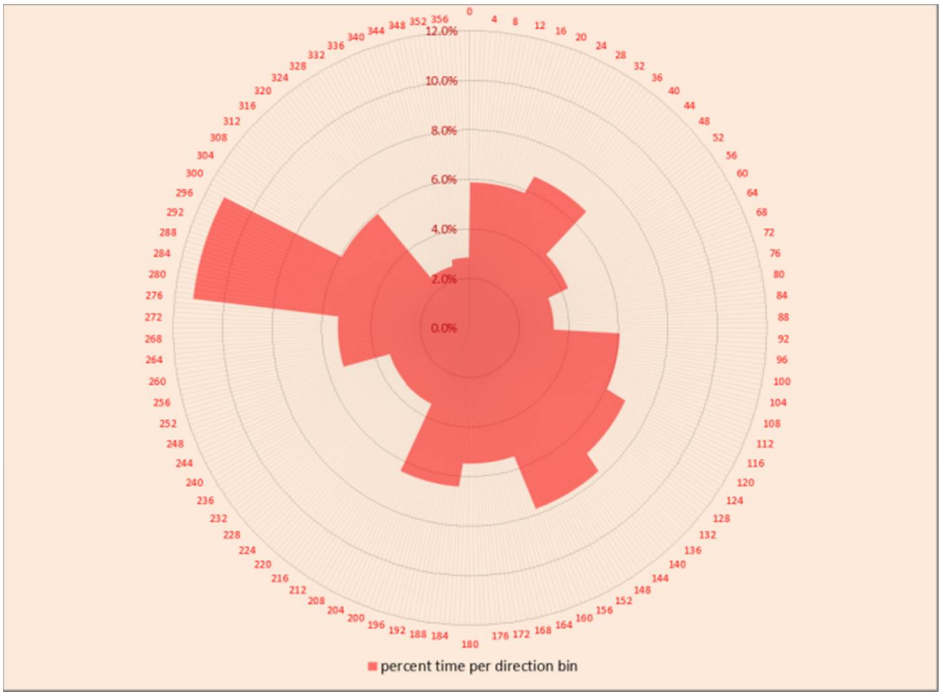

Figure B.14 Wind rose for percentage of time RG3

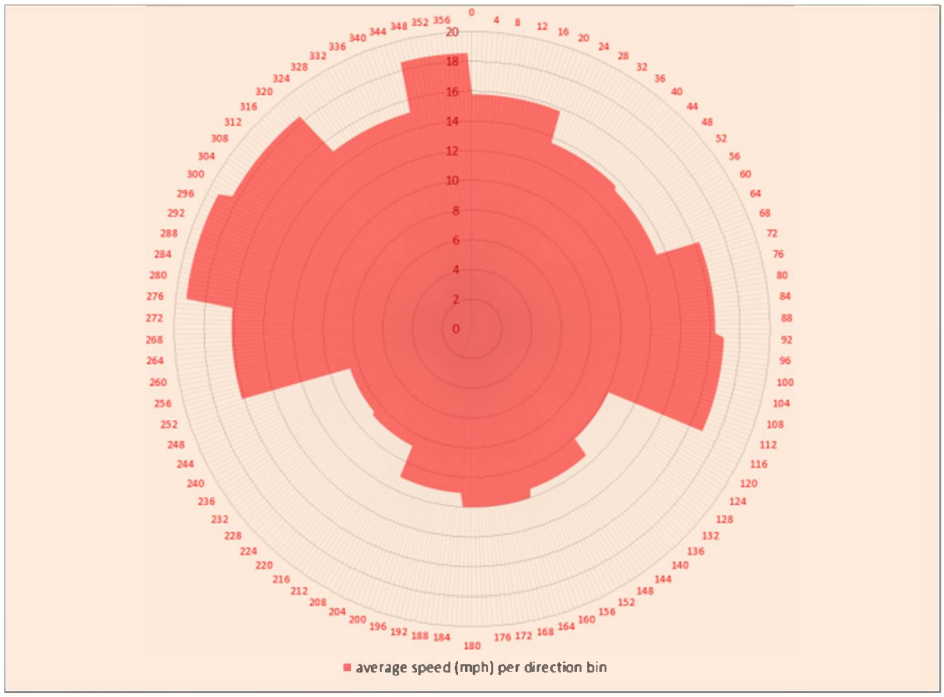

Figure B.15 Wind rose for average speed of RG4

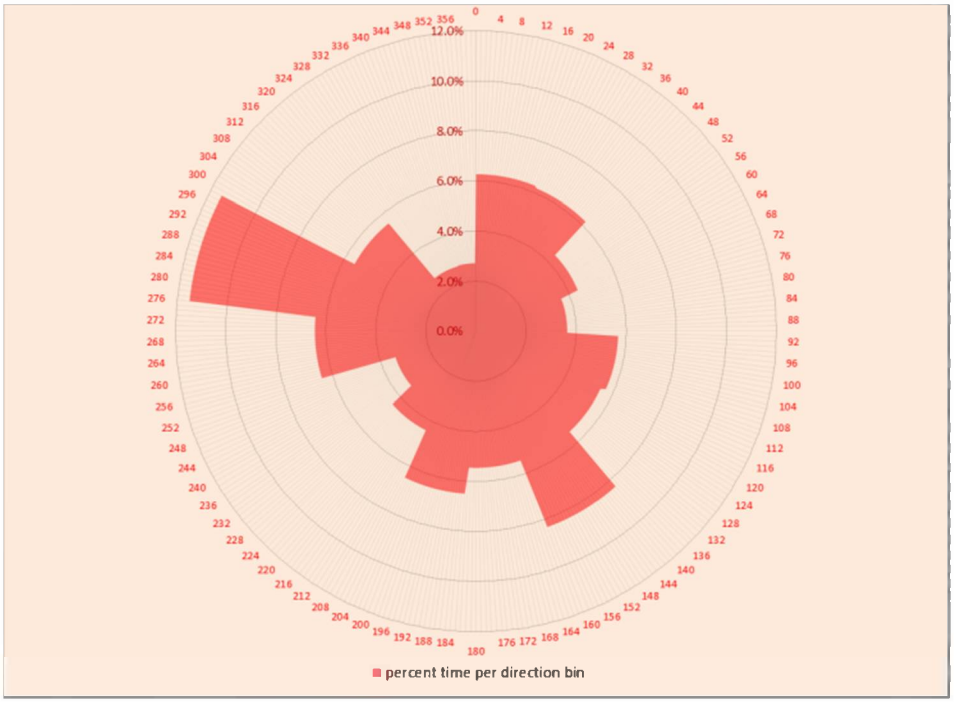

Figure B.16 Wind rose for percentage of time RG4

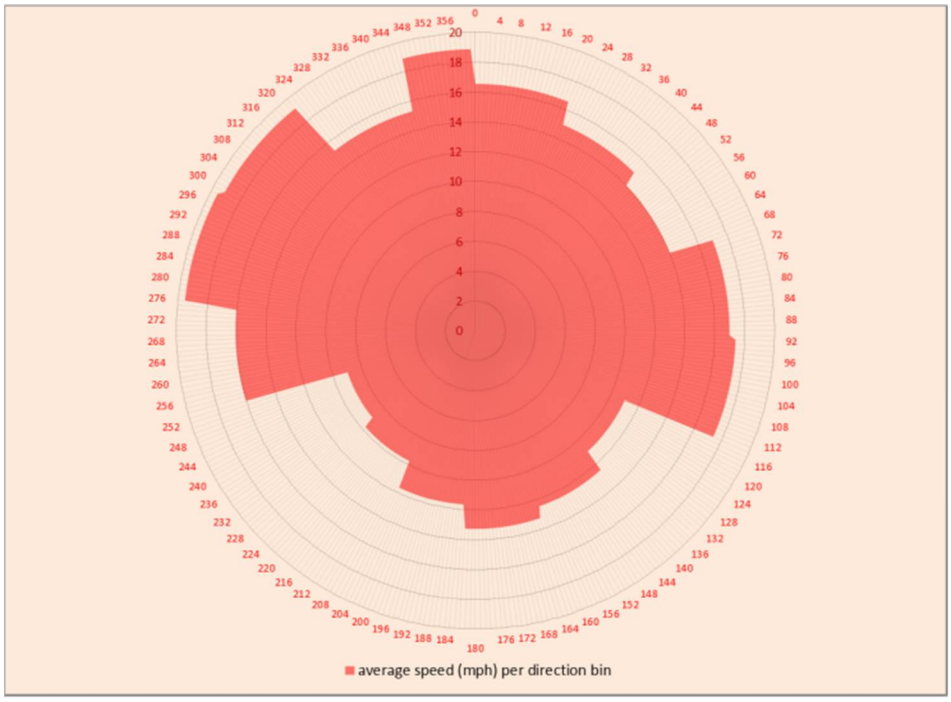

Figure B.17 Wind rose for average speed of RG5

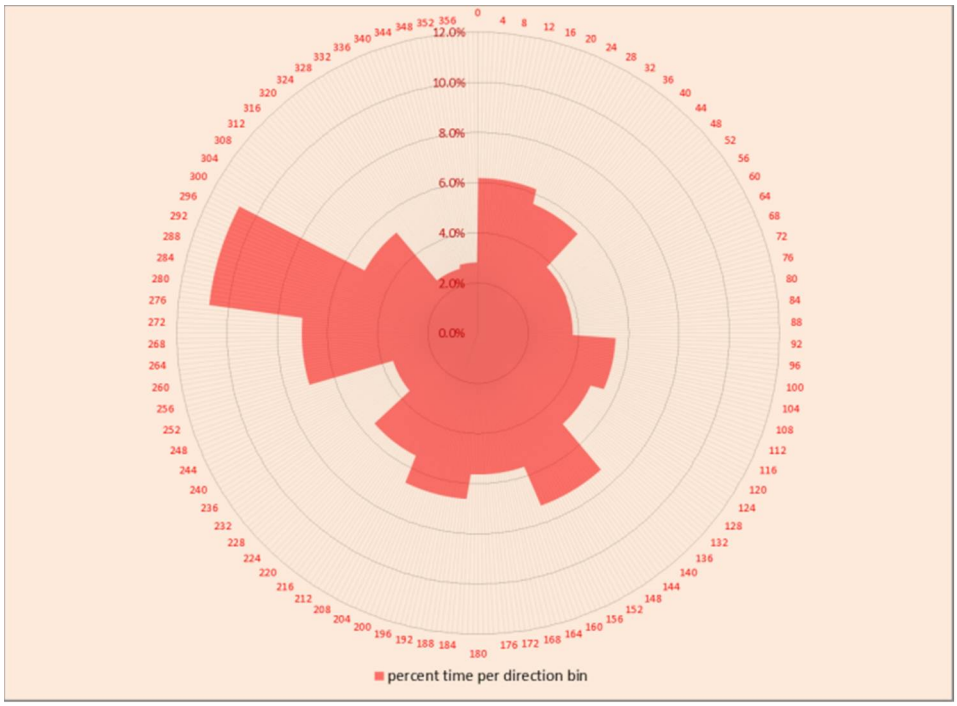

Figure B.18 Wind rose for percentage of time RG5

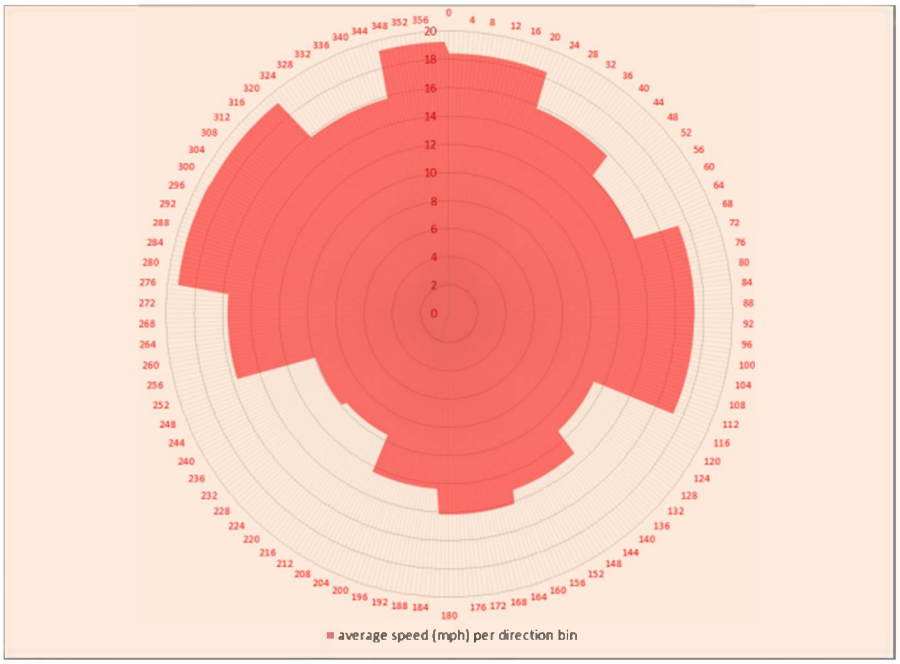

Figure B.19 Wind rose for average speed of RG6

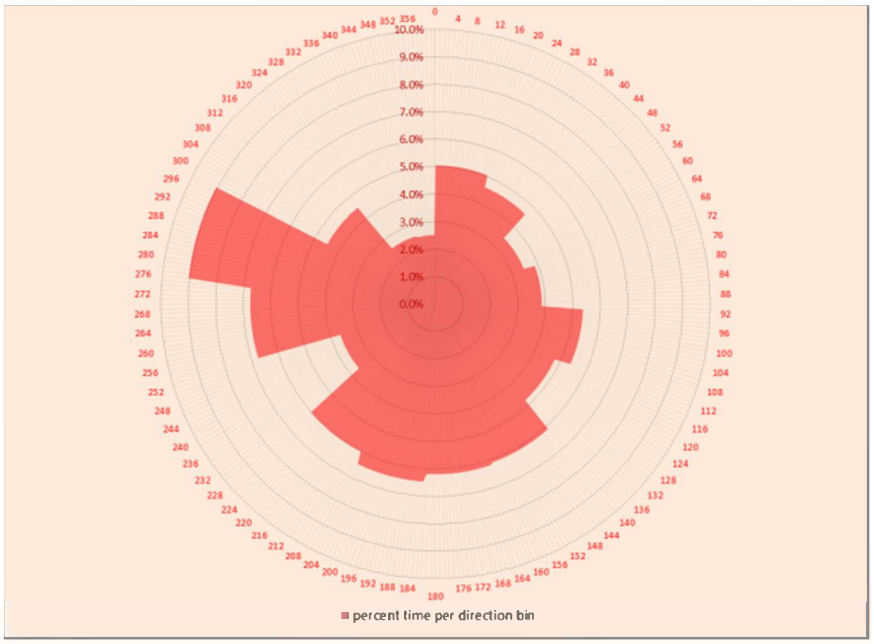

Figure B.20 Wind rose for percentage of time RG6

B.2 Lake Michigan (near shore) results

Table B.32 Summary of results of different range gates

Range Gate	Altitude (m)	Average wind speed (mph)	Energy output (MWh)	Capacity factor
RG1	55	18.42	496.257983	45.90%
RG2	60	18.41	570.131649	52.73%
RG3	75	19.00	636.239385	58.85%
RG4	90	19.45	673.605597	62.30%
RG5	110	19.49	680.455134	62.94%
RG6	120	19.68	662.845907	61.31%

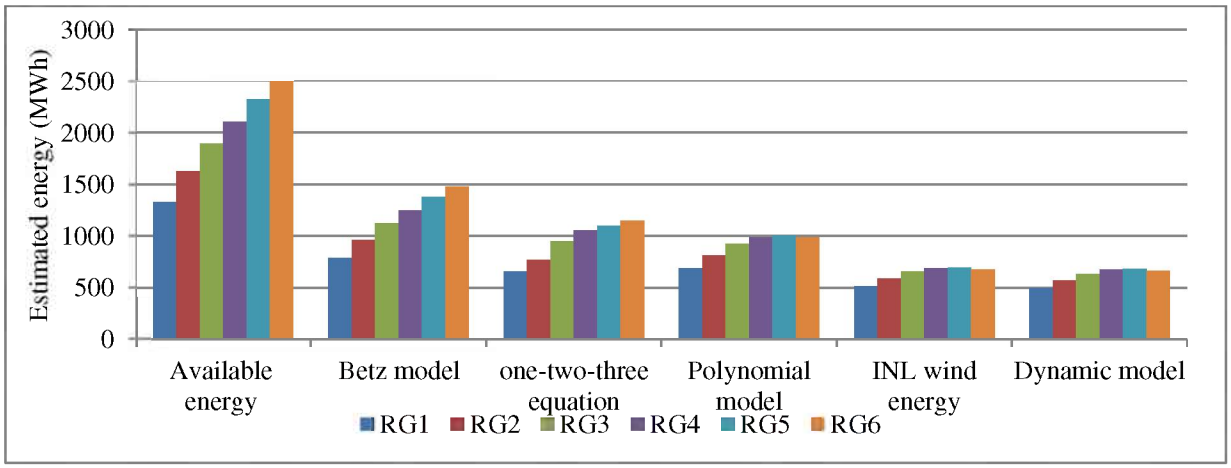

Figure B.21 Comparison of energy estimated by different models (1 min data set)

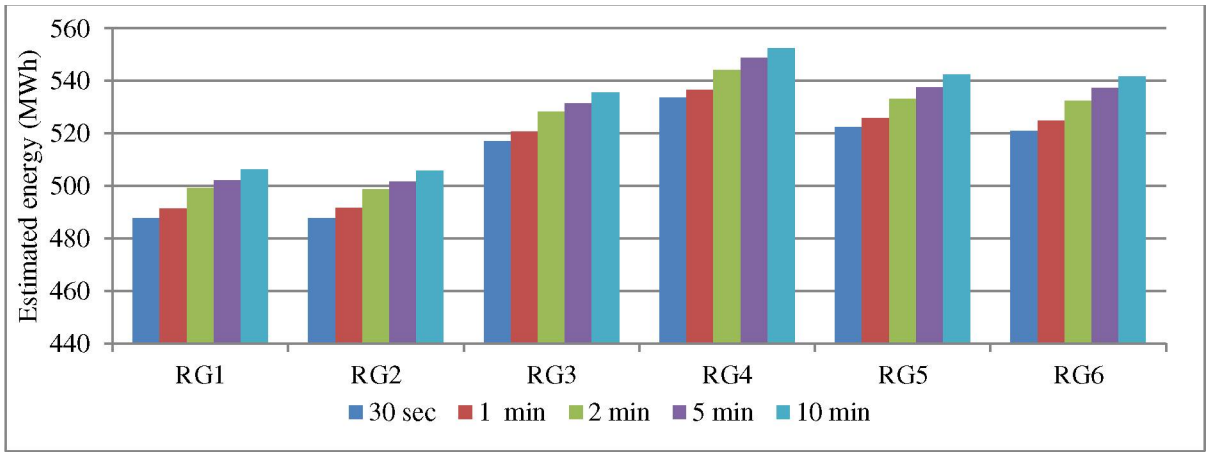

Figure B.22 Comparison of energy estimated by different frequency data sets (yaw rate 1 deg/sec)

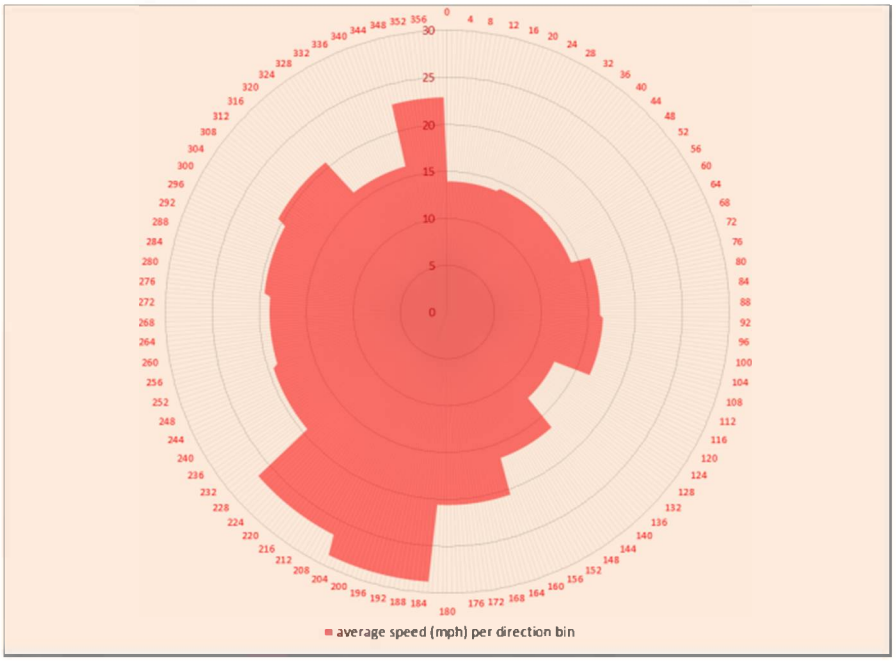

Figure B.23 Wind rose for average speed of RG4 (90 m)

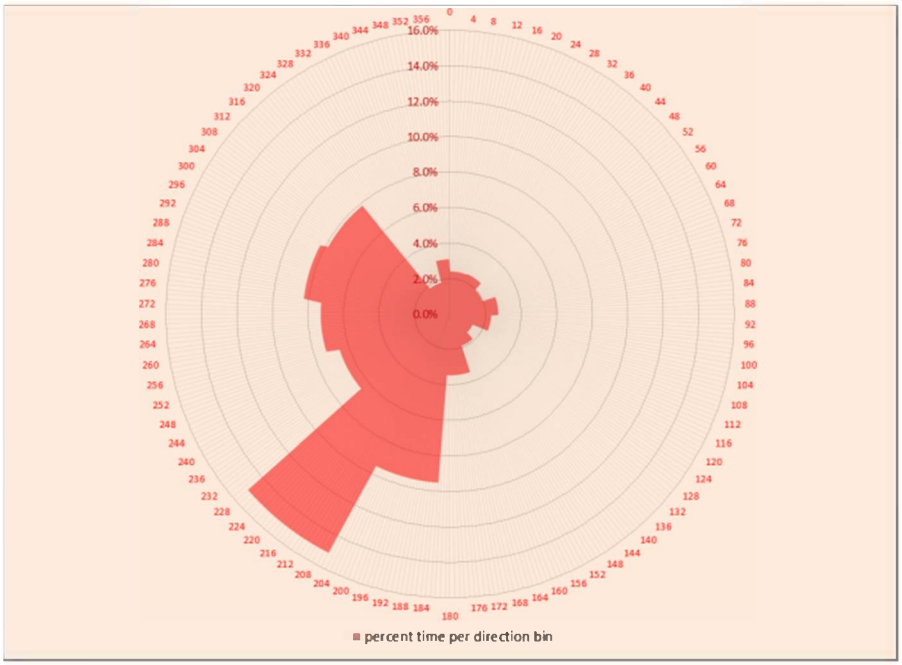

Figure B.24 Wind rose for percentage of time RG4 (90 m)

B.3 NOAA field station deployment results

Table B.33 Summary of results of different range gates

Range Gate	Altitude (m)	Average wind speed (mph)	Energy output (MWh)	Capacity factor
RG1	55	14.02	496.257983	19.62%
RG2	60	14.77	570.131649	22.54%
RG3	75	15.83	636.239385	25.15%
RG4	90	16.40	673.605597	26.63%
RG5	110	16.61	680.455134	26.90%
RG6	120	16.85	662.845907	26.20%

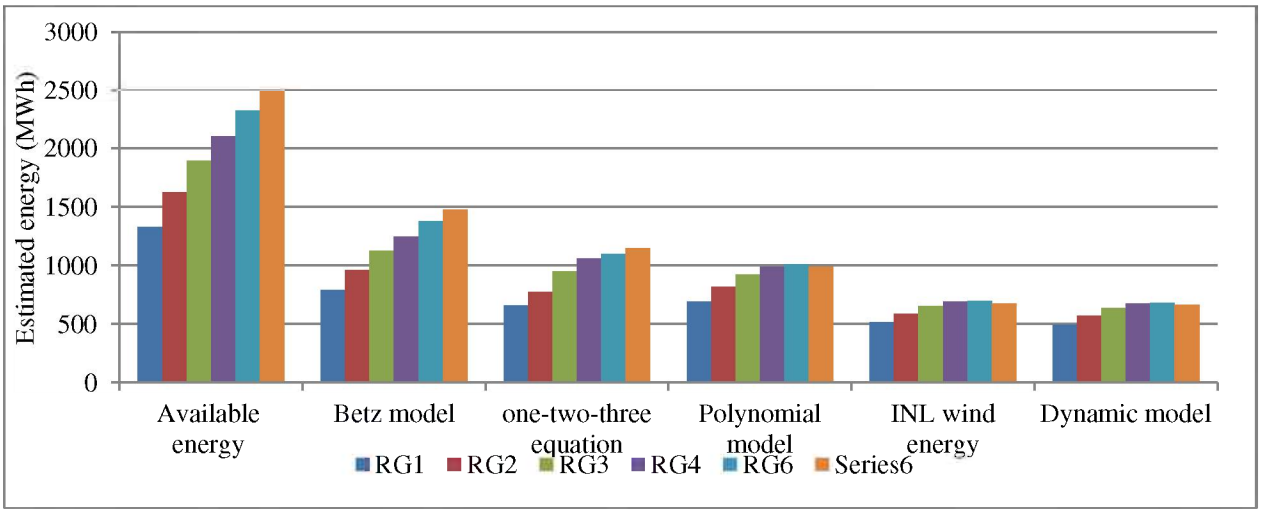

Figure B.25 Comparison of energy estimated by different models (1 min data set)

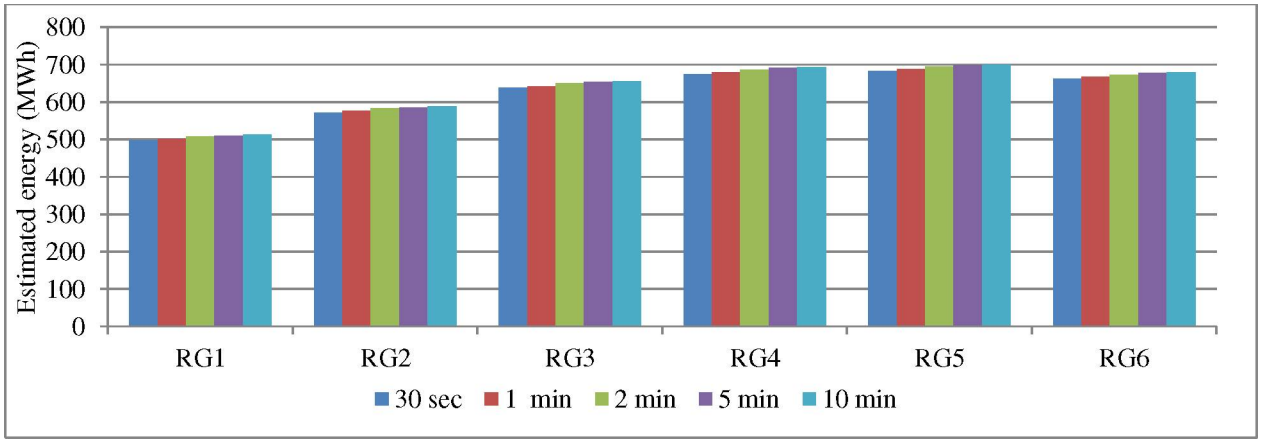

Figure B.26 Comparison of energy estimated by different frequency data sets (yaw rate 1 deg/sec)

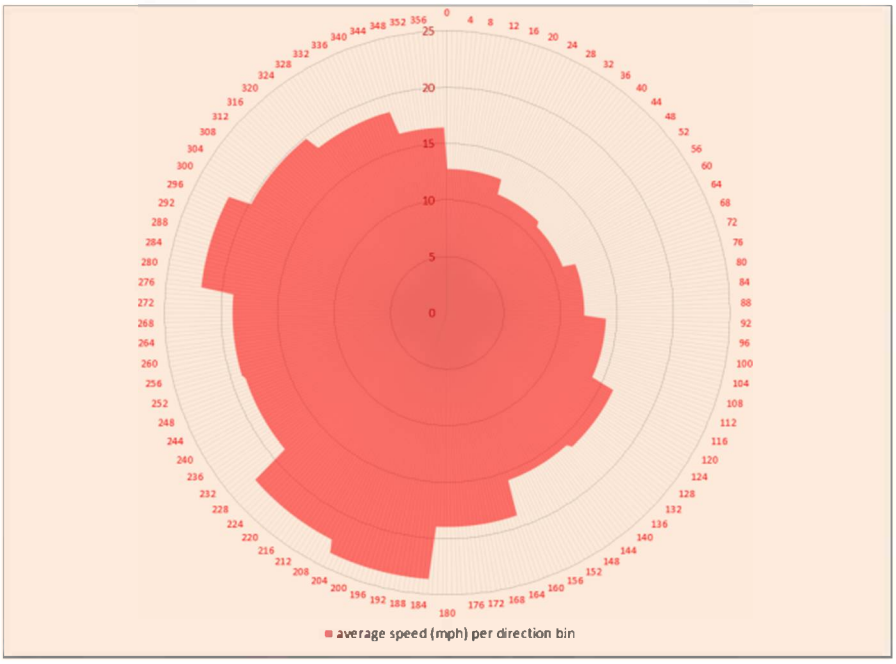

Figure B.27 Wind rose for average speed of RG4 (90 m)

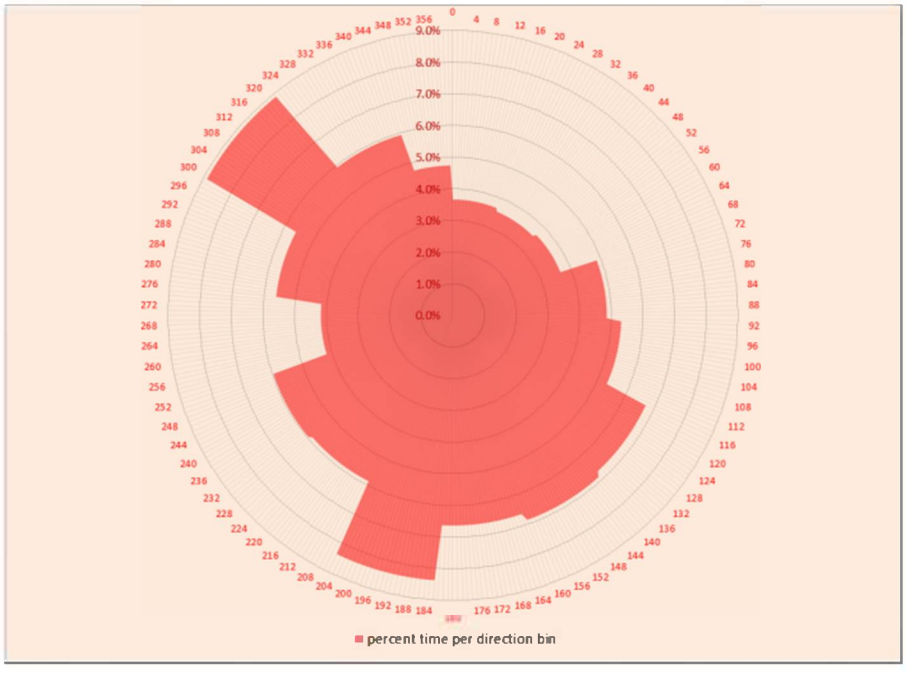

Figure B.28 Wind rose for percentage of time RG4 (90 m)

B.4 Mid-lake Plateau deployment results

Table B.34 Summary of results of different range gates

Range Gate	Altitude (m)	Average wind speed (mph)	Energy output (MWh)	Capacity factor
RG1	75	19.07	1707.732224	37.9%
RG2	90	19.64	1786.540252	39.3%
RG3	105	19.83	1805.26632	39.7%
RG4	125	19.55	1754.083151	38.5%

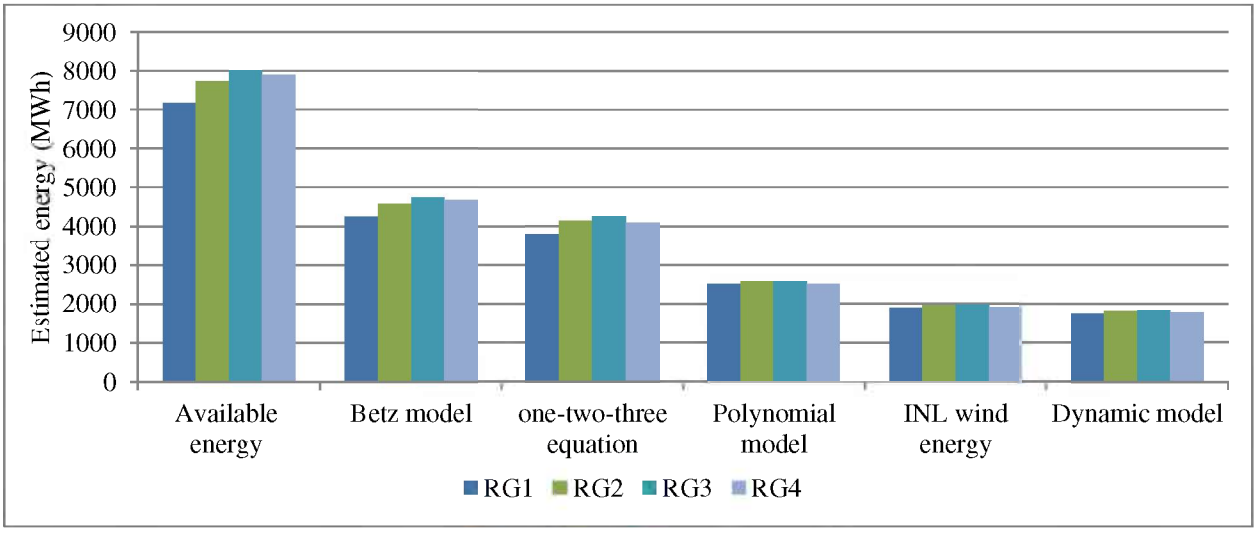

Figure B.29 Comparison of energy estimated by different models at mid-lake deployment (1 min data set)

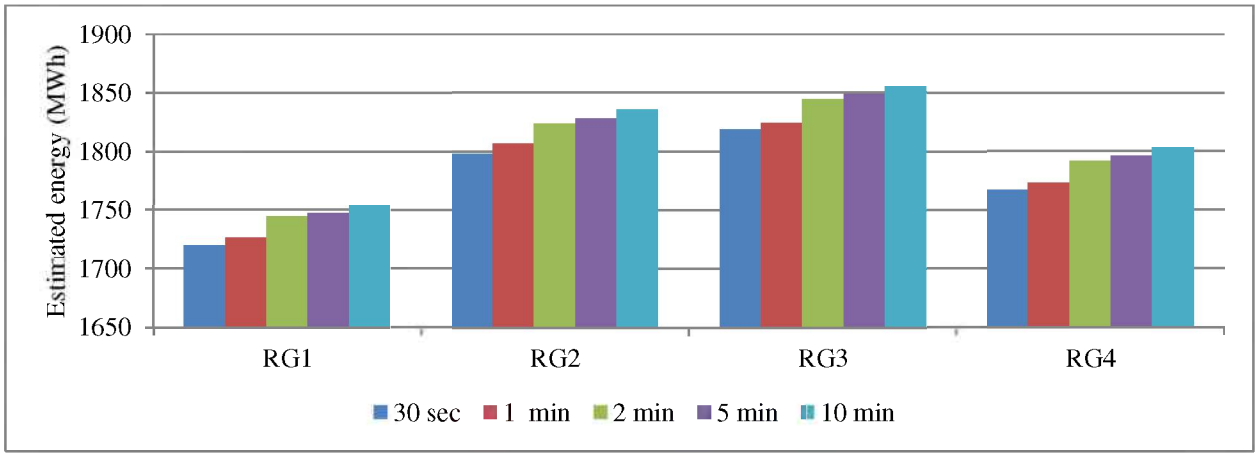

Figure B.30 Comparison of energy estimated by different frequency data sets (yaw rate 1 deg/sec)

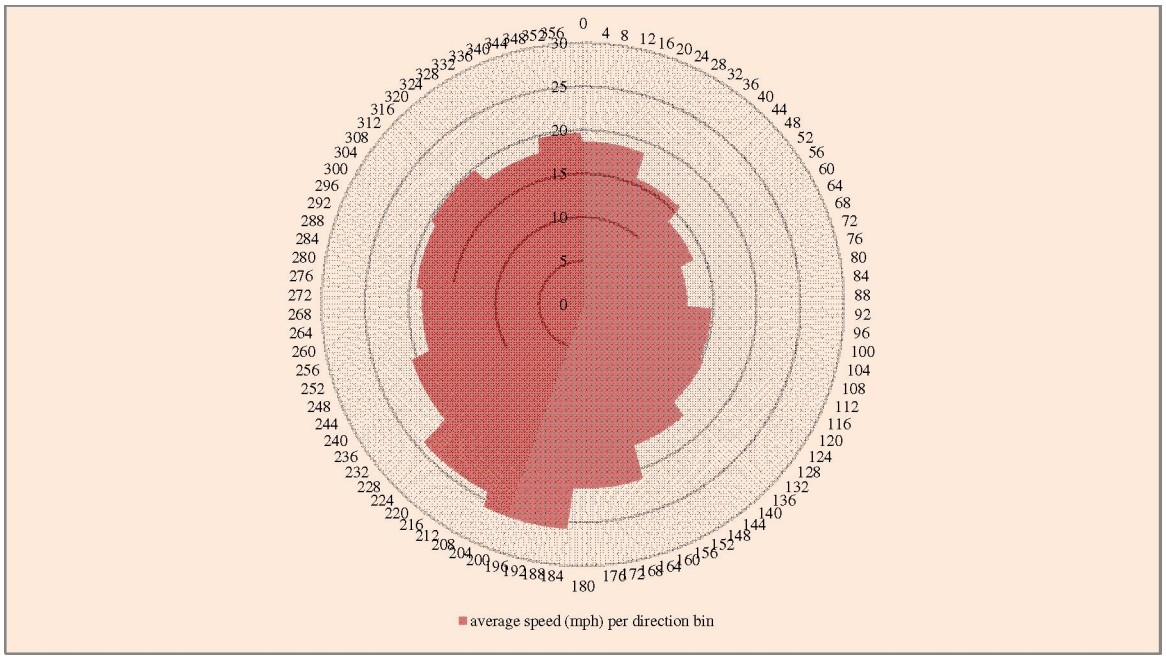

Figure B.31 Wind rose for average speed of RG2 (90 m)

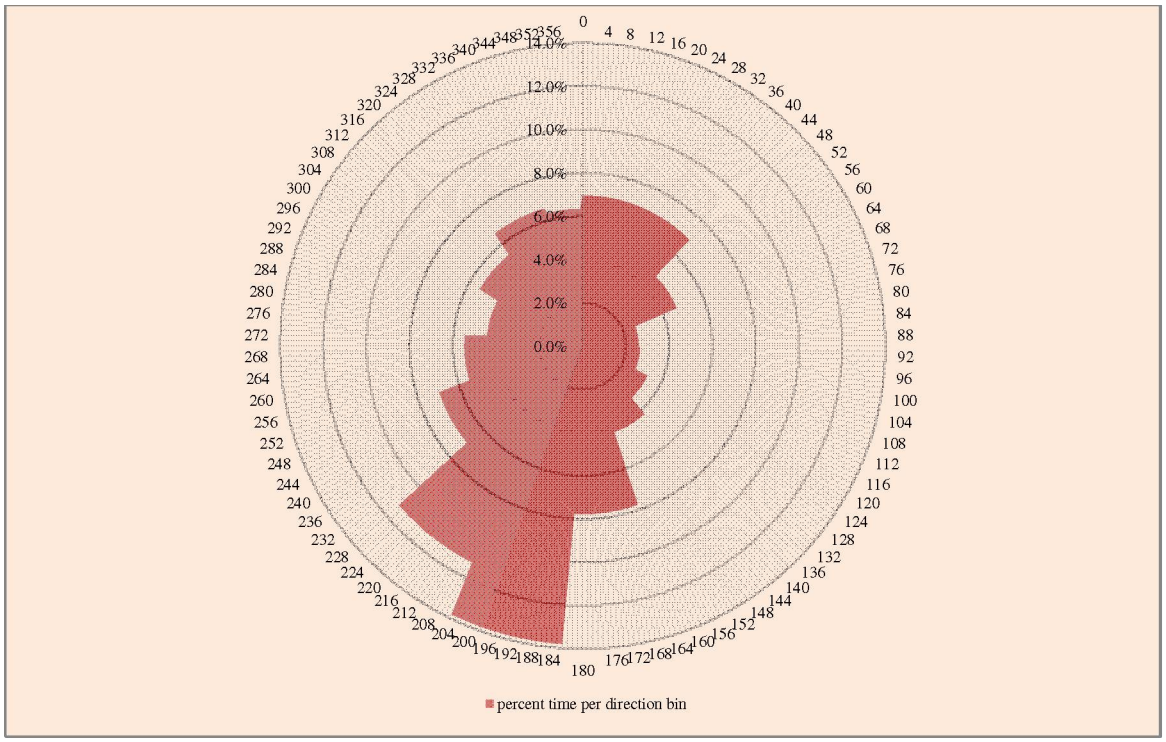

Figure B.32 Wind rose for percentage of time RG2 (90 m)

Appendix E

Great Lakes Wind Energy

Analysis of Turbulence and Temporal Averaging Time Constants

Neel Desai

University of Michigan, Ann Arbor

Acknowledgement and Disclaimer

Acknowledgements: "This material is based upon work supported by the Department of Energy; Grand Valley State University; Michigan Public Service Commission; We Energies; Sierra Club of the Great Lakes; Grand Valley State University; Michigan State University, Michigan Natural Features Inventory; and the University of Michigan, under Award Number DE-EE0000294. And the following organizations for technical support: National Oceanic and Atmospheric Administration/Great Lakes Environmental Research Laboratory; National Data Buoy Center; Pacific Northwest National Laboratory; United States Coast Guard; United States Army Corp of Engineers; Michigan Department of Natural Resources; and West Michigan Energy Partners."

- We tried to look at possible causes of the observed periods of high Turbulence Kinetic Energy (TKE).
- We saw that the TKE values seem to co-relate better with wind speeds rather than wave heights.
  - Stability
  - Time required for wave development at a given wind speed and fetch
- TKE values determined using Wind Sentinel Observations.
- TKE contours were compared with wind speed data obtained from GLERL buoy (MKGM4), as well as from the cup anemometers on the Wind Sentinel Buoy.

Enhanced TKE periods correspond to elevated surface winds from buoys

30

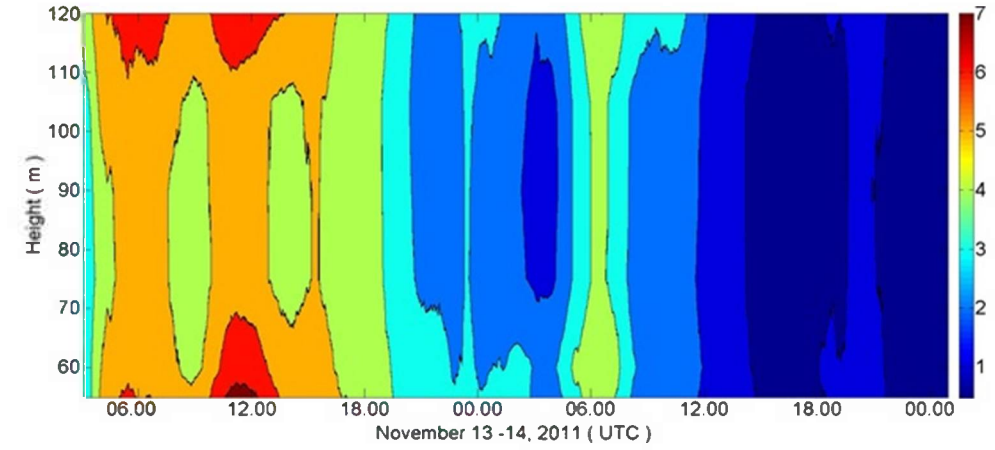

Turbulence Intensity
Second Averaging

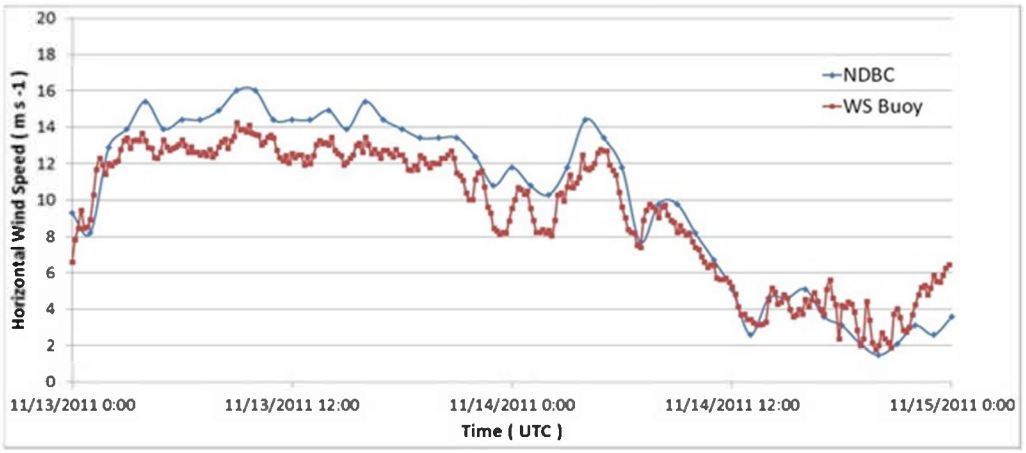

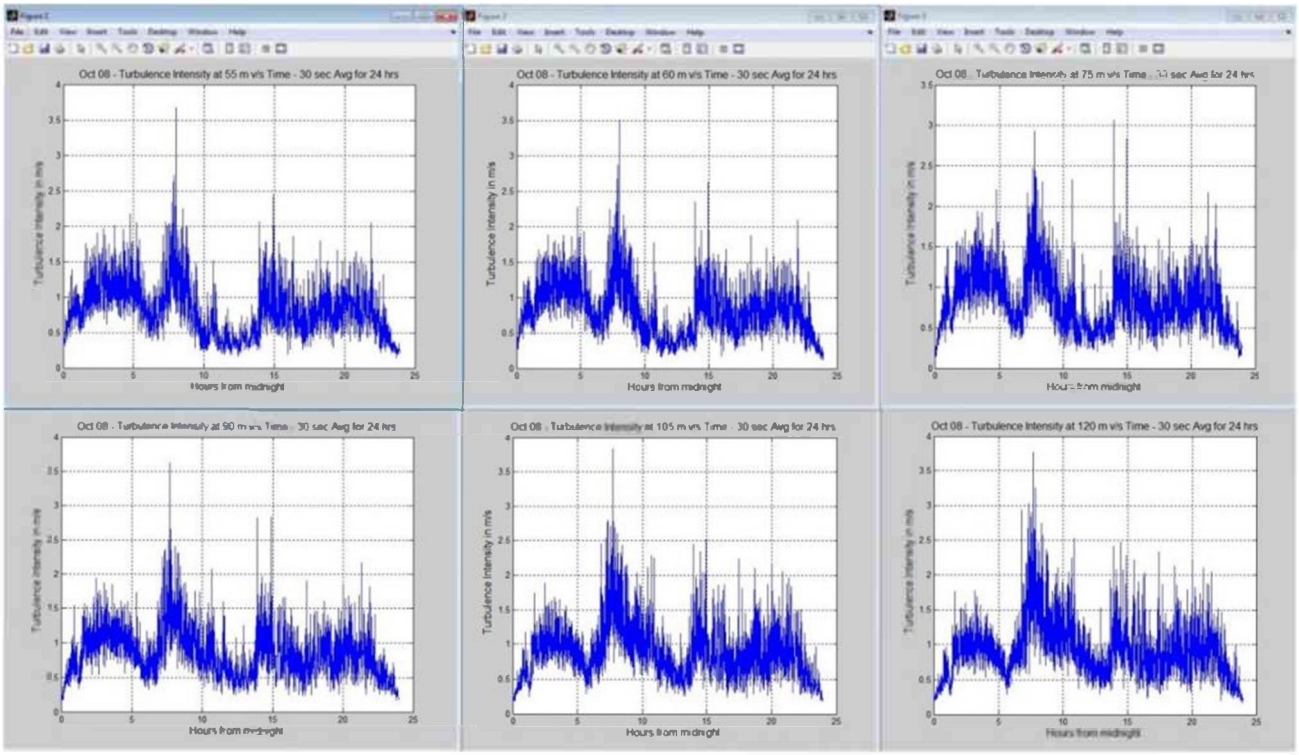

10 Minute Averaging

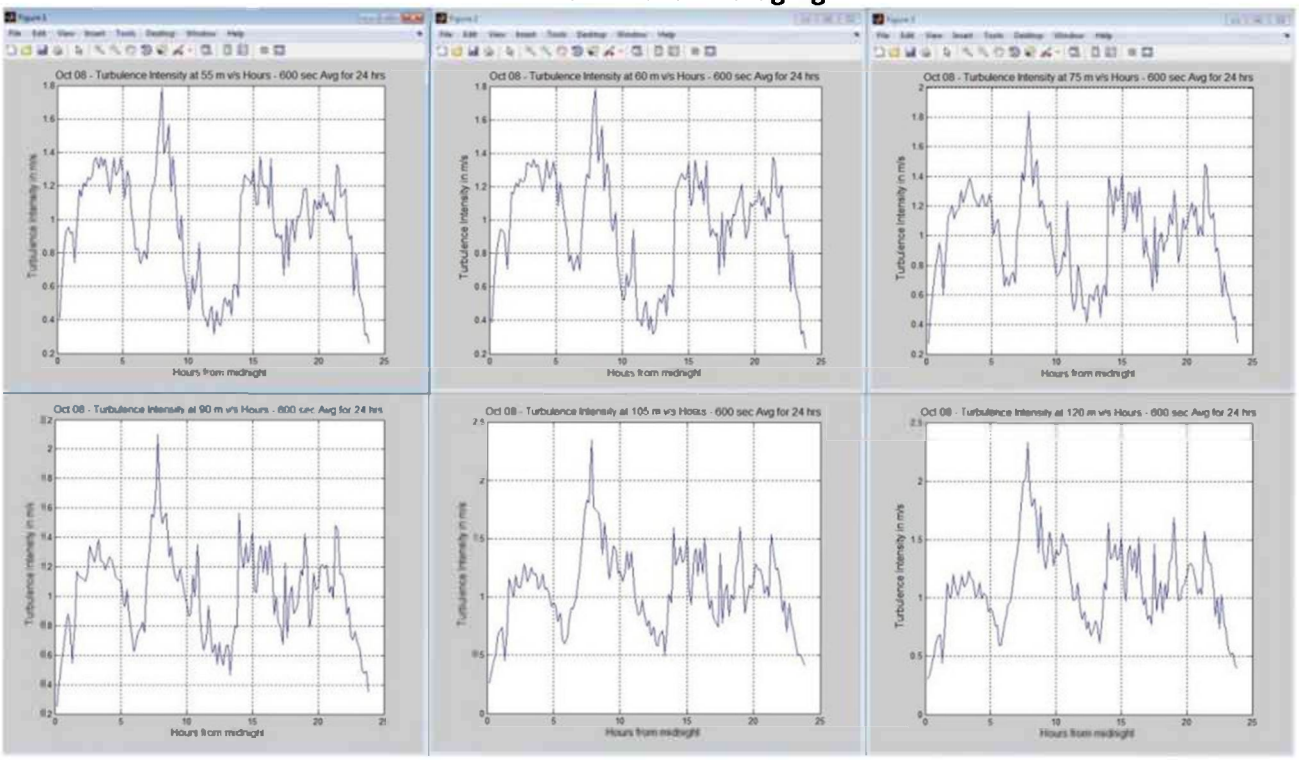

Turbulence Kinetic Energy

30 Second Averaging

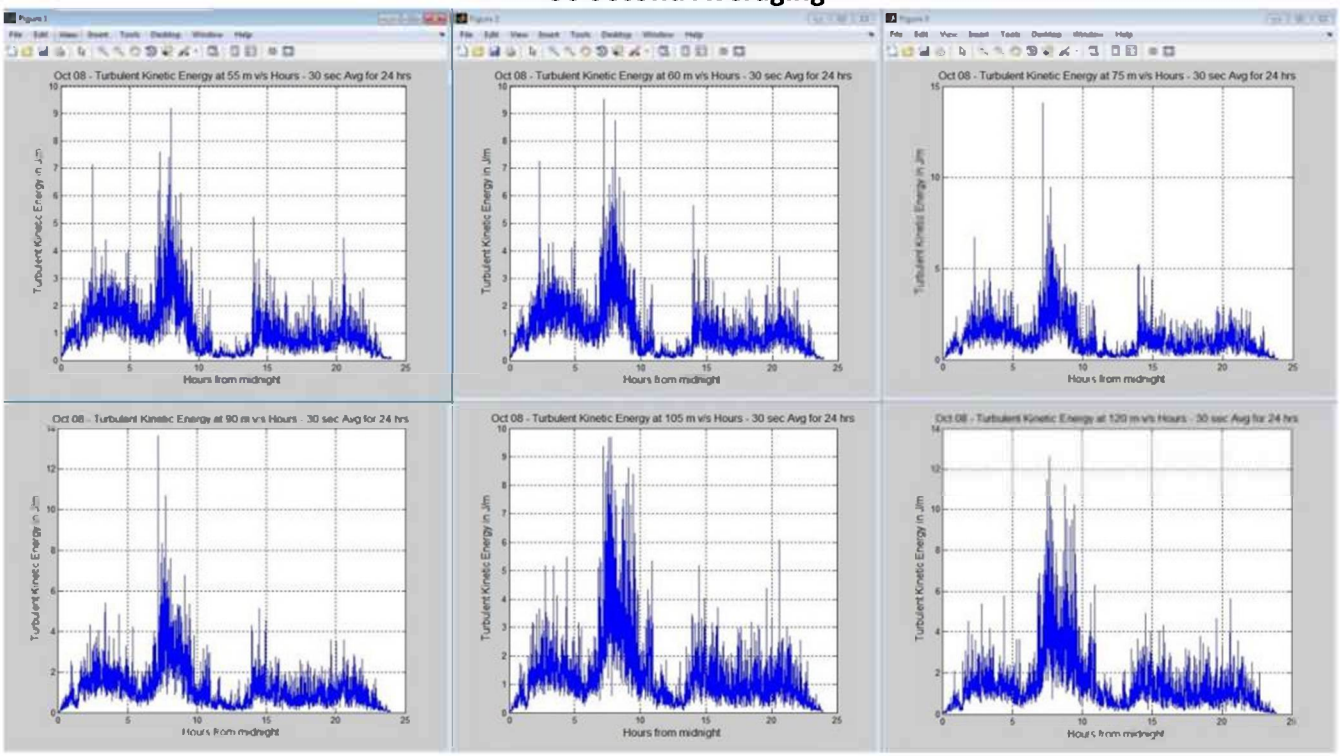

10 Minute Averaging

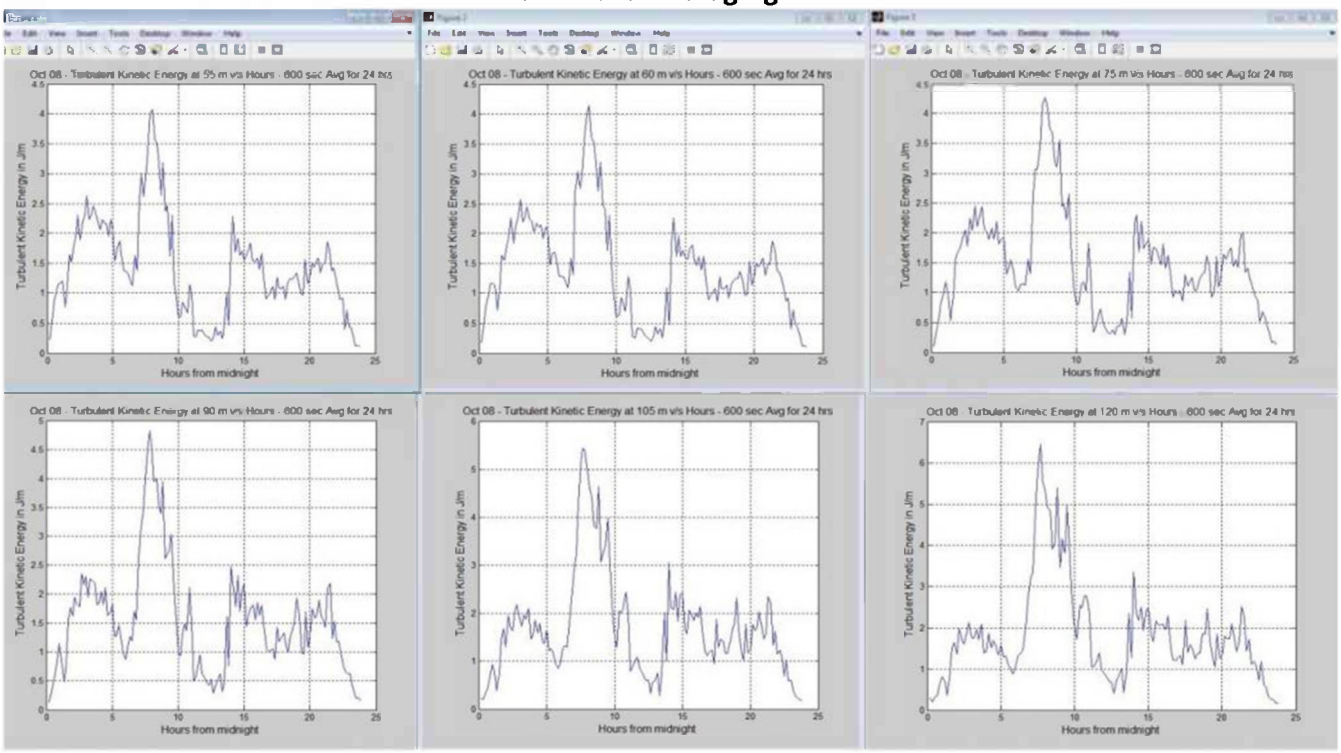

Shear Stress

XY Shear Stress – 10 Minute Averaging

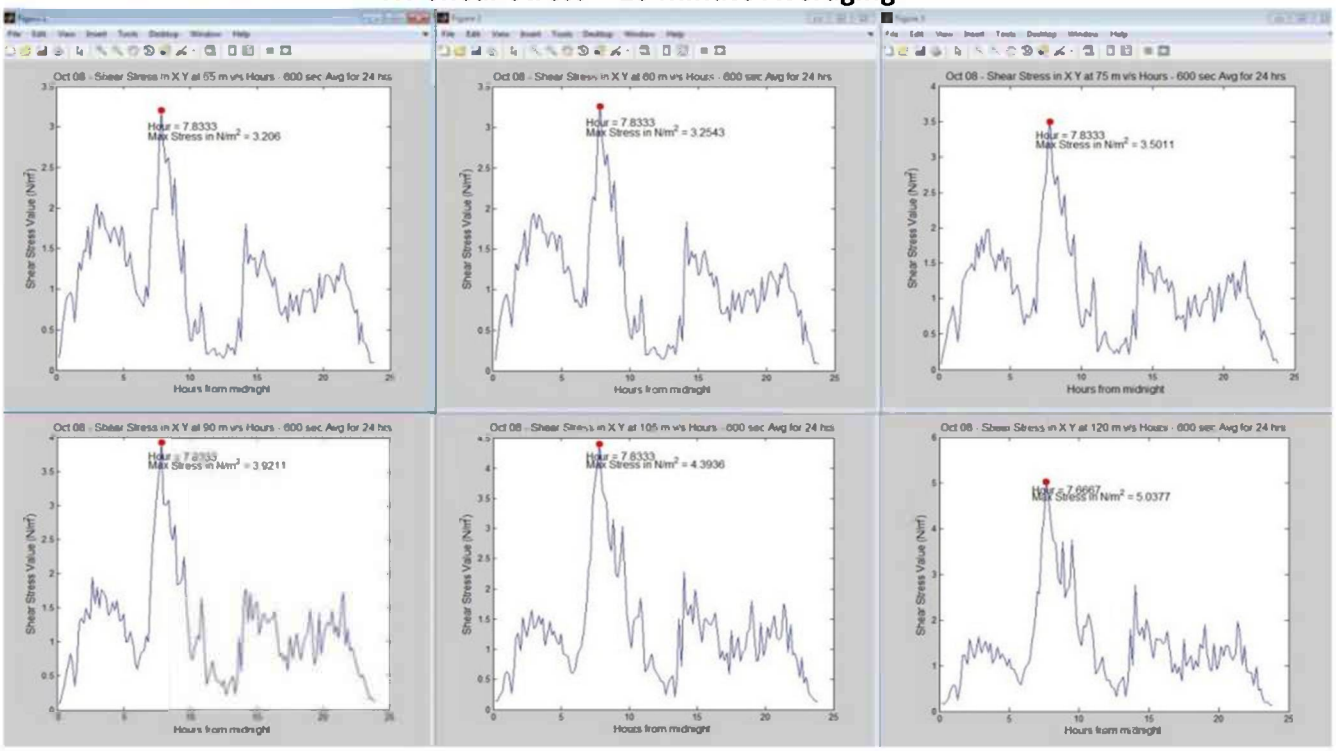

YZ and XZ Shear Stress – 10 Minute Averaging

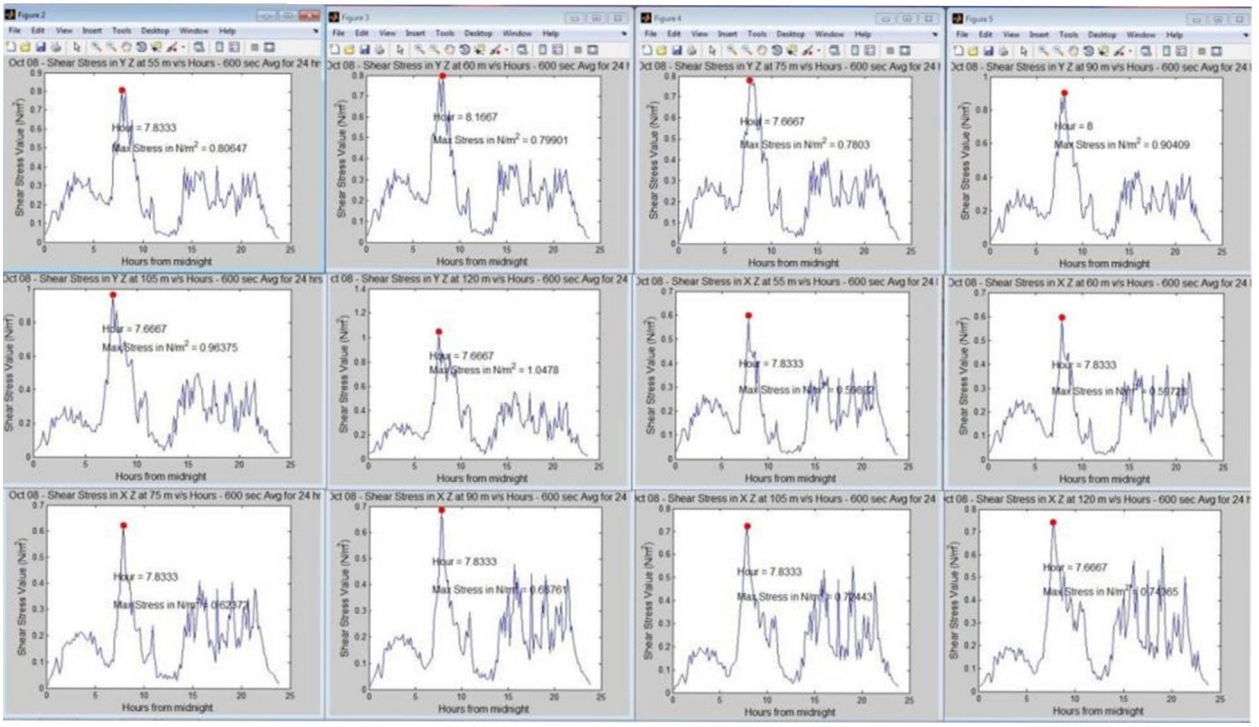

Appendix F

Wind Gust Frequency Analysis

Bruce M. Williams
University of Delaware
May 2013
brucew@udel.edu

Acknowledgement and Disclaimer

Acknowledgements: "This material is based upon work supported by the Department of Energy; Grand Valley State University; Michigan Public Service Commission; We Energies; Sierra Club of the Great Lakes; Grand Valley State University; Michigan State University, Michigan Natural Features Inventory; and the University of Michigan, under Award Number DE-EE0000294. And the following organizations for technical support: National Oceanic and Atmospheric Administration/Great Lakes Environmental Research Laboratory; National Data Buoy Center; Pacific Northwest National Laboratory; United States Coast Guard; United States Army Corp of Engineers; Michigan Department of Natural Resources; and West Michigan Energy Partners."

The first analysis was conducted to determine if, and how often. the wind speed ramp rate exceeded the ability of the pitch rate to keep up and maintain optimal pitch. An algorithm was written and run in "C" programming language which estimates the frequency of ramp events by durations and accelerations using a moving time window. As an example, results for a 4 second window are shown in *Figure 9*. The horizontal axis represents the acceleration of the wind, from -1.5 m/s per second to +1.5 m/s per second (pos. and neg around zero at center), and the vertical axis is the number of occurences. The highest frequency belongs to the lowest acceleration rates, and the tails belong to the largest acceleration rates.

The base case turbine pitch rate is about 8 degrees per second, and the Region 3 pitch range is about 23 degrees. The wind speed range of Region 3 (active pitch) is from about 12 m/s to about 25 m/s (see **Error! Reference source not found.**). Although optimal steady state pitch is not directly proportional to wind speed, the assumption of linearity is close enough for this analysis, based on **Error! Reference source not found.**. This assumption yields a ratio of *(23 deg/ 13 m/s=)* 1.8 degrees per 1 m/s. In other words, the pitch must be changed approximately 1.8 degrees for every 1 m/s change in wind speed in Region 3 to maintain optimal TSR. Since the pitch servos are capable of 8 degrees per second, they can theoretically match a gust rate of 4.4 m/s per second. Figure 34 shows a 3-D surface plot of the acceleration distributions for all time windows up to 29 seconds. Only a few events with acceleration above ~1.5 m/s per second were observed. Therefore it can be concluded that the energy loss from gust ramp rates exceeding pitch rate is not significant. However, the out-of-sync response to the gust is what creates the power drops. Further data analysis was performed to determine the frequency and magnitude of these power losses.

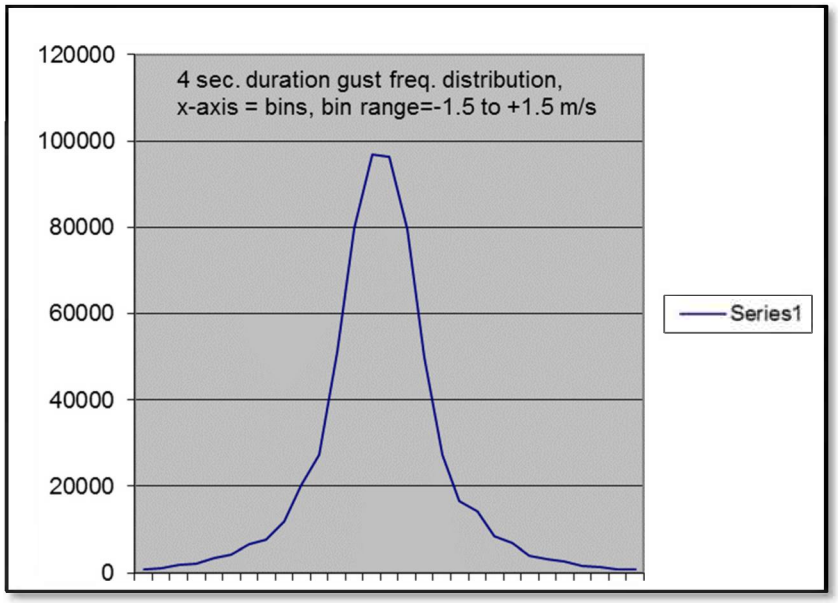

Figure 61- Wind Acceleration Frequency Distribution for a 4 Second Averaging Time. Acceleration range is from -1.5 m/s/s to +1.5 m/s/s. . Raw data provided by GVSU-Arn Boezaart

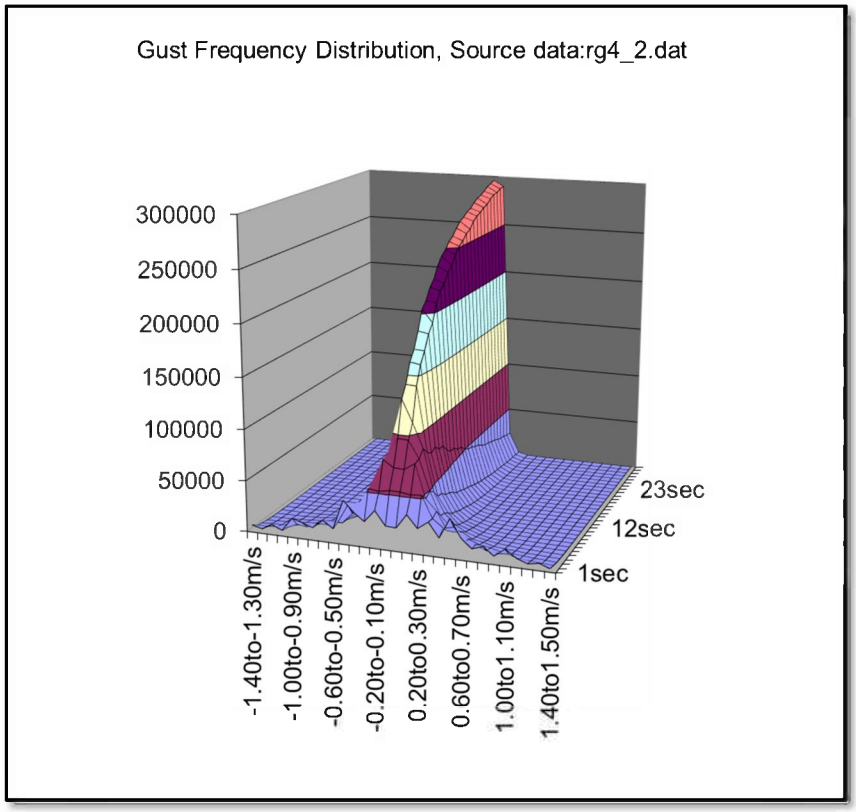

Figure 34- Frequency Distrubution of Wind Acceleration WindSentinel Lidar data at 90m, Jan 4 – 14, 2012. Raw data provided by GVSU-Arn Boezaart

To estimate the frequency of conditions which create these losses, a data set was obtained and analyzed from a WindSentinel deployed in Lake Michigan in 2012 by Grand Valley State University. The data set includes wind speeds and directions at 90 m height, sampled at 1 Hz. Ten sequential days in January 2012 were selected as being representative of gusty winter conditions. The data were scrubbed by removing all strings of invalid data exceeding 1 minute and extrapolating to fill in gaps of less than one minute. This left 665,027 records, or the equivalent of about 8 days of measurements. A simple analysis was performed to identify gust events, defined as "saw tooth" events, where a sudden rise in velocity is followed by a sudden drop. These events are what causes out-of-sync pitch response and power drops. The data stream was scanned multiple times by an algorithm written in the "C" programming language. The algorithm looked for waveforms matching the defining critieria for a "sawtooth gust" event on each pass, and accumulated counts of qualifying events. Those counts were written to a file/table and imported into an excel spreadsheet for presentation. Search criteria were set for 1, 2, 3, and 4, and 5 second windows, and changes in wind speed were binned according to magnitude, from 0 to 11 m/s, in bins of 1 m/s. For example; 99 events were observed where the wind speed increased by between 3.0 and 4.0 m/s in on second, and then immediately following that ramp up, the wind speed fell by the same amount in one second. A spectral analysis of the data would

provide the most accurate estimate of the potential loss of power, but that is beyond the scope of this study. For a first order analysis, to determine if the benefits pass the threshhold of significance (greater than 0.5%), the number of events similar to the reference EOG was estimated.

Figure 63 shows the output data plotted as a 3-D surface for all ramp rates and window widths. The reference "mexican hat" EOG has a trough to peak duration of about 3 seconds, and raises the wind speed by about 6 m/s in that period, for a ramp rate of about 2 m/s per second. In Table 35, for the 3 second sliding window, there were 996 events where the wind increased by 6 m/s over a 3 second period, then dropped back to the baseline over the following three seconds. Since this represents about 7.7 days of data, a first order estimate for one year would be *(996 x 365 / 7.7 =)* 47,212 similar events. Assuming conservatively that about 25% of the events occur in Region 3 leaves about 11,800 qualifying events per year. If each event can be mitigated with Lidar control, saving 0.3 kWhr per event, this would yield about 3,540 kWhr annually. This translates to only $531, which is insignificant.

Although this analysis has high levels of uncertainty, and is based on data from Lake Michigan, not the study area, it does not show any evidence of significant gains in AEP from this methodology of pitch control. This agrees with other simulation studies reviewed, which found no direct, significant increase in power production through Lidar assisted pitch control. Further research is warranted to confirm or revise this obervation. However, the reduction in fatigue loading is confirmed by several studies, and can be monetized, as discussed in the following sections.

Table 35- Sawtooth Gust Frequency from WindSentinel Data, Lake Michigan

	Frequency Count by Change in Wind Speed, m/s, binned.			
Sliding Window Width (seconds, trough to peak)	0 to 1	1 to 2	2 to 3	3 to 4
1	11514	1491	328	99
2	13939	2505	675	215
3	15474	3292	996	376
4	16423	3775	1243	456
5	16692	4141	1348	568
6	17148	4288	1370	555

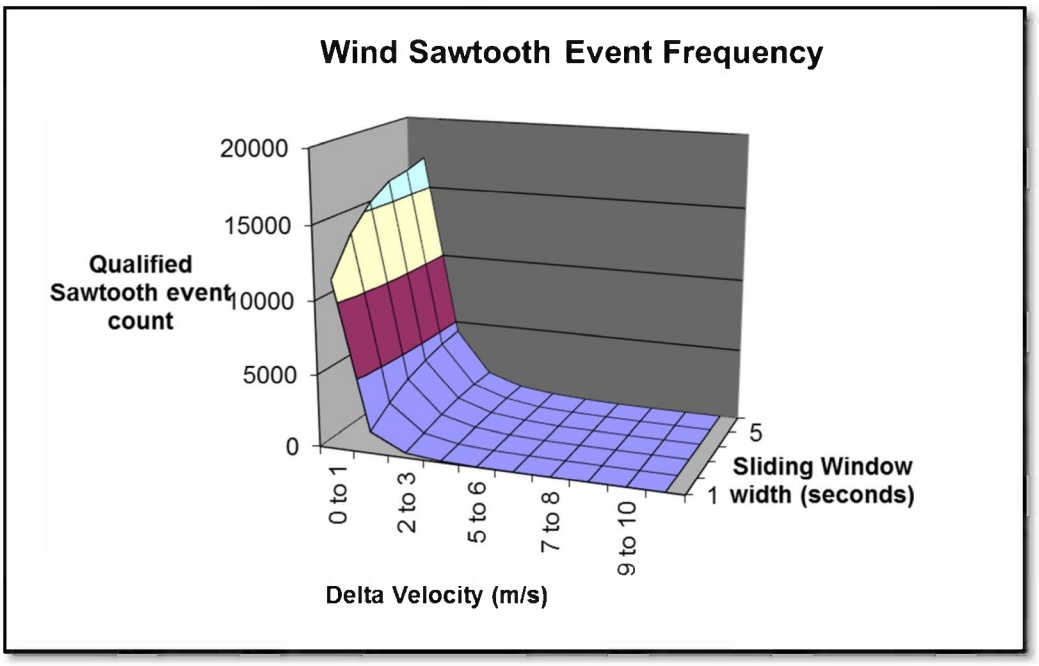

Figure 63- Sawtooth Gust Event Frequency

Appendix G

Visualizing Lake Michigan Wind with SAS® Software

Aaron C Clark, Grand Valley State University; David Zeitler,
Grand Valley State University

ABSTRACT

A wind resource assessment buoy, residing in Lake Michigan, uses a pulsing laser wind sensor to measure wind speed and direction offshore up to a wind turbine hub-height of 175m and across the blade span every second. Understanding wind behavior would be tedious and fatiguing with such large data sets. However, SAS/GRAPH® 9.4 helps the user grasp wind characteristics over time and at different altitudes by exploring the data visually. This paper covers graphical approaches to evaluate wind speed validity, seasonal wind speed variation, and storm systems to inform engineers about the energy potential of Lake Michigan offshore wind farms.

KEYWORDS

Big data, time series, visualization, offshore wind farms, renewable energy, Lake Michigan, moving window, PROC SGPLOT, PROC GRADAR

INTRODUCTION

Wind speeds off of large bodies of water have often been hailed for their prime wind energy candidacy, and Lake Michigan is no exception. The U.S. Department of Energy's (DOE) National Renewable Energy Laboratory (NREL)
has cited Lake Michigan with an "outstanding" wind resource with the potential of generating and estimated 600- 800 watts/minute^2 at 50 meters above the water surface in 2007. In a continued effort to explore the candidacy of wind
energy on Lake Michigan and to compromise with shoreline property owners' claim that turbines contribute to visual pollution, offshore wind farms propose a promising alternative. In 2012 Grand Valley State University deployed a wind resource assessment buoy called the WindSentinel™ in Lake Michigan's mid-lake plateau, 35 miles west of Muskegon, MI, a prime area for development in approximately 250 feet of water. The feature technology: a pulsing laser wind sensor (LWS) is mounted on the buoy to accurately measure wind speed and direction up to a wind turbine hub-height at 175m and across the blade span every second. Predecessors to the WindSentinel™ would aggregate wind speeds to ten minute averages only a few feet above the water, lacking detailed data. The WindSentinel's™ primary objective is wind monitoring using the LWS, but many water, atmospheric, and bird/bat characteristics are also captured using other onboard devices.

One challenge to determining wind farm plausibility on Lake Michigan is confirming the validity of the wind measurements we observe in preparation for data analysis. In some experimental high altitude cases, the LWS struggles to collect consistent and validated wind speed records due to lack of reflective particulates and movement of existing particles in the atmosphere over the open water. Data quality

indicators provided by the LWS vendor have proven to flag relatively good data as bad. Therefore, before exploration of seasonal and storm activity on the lake for a turbine-friendly assessment, we need to ensure we are examining all valid data values. Visualizing the state of these data using SAS® 9.4 will prove useful to identify "bad data" and inform an algorithm to sort it from the "good data." For example, at times, reported wind speeds are too constant or too extreme to be real.

The second challenge is previewing seasonal variation with inherent patterns in the wind behavior. Understanding the seasons will be important in forecasting how often a wind turbine is operating with optimal power output limitations. That is, optimal power output cannot be achieved if the wind is too fast or too slow; when it is, the turbine will not collect any wind, and will shut itself off. Since wind is cyclical, we need to understand how often our target wind speed is maintained during these seasonal variations.

The last undertaking is to explore the phenomenon of storms to reveal any possible challenges for turbines in the middle of the lake. During high wind storms, can we expect the turbines to operate? Is the WindSentinel™ collecting valid wind during these storm periods? These concerns will be addressed.

Considering all these challenges, visualizations of these data will help the user gain a clear perspective on activity and key wind characteristics much easier for short periods of time than descriptive statistics would be able to portray. This paper will serve as a guide to how we approached these large time series datasets using visualizations.

THE WIND TECHNOLOGY AT A GLANCE

The Grand Valley State University-owned WindSentinel™ is a product of AXYS Technologies Inc., and the first wind assessment tool of its kind in the world. Its monitoring systems include wave, current, water quality, water temperature, basic wind (anemometers), atmospheric pressure, solar radiation, laser wind, sonar, and audio recordings. The vessel is approximately 15 feet in length and capable of powering all its systems with an onboard turbine and solar panels and storing the energy in forty batteries located in the hull. In case no wind or sun energy is available, a backup diesel generator lies within the hull as well. As you can see in diagram 1 (right), the LWS monitors wind at six distinct altitudes called range gates (RG). Their altitudes are 75m, 90m, 105m, 125m, 150m, and 175m for range gates 1 through 6, respectively. The laser sensor pulses more than 600 times per second in three angled directions, auto-correcting for buoy movement.

The buoy's location during the 2012 season (May 7 to December 19) was approximately W43^{O} 20' 31.20'', N -87^{O} 7'
12.00''. The offshore wind assessment project is three years in total, spending time on Muskegon Lake, the Mid-Lake Plateau, and various other locations on Lake Michigan. To date, over 65 individuals from various institutions have collaborated on the project, including the U.S. Department of Energy, Federal and State agencies, Grand Valley State University, Michigan State University, University of Michigan, University of Delaware, and Michigan Tech University.

VISUALIZING WIND VALIDITY

We have a number of SAS/GRAPH® tools at our disposal to visualize invalid data. Range gate 6 (175m) is a test range gate to observe the performance of the LWS at an extreme operating height limit for this configuration. Thus, performance degradation was expected. To analyze only valid data at each range gate, we will build a quantitative and indicator measure to identify wind speeds that are extremely high or too constant to be real.

The former two scenarios are displayed in figure 1 (bottom right) which previews wind at RG6 on July 1st, 2012. A trivial
PROC SGPLOT with a SCATTER statement produce figure 1:

```
PROC SGPLOT DATA=LIB2.JULY1;
SCATTER Y= WindSpeedHorRG6
X=TS;
RUN;
```

Occasionally, the LWS will record an observation not characteristic of the wind speeds surrounding it. For example, figure 1 displays an extreme point at around 4am nearing 48 m/s (~107 mph) which is clearly unrealistic, especially considering the wind activity during the rest of the day. Therefore, we must train our validity indicator to recognize such occurrences. This is easily achieved by scanning the data for high wind speeds, taking into account wind before and after each occurrence. Visualizations such as figure 1 are all that
are needed to show these instances.

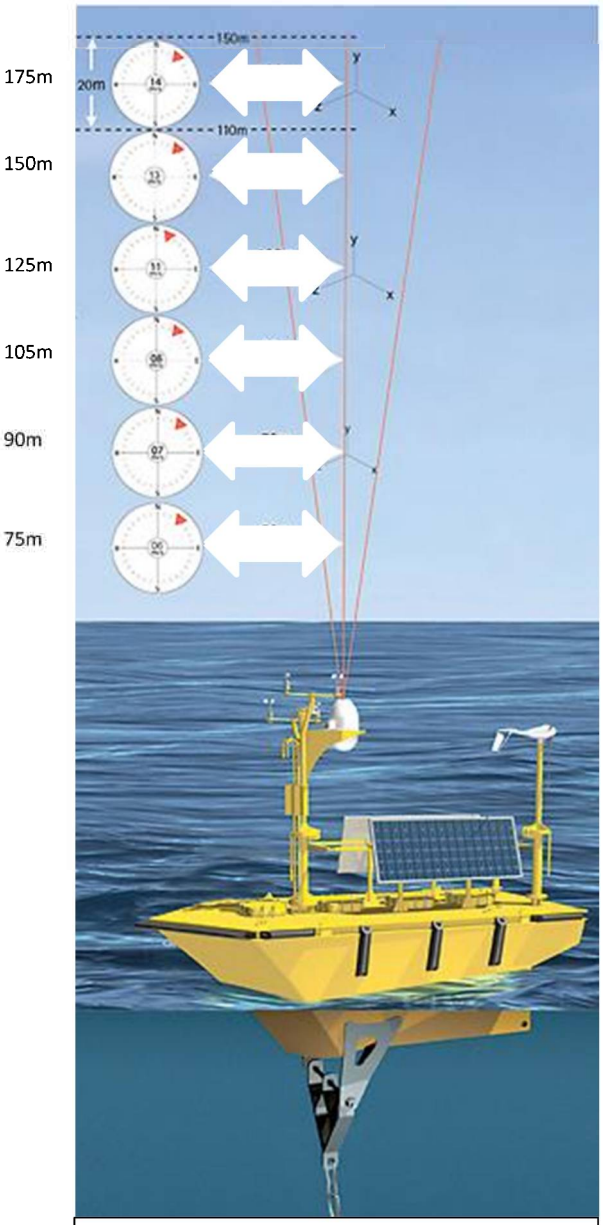

Figure 1: Range Gate 6 (175m) wind speeds on July 1st, 2012

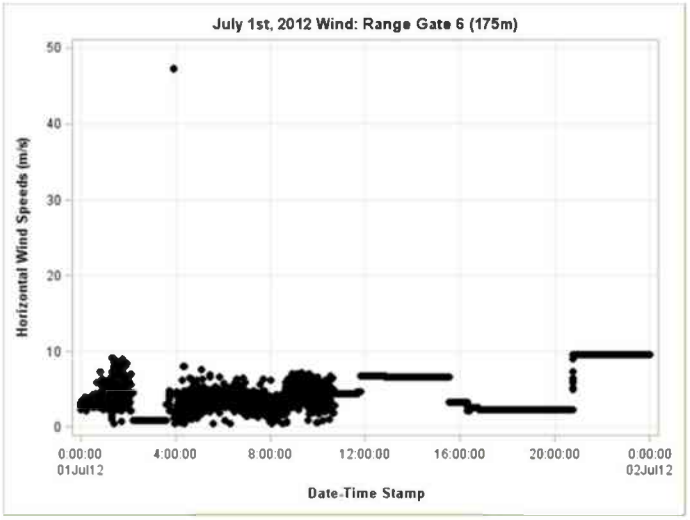

Diagram 1: Conceptual view of WindSentinel™ configuration and the Laser Wind Sensor's 6 range gates

Next, identifying wind speeds that are too constant to be real is slightly more complex and requires a computational solution since short time intervals of "dead wind" are difficult to observe with the naked eye. Figure 1 has some obvious instances of this, especially after noon. These winds cannot be real for three reasons:

1. Winds come and pass in gusts. That is, it is unlikely for wind to maintain a constant speed for more than a couple seconds.
2. Our measurements extend out to the tenth of an m/s, so exact readings for consecutive time stamps are less probable to this degree.
3. The LWS measurements are inherently variable. As a result, it will likely never measure the exact same wind speed for consecutive time stamps.

Our solution utilizes a 5-second moving window standard deviation (5-sec stddev). This statistic satisfies our need for a quantitative measure of variability because the window is short enough to measure delicate spikes in wind and long enough to be conservative about how long wind can remain constant. Using this information, we produce figure 2, a display of the relationship between wind speeds and their 5-sec stddev by adding another SCATTER statement to the code that produced figure 1. Focusing on figure 2, whenever the wind speeds remain constant, the 5-sec stddev equals zero. Thus, we can train our validity indicator to classify "bad data" as having a zero value for this statistic. Grouping by the validity indicator using a GROUP= option on the SCATTER statement produces figure 3 below.

```
PROC SGPLOT DATA= JULY1;  SCATTER
 Y= WindSpeedHorRG6 X=TS; SCATTER
 Y=_5sSdRG6 X=TS;
 YAXIS MIN=0 MAX=11 LABEL="Horizontal Wind Speeds
(m/s)"; RUN;
DATA JULY1;
 SET JULY1;
 IF _5sSdRG6 = 0 THEN ValidRG6 =
                  0; ELSE ValidRG6 =
                  1;
RUN;
PROC SGPLOT DATA= JULY1;
 SCATTER Y= WindSpeedHorRG6 X=TS / GROUP=ValidRG6;
 YAXIS MIN=0 MAX=12.5 LABEL="Horizontal Wind Speeds
 (m/s)";
RUN;
```

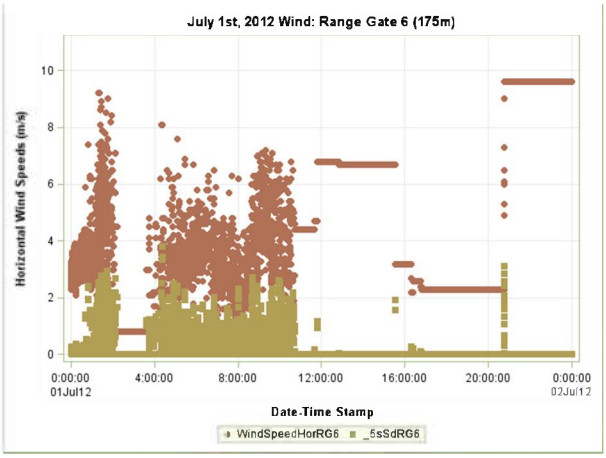

Figure 2. Display of 5-second moving window
standard deviation against wind speeds

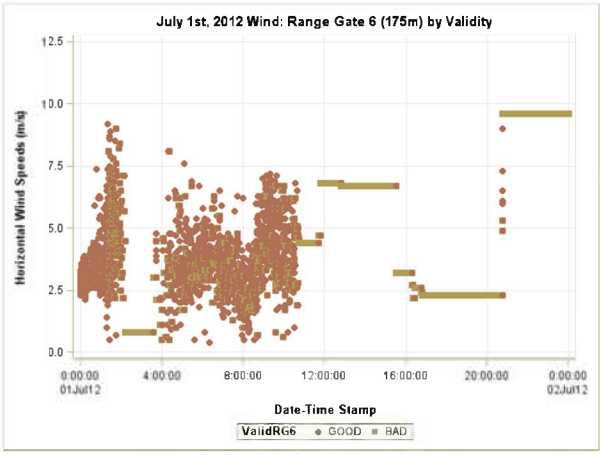

Figure 3. Display of wind speeds grouped by manually built validity indicator

Note that we not only identify obvious constant wind that occurs after noon on July 1st, but we also captured short time intervals (1 to 3 minutes, for example) where the wind remained constant that were not visible at this day-level visualization. Now that the data has been classified as "good" and "bad", it is appropriate to explore the data further. The tools identified in this section will prove useful in dissecting key wind characteristics in the remainder of the report.

VISUALIZING SEASONAL VARIATION

Your average 850kW wind turbine, the prospective model appropriate for offshore wind farms in Lake Michigan, generates the most energy when capturing wind between 11 and 14 m/s. However, the turbine will remain ON as long as the wind is between 4 and 14 m/s. Any wind outside of this range is not sufficient on the low end and potentially damaging to the turbine on the high end, so the turbine will shut off. Seventy-three percent of the 2012 data from the mid-lake plateau location was between these values. From now on, our visualizations will include a horizontal reference lines at 4 and 14 to offer this perspective. To accomplish this, we only need the following in any SGPLOT procedure:

```
REF 4 14;
```

To attain the "big picture" perspective that visualizing seasonal wind activity seeks, detail of second-level data in our plots would be quite excessive. That is, the 2012 season is composed of roughly 23 million data observations. To plot such detail on in one pass would prove useless as the points would be too packed, plotted over one another, and take the form of a big blob. Therefore, we have opted to utilize ten minute averages of the data, reducing our total observation count to approximately 38 thousand and smoothing out possible outliers. To reduce the detail even more, we ask SAS® for only two of these observations be plotted for each day: the max and min. The result (figures 4- 6) will provide a "channel" of possible wind values measured by day when using two SERIES statements (one for day-minimums and one for day-maximums) in PROC SGPLOT, viewed by season. An alternative would be to use PROC SGPANEL and a statement to PANELBY season. We will choose the former so that we can append more graphics that assess seasonal data, and group them accordingly.

Namely, we will create a windrose plot for each season to evaluate the frequency of several wind speed magnitudes and wind directions in one plot. To do so, we create discrete categories for wind speeds and directions and produce a cross tabulation of their frequencies for input into PROC GRADAR.

The SAS® syntax below illustrates the entire seasonal visualization process:

```
PROC SGPLOT DATA= Seasons;
  SERIES Y=dayMIN X=DateStamp;
  SERIES Y=dayMAX X=DateStamp;
  BY Season;
  REFLINE 4 14;
RUN;
PROC FREQ DATA = Midlake;
  TABLES DiscreteAvgDir*DiscreteAvgSpd/ NOROW NOCOL OUT= Freqs;
BY Season;
RUN;
DATA FALLFREQS; SET Freqs; IF Season="Fall"; RUN;
DATA SPRINGFREQS; SET Freqs; IF Season ="Spring"; RUN;
DATA SUMMERFREQS; SET Freqs; IF Season ="Summer"; RUN;
PROC GRADAR DATA= SPRINGFREQS;
  CHART DiscreteAvgDir / sumvar=percent windrose noframe speed=DiscreteAvgSpd;
RUN;
```

Note that PROC GRADAR does not operate with a BY statement, so three separate procedures are executed, one for each season. The spring season was slightly shorter than the summer and fall seasons as the buoy was deployed May 7, well into this time period. As a result, figure 4 may appear less cluttered than the others. Generally, the averaged wind speeds are mostly within the 4 and 14 m/s turbine constraints, with a tendency to drop below the lower bound more frequently than rise about the upper bound. The percentage of usable wind during the spring season is about 71.18%, not far from the overall percentage of usable wind in 2012 (73%). The wind is primarily out of the south with wind speeds frequent in the 5-10 m/s range.

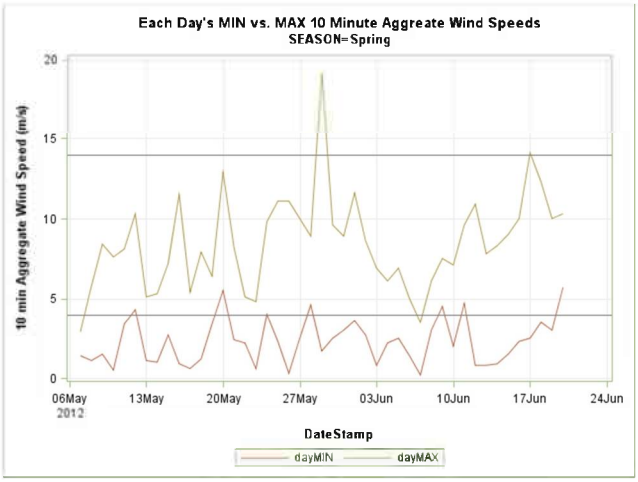

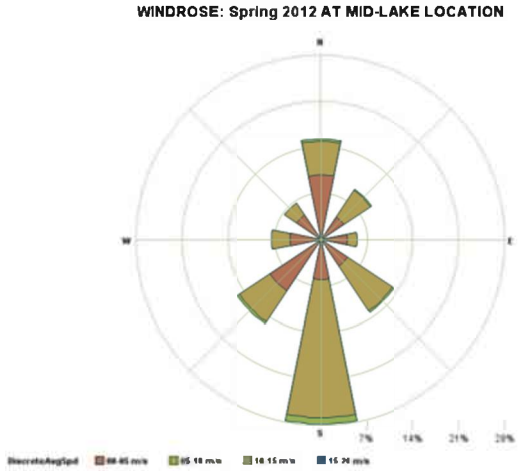

Figure 4. Min and max 10-minute wind speed averages per day, for spring 2012 season with windrose

Next, figure 5 (below) displays a similar trend observed in figure 4. That is, there is more unusable wind below the lower constraint than above the upper constraint. Sixty five percent of the wind speeds during this season were between 4 and 14 m/s, much lower than in the spring. Last, wind from the south and southwest at 5-10 m/s is most frequent, though there seems to be some stronger winds (10-15 m/s) that came from the north briefly.

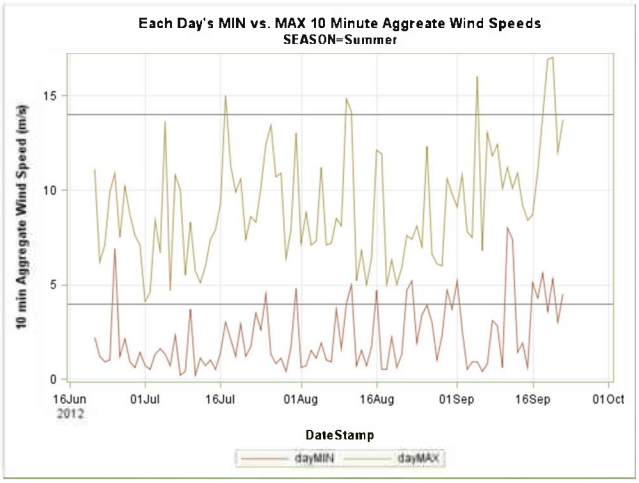

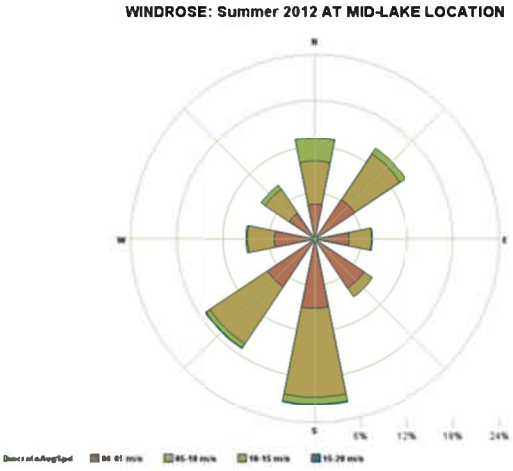

Figure 5. Min and max 10-minute wind speed averages per day, for summer 2012 season with windrose

Finally, figure 6 (below) displays the results for the fall season:

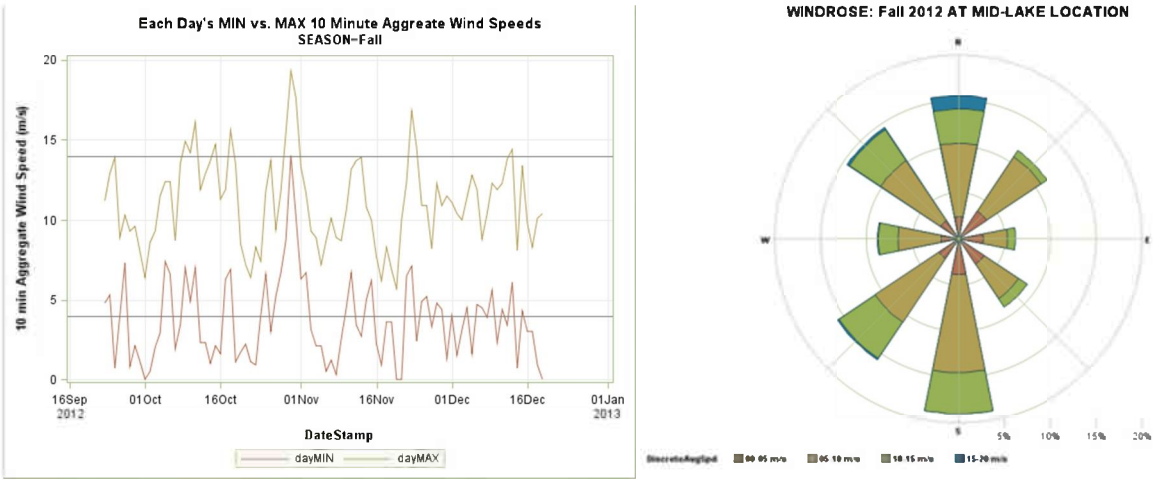

Figure 6. Min and max 10-minute wind speed averages per day, for fall 2012 season with windrose

During the fall season, 82.8% of the wind fell within the usable constraints defined by an 850kW turbine. That makes this season's usable wind the highest out of all other season. However, around the end of October, the min and max 10-minute averaged wind speeds rise above 14 m/s. This phenomenon is due to residual effects of the devastating Hurricane Sandy that hit the east coast impacting the U.S. all the way up into Lake Michigan. Actual (not averaged) wind speeds reached gale force levels of 26 m/s (58 mph). One gust reached 29.9 m/s (or nearly 67 mph). As such, the windrose also displays significantly higher winder wind speeds in accordance with this finding, but with wind coming from the S, SW, NW, and N a fairly uniform amount of time. The may be due to the circular motion of hurricane storm systems.

In conclusion, the summer months produced the least amount of usable wind while the fall produced the most. However, it is unknown whether the fall season yielded more wind due to high winds from Hurricane Sandy, or for some other reason. A SERIES statement for the mean day 10-minute averaged wind is an alternative to using the min and max. We chose the latter route solely for its "channel" like properties described earlier. A secondary method of visualizing this "channel" is to use a HILOW statement in SGPLOT procedure. This method will plot vertical lines between any two values specified for each day, such as max/min values or even upper/lower bounds to a 95% confidence interval.

VISUALIZING STORM SYSTEMS

As discussed for figure 6's display of hurricane Sandy in *Visualizing Seasonal Variation*, storms play an important role in the functionality of turbines and in the data collected on Lake Michigan. From figure 6 (above), we know that the turbine would shut off because the winds were much too extreme during Hurricane Sandy, a truly powerful storm. However, those winds were not typical of most storms on Lake Michigan. In other words, some storm's wind speeds may be in the "usable range" (between 4 and 14 m/s), but if they are too variable, then the turbine has potential to cease function until winds are more optimal. Additionally, we will explore if storms are affecting the validity of the data collected by the LWS at different altitudes. To achieve both goals, we provide the following example that summarizes what we found to be typical among storms during the 2012 season. Figure 7 displays a brief storm that took place on July 31st, 2012 from approximately 4am to 7am that uses three SCATTER statements (one for each range gate) in a PROC SGPLOT.

```
PROC SGPLOT DATA= Midlake_JULY;
```

```
  WHERE DATATIMESTAMP>="31JUL12:00:00:00"DT AND DATATIMESTAMP <="31JUL12:23:59:59"DT;
  SCATTER X=DATATIMESTAMP Y=WindSpeedHorRG1;
  SCATTER X=DATATIMESTAMP Y=WindSpeedHorRG3;
  SCATTER X=DATATIMESTAMP Y=WindSpeedHorRG5;
RUN;
```

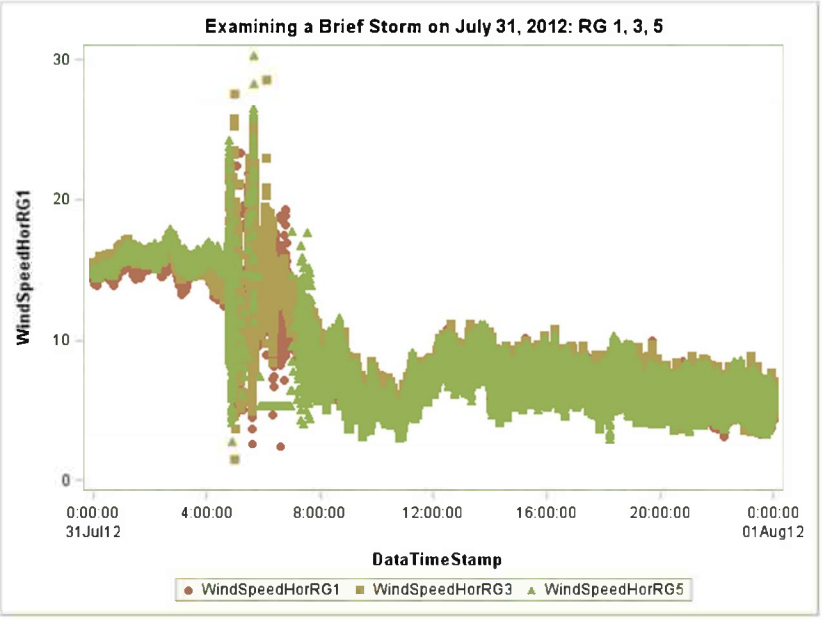

Figure 7. Display brief storm at RGs 1, 3, and 5 on July 31st, 2012

To summarize figure 7: there is data degradation in the higher range gates while the lower range gates records remain intact. There also appears to be a great deal of variation in wind speeds inside the storm vs. the wind before and after the storm. Therefore, we will consult our 5-sec stddev statistic discussed in *Visualizing Wind Validity* and zoom-in on the storm to understand what is happening here. Figure 8 is the result; below is the SAS® syntax required:

```
PROC SGPLOT DATA=JUL31;
  WHERE TS >="31JUL12:04:00:00"DT AND TS <="31JUL12:07:00:00"DT;
  SCATTER X=TS Y=WindSpeedHorRG2 /GROUP=StatusRG2DataGood;
  SCATTER X=TS Y=_5sSdRG2 / GROUP=StatusRG2DataGood;
  REFLINE 4 14;
  XAXIS GRID;
  YAXIS GRID LABEL="WIND SPEED (M/S)";
  TITLE "Examine Wind Variability using 5-sec Stddev by Validity";
RUN;
```

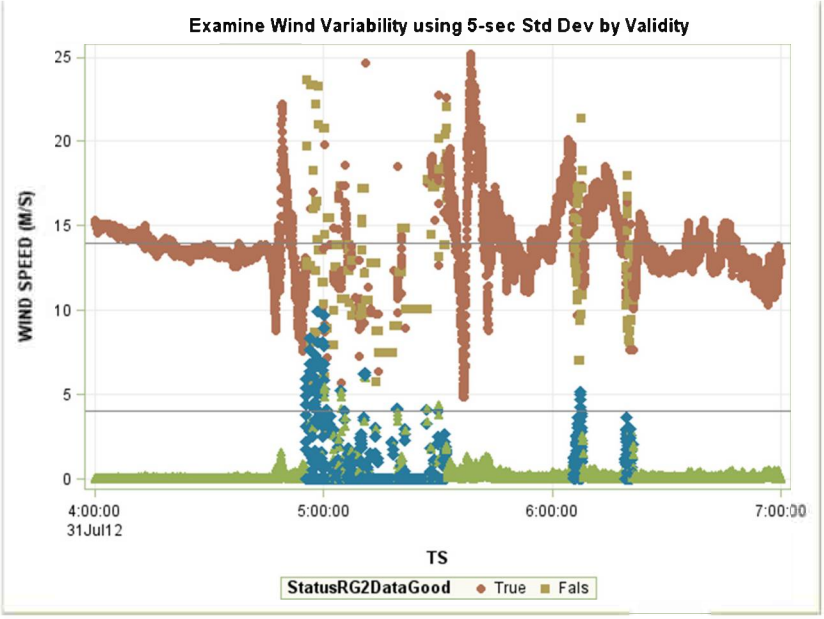

Figure 8. Zoomed-in display of July 31st, 2012 storm wind speeds and 5-sec stddev at Range Gate 2, by validity indicator

By default, SAS® displays a legend for the first grouped data supplied via SCATTER statement with a GROUP= option (the validity indicator for wind speeds), but it is easy enough to understand that the blue diamond symbols correspond to "bad data" and the green triangle symbols correspond to "good data" for the 5-sec stddev. From figure 8, we learn that the variability we observed in figure 7 is not real wind, but is actually invalid data. From the valid data, we can conclude that storm winds vary slightly more than non-storms, but not by as much as originally anticipated. The highest valid 5-sec stddev appears around "5" at 5am, which is half the invalid value observed only few minutes early at "10". In conclusion, most storms we examined displayed this characteristic: anticipated variable winds were not actually variable, but just invalid. Therefore, further exploration is needed to determine if turbines are subject to winds that are "too variable" and, thus, require shutting down due to inconsistency.

CONCLUSION

Now that we know how to watch out for invalid wind data, wind analysts can properly address how seasonal wind variation and storms will relate with turbine function for an offshore wind farm in Lake Michigan. Undoubtedly, SAS/GRAPH® 9.4 is an exceptionally capable visualization tool to dissect and interpret key wind attributes. The SAS® software will surely aid wind analysts in informing engineers, investors, and developers on the plausibility of Wind Farms on Lake Michigan. However, the wind candidacy is only one small component of wind farm development. Other assessments need to be made on social, economic, political, technologic, and environmental concerns before justifying renewable wind energy on the great lakes. As far as this assessments goes, the wind is there.

CONTACT INFORMATION

Your comments and questions are valued and encouraged. Contact the author at:

Name: Aaron Clark
Organization: Grand Valley State University, Padnos College of Engineering and Computing, Grand Rapids, MI Email: clarkaa@mail.gvsu.edu
Web: www.linkedin.com/in/dataAaronClark

Appendix H

AWRI Summary Report of Water Quality Data from Wetlab's WQM Sensor on board GVSU's Windsentinel Buoy during 2012 and 2013.

Acknowledgement and Disclaimer

Acknowledgements: "This material is based upon work supported by the Department of Energy; Grand Valley State University; Michigan Public Service Commission; We Energies; Sierra Club of the Great Lakes; Grand Valley State University; Michigan State University, Michigan Natural Features Inventory; and the University of Michigan, under Award Number DE-EE0000294. And the following organizations for technical support: National Oceanic and Atmospheric Administration/Great Lakes Environmental Research Laboratory; National Data Buoy Center; Pacific Northwest National Laboratory; United States Coast Guard; United States Army Corp of Engineers; Michigan Department of Natural Resources; and West Michigan Energy Partners."

During the 2012 and 2013 deployments of the Windsentinel buoy, an onboard Wetlab's Water Quality Monitor (WQM) collected data on several core parameters important for monitoring water quality in Lake Michigan surface waters. Data were collected from May-December in 2012 and April-December in 2013 at 10 minute intervals for conductivity, temperature, sensor depth, dissolved oxygen (2012 only), chlorophyll fluorescence and turbidity. Seasonal patterns of these parameters in Lake Michigan were observed at the mid-lake plateau location in the central basin of southern Lake Michigan during 2012 and the near shore location near Whitehall, Michigan during 2013.

The WQM sensor is a multi-parameter sonde equipped with multiple sensors and several biofouling control features (Figure 1). At the top, water is pumped into an intake port and through tubing and analyzed with sensors for conductivity, temperature, and dissolved oxygen. Biofouling is controlled using a combination of means including a BLIS system which injects bleach into the tubing following measurements and copper cladding. Adjacent to the top pump/sensor housing is a pressure sensor for monitoring water depth. At the bottom, a dual optical sensor measures chlorophyll fluorescence and turbidity. Biofouling of the optical window was controlled by a mechanical wiper system and copper cladding. The WQM was mounted in the center moon pool at the rear of the Axys buoy (Figure 1). According to Axys, the top of the WQM was approximately ~13 inches below the water surface. As such, conductivity, temperature, and dissolved oxygen measurements represent waters at that depth (i.e., ~13 inches below water surface) and chlorophyll fluorescence and turbidity measurements represent waters at ~38 inch depth. Prior to each deployment, the sensors were calibrated at AWRI according to manufacturer's specifications.

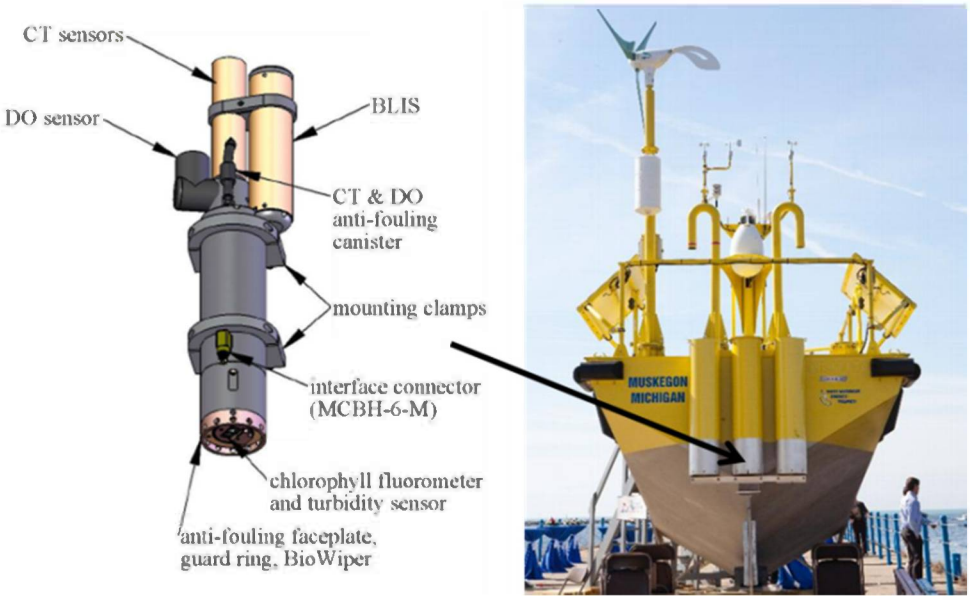

Figure 1. Wetlabs WQM Sensor and deployment location in center moon pool on Axys buoy during 2012-2013 deployments in Lake Michigan.

Seasonal trends for the 2012 mid-plateau and 2013 nearshore deployments in Lake Michigan are shown in Figures 2-6 for each water quality parameter.

Water temperature data (Figure 2) show similar seasonal warming and cooling trends for the two years. Peak water temperature at each location occurred during late July at about 25°C. However, while this temperature was sustained longer at the mid-lake plateau location, the nearshore location shows more cool temperatures quickly following the peak temperature. While the mid-lake location shows a more stable trend during 2012, more variability is observed during 2013 at the near shore location. This is likely due to water circulation dynamics in the nearshore during upwelling events as well as the influence of riverine inputs.

Fig 2. Water Temperature (°C)

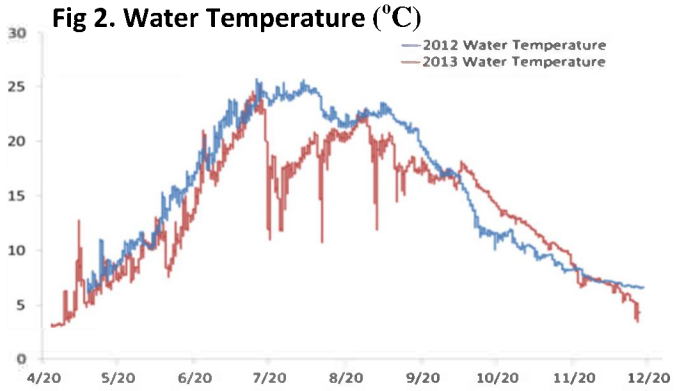

Fig 3. Dissolved Oxygen (mg/L)

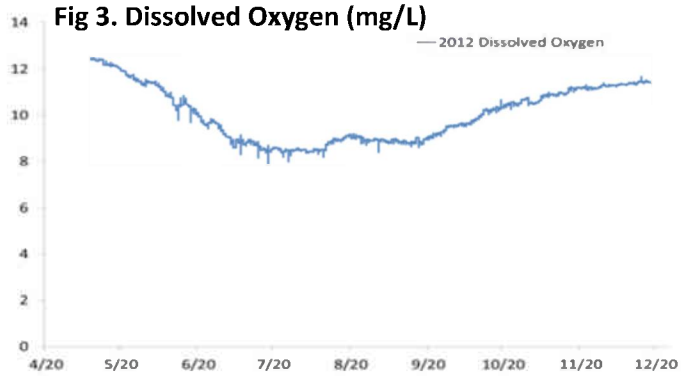

Dissolved oxygen (mg/L) data (Figure 3) show a well-oxygenated environment during 2012 at the mid-lake plateau location, with relatively lower oxygen concentration observed during the middle of the monitoring period. This dip in oxygen concentration coincides with a rise in water temperature suggesting reduced oxygen solubility as a cause. Also, another contributor to lower summer time oxygen could be from high respiration rates of non-photosynthetic organisms, such as that suggested by Cuhel and Aguilar (2013) for the extensive quagga mussel communities on the mid-lake reef complex. No data were collected during 2013 due to malfunction of the oxygen sensor.

Fig 4. Chlorophyll

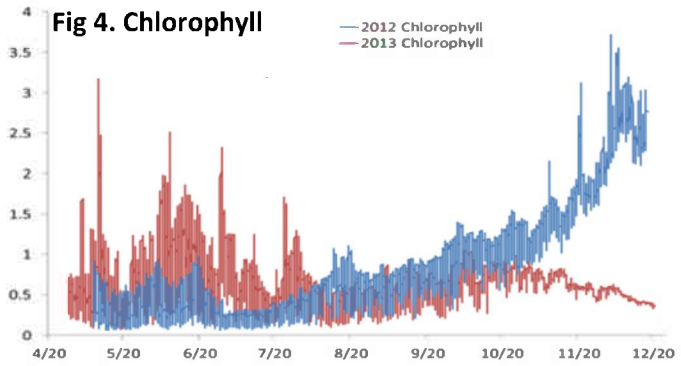

Fig 5. Turbidity (NTU)

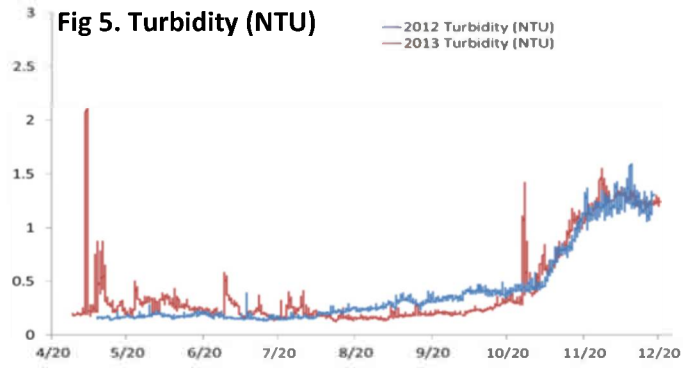

Chlorophyll fluorescence (µg/L) data (Figure 4) during 2012 show an increasing trend through the year at the mid-lake plateau, while the 2013 nearshore location showed more variability with higher chlorophyll levels during the earlier part of the year. The 2012-year also showed more algal

biofouling of the buoy hull and it is not clear whether the sensor is measuring conditions related to the ambient lake water or accumulated biofouling algae. Information on biofouling of the hull during 2013 was not available.

Turbidity (NTU) data (Figure 5) show similar seasonal trends at both locations, with the overall level of turbidity representative of fairly clear waters. The increase during the fall months indicates non-photosynthetic particulates in the absence of a corresponding trend in the chlorophyll fluorescence data (e.g., 2013-year). However, during the 2012, some influence of epiphytic algae on the buoy hull on the data quality is suspected, and that may explain the somewhat close correlation of chlorophyll with turbidity for that year. The 2013 spring turbidity peak may be associated with runoff during the significant storm events in April that year; events that may have driven the algal bloom indicated in the chlorophyll data during May through July.

Conductivity (S/m) data (Figure 6) for the two data sets are very similar, and appear to show higher conductivity during late summer/early fall period with more variability observed at the nearshore location during 2013. Also, there appears to be a trend of lower conductivity during December. The nearshore region is commonly subject to more variability due to influences of upwelling and riverine inputs, and this typically is observed in some of the water parameters like temperature, conductivity, and dissolved oxygen. While we are lacking dissolved oxygen data for 2013, the variability is observed in the conductivity and temperature data. However, the sensor was calibrated in too broad of a conductivity range to make rigorous interpretations of the much smaller changes in conductivity data.

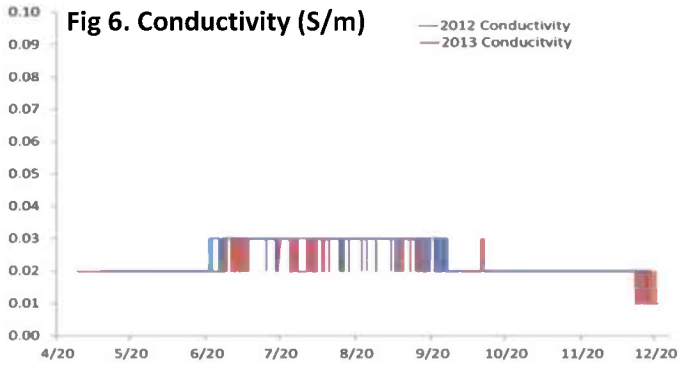

In summary, these data show seasonal trends during the April-December months at the 2012 mid-lake plateau and 2013 coastal locations. The data also allow for a general comparison between the sites, albeit in different years. More effort is needed to determine if the mounting location of the WQM in the moon pool is impacting data quality through such artifacts as biofouling of the buoy hull.

Report Authors:

Scott Kendall, Bopi Biddanda, Alan Steinman

Date: 4/3/2014

Annis Water Resources Institute
Grand Valley State University

740 West Shoreline Dr.
Muskegon, MI 49441.

Literature Cited:

Cuhel, R.L., and C. Aguilar. 2013. Ecosystem transformations of the Laurentian Great Lake Michigan by Nonindigenous Biological Invaders. Annu. Rev. Mar. Sci. 5: 289-320.

Appendix I

Offshore Bat and Bird Activity at the Lake Michigan Mid-lake Plateau, – Considerations for Wind Energy Development

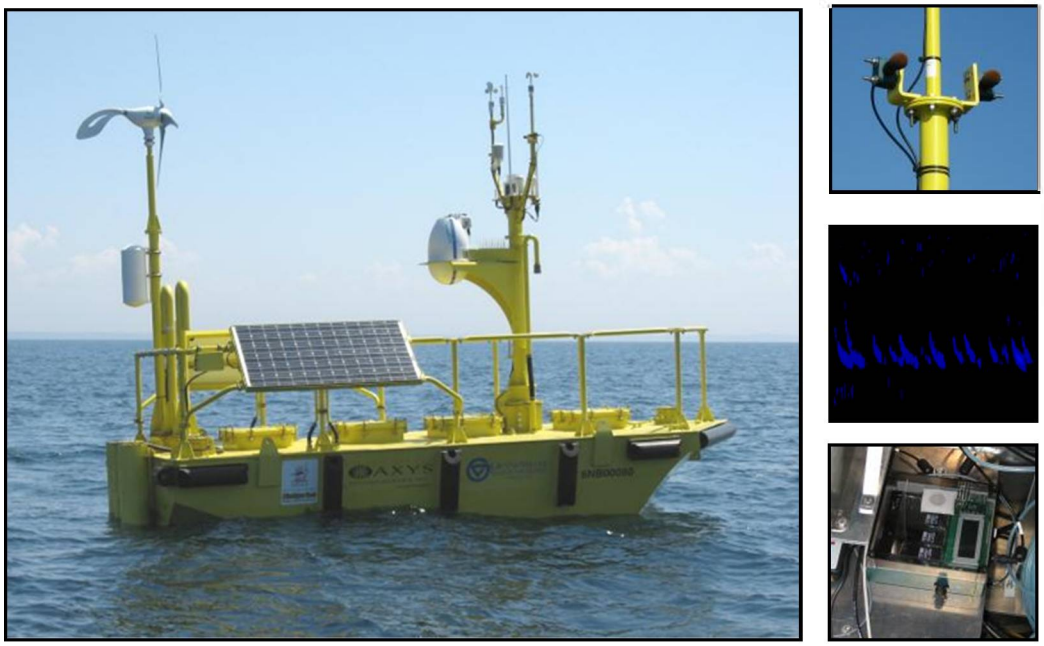

Prepared By:

Brian J. Klatt[1], T. Arnold Boezaart[2], Joelle L. Gehring[3], Kristen Walter[1], James B. Edmonson[4]

[1]Michigan Natural Features Inventory
Michigan State University
P.O. Box 30444
Lansing, MI 48909-7944

Prepared For:

Michigan Alternative and Renewable Energy Center
Grand Valley State University
200 Veridian Drive
Muskegon, MI 49440

25 April 2014

MNFI Report No. 2014-05

Author contact information:

[2] T. Arnold Boezaart, Michigan Alternative and Renewable Energy Center, Grand Valley State University, 200 Veridian Drive, Muskegon, MI 49440

[3] Joelle L. Gehring, Federal Communications Commission, 445 12th St SW, Washington, DC 20536

[4] James B. Edmonson, Edmonson Associates, Baton Rouge, La, and Muskegon, MI.

Acknowledgement: This material is based upon work supported by the Department of Energy; Grand Valley State University; Michigan Public Service Commission; We Energies; Sierra Club of the Great Lakes; Grand Valley State University; Michigan State University, Michigan Natural Features Inventory; and the University of Michigan, under Award Number DE-EE0000294. And the following organizations for technical support: National Oceanic and Atmospheric Administration/Great Lakes Environmental Research Laboratory; National Data Buoy Center; Pacific Northwest National Laboratory; United States Coast Guard; United States Army Corp of Engineers; Michigan Department of Natural Resources; and West Michigan Energy Partners.

The authors would like to acknowledge the help of Leonard Zaug of Andrie Marine Services for his invaluable aid in logistics in servicing the buoy and its monitoring equipment throughout this study.

Suggested Citation:

Klatt, B. J., T. A. Boezzart, J. L. Gehring, K. Walter, and J. Edmonson. 2014. Offshore Bat and Bird Activity at the Lake Michigan Mid-lake Plateau – Considerations for Wind Energy Development. Michigan Natural Features Inventory, Michigan State University, Report Number 2014-XX, Lansing, MI.

Cover photographs by Brian Klatt.

Table of Contents

List of Figures

List of Tables

EXECUTIVE SUMMARY

Many offshore areas of the Great Lakes are believed to possess wind resources adequate for the efficient generation wind energy. However, this supposition is based on modeling of onshore winds projected out into the lakes. To better assess the actual wind resources available, the Michigan Alternative and Renewable Energy Center (MAREC) of Grand Valley State University assembled a team of researchers to study the issue of offshore wind energy development. The team oversaw the design and construction of a research buoy that included instrumentation to assess a variety of offshore conditions, including actual wind speeds at various assumed wind turbine hub heights. As a member of the MAREC team, the Michigan Natural Features Inventory (MNFI) of Michigan State University installed acoustical monitoring instrumentation on the buoy to monitor bird and bat activity over the lake. The buoy was deployed at the Mid-lake Plateau of Lake Michigan during the period of April to December 2012.

During the deployment, bat activity was assessed by monitoring for bat echolocation calls from one half hour before sunset until one half hour after sunrise, using a SM2Bat+ monitor, recording in full spectrum. Recorded calls were analyzed using Sonobat software, which attempts to classify bat calls as to species based on over 60 call characteristics. 177 calls were classified to species, with 3 species accounting for the majority of the calls; the eastern red bat, silver-haired bat, and hoary bat; each accounted for approximately 40-60 calls. Calls from the little brown bat and the big brown bat were also represented in the recordings. The distribution of calls throughout the deployment indicate that there is a fairly steady level of bat activity over the lake throughout the spring, summer, and fall months, with the last bat call recorded at the end of October. This is the first systematic documentation of bat activity in far offshore (over the horizon) areas of the Great Lakes.

Bird activity was monitored during daylight hours, also using the SM2Bat+ monitor. The bird call recordings were analyzed using Raven software. A total of 2773 bird calls were classified with the majority (2697) being identified as gulls. Also represented were Forster's Tern, Red-winged Blackbird, and American Goldfinch; 36 calls could not be identified beyond general groups (e.g. passerine). All non-gull calls were recorded by early June, after which bird activity remained

constant but low.

INTRODUCTION

Wind energy is generally considered "green" from an environmental point of view due to the fact that it does not depend on non-renewable natural resources as fuel and consequently avoids some of the adverse effects of greenhouse gases and other air pollutant production, as well as the effects of coal mining and oil and gas drilling. Nonetheless, the development and operation of wind energy facilities is not without the potential for negative environmental impacts. The potential impacts of wind energy development, both positive and negative, have been reviewed by the National Academy of Sciences (NAS 2007) and included examination of impacts related to: air quality, culture, human health and well-being, local economic and fiscal conditions, electromagnetics, and ecological resources, with a focus on birds and bats.

Bird and bat fatalities associated with land-based wind energy facilities in North America have been well documented (NAS 2007). While at the time of the NAS study, reliable estimates of the fatality rates for birds and bats associated with wind turbines were considered not readily available, it was generally thought that mortality rates for both birds and bats were dependent on the specific situation, with higher bat fatality rates being reported in the Eastern United States (NAS 2007). Since the NAS study, more data has become available and separate reviews of fatalities for birds and bats have been conducted and estimates considered more reliable have been made.

Strickland et al. (2011) reviewed bat fatality rates and found them to vary from 0.07-39.7 fatalities/MW/Year, with the highest rates associated with forested, mountain ridge tops. Based on reported fatality rates in the literature, Smallwood (2013) estimated that there were 888,000 bat fatalities at 51,630 megawatts (MW) of installed wind-energy capacity in the United States (U.S.) in 2012, or approximately 17 bat fatalities/MW/year, or 34 bat fatalities/turbine assuming an average 2MW turbine. Hayes (2014) estimated that 600,000 bats

were killed in 2012 in connection with wind turbines at 51,000 MW of installed capacity, or approximately 12 bat fatalities/MW/year, or 24 bat fatalities/turbine.

For birds, Smallwood (2013) estimated 573,000 bird fatalities/year (including 83,000 raptor fatalities) at 51,630 MW of installed wind-energy capacity in 2012, or approximately 11 bird fatalities/MW/year, or 22 bird fatalities/turbine.

Fatalities can result from either direct interaction with turbines, i.e. individuals are struck by turbine blades or they collide with monopoles (Kunz et al., 2007). Additionally, bats may die from barotrauma, i.e. lung damage resulting from rapid decompression due to turbulence associated with wind turbines (Baerwald et al. 2008). Regardless of the exact mechanism, a wide variety of bird and bat species are known to suffer morality due to wind turbines, including 15 of the 45 species of bats in the U.S. and 8 of the 9 species of bats that occur in Michigan (NAS 2007). Wind farm fatalities include a variety of high-profile species, such as bald and golden eagles, and have included at least one endangered species of bat, the Indiana bat (*Myotis sodalis*), as well as three bat species currently at various stages of consideration for listing under the Endangered Species Act, these are: northern long-eared bat (*Myotis septentrionalis*), eastern small-footed bat (*Myotis leibii*), and the little brown bat (*Myotis lucifugus*).

The above discussion is based entirely on land-based wind energy facilities, which reflects the current state of wind energy development in the U.S.. However, onshore measures and modeling suggest that significant wind resources exist in various offshore areas of the U.S., including the Great Lakes. The Wind Energy Resource Zone Board (WERZB), a group commissioned by the Michigan Economic Development Council to investigate the potential of offshore wind resources, reports that winds adequate for the efficient generation of electrical energy on a commercial scale are associated with many of the coastal areas of Michigan (WERZB 2009). Also in light of this potential, Governor Jennifer Granholm created the Great

Lakes Wind Council "to identify permitting criteria and the most favorable and least favorable places for wind development because it is likely that in the near future wind energy developers will approach the State of Michigan with proposals to build offshore wind energy systems in the Great Lakes" (Great Lakes Wind Council (GLWC 2009)). The Council's report, often referred to as the Great Lakes Offshore Wind Report (GLOW Report), identified a number of areas considered suitable for offshore wind facility development (GLWC 2009).

These reports were based primarily on "desk top studies", i.e. on information not collected in the field, such as modeling of wind speeds out into the lakes based using onshore data. So too, the assessment of environmentally suitable areas identified in the GLOW report were based primarily on non-ecological information, which, except for substrate, near-shore, and fisheries information, is largely not available. Yet, decision makers need sound information on both the actual wind and biological resources present in offshore areas for development of wind energy facilities that are sound from both economic and environmental perspectives. The very real need by decision makers for such information provided the impetus for the study being reported on here, which is part of a multi-disciplinary, multi-institutional effort.

The Michigan Alternative and Renewable Energy Center (MAREC) of Grand Valley State University (GVSU) obtained funding for and assembled a research team including representatives from GVSU, the Michigan Natural Features Inventory (MNFI) of Michigan State University Extension, Michigan Technological University, and the University of Michigan for the "Lake Michigan Offshore Wind Assessment Project". The team established a number of research objectives related to the development of offshore wind energy facilities; these objectives, among others, included collecting data on the following offshore aspects: 1) actual wind speeds at various potential wind turbine hub heights; 2) physical conditions in terms of wave action; 3) water chemistry; and 4) biological resources. This report focuses on the fourth objective, namely the presence and activity levels of birds and bats in offshore areas. While bird activity in the Great Lakes has received attention in the past and has been addressed in other

studies by MNFI, as well as herein, this study represents the first systematic assessment of bat activity in far offshore ("over the horizon") areas of the Great Lakes.

MONITORING METHODS AND ANALYSIS PROTOCOLS

General

The Lake Michigan Offshore Wind Assessment Project Research Leadership Team (RLT), led by MAREC-GVSU, oversaw the design and construction of a buoy that served as a research platform (see cover photo). This buoy was constructed by AXYS Technologies, Inc. of Vancouver, British Columbia, Canada, and was used to support instrumentation used by the RLT members in their respective studies.

The buoy was deployed at the Mid-lake Plateau of Lake Michigan (latitude 43.34°N, longitude 87.12°W) from 8 April through 17 December 2012 (Figure 1).

For the bird and bat activity assessment, an acoustical monitoring approach was selected, as it allowed for long-term monitoring without the need for constant human attendance of the instrumentation. In this approach, ultrasonic bat echolocation calls and audible bird calls are recorded and subsequently analyzed in order to classify the calls. Calls were recorded in a full-spectrum, compressed format using a SM2Bat+ acoustic monitor (see cover photo) equipped with a SMX-US ultrasonic and a SMX-II audible range microphones (Wildlife Acoustics, Inc.) connected to the monitor by 10-m cables. The microphones were mounted to the main mast of the buoy (see cover photos) and oriented toward the stern of the buoy to minimize spray reaching the microphones. Calls were recorded onto 32G SDHC cards. The monitor was powered by the onboard electrical system, which included a small wind turbine, solar panel, battery bank, and back-up generator.

For bats, the SM2Bat+ monitors were programmed to record in the ultrasonic range on a 15-minutes-on/15-minutes-off mode from one-half hour before sunset until one-half hour after sunrise (adjusted for specific latitude and longitude of the buoy) on a daily basis. To monitor for bird activity, the SM2Bat+ unit was programmed to record in the audible range in a 10-

minute-on/50-minute-off mode, when not monitoring for bats in the ultrasonic range, i.e. bird monitoring was during day light hours. The monitor was not run continuously in order to avoid over filling of the data cards, as the buoy could be serviced only infrequently due to its remote location.

Figure 1. Location of Buoy and Mid-lake Plateau, Lake Michigan

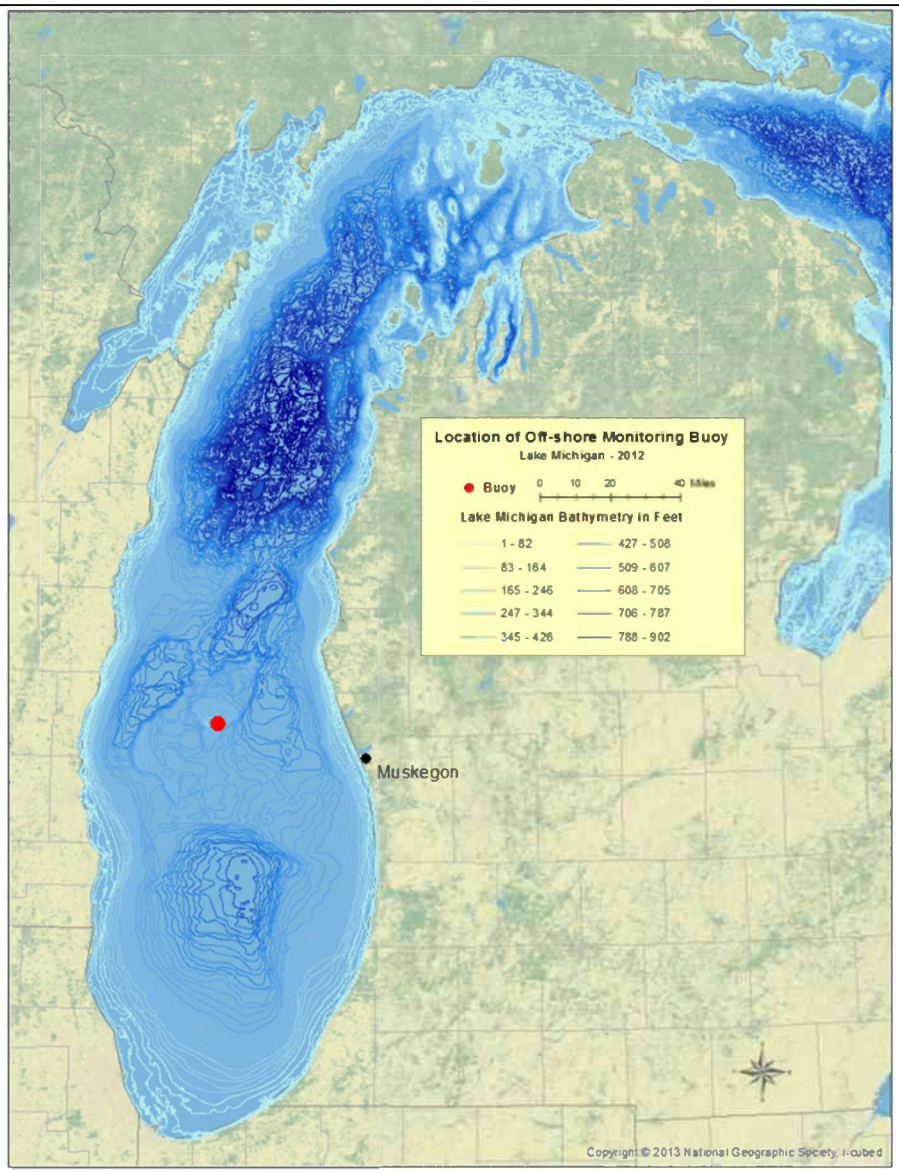

Bat Call Analyses

The compression format for field recordings, i.e. those actually made by the SM2Bat+ units, was a proprietary format referred to as ".WAC" (Wildlife Acoustics Compressed). Compressed field recordings were converted from .WAC format to standard .WAV format using Wildlife Acoustics, Inc.'s Kaleidoscope (v 0.3.1) software. To insure compatibility of .WAV files with subsequent Sonobat call analysis software, Kaleidoscope split the files into a maximum of 8-second segments; resulting files were filtered ("scrubbed") using a signal of interest of 8-120 kHz and 1-500 milliseconds duration. "Scrubbed", or noise files, i.e. those not containing a signal of interest, were not analyzed further.

Non-noise files were batched analyzed using Sonobat 3.1 NNE. The Sonobat software attempts to classify bat call passes/calls ("passes" consist of a series of individual "calls" made by a bat as it passes within range of the recorder). Passes containing calls of sufficient quality may be classified to species, species complex, or as "High" or "Low" frequency calls, using a discriminant function analysis of the highest quality individual call, discriminant classification "voting" on a series of individual calls, and expert opinion. While recorded passes were identified to species if possible, many species of bats are difficult to separate from one another using acoustic data; of particular note, the calls of the little brown bat and the Indiana bat overlap in many quantitative call measurements and may not be separable, as might also some calls of the silver-haired and big brown bats. For this study only the passes/calls classified with the highest confidence are reported. Pass classifications were generally accepted if Sonobat indicated the majority of individual calls in the pass were classified to a given species ("majority vote") or, there was even stronger evidence of a "consensus" on the pass, i.e. agreement between the votes and a high discriminant probability for a the highest quality call. While Sonobat is the most sophisticated software currently available and greatly facilitates classification (it simultaneously considers over 60 variables in each attempted discriminant classification), visual inspection of some sonograms indicated some misclassification by the software (echoes are particularly problematic in analyses); if clear

evidence of a different classification was present, the classification was adjusted accordingly.

Classified calls were tabulated and summarized as to species. It must be emphasized that screening and classification acceptance procedures outlined above underestimate actual bat activity. Many passes/calls recorded could only be classified to the "low frequency call" or "high frequency call" levels. Because these classifications can include signals that are of a mechanical or electrical origin, those passes are not reported here. Additionally, some recorded calls, though they may be visually observable in the sonograms, are of such poor quality (usually due to background interference or distance of the bat from the microphone), they too are not reported here.

Bird Call Analyses

As with the bat echolocation calls, the bird calls were recorded in .WAC format and converted to .WAV format using the Kaleidoscope software. The resultant .WAV files were analyzed using Cornell University Laboratory of Ornithology's Raven Pro 1.5 software. Files were analyzed in batches of one to five days at a time, depending on the number of selections generated. First, the spectrogram was altered for premium visibility. Overlap was increased to 96.1%, and brightness and contrast were both increased to 60. Then the Band Limited Energy Detector (BLED) was run using the following parameters:

- Minimum Frequency: 1000 Hz
- Maximum Frequency: 8000 Hz
- Minimum Duration: 0.1975 seconds
- Maximum Duration: 3 seconds
- Minimum Separation: 0.09875 seconds
- Minimum Occupancy (%): 70
- SNR Threshold (dB): 4.5 (above)

- Block Size: 1.99688 seconds
- Hop Size: 0.49938 seconds
- Percentile: 20.0

After running the BLED, if the selections made using these parameters exceeded 1,000 for one day's worth of data, then an exclusion band was used, filtering selections from 7500-8000 Hz at an SNR of 4.5. This largely eliminated many full-spectrum noises, such as waves or noise produced by the on-buoy generator. The selections were viewed in a grid of 36 at a time using the selection review tool. Each selection was inspected, and if a bird call was suspected, then the selection was played. The listener determined whether the noise was avian, and if so, which species, if possible. This was determined by personal identification skills supplemented by comparison to known calls in audio and/or spectrogram form. A keystroke marked the selection with a four digit alpha code, for example "g" for GULL, or "f" for FOTE. If more than one bird call existed in a visible time window and it was not obvious that more than one bird was vocalizing (for example, overlapping), only one call would be counted in order to minimize exaggerating bird counts. Once all valid selections were marked, all empty selections were then deleted from the table, and the remaining bird calls had the "Begin File" feature added in order to add the exact date and time to each call. Both the audio files and the text table for those selections were then saved.

RESULTS

Bats

Figure 2 presents the first bat call recorded from "over the horizon" areas of Lake Michigan and was made on 12 May 2012. As indicated in the screen shot, Sonobat classified this pass as being made by a silver-haired bat.

Figure 2. Sonogram of First Bat Call Recorded from "Over the Horizon" areas of the Great Lakes (Lake Michigan).

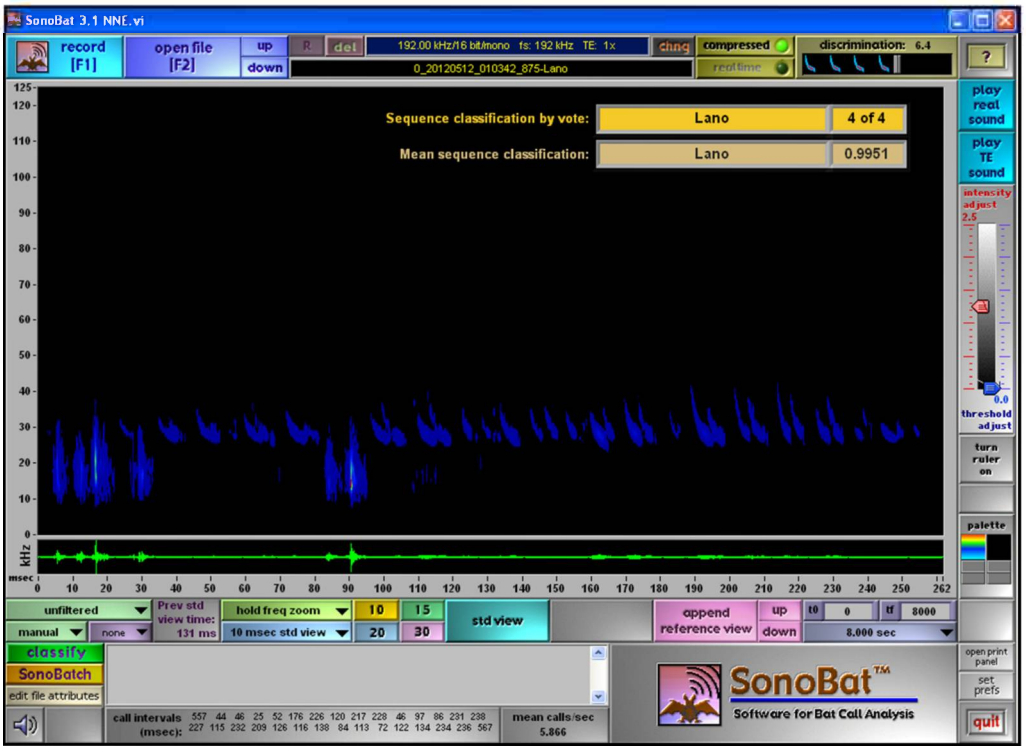

In all, 5 of the 9 species of bats native to Michigan were detected during the study. Table 1 presents a list of the species as well as a tabulation of the number of call passes attributed to each during the May to December deployment. The three species of tree bats (eastern red bat, silver-haired bat, and hoary bat), which are also the long-distance migrating species in Michigan, dominated the calls from a frequency perspective.

Table 1. Bat Species Detected and Number of Detections.	
Species	**Number of Pass Calls Classified**
Eastern Red Bat	66
Silver-haired Bat	63
Hoary Bat	42
Little Brown Bat	5
Big Brown Bat	1
Total	177

Figure 3 presents the distribution of calls by the different bat species throughout the study period. As is evident from the figure, there was a sustained level of activity out in the lake throughout the season.

Figure 3. Number of Classified Bat Call Passes by Study Week (2012).

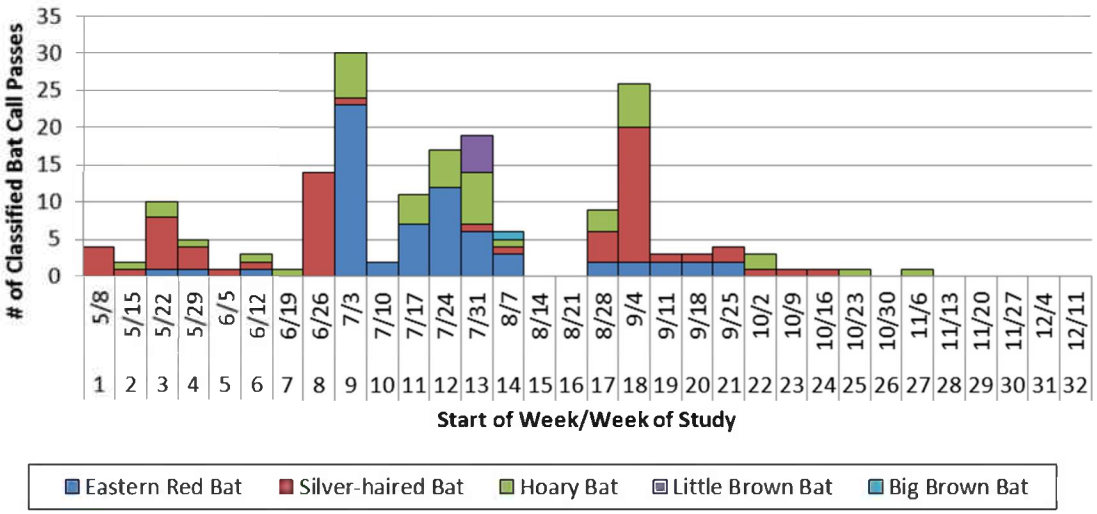

Birds

Table 2 presents the number of bird calls recorded throughout the deployment, totaled by

species or group. As can be seen, gulls were overwhelming represented in the calls. Only three species of birds could be unambiguously identified from the recordings.

Table 2. Number of Bird Calls Recorded by Species or Group.	
Group/Species	**# of Calls**
Gull	2697
Red-winged Blackbird	15
Forster's Tern	18
American Goldfinch	7
Unknown passerine	20
Unknown low frequency	3
Unknown high frequency	13
Total	**2773**

Figure 4 presents the distribution of calls by the different bird species throughout the study period. As with the bats, there was a low but persistent level of activity indicated throughout the deployment.

Figure 4. Classified Bird Calls by Study Week (2012).

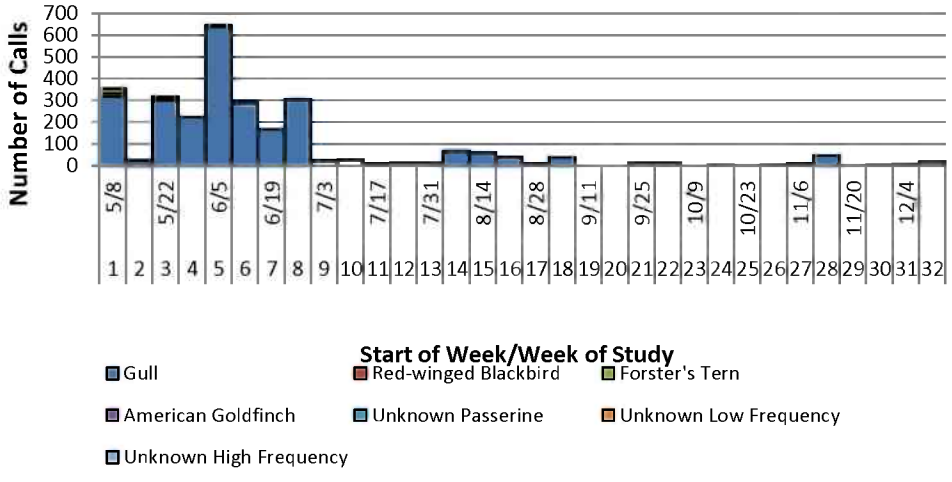

DISCUSSION

The development of offshore wind energy facilities in the U.S. is in its infancy. It has lagged development of on-shore facilities in the U.S. due to the technical and financial challenges of construction and operation in offshore areas and has lagged development of offshore facilities in Europe due to both differing conditions (the North Sea is relatively shallow) and differences in the general interest in development of alternative energy. However, it can be presumed that as technical challenges are met and associated costs are reduced, offshore wind energy will increase in development in the U.S. due to the abundance of wind resources along the coasts, including the Great Lakes.

While wind energy is generally considered a "green" energy source, like any other industrial scale effort, there are environmental concerns with wind energy production. One of the primary concerns with development of on-shore wind energy has been the association of wind farms with bat and bird fatalities (NAS 2007). We have learned a lot from the various studies conducted in association with on-shore facilities, such as those at the Altamont Pass facilities, and we have the opportunity to apply those lessons as we go forward with offshore facilities. One of the first steps in sound decision making is to insure that the decision makers have the most complete and reliable information possible. Consequently, studies such as the Lake Michigan Offshore Wind Assessment are necessary in gathering the information that can guide offshore wind farm development. This study will help fill essential information gaps, such as what, in fact, are the wind resources in offshore areas and do we have the same concerns regarding potential bird and bat fatalities as we do with onshore facilities. While some information exists regarding offshore bird activity, primarily in terms of waterfowl, virtually nothing is known concerning bat activity in far offshore, or "over the horizon", areas of the Great Lakes. The Lake Michigan Offshore Wind Study is the first systematic assessment of bat activity in offshore areas of Lake Michigan in relation to wind energy development.

Nine species of bat are known to occur in Michigan: big brown bat (*Eptesicus fuscus*), silver-

haired bat (*Lasionycteris noctivagans*), eastern red bat (*Lasiurus borealis*), hoary bat (*Lasiurus cinereus*), little brown bat (*Myotis lucifugus*), northern long-eared bat (*Myotis septentrionalis*), Indiana bat (*Myotis sodalis*), evening bat (*Nycticeius humeralis*), and the tri-colored bat (*Perimyotis subflavus*). Of these, all but the evening bat have been reported to incur mortality associated with wind turbines. However, mortality rates among species are not evenly distributed and on a nation-wide basis, the tree bats, i.e. silver-haired bat, eastern red bat, and hoary bat, account for 75% of all bat fatalities at wind energy facilities. Thus, it is significant that this study found that the vast majority of bat activity, as measured by call frequency, is attributable to these species.

Various explanations have been put forward as to why these species seem particularly vulnerable to wind turbine associated mortality. It is also noted that the highest rates of bat fatalities are found at mountain-ridge wind facilities; it has been suggested that the high rates of tree bat mortality is due to the bats using ridge tops as landmarks in navigation. The current study, along with others conducted by MNFI, suggests a different explanation is possible. Our study showed that the silver-haired, eastern red, and hoary bats all maintained a steady level of activity out over Lake Michigan throughout the study. While one might expect to detect these species out in the lake during migration periods (they are known long-distance migrators, spending the summers in the northern portion of the U.S., but migrating to southern states for the winter), their regular presence out in lake suggests that they are, in fact, foraging in the offshore areas.

This observation is consistent with findings by Klatt and Gehring (2013a, 2013b), who compared levels of bat activity in riparian areas versus adjacent open agricultural fields in southern Michigan and found that that the tree bats used the open areas to a greater extent than non-tree bats. This propensity to forage in open areas would put them in greater risk of encountering wind turbines, as wind farms are preferentially located in open areas, or as in the case of many ridge-top facilities, in areas where the forest has been opened up. Thus, it is

likely that, in the event of development of offshore wind facilities, that tree bat species will likely continue to incur a greater risk of fatalities that non-tree bats.

Total fatalities and risk at any given turbine, however, is also dependent on the likelihood of a bat encountering the turbine. While tree bats may forage in offshore areas, there appears to be far fewer individuals in offshore areas compared to nearshore or onshore areas. For example, in a study of bat activity along the shores of Lakes Michigan near Pentwater, Klatt and Gehring (2013b) recorded a number of calls for the eastern red bat, silver-haired bat, and hoary bat an order of magnitude larger in a shorter time frame than the number reported here for the entire deployment period. This pattern of reduced numbers of bats in offshore areas was also found on a finer scale by Ahlen, et al. (2007) who looked at levels of bat activity onshore and offshore, and in relation to prey abundance, in southern Scandinavia. Thus, while the tree bats may continue to be at risk at offshore wind facilities, the rate of fatalities in terms of fatalities/MW/year are likely to be far lower for offshore facilities relative to onshore facilities, due to a presumed lower density of bats out in the lake.

The low level of bird activity and diversity found in this study is somewhat surprising. Monfils and Gehring (2012, 2013) and Monfils (2014) have conducted aerial surveys of birds in northern and central Lake Huron and have found a wide range of species, including: Canada Goose (*Branta canadensis*), Mallard (*Anas platyrhynchos*), Canvasback (*Aythya valisineria*), Common Eider (*Somateria mollissima*), Surf Scoter (*Melanitta perspicillata*), White-winged Scoter (*Melanitta deglandi*), Long-tailed Duck *(Clangula hyemalis),* Bufflehead (*Bucephala albeola*), Common Goldeneye *(Bucephala clangula),* Common Merganser (*Mergus merganser*), Common Loon (*Gavia immer*), Double-crested Cormorant *(Phalacrocorax auritus),* Herring Gull (*Larus argentatus*), Great Black-backed Gull (*Larus marinus*), and Bald Eagle (*Haliaeetus leucocephalus*). However, waterfowl observations on offshore transects were dominated by sea ducks, especially Long-tailed Duck. Raw densities of waterfowl were greatest on nearshore transect segments and low on offshore segments, but very few

offshore segments lacked any waterfowl detections. Additionally, they recorded over 55,000 sitings of birds in ten surveys conducted in 2012 and 2013.

There are various possible explanations for the qualitative difference in results of the Gehring and Monfils studies and the current one. For example, the Lake Huron surveys included both nearshore, as well as offshore areas. The bird species that we detected in audio recordings (larids, passerines) were those that might be attracted to the buoy for loafing, whereas waterfowl species using offshore areas (i.e., sea ducks) are not likely to loaf on structure and might even avoid the buoy far enough to be outside the range of audio detection. These differences can have important implications for offshore wind energy development. Monfils and Gehring (2013) reviewed the literature related to waterbirds and waterfowl in relation to wind energy development. They found that the environmental concerns related to birds and wind energy development share similarities with those related to bats, including: direct mortality due to collision risk, habitat loss both during and after construction, and habitat fragmentation to mention a few. Additionally, as with bats, both onshore and offshore studies have determined that bird fatalities are most related to the location of the turbine in relation to landscape features and the frequency of use of that area by birds. If the differences between this study and the Lake Huron studies are related to the relative distances from shore and/or water depths, it would suggest that avian risks could be reduced by avoiding nearshore areas and placing turbines in over the horizon locations, perhaps using floating platforms.

It is interesting to note that the Red-winged Blackbird, American Goldfinch and the other unknown passerines were detected only early in the study, suggesting the detections reflected migration patterns. If such is the case, it would suggest that, given the limited range of the microphones, these migrating passerines may be flying at lower altitudes than commonly thought. Using NEXRAD radar, Schools, et al. (2012) demonstrated that migrating birds regularly form concentrations while ascending and descending during migration. As

they note, “While most nocturnal migrants fly at heights above typical rotor swept areas, birds may be particularly vulnerable to adverse interactions with wind turbines during periods of ascent and descent. Additionally, inclement weather may increase the probability of adverse interactions and decision makers should be particularly sensitive to these factors in high concentration areas.”

While the current study has developed significant new information with respect to the offshore activity of birds and bats, this is only a necessary first step in developing the information necessary for wind energy development in the Great Lakes. Siting of wind farms on the landscape and placement of individual turbines on a finer scale is likely one of the most important variables when attempting to minimize ecological impacts and we need to continue to develop information in this area.

LITERATURE CITED

Ahlen, I., L. Bach, H. J. Baagoe, and J. Pettersson. 2007. Bats and offshore wind turbines studied in southern Scandinavia. The Swedish Environmental Protection Agency, Bromma, Sweden.

Baerwald, E. F., G. H. D’Amours, B. J. Klug, and R. M. R. Barclay. 2008. Barotrauma is a Significant Cause of Bat Fatalities at Wind Turbines. Current Biology 18(16):R695-R696.

Great Lakes Wind Council. 2009. Report of the Great Lakes Wind Council. Public Sector Consultants and Mikinetics, Lansing, MI.

Hayes, M. A. 2013. Bats Killed in Large Numbers at United States Wind Energy Facilities. Bioscience 63:975-979.

Klatt, B. J. and J. L. Gehring. 2013a. Monitoring Bat Species Diversity in the Northern Thumb Area of Michigan Through the Use of Mobile Surveys. Michigan Natural Features Inventory Report No. 2013-04. Michigan Natural Features Inventory, Michigan State University Extension, East Lansing, MI.

Klatt, B. J. and J. L. Gehring. 2013b. Assessing Bat Community Structure in Riparian and Agricultural Habitats in a High Wind Resource Area of Southeast Michigan – A Preliminary Analysis. Michigan Natural Features Inventory, Michigan State University, Report Number 2013-05, Lansing, MI.

Klatt, B. J. and J. L. Gehring. 2013c. Bat Activity in High Wind-Energy Coastal Areas of Michigan - A Preliminary Analysis. Michigan Natural Features Inventory, Michigan State University, Report Number 2013-06, Lansing, MI.

Kunz, T. H., E. B. Arnett, B. M. Cooper, W. P. Erickson, R. P. Larkin, T. Mabee, M. L. Morrison, M. D. Strickland, and J. M. Szewczak. 2007. Assessing Impacts of Wind-Energy Development on Nocturnally Active Birds and Bats: A Guidance Document. Journal of Wildlife Management 71: 2449–2486.

Monfils, M. J. 2014. Monitoring and mapping avian resources in the nearshore and open waters of Lakes Erie, Huron and Michigan as an evaluation tool for potential offshore wind development and conservation planning: Michigan Natural Features Inventory Phase I final report. Michigan Natural Features Inventory, Report Number 2014-02, Lansing, MI.

Monfils, M. J., and J. L. Gehring. 2012. Identifying migrant waterfowl and waterbird stopovers to inform offshore wind energy development within Saginaw Bay. Michigan Natural Features Inventory, Report Number 2012-19, Lansing, MI.

Monfils, M. J., and J. L. Gehring. 2013. Identifying migrant waterfowl and waterbird stopovers to inform offshore wind energy development in the eastern Upper Peninsula. Michigan Natural Features Inventory, Report Number 2012-14, Lansing, MI.

National Academy of Sciences. 2007. Environmental Impacts of Wind-Energy Projects. Committee on Environmental Impacts of Wind Energy Projects, National Research Council. 394 pp. http://www.nap.edu/catalog/11935.html.

Schools, E. H., H. D. Enander, J. L. Gehring, B. J. Klatt, and C. A. Forgacs. 2012. Utilizing NEXRAD Weather Data and a Hotspot Analysis to Determine Bird Migration Concentration Areas. Michigan Natural Features Inventory, Report Number 2014-21, Michigan State University, Lansing, MI.

Smallwood, K. S. 2013. Comparing Bird and Bat Fatality-Rate Estimates Among North American Wind-Energy Projects. Wildlife Society Bulletin 37(1):19-33.

Strickland, M.D., E.B. Arnett, W.P. Erickson, D.H. Johnson, G.D. Johnson, M.L., Morrison, J.A. Shaffer, and W. Warren-Hicks. 2011. Comprehensive Guide to Studying Wind Energy/Wildlife Interactions. Prepared for the National Wind Coordinating Collaborative, Washington, D.C., USA.

Wind Energy Resource Zone Board. 2009. Final Report of the Michigan Wind Energy Resource Zone Board. Michigan Public Services Commission. Lansing, Michigan.

Appendix J

Estimating sound levels from a hypothetical offshore wind farm in Lake Michigan

Erik E. Nordman, Ph.D.

Acknowledgement and Disclaimer

Acknowledgements: "This material is based upon work supported by the Department of Energy; Grand Valley State University; Michigan Public Service Commission; We Energies; Sierra Club of the Great Lakes; Grand Valley State University; Michigan State University, Michigan Natural Features Inventory; and the University of Michigan, under Award Number DE-EE0000294. And the following organizations for technical support: National Oceanic and Atmospheric Administration/Great Lakes Environmental Research Laboratory; National Data Buoy Center; Pacific Northwest National Laboratory; United States Coast Guard; United States Army Corp of Engineers; Michigan Department of Natural Resources; and West Michigan Energy Partners."

Introduction

Operating wind turbines generate sounds from the spinning blades and electrical components. The sound from operating land-based turbines, and its potential impacts, has been thoroughly studied but the sound from offshore wind turbines has received less attention. This paper seeks to review the existing literature on sound propagation from offshore wind farms and estimate the potential sound impact on coastal residents and beachgoers from a hypothetical offshore wind farm in Lake Michigan, USA. The paper focuses on the airborne sound propagation from operating turbines. Sounds from the construction and decommissioning phases, as well as underwater sounds, are beyond the scope of this project, but are important considerations for wind farm developers.

Sound propagation from offshore wind farms

Sounds from offshore wind farms are produced during the construction, operation, and decommissioning phases of the wind farm life cycle. Construction of wind turbines using "monopile" foundations in which steel tubes are hammered into the sea or lake bed can emit significant sounds. This occurs for a relatively short time during the construction phase. Van Renterghem et al. (2014) found that sounds levels from piledriving depend strongly on several factors, including the size of the hammer, dimensions of the pole, characteristics of the sea floor, and weather conditions. A flat sea surface is most favorable to sound propagation. Waves and rough seas scatter the sound waves and inhibit propagation. Under most conditions, however, the noise impact would be very low (<40 dB(A)) at a distance of 10 km from shore.

Bolin et al. (2009) also emphasized the important role of weather conditions in propagating sounds from offshore wind turbines. In addition to the flat sea surface described above, atmospheric turbulence can also affect sound propagation. Under certain conditions in which an air current at relatively low height (<500 m) can trap sound causing it to reflect between the sea surface and air current. This results in greater propagation of the sound. Most of the sound, however, is dissipated as the range approaches 10 km. Under more turbulent atmospheric conditions, the sound is dissipated more quickly.

The Cape Wind project is currently under development off the coast of Massachusetts. The US Minerals Management Service (2009) conducted an environmental impact analysis which included estimates of sound propagation from the offshore turbines. Background sound levels were estimated to be as low as 35-40 dBA in some locations at certain times. The project proposes using 3.6 megawatt (MW) turbines located in Nantucket Sound about five miles from the mainland and nine miles from Martha's Vineyard. Sounds from operating wind turbines were estimated to be 12-26 dB(A) at onshore locations on mainland Cape Cod and Martha's Vineyard (five and nine miles away, respectively) which would be below the background sound levels. The assessment's noise impact from operating wind turbines was deemed negligible (Minerals Management Service 2009).

Zhao et al. (2011) conducted a study of offshore wind turbine noise for a hypothetical project in the Canadian waters of Lake Erie. The analysts used the WindPRO software package to estimate the sound levels at coastal residences. WindPro's noise module is based on the ISO 9613 sound propagation standard. The project featured fifteen 2 MW wind turbines located about 1 km from shore. Ontario's Ministry of Environment imposes a 43 dB noise limit from industrial noises in rural areas, including the study site. The study results showed that, under the assumed conditions, the turbine sounds would not exceed the 43 dB standard and, in fact, would not exceed 39 dB(A) at any of the coastal residences.

The literature on offshore wind farm sound propagation is limited but growing. The consensus is that offshore wind farms pose less of a noise nuisance than onshore wind farms. Sound may propagate farther because of the higher reflectivity of water compared to land, but the greater distances to receiver sites more than compensates for this. Examples from North America indicate that noise from

properly sited offshore wind farms will have a negligible impact on coastal residents. The next section describes the estimated impact from a hypothetical offshore wind farm in Lake Michigan, off the coast of Muskegon, Michigan, USA.

Analytical Methods

Baseline measurements

The study site was at the National Oceanic and Atmospheric Administration's Great Lakes Environmental Research Laboratory (GLERL) in Muskegon, Michigan. The GLERL office is located on the beach at the intersection of Lake Michigan and the Muskegon Lake channel. GLERL records meteorological data at the site, including wind speed at 24.4 m above ground level. Grand Valley State University has deployed the WindSentinel buoy which measures, among other things, wind speed at hub heights using a laser wind sensor. Wind data were collected at the GLERL weather station and at the buoy location six miles offshore in Lake Michigan.

Sound data were recorded using an industry-grade sound level meter. The microphone was mounted on a 2 meter stand outside of GLERL near the beach (Figure 1).

Sound levels were measured from 14 November 2014 to 25 November 2014. On 17 November, however, the study site experienced an intense thunderstorm with a tornado watch. The sound monitoring equipment was dismantled on 17 November and restarted on 19 November. This analysis is based on the post-storm data set. L_{90} is the sound level that is exceeded 90% of the time is an appropriate estimate for background noise at the receiving site.

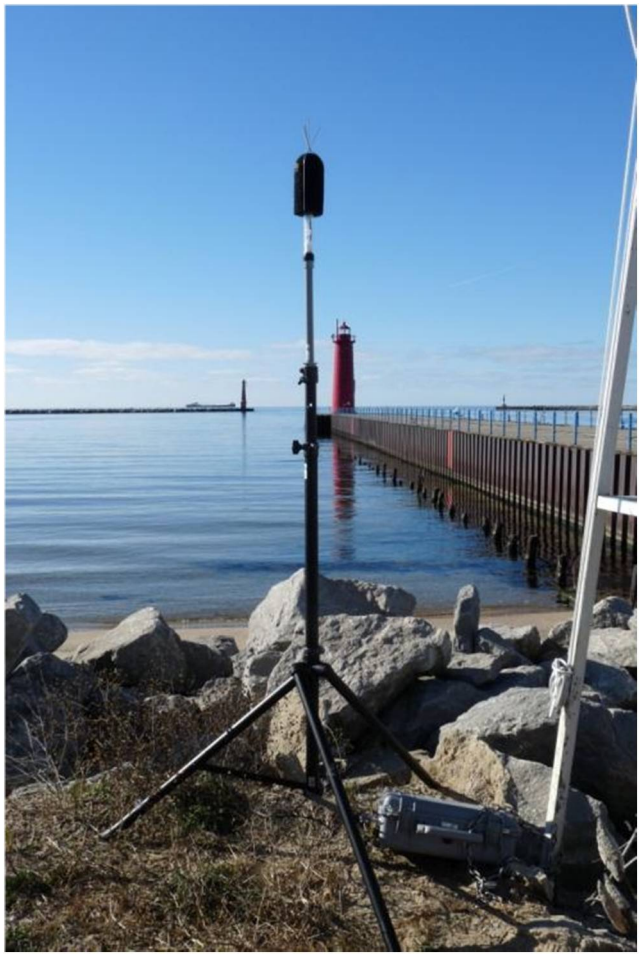

Figure 64: Microphone and sound level meter at the Great Lakes Environmental Research Laboratory.

Sound propagation model

Sound propagation from offshore wind turbines was estimated using sound models in the WindFarm software package (ReSoft 2014). WindFarm includes two industry-standard sound propagation models: one from the Danish Ministry of the Environment, National Agency for Environmental Protection (henceforth referred to as the Danish model); and the International Organization for Standardization (ISO 9613 Parts I and II, henceforth referred to as the ISO model).

The Danish model uses the following equation to estimate the sound level at a receiving house at 1.5 m above ground from one turbine:

$$L_p = L_{wa} - 10log_{10}\{2\pi r^2\} - ar$$

Where:

- L_{wa} is the sound source level in dB(A) re 1 pW
- *Lp* is the sound pressure level at the receiver in dB(A) re 20 µPascal
- *r* is the line of sight distance in meters between the source and receiver
- *a* is the attenuation coefficient in dB/m
- If L_{wa} exists as a single broadband sound power level, then a=0.005 dB m/s

Multiple turbines in a wind farm can be accommodated using the following equation:

$$L_p = 10log_{10}\left\{\sum_{j=1}^{j=m} 10^{L_{p(j)/10}}\right\}$$

Where:

- Turbines are numbered *j*=1…m
- All other elements same as above

The ISO 9613 model uses eight octave bands (63 Hz to 8000 Hz) to model sound propagation using the following equations

$$L_R = L_W + D_C - A$$

Where:

- L_R is the octave band sound power level (dB) at the receiver
- L_W is the octave band sound power level (dB) produced by the turbine
- D_C is the directivity correction which, for an omnidirectional point sound source, is zero
- *A* is the octave band attenuation (dB) between the source and receiver

Furthermore, octave band attenuation *A* is given by:

$$A = A_{div} + A_{atm} + A_{gr} + A_{bar} + A_{misc}$$

Where:

- A_{div} is the geometrical divergence
- A_{atm} is the atmospheric absorption
- A_{gr} is the ground effect
- A_{bar} is the barrier effect
- A_{misc} is the attenuation due to miscellaneous effects

WindFarm does not consider A_{bar} and A_{misc} in its noise propagation estimation. WindFarm uses the standard representation for divergence (spreading):

$$A_{div} = 20\log(d) + 10\log(4\pi) = 20\log(d) + 11$$

The atmospheric absorption coefficient is calculated for each octave band and is dependent on humidity and temperature. These values are included automatically by WindFarm when the humidity and temperature are specified. During the study period, temperature averaged 1.1°C and relative humidity averaged 69%. The ground attenuation effect is a function of the reflectivity of the ground surface. Water (and ice) is highly reflective and has a coefficient of 0. The roughness of water is 0.0002 m (Zhao et al. 2011).

Both the Danish model and the ISO 9613 model were used to estimate sound propagation from the hypothetical offshore wind farm in Lake Michigan. Researchers have noted that the ISO 9613 model is more accurate for calculating air absorption of sound (Søndergaard and Plovsing 2005)

Hypothetical wind farm

The hypothetical wind farm was composed of Vestas V90 3 megawatt (MW) turbines. This turbine model is in use at several European offshore wind farms. Two project configurations were considered: a single row of five turbines and two rows (offset) of five turbines each. In both scenarios, the turbines were spaced 800 meters apart within and between rows.

Vestas 90 turbines have a broadband sound power level at the source of 109.3 dB(A) and the following octave band sound power levels (Table 1) (Environmental Resource Management 2010).

Table 36: Sound power levels from eight octaves for the Vestas V90 3 MW wind turbine.

Frequency (Hz)	63	125	250	500	1000	2000	4000	8000	dB(A)
Sound Power Level	93.5	96.9	102.0	104.0	104.0	99.7	93.7	80.7	109.3

Results

Wind speeds at 24.4 m as measured by the GLERL weather station are listed in Table 2. Figure 2 illustrates the wind direction at GLERL during the study period.

Table 37: Wind speeds measured at GLERL (24.4 m) in 2013.

Time frame	Average wind speed (m/s)
2013 daily mean	5.9
2013 summer daily mean	4.4
6 day study period	7.3

The WindSentinel buoy, six miles offshore, recorded an average wind speed for November 2013 of 11.6 m/s and a maximum of 30.9 m/s at 125 m above water level. The maximum wind speed was observed during the storm on 18 November 2013.

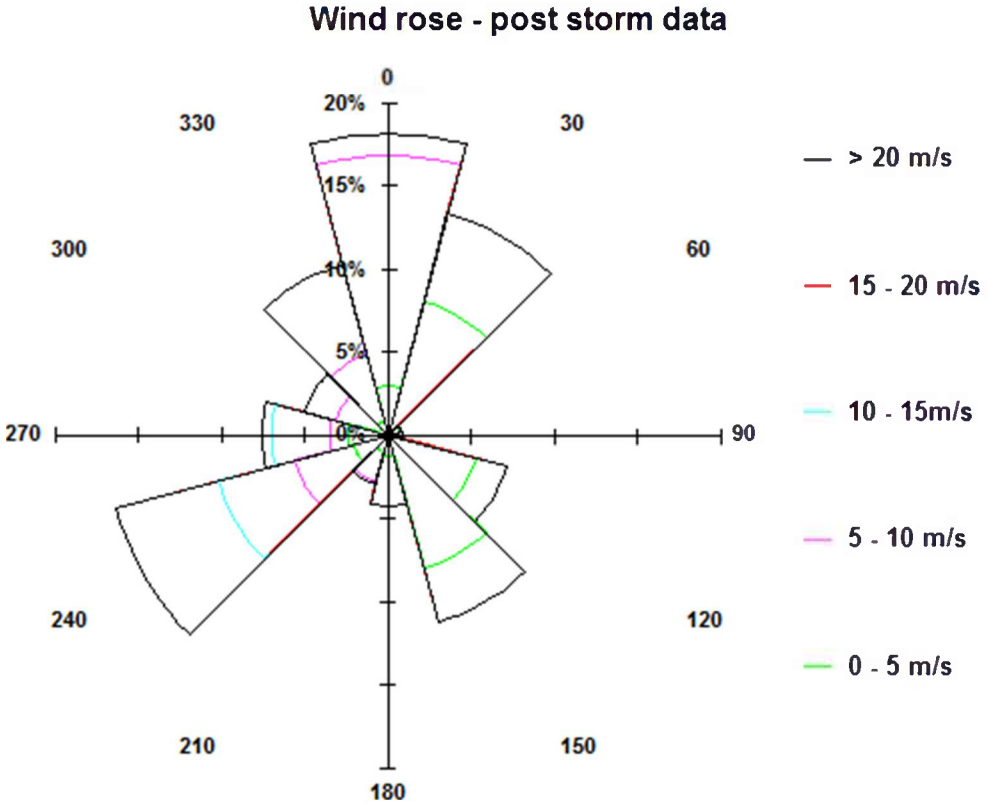

Figure 65: Wind rose for the study period.

The background noise at the receiver site (outside GLERL) during the study period was L_{AS90}=49.5 dB(A). The wind speed during the November study period was higher than the summer 2013 average, so it would be expected that summer background noise might be lower than 49.5 dB(A). Short-term sound measurements (~1 minute each) were taken right at the beach on a calm day. The lowest L_{AS90} reported during these short measurements was 47.4 dB(A) during which the 10 minute average wind speed was 3.9 m/s. The location of the short term measurements was about 10 meters closer to the water than the long-term measurements at the GLERL site.

The resulting sound levels at the receiver site for each sound propagation model and wind farm configuration under the most extreme wind conditions (30.9 m/s at 125 m) are listed in Table 3. The sound level under average wind conditions for November 2013 (11.6 m/s at 125 m) from the ten turbine configuration, ISO octave model, was 23.4 dB(A).

Table 38: Estimated sound levels at GLERL from a hypothetical wind farm six miles offshore.

Configuration	Danish, broadband	Danish, octave	ISO, octave
Five turbines	25.41 dB(A)	35.6 dB(A)	36.5 dB(A)
Ten turbines	27.4 dB(A)	38.2 dB(A)	39.0 dB(A)

Figure X illustrates the sound propagation using the ISO model, where numbers 1 through 10 are the turbines and H1 is the receiver location at GLERL.

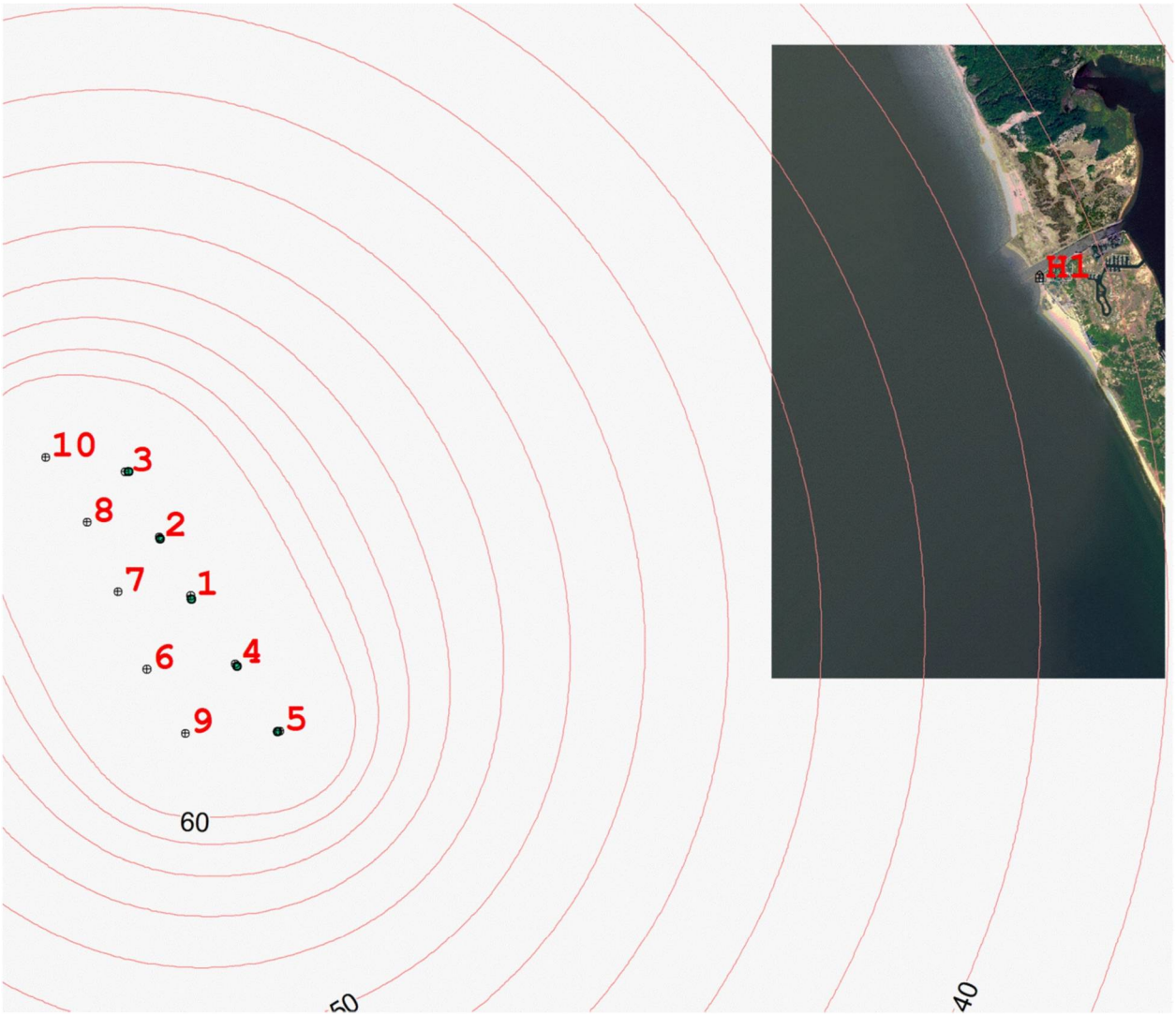

Figure 66: Estimated sound propagation from a ten turbine wind farm six miles offshore.

Discussion and conclusions

The background sound level (L_{AS90}) during the study period was 49.5 dB(A). The ten turbine configuration, under the most extreme wind conditions measured during the study period, produced a sound level at the receiver of 39.0 (ISO model). Under these conditions, the sound produced by the turbines would not be audible above the background noise (L_{AS90}) at the GLERL site. Only 0.89% of the sound observations during the study period fell below 39.0 dB(A). It is possible, but unlikely, that such conditions would occur it is extremely windy at the turbine site and very calm at the receiving site at the beach. The scenario presented here is a worst-case scenario and under these conditions the turbine sounds are masked by the background noise.

Winds are generally calmer in the summer months when people spend more time at the beach. The GLERL daily average data indicate that summer (Memorial Day to Labor Day) wind speeds average 4.4 m/s. The wind measurements on the calm November day averaged 3.9 m/s which is similar to a calm summer day. The background sound level (LAS90) right at the beach was 47.7 dB(A). This suggests that even under calm summer-like conditions, wind turbines sounds will not be audible above the background noise. Additional data are needed to understand the background noise levels at coastal locations during the summer months.

Literature Cited

Van Renterghem, T., D. Botteldooren, and L. Dekoninck. 2014. Airborne sound propagation over sea during offshore wind farm piling. Journal of the Acoustical Society of America 135(2):599-609.

Bolin, K., M. Boue, and I. Karasalo. 2009. Long range sound propagation over a sea surface. Journal of the Acoustical Society of America 126(5):2191-2197.

US Minerals Management Service. 2009. Cape Wind Energy Project Environmental Impact Statement. OCS Publication No. 2008-040.

Zhao, L., J. Liovas, and B. Danesh. 2011. Perspectives from the field: Environmental noise impact – Study for the proposed 30-MW offshore wind farms in Lake Erie. Environmental Practice 13(2):101-112.

ReSoft Ltd. 2014. WindFarm Release 4.2.

Søndergaard, B. and B. Plovsing. 2005. Noise from offshore wind turbines. Danish Ministry of the Environment – Environmental Protection Agency. Environmental Project No. 1016 2005.

Environmental Resource Management. 2010. Noise assessment: Hermosa West Wind Farm Project. Available at: https://ww2.wapa.gov/sites/western/transmission/interconn/Documents/hermosawest/noiseassessment_030210.pdf. Accessed 9 March 2014.

Appendix K

RESEARCH ARTICLE

Behavioral approaches to environmental policy analysis: a case study of offshore wind energy in the North American Great Lakes

Erik Nordman

Natural Resources Management Program, Biology Department, Grand Valley State University, Allendale, Michigan 49401, USA

Acknowledgement and Disclaimer

Acknowledgements: "This material is based upon work supported by the Department of Energy; Grand Valley State University; Michigan Public Service Commission; We Energies; Sierra Club of the Great Lakes; Grand Valley State University; Michigan State University, Michigan Natural Features Inventory; and the University of Michigan, under Award Number DE-EE0000294. And the following organizations for technical support: National Oceanic and Atmospheric Administration/Great Lakes Environmental Research Laboratory; National Data Buoy Center; Pacific Northwest National Laboratory; United States Coast Guard; United States Army Corp of Engineers; Michigan Department of Natural Resources; and West Michigan Energy Partners."

Abstract

Behavioral economics, including prospect theory, offers new approaches to environmental policy analysis. The utility of behavioral approaches to environmental policy analysis is illustrated using a case study of offshore wind energy policy in Michigan, USA. Michigan has attempted to clarify the permitting process for offshore wind energy but those efforts have failed. Prospect theory suggests that Michigan legislators are, for the most part, risk averse to policy reforms as the state emerges from its "one-state recession" and into a gains domain. Legislators from some coastal districts perceive offshore wind development as a threat to coastal quality of life, are risk-seeking for policy reforms, and have introduced bills banning offshore wind energy. Framing the discussion from a loss perspective (losing out to competing states) may be an effective strategy for passing offshore wind policy reforms. Results suggest behavioral approaches have utility for other environmental policy challenges, such as climate change.

Keywords: offshore wind energy; Great Lakes; Michigan; prospect theory; behavioral economics

Introduction

Offshore wind energy, though well-established in Europe and gaining traction in Asia, is only taking tentative steps in North America. The US Department of Energy identified cost and permitting

uncertainties as two critical roadblocks that must be overcome for offshore wind to be competitive with other energy sources (Beaudry-Losique *et al.* 2011). The US federal government, particularly the Bureau of Offshore Energy Management, Regulation, and Enforcement (BOEMRE) has clarified and streamlined the permitting process for offshore wind energy development in the federal waters of the outer continental shelf. BOEMRE, however, has no jurisdiction in the US waters of the North American Great Lakes – these are left, primarily, to state governments.

Michigan, like most other Great Lake states, lacks a clear permitting process for offshore wind energy development. Michigan's offshore wind resources could support as much as 36,000 MW of generating capacity after accounting for suitably shallow waters and a shoreline buffer (Adelaja *et al.* 2012) and even more if the potential for deep-water floating turbines is included. The permitting uncertainty also causes anguish among lakeshore community residents, some of whom would rather not see such development at all. A promising start to regulatory clarification in Michigan has bogged down into policy paralysis. Understanding the underlying causes of the policy paralysis is a necessary first step toward the appropriate regulation of this energy resource in Michigan, other Great Lakes states, and the Canadian province of Ontario (which shares jurisdiction of the Great Lakes). Behavioral approaches to environmental policy, such as prospect theory, may be appropriate tools for understanding, and breaking through, the policy paralysis on offshore wind energy and other environmental challenges.

My goal in this paper is to understand, using prospect theory, how policy processes may become paralyzed. I use the example of offshore wind energy in Michigan, USA, as a case study in the causes of policy paralysis and the means to advance the process. The paper begins with an introduction to prospect theory followed by a summary of the current state regulations, why they are insufficient, and the outcomes and recommendations of an expert panel convened. The section also includes relevant actions at the federal level. Next, I use prospect theory to analyze two proposed bills: one facilitating offshore wind energy and the other banning it. I suggest options to move the policy process ahead including those suggested by other authors. Finally, I move out of the case study to look at the broad implications for using behavioral approaches to understand environmental policy challenges more broadly, such as climate change and hydraulic fracturing ("fracking") for natural gas.

Behavioral approaches to environmental policy analysis

Behavioral economists have shown that people often deviate from the actions expected under rational choice theory and make decisions that, on the surface, appear less than optimal. Over the last twenty years, prospect theory has both illuminated the limitations of the rational choice model and provided more refined insights into human decision-making. What follows is a brief summary of prospect theory and its application to governmental choices.

Prospect theory, as first described by Kahneman and Tversky (1979), presents an alternative approach for analyzing decision-making behaviors. Prospect theory

> "posits that individuals evaluate outcomes with respect to deviations from a reference point rather than with respect to net asset levels, that their identification of this reference point is a critical variable, that they give more weight to losses than to comparable gains, and that they are generally risk averse with respect to gains and risk acceptant with respect to losses" (Levy 1992 p. 171).

These three concepts of prospect theory – the reference point or frame; the idea that "losses loom larger than gains" (Kahneman and Tversky 1979); and risk averse behavior are described in more detail below. Kahneman and Tversky's work was summarized well in *Thinking, Fast and Slow* (Kahneman 2011). According to prospect theory, people are sensitive to *changes* in wealth – gains, losses and neutral outcomes – rather than *states* of wealth. The theory also suggests that the pleasure of a gain is weaker than the pain of a loss of an equivalent amount. For example, a purely rational actor would accept a bet in which a coin toss of heads won her $150 and tails lost her $100 – the expected value of the coin toss is a win of $25. However, experiments show that the pain of losing $100 is greater than the pleasure of winning $150 and the bet is often rejected. This anomaly to rational expectations is called loss aversion (Kahneman 2011).

Because losses loom larger than gains when people are faced with choices, they tend to stick with the status quo. Moving away from the status quo involves some risk. People tend to fear the pain of the downside risk more than they enjoy an equivalent degree of upside risk. This "status quo bias" can prevent people from making choices that may otherwise be beneficial. Levy describes the status quo bias as follows:

> "If an individual frames a choice problem around the existing status quo, she will treat the costs of moving away from the status quo as a loss and the benefits of moving away from the status quo as a gain, overweight the former relative to the latter, and consequently demonstrate a tendency towards remaining at the status quo" (Levy 1992, p 222).

Another reason for status quo bias is what Richard Thaler (1980) called the endowment effect. People evaluate changes from a reference point and people are less willing to part with something they already have than are willing to make a purchase to obtain it.

Prospect theory also illustrates the consequences from the way in which the choice is framed. That is, changing the reference point can alter a person's preference. In one experiment using a hypothetical disease outbreak, respondents chose between conservative (risk averse) and aggressive (risk seeking) disease mitigation options. The options were variously presented in terms of how many people would survive or how many would die, even though the death rate in both scenarios was identical. When presented with the survival frame, more respondents chose the more conservative (risk averse) program but chose the more aggressive approach (risk seeking) when presented with the mortality frame (Kahneman 2011). Businesses use the framing effect when offering, for example, cash discounts rather than credit card surcharges (Levy 1992).

The elements of prospect theory combine into a "fourfold pattern" of decision making under risk and uncertainty. Decision outcomes (Table 1, Boxes 1-4) can be grouped according to whether their risk (high or low probability) and the type of outcome (gain or loss). Table 1 describes an actor's likely decision-states (risk averse or risk seeking) relative to a hypothetical $10,000 bet. The alternative choice (B) in each case is a guaranteed outcome that is the expected value of Choice A (e.g. $95\% \times \$10{,}000 = \$9{,}500$). The rational decision-maker should be indifferent between the choices because the expected outcomes are identical. However, behavioral economists have shown that people predictably deviate from this rational expectation. Box 1 explains why some litigants accept less favorable settlements even though they are almost sure to win. Box 2 explains the popularity of lottery tickets. Box 3 explains why gamblers continue to make risky bets when they are down. Box 4 explains why people buy insurance (Kahneman 2011).

[Insert Table 1 approximately here]

Policy reforms involve risk and uncertainty, losses and gains, and reference points. Prospect theory, therefore, can provide some guidance on how the actors make or do not make these reforms. Vis and van Kersbergen (2007) applied prospect theory to the workings of political actors.

Vis and van Kersbergen (2007) predict that "policy makers avoid risks as long as they consider themselves in the domain of gains, that is, they see their current situation as still acceptable or tolerable" (p. 159). That is, the policy maker is in Box 1 in Table 1 and is in a risk-averse setting. When presented with the options of a) preserving the status quo (no reform) or b) a reform that has an overall positive expected value but does involve some smaller risk of loss, then the policy maker is likely to be risk averse to gains and choose the status quo. Policy makers will choose the risky reform when they perceive themselves in a loss domain and "are confronted with a choice between (a) the status quo (no reform) and (b) some gamble (reform) with both an expect value of *further loss* (further electoral loss) and some smaller prospect for improvement (an electoral reward smaller than the expected loss)" (Vis and van Kersbergen 2007, p. 159). This position aligns with Box 3 in Table 1.

Vis and van Kersbergen (2007) also applied the logic of prospect theory to voters. Like their policy maker counterparts, voters in a gains domain and choosing between the status quo and an uncertain but likely positive reform will opt for the status quo (Box 1). Voters in a loss domain choosing between the status quo and an uncertain but likely further loss – but a small opportunity for improvement – will be risk seeking and opt for the reform (Box 3).

Behavioral economics, including prospect theory, is increasingly being applied to environmental policy analysis. Pollitt and Shaorshadze (2013) described how behavioral economics affected household energy consumption habits, energy efficiency investments, and pro-environmental behavior. Venkatachalam (2008) reviewed some of the behavioral anomalies that plague environmental policy-making and implementation, such as the endowment effect, gaps between willingness to pay and willingness to accept for environmental goods and services, and time-inconsistent behavior. Most of the behavioral

critiques of environmental and energy policy, including those above, focuses on the individual consumer. Environmental and energy policy analysis can benefit by incorporating behavioral approaches such as prospect theory, as demonstrated in this paper.

Tentative steps toward offshore wind policy: 2008-2010

The Permitting "Dry Run" and the Michigan GLOW Council

In 2008, the Michigan Economic Development Corporation convened a workshop to assess the legal barriers to permitting offshore wind energy development in Michigan's portion of the Great Lakes. The offshore turbines can access the lakes' outstanding wind resources and thus can produce more electricity but they require specialized foundations and vessels and pose challenges for operations and maintenance in bad weather – all of which increase project costs. Given the tedious (now completed) permitting process for the Cape Wind offshore wind project in Massachusetts, it was believed that Michigan's untested regulatory process could inhibit prospective developers. The "dry run" was an attempt to explore the existing permitting and bottomland leasing process, identify shortcomings and uncertainties, and develop proposals to make Michigan "development ready" for offshore wind energy.

The dry run used two hypothetical offshore wind proposals to assess which state and federal agencies would be involved, which legal statutes would be invoked, and how the public would be involved. The dry run itself, however, did not include public participation though the conveners recognized that such participation would be an essential component of any permitting process. The details of the dry run can be found in the project's final report (Klepinger 2008).

The dry run and subsequent Great Lakes Wind (GLOW) Council report found that the state's current review process "would prove inadequate and would likely lead to confusion within government agencies as well as for the applicant and the public" (Klepinger and Public Sector Consultants 2009, p. 4). The dry run participants found that the main permitting tool – the so-called Joint Permit – as currently written is not suitable for regulating offshore wind energy. The Joint Permit is administered jointly by the Michigan Department of Environmental Quality (MDEQ) and the US Army Corps of Engineers (USACE). The Joint Permit process allows applicants to file a single permit request for various construction activities in Great Lakes waters or on the bottomlands. The process was written with coastal and near-shore activities in mind, such as wharfs and marinas, and therefore only riparian landowners may file for a joint permit. Offshore wind developers presumably are not riparian owners (though they could be) and thus would be ineligible for a Joint Permit (Klepinger 2008, Mausolf 2012).

The Michigan Natural Resource and Environmental Policy Act (NREPA) Part 325 regulates the Great Lakes submerged lands. Michigan's Great Lakes bottomlands are held in public trust and as such the state has an obligation to "preserve and protect the interests of the general public in the lands and waters described" and "shall provide for the sale, lease, [or] exchange" of bottomlands whenever the public use of those lands and waters is not substantially affected or the public trust in the state will not

be impaired (M.C.L. 324.32502). Compliance with the law is detailed under Administrative Rule 322.1001 *et seq*. The USACE derives its regulatory authority on the Joint Permit from the Rivers and Harbors Act of 1899 (Section 10.33 U.S.C. §403) and the Clean Water Act (33 U.S.C. §1344 and §1251) (Klepinger 2008).

NREPA also provides the Michigan Department of Natural Resources (DNR) with some regulatory authority regarding activities related to offshore wind energy development including, but not limited to, endangered species protection (Part 365), wildlife conservation (Part 401), commercial fishing (Part 473), and marine safety (Part 801) (Klepinger 2008). Other state and federal agencies have coordinating roles, such as the Federal Aviation Administration (FAA), US Coast Guard (USCG), US Environmental Protection Agency (EPA), Federal Energy Regulatory Commission (FERC), Michigan Department of Transportation (MDOT), Michigan Public Service Commission (MPSC), and local planning and zoning boards under the Michigan Zoning Enabling Act (MZEA). These directives are summarized in Table 2 and the complete list can be found in the dry run report (Klepinger 2008).

[Insert Table 2 approximately here]

Recommended legal changes

In 2008 Governor Jennifer Granholm convened an expert panel (the Great Lakes Wind (GLOW) Council) to analyze the permitting issues around offshore wind energy, identify most suitable areas for offshore wind energy development, and recommend offshore wind policy reforms. The GLOW Council, in its 2010 final report, recommended that new legislation be adopted to specify the permitting criteria, the bottomlands leasing and public compensation structure, and the public engagement process for offshore wind energy. The final report included the following recommendations:

- "An acknowledgement that the existing Part 325, Great Lakes Submerged Lands, of Michigan's Natural Resources and Environmental Protection Act of 1994 (PA 451) does not regulate offshore wind energy facilities
- A process for identifying sites for offshore wind energy leasing
- A detailed set of requirements for site assessment plans, development plans, construction plans, operation plans, and decommissioning plans
- A process for public involvement in decision making, including notice and comment opportunities throughout the auction, site assessment, and development processes
- A framework for collecting lease payments and operation royalties and for distributing those funds to administer the regulatory program, to foster renewable energy production and energy efficiency, and to monitor the impacts of offshore wind facilities and offset any impacts through habitat protection and improvements in the Great Lakes" (Klepinger and Public Sector Consultants 2010).

The GLOW Council also drafted a map of most favorable, conditional, and categorically excluded areas for the leasing processes (Figure 1). The most favorable areas were constrained by 22 environmental, economic, and social criteria and limited to bottomlands that are greater than six miles from shore and less than 45 meters in depth (Klepinger and Public Sector Consultants 2010). Technology continues to evolve, particularly floating turbines designed for deep-water applications. For example, Glosten Associates is testing a tension-leg floating wind turbine platform designed for use in depths greater than 40 meters (Moon and Nordstrom 2010). Though the GLOW Council's mapping criteria reflected the time's deployable technology, it is becoming outdated as the years pass and available technology rapidly advances. Once the GLOW Council's reports were submitted, it was left to the state legislature to take up the recommendations.

[Insert Figure 1 approximately here]

Policy coordination at the federal and regional levels

As Michigan debated the GLOW Council recommendations, the federal government and Great Lakes states explored a regional approach to permitting. In 2012 several federal agencies and five of the eight Great Lakes states signed a memorandum of understanding (MOU) to create a Great Lakes Offshore Wind Energy Consortium. The purpose of the consortium is to "support the efficient, expeditious, orderly and responsible review of proposed offshore wind energy projects in the Great Lakes by enhancing coordination among federal and Great Lakes state regulatory agencies" (White House Council of Environmental Quality *et al.* 2012). The participants include Illinois, Michigan, Minnesota, New York, and Pennsylvania as well as the following federal agencies:

- White House Council on Environmental Quality
- Dept. of Energy
- Dept. of Defense
- Dept. of the Army
- Advisory Council on Historic Preservation
- Coast Guard
- Environmental Protection Agency
- Fish and Wildlife Service
- Federal Aviation Administration
- National Oceanic and Atmospheric Administration

The MOU clearly defines each participant's roles and responsibilities for the regulation of offshore wind energy as well as the statutes from which each derives this authority. The participants agreed, among other things, to create a "regulatory roadmap" that clearly articulates the regulatory review process and the information needed for such a review. The participants agreed to publish the roadmap within 15

months of signing the MOU (in March 2012) but as of this writing (January 2014) the roadmap has not been released.

Any offshore wind energy development in the Great Lakes will trigger an environmental impact statement under the National Environmental Policy Act. Agencies can use programmatic environmental statements (PEIS) to analyze the broad landscape, regional, or cumulative effects of regulated activities to reduce the need to redundantly analyze the broad impacts at the project-specific level (National Environmental Policy Task Force 2003). The Great Lakes Wind Collaborative (a multi-sectoral group for which the Great Lakes Commission serves as the secretariat), the State of Ohio, the Council of Great Lakes Governors, and the Michigan Great Lakes Wind Council have all suggested or formally requested that the White House Council on Environmental Quality (CEQ) initiate a PEIS to identify the up-front issues and impacts that would be common to all Great Lakes offshore wind projects, look at the cumulative effects of multiple projects, and encourage the Great Lakes states to proactively develop common standards and practices (Great Lakes Commission 2010). As of January 2014, no PEIS has been conducted and the reason for the lack of progress is unclear.

In September 2013, the Great Lakes Commission – whose membership includes all eight Great Lakes states (Ontario and Quebec have associate membership)– formally adopted a resolution stating that "the Great Lakes Commission believes a small-scale demonstration or pilot project is the most direct means of assessing the potential environmental impacts, and evaluating economic viability and opportunities for job creation involving offshore wind projects in the Great Lakes" (Great Lakes Commission 2013). The Commission's Great Lakes Wind Collaborative published an economic impact analysis of offshore wind energy development in the Great Lakes. A low-deployment scenario of 1,000 MW of Great Lakes offshore wind energy by 2030 could result in 12,500 full-time equivalent (FTE) construction jobs and 750 FTE long-term jobs. Under a high-deployment scenario of 5,000 MW by 2030, the construction phase FTEs climb to 121,700 and 3,900 FTE long-term jobs. The high-deployment scenario capital cost is $4,642/kW (Loomis 2013) which translates to a levelized cost of energy of approximately $0.20/kWh (US National Renewable Energy Laboratory 2013). Though this levelized cost is higher than currently deployed onshore wind energy and fossil fuel generation, technological innovation, experience with pilot projects, and saturation of lower-cost onshore sites may close the cost gap. The difference between the low- and high-deployment scenarios, and their economic impacts, is whether state and federal policies are in place to facilitate the orderly development of offshore wind energy in the Great Lakes region, including Michigan.

Proposed legislation: 2010-2012

Bills that incorporated the GLOW Council recommendations were introduced at the end of the 2010 legislative session by Representative Dan Scripps (Democratic Party) (HB 6564) and Senators Patricia Birkholz and Gerald Van Woerkom (both from the Republican Party) (SB 1591). Each bill was referred to its respective committees but neither was brought to the full chamber for a vote. Both bills were

introduced in the lame duck session after the 2010 elections in which Rep. Scripps was defeated. Senators Birkholz and Van Woerkom were term limited and left office at the end of 2010. Since then no legislator has introduced a bill with the GLOW Council recommendations. The 2010 state elections mirrored the national trend with several winners self-identifying as members of the "Tea Party" conservative wing of the Republican Party. Some of these new legislators, such as Ray Franz (who defeated Rep. Scripps), ran on anti-offshore wind platforms (Stanton 2010). Offshore wind energy became a highly controversial issue along the Lake Michigan coast in 2010 as a Norwegian developer proposed an offshore wind farm in the area even without the regulatory clarity of the recommended legislation (the project was later shelved).

In 2011 and again in 2013, Representative Franz and other Republican colleagues introduced HB 4499 (2011) and HB 7778 (2013) which would have modified Part 325 of NREPA to prohibit the MDEQ from permitting or leasing land for activities, including research, related to offshore wind energy. The bills failed to move out of committee and were not enacted, but the opposition to offshore wind energy in Michigan's Great Lakes remains strong in some constituencies. This bill also failed to move out of committee (Disclosure: the author conducts offshore wind energy research that would be banned under such a bill).

Renewable energy advocates campaigned for expanding Michigan's 10% renewable energy standard which will be met in 2015. In 2012, voters were given the choice, through a proposed constitutional amendment (Proposal 3), to increase the state's RPS to 25% by 2025. The ballot initiative did not directly address offshore wind energy. The proposal was rejected with only about one-third of votes in favor of raising the RPS standard (Anders 2012). Governor Snyder continued the energy conversation in 2013 through his "Readying Michigan to Make Good Energy Decisions" program. The Michigan Public Service Commission (MPSC) hosted a series of public energy forums around the state and released four reports: renewable energy, electric choice, energy efficiency, and additional areas. The MPSC found that renewable energy targets of up to 30% are achievable and none of the scenarios evaluated included offshore wind energy. The report discussed several non-technical barriers to renewable energy adoption, including policy barriers, but the lack of offshore energy policy was not addressed (Quackenbush and Bakkal 2013).

Policy paralysis: a case of risk aversion?

Has offshore wind energy become the "third rail" of Michigan politics? The following section usaes prospect theory to examine why, three years after the GLOW Council submitted its recommendations, Michigan still lacks a clear policy for regulating offshore wind energy.

One of the key elements of prospect theory is whether the decision is being made from a gain or loss domain. The State of Michigan was in a "one-state recession" for the first decade of the 21st century (Darga 2011). Michigan, particularly the state government and many unemployed and underemployed voters, perceived itself in a loss domain. Offshore wind energy development presented an opportunity

for Michigan to become the leader in this emerging technology. No full-scale offshore wind turbines had been constructed in North American waters (as of January 2014), though the University of Maine deployed a 1/8-scale, grid-connected floating wind turbine prototype in June 2013 (Viselli 2013). The technology was, and is, more expensive than other clean energy options but the hope was that a clear regulatory pathway could spur innovation and investment and drive costs down in the future. In this context Governor Granholm convened the GLOW Council in 2008 and supported its recommendations for policy reform in 2010. The actual likelihood of attracting offshore wind energy investments, particularly in the near term, were low but the status quo in which further losses were likely was untenable – that is, Michigan found itself in Box 3 of Table 1. In this sense, the risk-seeking policy reform of the GLOW Council recommendations was a reasonable course of action even if the likelihood of Michigan becoming the offshore wind energy manufacturing and logistical hub for the Great Lakes was low.

Prospect theory also explains the timing and authors of the GLOW Council-recommended reform bills introduced in 2010. The bills were introduced during the lame duck session by Rep. Scripps, who had been defeated but had not yet left office, and Senators Birkholz and Van Woerkom, both of whom were unable to run for re-election because of term limits. All of these legislators, therefore, can be described as being in a loss domain (Table 1, Box 3) in which they are risk-seeking toward policy reforms. Each of these legislators had a strong record on environmental issues so it not surprising that they proposed the reform bills. It does suggest, however, that future bills implementing the GLOW Council recommendations may similarly come from legislators who find themselves, for one reason or another, in a loss domain.

One plausible, but not exclusive, explanation for why the GLOW Council recommendations were not enacted and why the 25% renewable energy initiative failed is risk aversion. By late 2010, Michigan's economy was improving (Darga 2011). Legislators and their constituents may have perceived themselves to be in a gains domain and thus more averse to risky policy reforms. Other factors have been noted as reasons why the 25% renewable energy initiative failed, such as it being an amendment to the state constitution. Of the six initiatives on the 2012 ballot for voter approval, none passed.

The Michigan government, and its citizens, is not a monolithic actor. The legislators represent diverse constituencies and not all of them experienced the "one-state recession" equally. The Michigan GLOW Council held a series of public meetings in 2009-2010. A disproportionately large number of attendees (24%) reported being able to see the Great Lakes horizon from his or her primary residence. Additionally, 62% of the attendees reported owning a second residence and about one-third of them had a view of the Great Lakes horizon (Klepinger and Public Sector Consultants 2010). It is plausible that residents of lakeshore communities, particularly those with homes on the coast, perceived themselves in a gains domain. That is, their particular economic conditions were tolerable under the status quo (no reform). Prospect theory predicts that the lakeshore voters and their legislators should be risk averse with respect to reform (the GLOW Council recommendations). The legislators who sponsored the ban on

offshore wind energy represent some of the coastal regions where offshore wind energy has been controversial. Additional evidence from the GLOW Council's stakeholder meetings supports this view. Coastal residents who attended the meetings expected offshore wind turbines to "strongly harm" aesthetics and coastal property values – the potential losses loom large. Inland residents, on the other hand, expected offshore wind farms to neither benefit nor harm these aspects (Five-point Likert scale, median=5 (coastal) vs. 3 (inland), Mann-Whitney U $p<0.05$). These results were not drawn from a random sample so the conclusions cannot be generalized to the whole population.

Framing (the reference point) is an important component of prospect theory and plays a role here. In the discussion above, the status quo is presented an uncertain regulatory framework that inhibits (though does not outright prevent) offshore wind energy development. Reform is presented as the GLOW Council recommendations that would rationalize the permitting and lease process while protecting scenic amenities, spawning habitats, and other locations.

Another frame can be applied to the problem. Offshore wind is currently legal but the permitting process is uncertain and untested (status quo). An alternative policy reform is to ban offshore wind energy from Michigan's Great Lakes altogether. In this case, lakeshore property owners can see an uninterrupted horizon. Any development that might disrupt that view, no matter how far or visible it might be, is perceived as a loss. Peer-reviewed economic analyses of the property value impacts of wind turbines have consistently failed to find a meaningful loss of value from wind turbines (e.g. Hoen *et al.* 2011; see Isely *et al.* 2013 for review). Property owners, however, have often voiced concerns that offshore wind energy could cause lakeshore property values to decline (Nordman *et al.* 2013a, Klepinger and Public Sector Consultants 2010). From this perspective, lakeshore property owners are in Box 3 in Table 1 and are risk seeking as voters for reform that would ban offshore wind energy. That is, coastal residents are risk seeking toward reform to prevent losses but risk averse toward reforms that seek additional gains.

Moving forward

This leaves offshore wind at a legislative impasse. Legislators from coastal communities who are concerned about the potential (though unlikely) property value and aesthetic effects of offshore wind will continue to press to ban offshore wind energy technology even if the bill has little chance of passing. On the other hand, there is little incentive for any particular legislator, especially one not facing defeat or term limits, to sponsor a bill embracing the GLOW Council recommendations. The lesson from previous elections is to sponsor the bill only if you are a lame duck, otherwise you may find yourself touching the "third rail" of Michigan politics. This section presents some options for overcoming the policy gridlock on offshore wind energy in Michgian.

Working from a loss domain: fear of missing out

While Michigan still struggles with higher than average unemployment and weak growth, its "one state recession" was declared at an end in 2011 (Darga 2011). Prospect theory predicts that a government may be more likely to take a chance on a reform when it perceives itself to be in a loss domain. As Michigan's economic climate improves it may find itself moving toward a gains domain in which the appetite for reform is weaker. While this is undoubtedly a positive economic trend, it does seem to be closing on an opportunity to reform the permitting process for offshore wind energy development. There are other factors that could shift Michigan from a gain to a loss frame such as if other states made notable progress on offshore wind energy. For example, if Lake Erie Energy Development Corporation's (LEEDCO) "Icebreaker" 18 MW offshore wind farm in Lake Erie off of Cleveland, Ohio were to move forward as planned, Michigan may fear being "left behind" and missing out on attracting the manufacturing and shipping industries associated with offshore wind energy. External developments like that could change Michigan to a domain that is more favorable to reforming the permitting process. Proponents of the GLOW Council reforms may consider framing the issue from such a loss perspective in which Michigan is losing out to its neighbors.

Strategic positioning as the Great Lakes energy hub

If Michigan is in a gains domain, reform is best approached as an opportunity to obtain a large gain – an incremental gain is unlikely to overcome the risk of disproportionately looming losses. For offshore wind energy, this might be portraying Michigan as the offshore wind energy hub for North America. The offshore wind sector, still in its infancy in North America, lacks an industrial hub. Michigan has an opportunity to strategically position itself as the industrial hub for offshore wind energy manufacturing, logistics, and deployment for the entire Great Lakes region, but only if it acts in a coordinated, timely manner.

Michigan, with coasts on four of the five Great Lakes, lies at the center of a region that includes 10 percent and 31 percent of the US and Canadian populations, respectively (US Environmental Protection Agency 2012). Michigan also has skilled workers with experience in manufacturing. Other regions have leveraged their human resources, natural capital, and infrastructure to become hubs for offshore wind energy, namely the North Holland region of the Netherlands. North Holland is home to several energy research and development organizations, including the Energy Centre Netherlands, the European Commission Joint Research Centre-Institute for Energy, the Wind Turbine Materials and Construction Knowledge Centre, and the Royal Netherlands Institute for Sea Research. This spatial concentration of skills and expertise, combined with a long history in North Sea oil and gas development, public comfort with a working seascape, and suitable coastal conditions, enabled the Netherlands to become a leader in offshore wind energy (Nordman et al. 2013b). The Netherlands plans to increase its offshore wind capacity to more than 4,000 MW by 2023 from about 1,000 MW installed or currently under development (Bakewell 2013).

For Michigan to become the industrial hub of Great Lakes offshore wind energy development would require more than permitting legislation. It would require comprehensive industrial policy to leverage the knowledge of Michigan's world-class universities, the skills of its renowned private manufacturing sector, and the expertise of the regulatory agencies to spur investment. Amassing the human, physical, and financial capital required is unlikely to occur without comprehensive public policy. Michigan does have the required capital to do this, but it is not concentrated in one small geographic area as it is in North Holland. The automotive industry, the closest analogue to offshore wind manufacturing, is concentrated in Detroit but parts suppliers are located throughout the state. The broad spatial distribution may limit the opportunity for knowledge spillovers across sectors and companies, it may help build statewide support across many constituencies.

Waiting for a lame duck session

In a risk-averse climate, prospect theory predicts that reform legislation will more likely be introduced during lame-duck sessions. This was the case in 2010, but no GLOW Council reform bills have been sponsored since then either in the lame duck or general session. It remains to be seen if the issue will be taken up during the lame-duck session in November 2014.

Compacts and regional approaches

Other scholars have offered ideas to move the process forward. Saks (2011) encouraged harmonized regional approach that fosters collaboration among the Great Lakes states and with the federal agencies, as has happened with the MOU. This would be especially relevant if proposed sites spanned state jurisdictions such as in southern Lake Michigan or western Lake Erie. Conger (2011) proposed forming a multi-state offshore wind energy compact similar to the Great Lakes Basin Compact and its implementing agency, the Great Lakes Commission. A multi-state offshore wind energy commission could serve as a lead agency for the harmonized permitting process. A regionally uniform permitting process – perhaps even in coordination with Ontario provincial regulations – in consultation with the appropriate federal agencies might better attract offshore wind energy investment to the region more broadly (Conger 2011). Pressure from neighboring states could put Michigan in a position of "losing out" on the industry and thus in a frame that is more amenable to offshore wind energy policy reform – in this case, relinquishing some permitting authority to a multi-state regulatory body.

Implications beyond Michigan offshore wind

This case study of Michigan's offshore wind energy policy paralysis illustrates how prospect theory can be applied to understanding environmental policy challenges. The results of the Michigan case study add to the growing body of literature using behavioral approaches to environmental policy (see, for example, Pollitt and Shaorshadze 2013; Shogren *et al.* 2010; Venkatachalam 2008). Most of this literature has focused on choices of individuals in a market context. We have, following the example of

Vis and van Kersbergen, have extended the behavioral approach of prospect theory to the policy process itself.

Our findings suggest that prospect theory may be a suitable tool for analyzing other environmental policy challenges. For example, the United States has struggled to produce a comprehensive federal energy and climate policy. If, as our results suggest, policy reform is more likely to be successful when framed from a loss domain, then a future in which climate-related losses (such as "Superstorm" Sandy in 2012) are increasing becomes less tolerable. In such a loss frame, policy-makers may be more risk-seeking in their approach toward reform, making energy and climate legislation more likely.

Prospect theory may also have utility in explaining attitudes toward hydraulic fracturing ("fracking") of natural gas and oil. Oil and gas development, including fracking, is legal and regulated. In some cases, however, the regulations for new fracking techniques are not as strict as some would prefer. Opponents of fracking are concerned about the environmental risks, especially those to groundwater (Krupnick and Siikamäki 2013). That is, they approach the problem from a loss domain and are risk-seeking toward reform of fracking regulations. There is evidence to support this idea: a recent study found that environmental NGO messages which highlight the risks of fracking (loss frame) elicited a higher willingness to pay for risk reduction compared to neutral and industry messages (Krupnick and Siikamäki 2013). Both of the examples above are superficial analyses of complex challenges that deserve more detailed investigation. Our results suggest that future studies of these and other environmental and energy policy challenges may benefit from using a behavioral theoretical lens.

Conclusions

Behavioral approaches to environmental policy analysis are gaining traction. Though the standard rational choice model of policy actors, including consumers, works well in most cases, environmental economists and policy analysts have catalogued "behavioral failures" in which actors do not make optimizing choices. While the research focus so far has been on consumers of environmental goods and services, behavioral approaches, including prospect theory, can apply to the actions of policy-makers as well. We have illustrated the utility of the behavioral approach to environmental policy analysis using a case study of offshore wind energy in Michigan's Great Lakes. Our results also suggest that behavioral approaches may be useful for analyzing other environmental policy challenges, including climate change and fracking.

Michigan has outstanding offshore wind energy resources but lacks a clear policy framework through which the private sector can access the state-owned lake bottomlands. While offshore wind energy is not prohibited, the regulatory uncertainty provides a strong disincentive toward such infrastructure investments. Attempts to clear the regulatory hurdles have failed to pass through the state legislature and there seems to be little enthusiasm to sponsor a bill that would facilitate offshore wind energy development in Michigan. On the other hand, several bills have been introduced that would ban offshore wind energy development from Michigan's Great Lakes. Prospect theory can explain some

aspects of this policy paralysis. The benefits of offshore wind energy – particularly in reducing air pollution from other generating sources – accrue to a broad range of residents inside and outside Michigan, while the potential, but uncertain and relatively smaller, property value and aesthetic impacts accrue to a particular constituency. There is little incentive for a legislator to advocate for offshore wind energy policy and strong incentives for particular legislators to advocate a ban. Prospect theory's emphasis on risk aversion, status quo bias, and framing add to the explanation and offer ways forward.

We offer several approaches for moving the policy discussion forward. Framing the issue from a loss domain – such as losing out to neighboring states on an emerging industry – could encourage voters and legislators to be more open to the regulatory reform needed to facilitate offshore wind energy development in Michigan's Great Lakes. Framing the policy reform from a gains domain requires the potential for a large, rather than incremental, benefit. The reform would need to go beyond simply permitting to perhaps an industrial policy aimed at making Michigan the Great Lakes hub for offshore wind energy. Regional collaborative approaches, from a federally coordinated MOU to a multi-state compact, could encourage Michigan to adopt a coherent, basin-wide offshore wind permitting system. A ban on offshore wind energy (and associated research) has been proposed but does not, at the moment, have much support. However the uncertainty surrounding Michigan's offshore wind energy permitting system discourages investment and the status quo may be as good as a ban.

The behavioral turn in environmental policy analysis is just beginning. Additional empirical evidence is needed from natural and laboratory experiments to advance the field. Our research, as well as that of others, suggest that prospect theory holds promise for understanding how individuals, whether consumers, citizens, or policy-makers, make decisions under conditions of uncertainty. The 20th century generation of energy infrastructure was built largely without much public input. The 21st century transition to low-carbon, distributed energy systems is happening with a large degree of public input, making the need for a behavioral approach to policy analysis that much greater.

Acknowledgements

This work was supported by the US Department of Energy under Grant DE-EE0000294. The author thanks project collaborators Arn Boezaart, Charlie Standridge, and Jim Edmonson. The author also thanks Lauren Knapp at the Great Lakes Commission whose suggestions have improved this manuscript. Any errors are strictly the author's.

References

Adelaja, S., McKeown, C., Calnin, B., and Hailu, Y. 2012. Assessing offshore wind potential. *Energy Policy* 42, 191-200.

Anders, M., 2012. Michigan Proposal 3: Voters reject 25 by 25 renewable energy mandate. MLive 6 November 2012. Available from http://www.mlive.com/politics/index.ssf/2012/11/proposal_3_michigans_renewable.html [Accessed 5 November 2013].

Bakewell, S., 2013. Netherlands to increase offshore wind fourfold in next decade. Bloomberg 6 September 2013. Available from http://www.bloomberg.com/news/2013-09-06/netherlands-to-increase-offshore-wind-fourfold-in-next-decade.html [Accessed 3 December 2013].

Beaudry-Losique, J., Boling, T., Brown-Saracino, J., Gilman, P., Hahn, M., Hart, C., Johnson, J., McCluer, M., Morton, L., Naughton, B., Norton, G., Ram, B., Redding, T., Wallance, W. 2011. *A National Offshore Wind Strategy: Creating an offshore wind energy industry in the United States.* Department of Energy Technical Report DOE/GO-102011 2988.

Conger, H., 2011. A lesson from Cape Wind: Implementation of offshore wind energy in the Great Lakes should occur through multi-state cooperation. *Loyal University Chicago Law Journal* 42, 741-793.

Darga, K., 2011. Is Michigan's economic recovery real? Re-thinking the one-state recession. Available from http://www.michigan.gov/cgi/0,4548,7-158-54534-260315--,00.html [Accessed 26 September].

Great Lakes Commission, 2013. *Support for Great Lakes offshore wind demonstration (pilot) projects*. Resolutions adopted at the Great Lakes Commission's 2013 Annual Meeting, 9 September 2013. Available from http://www.glc.org/about/resolutions/index.html#2013ann [Accessed 14 September 2013].

Isely, P., Fan, Y., Nordman, E., 2013. Wind energy economics: Production costs and additional impacts. West Michigan Wind Assessment Issue Brief 6. Available from http://www.gvsu.edu/wind/project-documents-3.htm [Accessed 26 September 2013].

Kahneman, D. 2011. *Thinking, Fast and Slow*. New York: Farrar, Straus and Giroux.

Kahneman, D., Tversky, A., 1979. Prospect theory: An analysis of decision under risk. *Econometrica* 47, 263-291.

Klepinger, M, 2008. *Michigan Great Lakes Offshore Wind Permitting Dry Run. Final report submitted to the Michigan Economic Development Corporation and the Great Lakes Renewable Energy Association.* Available from http://www.michiganglowcouncil.org/resources.html [Accessed 14 September 2013].

Klepinger, M. and Public Sector Consultants, Inc., 2010. *Report of the Great Lakes Wind Council – 1 October 2010*. Available from http://www.michiganglowcouncil.org/resources.html [Accessed 14 September 2013].

Klepinger, M. and Public Sector Consultants, Inc., 2009. *Report of the Great Lakes Wind Council – 1 September 2009*. Available from http://www.michiganglowcouncil.org/resources.html [Accessed 7 January 2014].

Krupnick, A., Siikamäki J. 2013. The shale gas debate: How industry and environmental messages stack up. Resources for the Future briefing webinar 6 December 2013. Available from http://www.rff.org/Events/Pages/The-Shale-Gas-Debate-How-Industry-and-Environmental-Messages-Stack-Up.aspx [Accessed 7 January 2014].

Levy, J., 1992. An introduction to prospect theory. *Political Psychology* 13(2), 171-186.

Loomis, D. 2013. The potential economic impact of offshore wind energy in the Great Lakes. Great Lakes Wind Collaborative research paper. Available from http://glc.org/docs/2013-potential-economic-impact-offshore-wind/ [Accessed 6 January 2014].

Mausolf, A., 2012. Clearing the regulatory hurdles and promoting offshore wind development in Michigan. *University of Detroit Mercy Law Review* 89, 223-255.

Moon, W. Nordstrom, C., 2010. Tension leg platform turbine: A unique integration of mature technologies. *Proceedings of the 16th Offshore Symposium, 9 February 2010, Houston, Texas. Texas Section of the Society of Naval Architects and Marine Engineers*. Available from www.glosten.com/pdfs/glosten_tltp_paper_2010.pdf *[Accessed 14 September 2013].*

National Environmental Policy Task Force, 2003. *Modernizing NEPA Implementation*. Report to the Council on Environmental Quality.

Nordman, E., O'Keefe, D., Arndt, E., 2013a. Enhancing public engagement on offshore wind energy using *genius loci*: A case study from a Lake Michigan coastal community. Working paper available at http://works.bepress.com/erik_nordman/ [Accessed 3 December 2013]

Nordman, E., VanderMolen, J., Gajewski, B., Ferguson, A., 2013b. Great Lakes, great debates: Facilitating public engagement on offshore wind energy using the Delphi Inquiry approach. *In*: Richardson, Robert B. (ed.), *Building a Green Economy: Perspectives from Ecological Economics*. East Lansing, MI: Michigan State University Press, 211-222.

Pollitt, M., Shaorshadze, I. 2013. The role of behavioural economics in energy and climate policy. *In* Fouquet, Roger (ed.), *Handbook on Energy and Climate Change*. Northampton, MA, USA: Edward Elgar, 523-546.

Quackenbush, J., Bakkal, S., 2013. *Readying Michigan to Make Good Energy Decisions: Renewable Energy*. Report from the Michigan Public Service Commission and Michigan Energy Office. Available from http://www.michigan.gov/energy [Accessed 5 November 2013].

Saks, K., 2011. Great Lakes, Great Potential: Examining the regulatory framework for wind farms in the Great Lakes. *Canada-United States Law Journal* 35(1-2), 209-235.

Shogren, J., Parkhurst, G., Banerjee, P. 2010. Two cheers and a qualm for behavioral environmental economics. Environmental and Resource Economics 46: 235-247.

Stanton, A., 2010. *Scripps vs. Franz: State rep candidates battle for the 101st*. Northern Express 1 November 2010. Available from http://www.northernexpress.com/michigan/article-5127-scripps-vs-franz.html [Accessed 5 November 2013].

Thaler, R., 1980. Toward a positive theory of consumer choice. *Journal of Economic Behavior and Organization* 1, 39-60.

US Environmental Protection Agency, 2012. Great Lakes Fact Sheet. Available from http://www.epa.gov/glnpo/factsheet.html [Accessed 3 December 2013].

US National Renewable Energy Laboratory. 2013. Levelized cost of energy calculator. Available from http://www.nrel.gov/analysis/tech_lcoe.html [Accessed 6 January 2014].

Venkatachalam, L. 2008. Behavioral economics for environmental policy. Ecological Economics 67:640-645.

Vis, B., van Kersbergen, K., 2007. Why and how do political actors pursue risky reforms? *Journal of Theoretical Politics* 19(2), 153-172.

Viselli, E., 2013. *Electrons from first offshore wind turbine in North America to flow into U.S. grid at noon*. University of Maine Advanced Structures and Composites Center press release 13 June 2013. Available from http://composites.umaine.edu/ [Accessed 5 November 2013].

White House Council of Environmental Quality, 2012. *Memorandum of understanding among the White House Council on Environmental Quality, the U.S. Department of Energy, the U.S. Department of Defense, the U.S. Department of the Army, the Advisory Council on Historic Preservation, the U.S. Coast Guard, the U.S. Environmental Protection Agency, the U.S. Fish and Wildlife Service, the Federal Aviation Administration, the National Oceanic and Atmospheric Administration, the Commonwealth of Pennsylvania, and the States of Illinois, Michigan, Minnesota, and New York to Create a Great Lakes*

Offshore Wind Energy Consortium to Coordinate Issues of Regional Applicability for the Purpose of Promoting the Efficient, Expeditious, Orderly and Responsible Evaluation of Offshore Wind Power Projects in the Great Lakes. Available from http://www.glc.org/energy/wind/windmou.html [Accessed 14 September 2013].

Table 1: Prospect theory's fourfold pattern (adapted from Kahneman 2011). The option (A or B) in **bold** reflects the outcome predicted by prospect theory.

		Level of risk	
		High probability	Low probability
Type of outcome	Gain	*Box 1: Risk Averse*	*Box 2: Risk Seeking*
		A: 95% chance of winning $10,000	**A: 5% chance of winning $10,000**
		5% chance of winning nothing	**95% chance of winning nothing**
		B: 100% chance of winning $9,500	B: 100% chance of winning $500
		Reason: Fear of disappointment	Reason: Hope of large gain
	Loss	*Box 3: Risk Seeking*	*Box 4: Risk Averse*
		A: 95% chance of losing $10,000	A: 5% chance of losing $10,000
		5% chance of losing nothing	95% chance of losing nothing
		B: 100% chance of losing $9,500	**B: 100% chance of losing $500**
		Reason: Hope to avoid large loss	Reason: Fear of large loss

Table 2: Key permitting actions, actors, and statutes regulating offshore wind energy development in Michigan's Great Lakes.

Action	Major Actor	Statute	Coordinating actors
Review and issue Joint Permit	MDEQ	NREPA Part 325	MDNR
	USACE	R&HA, CWA, NHPA	
Issue bottomland lease	MDEQ	NREPA Part 325	MDNR
Conduct EA/EIS	USACE	NEPA	EPA
Issue Notice of Proposed Construction	FAA and MDOT	MI Tall Structures Act, FAA 14 CFR 77	
Issue Permit for Private Aids to Navigation	USCG	33 CFR 64, 66. 67	USACE
Issue Certificate of Public Conveyance and Necessity	MPSC	PA 30 of 1995	FERC
Issue zoning permit for onshore transmission	Local planning and zoning boards	MZEA	

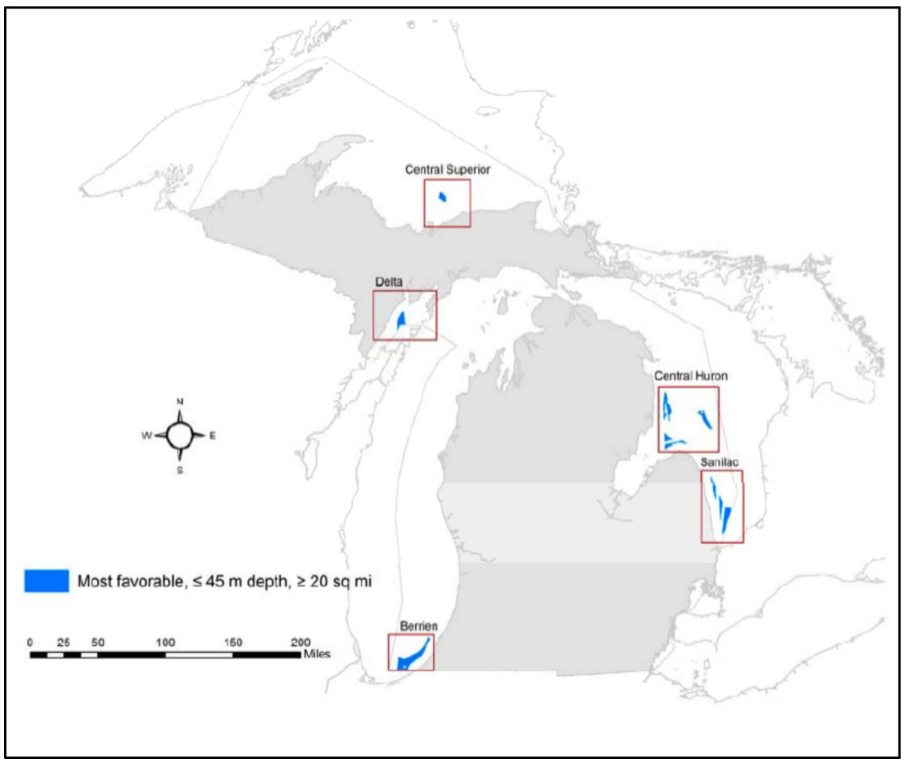

Figure 1: Most favorable areas for offshore wind energy development in Michigan's Great Lakes, based on GLOW Council mapping criteria (Klepinger and Public Sector Consultants 2010).